

Aerosol MALDI Mass Spectrometry for Bioaerosol Analysis

Proefschrift

ter verkrijging van de graad van doctor
aan de Technische Universiteit Delft,
op gezag van de Rector Magnificus,
Prof. dr. ir. J.T. Fokkema,
voorzitter van het College voor Promoties,
in het openbaar te verdedigen op

dinsdag, 16 september 2008, om 12.30 uur

door

Willemina Anna KLEEFSMAN

Doctorandus in de Farmacie en Technische Farmacie

geboren te
Groningen

Dit proefschrift is goedgekeurd door de promotor:

Prof. dr. A. Schmidt-Ott

Copromotor:

Dr. ir. J.C.M. Marijnissen

Samenstelling promotiecommissie:

Rector Magnificus	voorzitter
Prof. dr. A. Schmidt-Ott	Technische Universiteit Delft, promotor
Dr. ir. J.C.M. Marijnissen	Technische Universiteit Delft, copromotor
Prof. dr. F. Hillenkamp	University of Münster
Prof. dr. P.G. Kistemaker	FOM instituut AMOLF Amsterdam
Prof. dr. P.D.E.M. Verhaert	Technische Universiteit Delft
Dr. ir. P.J.T. Verheijen	Technische Universiteit Delft
Dr. M.A. Stowers	Technische Universiteit Delft
Prof. dr. ir. M.T. Kreutzer	Technische Universiteit Delft, reservelid

© Willemina Anna Kleefsman, 2008

ISBN 978-90-9023387-1

All rights reserved. Save exceptions stated by the law, no part of this thesis may be reproduced, stored in a retrieval system of any nature, or transmitted in any form or by any means, electronic, mechanical, photocopying, recording or otherwise, included a complete or partial transcription, without the prior written permission of the author. The author encourages the communication of scientific contents and explicitly exempts the use for scientific, non commercial purposes, provided the proper citation of the source. Parts of the thesis are published in scientific journals and copyright is subject to different terms and conditions.

Aerosol MALDI Mass Spectrometry for Bioaerosol Analysis

Thesis

presented for the degree of doctor
at Delft University of Technology
under authority of the Vice-Chancellor,
Prof. dr. ir. J.T. Fokkema,
Chairman of the Board of Doctorates,
to be defended in public in the presence of a committee on

Tuesday, September 16th, 2008, at 12.30 pm

by

Willemina Anna KLEEFSMAN

Doctorandus in de Farmacie en Technische Farmacie

born at
Groningen

This thesis is approved by the promotor:

Prof. dr. A. Schmidt-Ott

Copromotor:

Dr. ir. J.C.M. Marijnissen

Composition of Examination Committee:

Rector Magnificus	chairman
Prof. dr. A. Schmidt-Ott	Technische Universiteit Delft, promotor
Dr. ir. J.C.M. Marijnissen	Technische Universiteit Delft, copromotor
Prof. dr. F. Hillenkamp	University of Münster
Prof. dr. P.G. Kistemaker	FOM instituut AMOLF Amsterdam
Prof. dr. P.D.E.M. Verhaert	Technische Universiteit Delft
Dr. ir. P.J.T. Verheijen	Technische Universiteit Delft
Dr. M.A. Stowers	Technische Universiteit Delft
Prof. dr. ir. M.T. Kreutzer	Technische Universiteit Delft, reserve member

© Willemina Anna Kleefsman, 2008

ISBN 978-90-9023387-1

All rights reserved. Save exceptions stated by the law, no part of this thesis may be reproduced, stored in a retrieval system of any nature, or transmitted in any form or by any means, electronic, mechanical, photocopying, recording or otherwise, included a complete or partial transcription, without the prior written permission of the author. The author encourages the communication of scientific contents and explicitly exempts the use for scientific, non commercial purposes, provided the proper citation of the source. Parts of the thesis are published in scientific journals and copyright is subject to different terms and conditions.

Stellingen

Behorend bij het proefschrift

"Aerosol MALDI Mass Spectrometry for Bioaerosol Analysis"

door

Willemina Anna KLEEFSMAN

1. Met de juiste online monstervoorbewerkingsmethode kan aerosol MALDI standaard MALDI massaspectrometrie overtreffen
2. In de monstervoorbewerking voor MALDI, in het formuleren van geneesmiddelen en bij het koken bepaalt ook de samenstelling van ingrediënten het uiteindelijke resultaat: respectievelijk het massaspectrum, het moment van vrijkomen van het geneesmiddel en de smaak van het gerecht
3. Probleemgestuurd onderwijs gaat ten koste van het overbrengen van kennis
4. Iemand die denkt alleen op de wereld te zijn, maakt het moeilijk voor de andere mensen die er ook zijn
5. Een gedwongen immobiliteit kan de concentratie, voor bijvoorbeeld het schrijven van een proefschrift, ten goede komen
6. Wetenschap bedrijven is geloven
7. De conclusie van elk onderzoek is dat er meer onderzoek nodig is
8. Het toevoegen van een managementlaag in een organisatie doet de productiviteit afnemen

Deze stellingen worden opponeerbaar en verdedigbaar geacht en zijn als zodanig goedgekeurd door de promotor, Prof. dr. A. Schmidt-Ott

Propositions

Adjunct to the thesis

*"Aerosol MALDI Mass Spectrometry for Bioaerosol
Analysis"*

by

Willemina Anna KLEEFSMAN

1. With the right on-line sample preparation method aerosol MALDI can be superior to standard MALDI mass spectrometry
2. In the sample preparation in MALDI, in the formulation of drugs and in cooking it is also the choice of ingredients that determines the result: the mass spectrum, the moment of drug release and the taste of the dish, respectively
3. Problem-based learning is at the cost of the transfer of knowledge
4. Somebody who thinks to be the only person in the world makes it very hard for the others
5. Forced immobility can improve focus, for writing a thesis for instance
6. Practicing science is believing
7. The conclusion of each research project is that more research is necessary
8. Adding an additional management layer in an organization decreases productivity

These propositions are considered opposable and defensible and as such have been approved by the supervisor, Prof. dr. A. Schmidt-Ott

To My Parents

Summary

Aerosol MALDI mass spectrometry for bioaerosol analysis

In this thesis the development of the aerosol MALDI mass spectrometer for the analysis of single bioaerosol particles is described. A large part of this research project was by TNO Defence, Security and Safety and the primary goal of this research was to realize a sensing instrument to warn in case of a biological attack. An evaluation of a number of experimental studies in which the concentration of bacteria particles in the atmosphere were determined was made. The evaluation revealed that an outbreak (of harmful bacteria) can not be detected by measuring solely the (total) bacterial concentrations. The measured 'background' concentrations are highly variable and a sudden increase in concentration is usual and often related to normal (human) activities like harvesting. Therefore, identification of the aerosol particles is required. The NRC (National Research Council of the United States) defined design criteria for detection systems to provide rapid warning in case of a biological attack: detection of a broad range of biological agents, a small response time and a very low false alarm rate. Based on this evaluation is suggested to extend the design criteria of the NRC with two more criteria. Sensing instruments should be able to measure high absolute concentrations as well as wide concentration ranges, and the instruments should have the capability to measure and identify the total range of bioaerosol particles. With the currently available instruments it is impossible to measure and identify a biological attack within a short time range, and on-line techniques are re-

Summary

quired. Based on a discussion of these design criteria the aerosol MALDI mass spectrometer is proposed to be a sensing instrument that could meet the requirements of the NRC.

The strength of the aerosol MALDI mass spectrometer is based on three subsequent steps: particle detection, particle selection and the analysis of the particles based on MALDI mass spectrometry. At the start of this research project the aerosol mass spectrometer was not yet optimized for (on-line) bioaerosol analysis. The aerosol mass spectrometer has been improved to make the instrument suitable for bioaerosol detection. The implemented instrumental improvements include a new design of the repeller and the extractor plate as well as the implementation of delayed extraction. Due to the improvements, single particle mass spectra with a mass range up to 21 kDalton and with a resolution of 2000 at 6 kDalton are obtained. The sensitivity of the instrument is 1 zeptomole ($1 \cdot 10^{-21}$ mole) for a single component protein aerosol, and this is sufficient for bacterial analysis. Next to the instrumental improvements, the particle generation was optimized to be able to produce bioaerosol particles of natural sizes in a controllable way. Note that the developed particle generation system is only used for the experiments to prove the concept; in a 'real' instrument the particle generation system is not needed.

Since the bacteria particle concentration is low, compared to the total load of particulate matter, a selection step was already implemented to increase the sensitivity of the instrument. The selection of the bioaerosol fraction out of an aerosol is based on the fluorescence emission. In an experiment with atmospheric air approximately 20% of the analyzed aerosol particles were identified to be possibly bioaerosol particles. This percentage corresponds to a concentration of $1 \cdot 10^6$ bioaerosol particles/ m^3 , and is corresponding to the background values found in chapter 1. The effect of diesel soot particles on the preselection was investigated and diesel soot was found to be a minor source of interference. This type of interference is expected to be easily regnonized based on the mass spectra.

The developed aerosol mass spectrometer utilizes MALDI (matrix-assisted laser desorption/ionization) mass spectrometry for the analysis of aerosol particles. MALDI is a widely accepted technique for the analysis of biological material. This research project deals with a different kind of sample: single aerosol particles. Therefore different sample preparation techniques are required in aerosol MALDI. The quality and appearance of MALDI

mass spectra is influenced by the sample preparation method and by the sample composition. The application of the MALDI technique for *on-line* analysis of aerosol particles, implies the need of an on-line sample preparation method. Next to the off-line sample preparation methods (the premixed method and the crushed-crystal method), the on-line coating method was developed and investigated. The different sample preparation methods resulted in mass spectra with different appearance, but the target ions were detected with all the applied methods. The effect of the sample composition on the ion formation in aerosol MALDI was investigated for fifteen matrix-solvent combinations. Effects of sample composition in aerosol MALDI are less pronounced than reported in literature for standard MALDI mass spectrometry. It was found that the type of matrix material has more effect than the type of solvent on the ion formation of insulin in aerosol MALDI. The matrix PMC (a proprietary made compound, order number 0145GM02, kindly provided by TNO Defence, Security and Safety, Rijswijk, The Netherlands) is the matrix of choice for the analysis of biological aerosols and can also be used for the *on-line* analysis of aerosol particles.

The last part of this thesis describes the analysis of bacteria containing aerosol particles, to demonstrate the suitability of the instrument for on-line bioaerosol analysis. Bacterial analysis was performed using three different sample preparation methods: the crushed-crystal method, the impaction and evaporation/condensation method and the on-line coating method. The results with the impaction and evaporation/condensation method were unsatisfying and this method was not further investigated. The detectability of bacterial aerosol particles was demonstrated with the off-line crushed-crystal method. The obtained mass spectra covered a mass range up to 16 kDalton and the resolution was 200-400 up to 12 kDalton. In the obtained mass spectra peaks which can be correlated with ribosomal proteins are identified. Aerosol MALDI mass spectrometric analysis is also performed with bacterial spores and peaks which can be correlated with proposed biomarkers, the SASP's, are detected.

Finally, on-line bacterial analysis using the on-line coating technique was performed. It was attempted to perform on-line biomarker extraction and to create on-line mixing and co-crystallization of the matrix and analyte molecules (the biomarkers). The peaks in the obtained mass spectra had low resolution, but were found to be reproducible. The mass

Summary

range of the detected peaks was 4 kDalton. It was concluded that the applied on-line sample preparation method is not optimal. In the on-line sample preparation method on-line extraction and on-line mixing and co-crystallization of analyte and matrix has to take place. This requires a solvent in which matrix and analyte (biomarker) are soluble. Preliminary solubility experiments indicate that isopropanol may be such a solvent. A more extensive investigation of possible solvents and the solubility (rate) in these solvents is required.

The developed aerosol MALDI mass spectrometer has been demonstrated to have a high potential for the analysis of biological aerosol particles. The suitability has been demonstrated with an off-line sample preparation method. However, to obtain the same performance for on-line analysis, more research is required regarding the on-line sample preparation method.

The performed investigations and obtained results have led to more insight in the processes and mechanisms that occur (or are needed) in MALDI mass spectrometry, especially regarding the sample preparation and sample composition.

Ineke Kleefsman
Delft, September 2008

Contents

Summary	ix
List of Tables	xvii
List of Figures	xix
Introduction	xxiii
1 Bioaerosols	1
1.1 Introduction	2
1.2 Experimental	5
1.3 Results and Discussion	6
1.3.1 The effect of sampling location on bacteria concentration	7
1.3.2 Bacteria concentrations in urban areas	11
1.3.3 Bacteria concentrations in residential areas	13
1.3.4 Bacteria concentrations in rural areas	14
1.3.5 Bacteria concentrations at coastal sites	17
1.3.6 A comparison of the found background concentrations	18
1.4 Bioaerosol sampling instrumentation	20
1.5 Design criteria for sensing instruments	21
1.6 Conclusions	22
2 Instrumental Improvements for Bioaerosol Mass Spectrometry	25
2.1 Introduction	26
2.2 Previous improvements on the aerosol mass spectrometer	26
2.3 Latest improvements of the aerosol mass spectrometer	30
2.3.1 New high voltage ion source	30
2.3.2 Delayed extraction	34
2.3.3 Particle beam alignment	35

Contents

2.4	Calibration of the aerosol mass spectrometer	36
2.5	Description of the current aerosol mass spectrometer	38
2.6	Performance of the aerosol mass spectrometer	43
2.6.1	Improved resolution	43
2.6.2	Isotopic resolution	48
2.6.3	Sensitivity limit	50
2.7	Multicomponent aerosol analysis with the aerosol mass spectrometer	53
2.7.1	Internally mixed aerosol	53
2.7.2	Externally mixed aerosol	54
2.8	Particle generation and characterization	56
2.9	Applicability of IR-MALDI for bioaerosols	62
2.10	Conclusions	65
3	Particle Selection by Fluorescence	67
3.1	Introduction	68
3.2	Fluorescence principle	70
3.3	Experimental	70
3.4	Size selection and fluorescence preselection	71
3.5	Fluorescence properties of atmospheric air	75
3.6	Fluorescence properties of soot	77
3.7	Comparison of size and fluorescence of different aerosols	78
3.8	Conclusions	81
4	Effect of Sample Preparation and Composition in Aerosol MALDI	83
4.1	Introduction	84
4.2	MALDI mechanisms: desorption and ionization	85
4.3	MALDI matrices	86
4.3.1	MALDI matrix compounds	86
4.3.2	MALDI matrix properties	88
4.4	MALDI sample composition	89
4.5	Standard MALDI sample preparation methods	91
4.6	Aerosol MALDI sample preparation methods	93
4.6.1	Aerosol production by premixing	94
4.6.2	Aerosol production by the crushed-crystal method	94
4.6.3	On-line coating of aerosols	95

4.6.4	Aerosol analysis by impaction and matrix evaporation/condensation	99
4.6.5	On-line coating of aerosols using electrospray	100
4.7	The effects of sample composition in Aerosol MALDI	104
4.7.1	Aerosol generation	105
4.7.2	Data analysis	105
4.7.3	Results and Discussion	109
4.8	Conclusions	121
5	Detection of Bacteria by Aerosol MALDI Mass Spectrometry	123
5.1	Introduction	124
5.2	Crushed-crystal sample preparation method for bacterial analysis	128
5.2.1	<i>Erwinia herbicola</i>	130
5.2.2	<i>Escherichia coli</i>	132
5.2.3	<i>Bacillus atrophaeus</i>	140
5.2.4	Concluding and summarizing remarks for aerosol MALDI on bacteria using the crushed-crystal method	142
5.3	Semi on-line analysis of bacteria-containing aerosols	144
5.4	On-line analysis of bacterial aerosols	148
5.4.1	On-line analysis of <i>Escherichia coli</i>	148
5.4.2	On-line analysis of <i>Bacillus atrophaeus</i>	151
5.4.3	Discussion on on-line bioaerosol MALDI MS	152
5.5	Conclusions	154
6	Conclusions, Recommendations and Outlook	155
6.1	Summarized conclusions	156
6.2	Recommendations	158
6.2.1	Suggested improvements for aerosol sampling	159
6.2.2	Instrumental improvements	159
6.2.3	Improvements for the sample preparation	162
6.3	Outlook	163
A	Overview of standard MALDI MS analysis on bacteria	165
	List of Symbols	167

Contents

Bibliography	169
Samenvatting	193
Acknowledgement	197
Curriculum Vitae	201

List of Tables

1.1	Experimental data for concentrations of airborne bacteria in urban areas	5
1.2	Experimental data for concentrations of airborne bacteria in suburban/residential areas	7
1.3	Experimental data for concentrations of airborne bacteria in rural areas	8
1.4	Experimental data for concentrations of airborne bacteria in rural areas - continued	9
1.5	Experimental data for concentrations of airborne bacteria in coastal/marine/desert areas	10
2.1	Adjustable parameters, typical settings and their effects and functions, of the aerosol mass spectrometer	43
5.1	Peaks detected in the mass spectra of <i>Escherichia coli</i> , figures 5.3 and 5.4	138
A.1	Overview of standard MALDI MS analysis on bacteria	166

List of Figures

1.1	Concentrations of airborne bacteria at urban, rural and coastal sampling locations	11
1.2	Culturable and total concentrations of airborne bacteria at urban sites	13
1.3	Culturable and total concentrations of airborne bacteria at suburban sites	15
1.4	Culturable and total concentrations of airborne bacteria at rural sampling locations	18
1.5	Culturable and total concentrations of airborne bacteria at coastal sampling locations	19
2.1	Schematic drawing of the instrument for on-line aerosol analysis as proposed by Marijnissen et al. [1988]	27
2.2	Configurations of the aerosol beam generator	28
2.3	Schematic drawing of a microchannel plate detector	31
2.4	Schematic drawing of the ion source in the aerosol time-of-flight mass spectrometer	33
2.5	Visualization of the aerosol beam	37
2.6	Schematic diagram of the current aerosol mass spectrometer	39
2.7	The arrangement of the optical components	41
2.8	Effect of the new ion source on single particle mass spectra	44
2.9	Effect of continuous and delayed extraction	45
2.10	Histograms of peak positions of 1000 single particle insulin spectra	47
2.11	Frequency distributions of single shot resolutions in continuous and delayed extraction	48
2.12	MALDI mass spectra of substance P showing isotopic resolution	50

List of Figures

2.13	MALDI mass spectra of 0.26 μm -insulin particles (sensitivity limit)	51
2.14	MALDI mass spectrum of an internally mixed aerosol . . .	55
2.15	Single particle MALDI mass spectra from an externally mixed aerosol	57
2.16	Effect of nebulizer on the particle size distribution	59
2.17	SEM-image of a <i>Bacillus atrophaeus</i> -spore produced with the ultrasonic nebulizer	60
2.18	Pattern of particle concentrations in the aerosol chamber .	61
2.19	Schematic drawing of the trigger scheme for the IR-laser .	64
3.1	Histogram of particle size and fluorescence intensity obtained from an aerosol containing <i>Escherichia coli</i>	73
3.2	Histogram of particle size and fluorescence intensity obtained from aerosol containing spores of <i>Bacillus atrophaeus</i>	74
3.3	Histograms of particle size and fluorescence intensity obtained from atmospheric aerosol	76
3.4	Particle number distributions of the collected soot particle	78
3.5	Histogram of particle size and fluorescence intensity obtained from the fluorescing fraction of the soot aerosol . . .	79
3.6	Contour plots of particle size versus fluorescence intensity for <i>Escherichia coli</i> , <i>Bacillus atrophaeus</i> and diesel soot . .	80
4.1	Chemical structures of common MALDI matrix materials .	88
4.2	Effect of matrix temperature on particle size distributions of on-line coated particles	98
4.3	Effect of sample preparation method on aerosol MALDI mass spectra of insulin	101
4.4	Schematic drawing of the electrospray set-up	103
4.5	Effect of electrospray flowrate on particle size distributions of on-line electrospray coated particles	104
4.6	Effect of matrix and solvent on aerosol mass spectra	111
4.7	Effect of matrix-solvent combination on the detection of ions in aerosol mass spectra	113
4.8	Effect of matrix-solvent combination on the peak area . . .	118
4.9	Effect of matrix-solvent combination on the variability of peak area	120

List of Figures

5.1	Aerosol mass spectra of <i>Erwinia herbicola</i>	129
5.2	Reproducible aerosol mass spectra of <i>Escherichia coli</i> . . .	132
5.3	Aerosol and standard mass spectra of <i>Escherichia coli</i> M15	134
5.4	Aerosol and standard mass spectra of <i>Escherichia coli</i> K12 XL1 blue	135
5.5	Aerosol mass spectra of two strains of <i>Escherichia coli</i> . .	136
5.6	Aerosol mass spectra of <i>Bacillus atrophaeus</i> spores	141
5.7	SEM images of the <i>Bacillus atrophaeus</i> aerosol prepared with the crushed-crystal method	143
5.8	Mass spectra of <i>Erwinia herbicola</i> obtained using the im- paction evaporation/condensation method	145
5.9	Mass spectra of <i>Escherichia coli</i>	149
5.10	On-line aerosol mass spectra of <i>Escherichia coli</i>	150
5.11	On-line aerosol mass spectrum of <i>Bacillus atrophaeus</i> . . .	152

Introduction

This thesis describes the development of the aerosol MALDI mass spectrometer for the analysis of single bioaerosol particles. A large part of this research project was sponsored by TNO Defence, Security and Safety. In this research project aerosol technology, analytical methods and microbiology are coming together, making it interesting, complex and scientifically challenging.

In the first chapter an evaluation of performed studies in which the atmospheric bioaerosol concentrations were measured is given. This evaluation was made to identify the need for a sensing instrument. The goal of such a sensing instrument is to warn in case of a biological attack. Design criteria for a sensing instrument need to be defined. It should be defined if a sensing instrument should measure the total (bio)aerosol concentration, if an attack can be identified based on an increase in concentration, if identification or classification of biological particles is required. Furthermore, the suitability of the aerosol mass spectrometer to be used as a sensing instrument is discussed.

The second chapter starts with the history and a description of the previous improvements on the aerosol mass spectrometer. At the start of this research project the aerosol mass spectrometer was not yet optimized for (on-line) bioaerosol analysis. In this research project improvements were made to the instrument to make it suitable for bioaerosol analysis. The principles of the improvements are described. Experiments in which the effect of the implemented improvements is demonstrated are also given in chapter 2.

Only a fraction of the particles in the atmosphere has a biological origin. To reserve the instrument only for the biological fraction a preselection step based on fluorescence was already implemented. The third chapter describes the principle of this preselection and experiments to demonstrate the suitability of the preselection, including the effect of interfering sources

Introduction

on this preselection.

The developed aerosol mass spectrometer utilizes MALDI (matrix-assisted laser desorption/ionization) mass spectrometry for the analysis of aerosol particles. MALDI is a widely accepted technique for the analysis of biological material. However, the standard MALDI technique is normally used to analyze small, but bulky samples. This research project deals with a different kind of sample: single aerosol particles instead of an aliquot of a bulky liquid. One can imagine that for this type of sample different sample preparation techniques are required. Sample preparation methods for *aerosol* MALDI analysis are described in chapter 4. The effect of sample composition on the mass spectra in aerosol MALDI is investigated. This investigation was performed, since it is known that the sample composition in standard MALDI plays an important role on the quality and appearance of the mass spectra.

In chapter 5 the analysis of aerosol particles containing bacteria is reported. This bacterial analysis was performed to investigate and demonstrate the suitability of the aerosol mass spectrometer for the on-line analysis of these bioaerosol particles. The identification of biological material in standard MALDI mass spectrometry is based on so-called biomarkers. In this chapter the possibility to use these biomarkers also in aerosol MALDI is discussed.

I am very thankful that I have been given the opportunity and possibilities to look a little deeper in the wonderful world named science. I hope that you, while reading this thesis, recognize the beauty of the world as well as the beauty of science. But that you also realize that even in this small niche of science a lot is known, but that there is even more unknown.

Ineke Kleefsman
Delft, September 2008

Chapter 1

Background Bacteria Concentrations - Can a Biological Attack be Measured and Recognized?

My child, I warn you to stay away from any teachings except these. There is no end to books, and too much study will wear you out.

(Ecclesiastes 12.12)

In this chapter an overview of performed measurements to determine atmospheric concentrations of bacteria is given. Studies reported in literature are evaluated, regarding the type of bacteria measured, the locations of the measurements, the instruments used and the concentrations found. A distinction is made between the culturable and the total bacterial concentrations. The influence of point and area sources of bacteria on the existing bioaerosol concentrations is investigated. Based on this evaluation design criteria for a sensing instrument defined by the National Research Council (NRC) of the United States are discussed.

This chapter will be submitted for publication to *Environmental Science and Technology*

1.1 Introduction

Atmospheric outdoor air contains aerosol particles of all sorts and sizes. The presence of aerosol particles becomes sometimes visible as smog, dust or haze [Friedlander, 2000]. The discoloring of the sky during sunrise and sunset can also be due to the presence of aerosol particles. After World War II and in particular in the 1970s and 1980s aerosol particles (air pollution) were associated with adverse health effects [Hinds, 1999] and from that time fundamental research into atmospheric aerosols started. One of the first systematic studies on the behavior of polluted atmospheres is the Los Angeles Smog Project, conducted in 1969 [Whitby et al., 1972].

A fraction of the atmospheric aerosol particles are biological aerosol particles. A primary biological aerosol particle is defined at the IGAP-workshop (International Global Aerosol Program) in Geneva (1993) as: ‘airborne solid particles (dead or alive) that are or were derived from living organisms, including microorganisms and fragments of all varieties of living things’ [Matthias-Maser and Jaenicke, 1995]. The microorganisms under consideration are viruses, bacteria, fungi, protozoa or algae. The atmospheric load of bioaerosols comes from many natural and anthropogenic sources and is highly variable.

Louis Pasteur was the first who demonstrated the presence of microorganisms in air samples in the middle of the nineteenth century. The first long term study on airborne microorganisms is reported by Miquel in 1883 [Lacey and West, 2006]. From that time on several studies have been carried out in the field of aerobiology, dealing with subjects as meteorological influences on bioaerosol concentrations and composition, dispersion models of bioaerosols, and bioaerosol concentrations and compositions in several environments like rural, urban, coastal, marine areas as well as high up in the sky: in the stratosphere and mesosphere.

Bioaerosol particles are not air pollutants, but should be considered as a factor affecting air quality [Mancinelli and Shulls, 1978]. The effect of bioaerosols on climate change, for instance, is studied by Kulmala et al. [2005] and Allan et al. [2006]. The bioaerosols that are considered in their research consist of organic molecules originating from trees. These molecules are nuclei for the formation of new particles [Kulmala et al., 2005, Allan et al., 2006].

Sometimes the effects of biological aerosol particles is seen far away from

1.1 Introduction

the source of the bioaerosols. Bovallius et al. [1978b] investigated the cause of the red snow observed in 1969 in Sweden. It was found that a sand storm near the Black Sea, was the cause of the colored snow. Together with the sand particles, also pollen originating from the Black Sea were identified in the snow samples, indicating that bioaerosol particles can be subject to long range transport [Bovallius et al., 1978b]. Bioaerosol particles not only affect air quality, they are also involved in the spread of diseases and epidemics. Inhalation experiments of Blackley in 1873 proved that fever was caused by airborne bioaerosols [Lacey and West, 2006]. Recent outbreaks and spreads of the foot-and-mouth disease are also due to bioaerosol particles, containing a virus.

Despite the high number of reported experimental studies, no good data are available on common values of bioaerosol concentrations. For instance, there is no definition of a background concentration. Despite the associated and demonstrated adverse health effects of bacterial aerosols, no definition of ‘bioaerosol toxicity’ exists. A possible reason for the lack on common values of bioaerosol concentrations might be that in the performed studies different samplers, very often impingers and cascade impactors, each with their own sampling efficiency and sampling size range were used. Therefore, comparison of experimental data of different studies has to be done carefully [Nevalainen et al., 1992]. The choice of sampler automatically determines the type of analysis, which is off-line for the above mentioned samplers. Very often the concentration of viable bacteria is determined only, therefore underestimating the real bioaerosol concentration [Lighthart, 1973, Wilson and Lindow, 1992, Tong and Lighthart, 1997, Lighthart, 1997, Tong and Lighthart, 1999]. Factors as solar radiation, unfavorable temperatures and the presence of chemical pollutants are lethal for bacterial survival [Mancinelli and Shulls, 1978, Di Giorgio et al., 1996, Tong et al., 1993, Tong and Lighthart, 1997]. In addition, the determination of the viable bacteria requires culturing of the bacterial aerosol particles. The species that are allowed to grow is dependent on the chosen growth medium. Pillai and Ricke [2002] and Lee et al. [2006a] recognize the problem that no guidelines exist for bioaerosol sampling and that no threshold values for microbial concentrations are defined. Thus few predictions regarding health risks associated with aerosolized pathogens can be made.

Bioaerosols are associated with adverse health effects and are therefore

used for biological warfare. Biological weapons include living organisms or their infective material (*e.g.* toxins) applied to cause a disease or death in humans, but also in animals or plants. The effect of biological weapons depends on the ability to multiply in the infected species. Early Persian, Greek and Latin literature already report examples of the negative effects on human health due to the presence of biological particles. Hippocrates described that men were attacked by epidemic fevers when they inhaled air infected with ‘such pollutions as are hostile to the human race’[Lacey and West, 2006].

The events 2001 in the United States, like the Anthrax letters and 9-11 raised a growing concern for biological attacks. As a result, the National Research Council (NRC) of the United States published a report in 2005 about (current) sensor systems and their applications to detect and to warn in case of a biological attack [National Research Council, 2005]. In the same report the Council defines as typical requirements for a ‘detection system to provide rapid warning’: the detection of a broad range of biological agents, a response time (including sample collection and preparation) approaching 1 minute and a very low false alarm rate (1 false alarm per 10^6 samples). The NRC foresees sensing instruments meeting the above-mentioned requirements within the next 5 to 10 years.

Any sensing system in this perspective has to deal with a background concentration of bioaerosols and should be able to recognize an elevated concentration of bioaerosols and/or an increase in the concentration of a certain (pathogenic) microorganism. In this chapter experimental data from a great number of experimental studies available in literature are compared to find an answer to the question if a biological attack can be measured and how this attack can be identified or classified. From the investigated data some background concentration ranges are derived. The effect of point and area sources, known to release bacteria into the atmosphere, on the background concentrations is investigated. These point and area sources are regarded to simulate a biological attack. The instruments used in the experimental studies are briefly discussed. From the (background) concentrations found and reported in this chapter, some design criteria are derived for a sensing instrument to provide rapid warning in case of a biological attack. Based on a discussion of these design criteria the aerosol MALDI mass spectrometer is proposed to be a sensing instrument that could meet the requirements of the NRC.

Table 1.1:
Experimental data for concentrations of airborne bacteria in urban areas

Average (geom) mean	Concentration (m^{-3})		Sample	Sampler	Reference	Source of bacteria
	lower limit	upper limit				
850	50	700	culturable bac- teria	impaction (by suc- tion) on filter	[Fulton and Mitchell, 1966]	
	706	1410	culturable bac- teria	Pady-Rittis slit sampler	[Pady and Kramer, 1967]	
	375	2490	culturable bac- teria	Anderson 6 stage cascade impactor	[Lee et al., 1973]	
	100	4000	culturable bac- teria	Anderson 6 stage cascade impactor	[Bovallius et al., 1978a]	
	13	1880	culturable bac- teria	impaction on filter -home made	[Mancinelli and Shulls, 1978]	
3400		culturable bac- teria	Anderson sampler	[Tong et al., 1993]		
791	193	1390	culturable bac- teria	Reuter Centrifug- al Air sampler	[Di Giorgio et al., 1996]	
609	539	688	culturable bac- teria	Anderson 6 stage cascade impactor	[Shaffer and Lighthart, 1997]	
	13	4300	culturable bac- teria	Anderson 6 stage cascade impactor	[Pastuszka et al., 2000]	
	3290	17,500	total bacteria	Hi-Vol sampler with PM10 inlet	[Harrison et al., 2005]	
	300	24,000	culturable bac- teria	impaction on a fil- ter	[Bauer et al., 2002]	wastewater treatment plant

1.2 Experimental

A literature search was performed for which experimental studies were selected that report measured *outdoor concentrations of airborne bacteria* at specified *locations*. Additional selection criteria were that the experimental results should be given in number concentrations and that the size range of interest covers the particles likely to contain bacterial cells (which is approximately all particles $> 0.5 \mu\text{m}$). The study by Bovallius et al. [1978a] was used as the starting study and by cross-references the rest of the articles were collected. Due to the great number of available studies, a selection was made, which has been tried to be a representative selection, but is certainly not complete. From all the selected articles

the following data were tabulated: location of sampling (city/urban, residential/suburban, rural or coastal/marine), the used sampler, the sample (viable or nonviable bacteria and if known the bacteria species) and the concentrations found. With respect to the concentrations the average, mean or geometric (geom) mean values were taken and/or a range was defined: the lower limit corresponding to the lowest concentration found in that study and the upper limit corresponding to the highest concentration in the same study. If necessary, the data were rounded off to 3 significant figures, an accuracy commensurate to this sort of measurements. The different durations of the sampling periods was neglected as well as the difference in sampling efficiency and the differences in measured particle size range¹.

Some of the selected articles describe the influence of a point source (waste water plants) or area source (application of pesticides on land or harvesting activities) on the bioaerosol concentration. These sources are regarded to simulate a biological attack. The concentrations found in these studies are compared to the other data, which are regarded as 'background' data.

1.3 Results and Discussion

The tables 1.1, 1.2, 1.3 and 1.5 show the reviewed experimental data organized for the type of sampling location and are presented in historical order. For each type of sampling location, except for the category city/urban (table 1.1), one or more studies with the influence of a point source or area source on the bacterial concentration was found. Wastewater treatment plants are suggested to have an unfavorable environmental impact [Brandi et al., 2000]. Therefore, data obtained by Bauer et al. [2002], who investigated the generation of bacterial aerosol from waste water treatment plants, were taken as a point source of bacteria for the city/urban location.² The type of point and area source per location are

¹As can be seen in section 1.3 these instrumental and experimental differences do not contribute to the observed variations, since the variation in the experimental data is high

²One might argue about the fact that a waste water treatment plant was chosen as a source of bacteria in the urban locations, since waste water treatment plants are

Table 1.2:

Experimental data for concentrations of airborne bacteria in suburban/residential areas

Average (geom) mean	Concentration (m^{-3})		Sample	Sampler	Reference	Source of bacteria
	lower limit	upper limit				
763	100	2500	culturable bacteria	Anderson 6 stage cascade impactor	[Bovallius et al., 1978a]	
	50	121	culturable bacteria	Anderson 2 stage	[Jones and Cookson, 1983]	
	65	270	culturable bacteria	Multistage impactor (Anderson)	[Fannin et al., 1985]	
$1.5 \cdot 10^6$			total bacteria	2 stage slit impactor and wing impactor	[Matthias-Maser and Jaenicke, 1994]	
$1.9 \cdot 10^6$			total bacteria	2 stage slit impactor and wing impactor	[Matthias-Maser and Jaenicke, 1995]	
	88	6630	culturable bacteria	Anderson sampler	[Zucker and Müller, 2004]	
	11.3	28.8	culturable <i>B. thuringiensis</i>	Anderson 6 stage cascade impactor	[Teschke et al., 2001]	
	0.4	7.9	culturable Gram negative bacteria	Anderson sampler	[Zucker and Müller, 2004]	
	6.6	98	culturable <i>Actinomycetes</i>	Personal sampler	[Lee et al., 2006b]	
	52	373	culturable bacteria	Multistage impactor (Anderson)	[Fannin et al., 1985]	wastewater treatment plant
	157	243	culturable <i>B. thuringiensis</i>	Anderson 6 stage cascade impactor	[Teschke et al., 2001]	aerial spraying

also listed in table 1.1, 1.2, 1.3 and 1.5.

1.3.1 The effect of sampling location on bacteria concentration

The data in table 1.1, 1.2, 1.3 and 1.5 are used to produce the graphs presented in the following. Figure 1.1 shows bacteria concentrations found by Bovallius et al. [1978a], Shaffer and Lighthart [1997] and Harrison et al.

usually located outside the cities.

Table 1.3:
Experimental data for concentrations of airborne bacteria in rural areas

Average (geom) mean	Concentration (m^{-3})		Sample	Sampler	Reference	Source of bacteria
	lower limit	upper limit				
99	150	1450	culturable bacteria	impaction (by suction) on filter	[Fulton and Mitchell, 1966]	
	2	3400	culturable bacteria	Anderson 6 stage cascade impactor	[Bovallius et al., 1978a]	
	237	5670	culturable bacteria	slit impactor	[Lighthart, 1984]	
	20	1200	culturable bacteria	Anderson 6 stage cascade impactor	[Lindemann and Upper, 1985]	
	32	165	culturable bacteria	slit impactor	[Lighthart and Shaffer, 1995]	
42	0	112	culturable bacteria	Reuter Centrifugal Air Sampler	[Di Giorgio et al., 1996]	242
202	290	culturable bacteria	Anderson 6 stage cascade impactor	[Shaffer and Lighthart, 1997]		
60	5000	culturable bacteria	Wet glass cyclone	[Tong and Lighthart, 1999]		
8000	$1 \cdot 10^5$	total bacteria	Wet glass cyclone	[Tong and Lighthart, 1999]		
$5.2 \cdot 10^5$	$5 \cdot 10^6$	total bacteria	2 stage slit impactor and wing impactor	[Matthias-Maser et al., 2000]		
236	224	248	culturable bacteria	Wet glass cyclone	[Tong and Lighthart, 2000]	104
98	110	culturable bacteria	Anderson 6 stage cascade impactor	[Tong and Lighthart, 2000]		
10,381	10,375	10,387	total bacteria	Wet glass cyclone	[Tong and Lighthart, 2000]	10,381
150	$8 \cdot 10^4$	culturable bacteria	Impinger SKC biosampler	[Brooks et al., 2005]		
4244	16,300	total bacteria	Hi-Vol sampler with PM10 inlet	[Harrison et al., 2005]		
1.5	56	culturable coliforms	Impinger SKC biosampler	[Tanner et al., 2005]		

Table 1.4:

Experimental data for concentrations of airborne bacteria in rural areas
- continued

Average (geom) mean	Concentration (m^{-3})		Sample	Sampler	Reference	Source of bacteria
	lower limit	upper limit				
	2150	18,500	culturable bac- teria	slit impactor	[Lighthart, 1984]	harvesting
$2.8 \cdot 10^6$			culturable bac- teria	Wet glass cyclone	[Tong and Lighthart, 1999]	grass har- vest
$9.6 \cdot 10^6$			total bacteria	Wet glass cyclone	[Tong and Lighthart, 1999]	grass har- vest
$1 \cdot 10^8$			culturable bac- teria	Impinger SKC biosampler	[Brooks et al., 2005]	land appli- cation of biosolids
	0.12	21	culturable <i>B.</i> <i>anthracis</i>	wet cyclone	[Turnbull et al., 1998]	dead car- casses
	$3.5 \cdot 10^5$	$1.4 \cdot 10^6$	culturable bac- teria	Personal sampler	[Lee et al., 2006a]	corn har- vesting
	$1.7 \cdot 10^4$	$2.6 \cdot 10^4$	culturable <i>Acti- nomycetes</i>	Personal sampler	[Lee et al., 2006a]	corn har- vesting
	$4.0 \cdot 10^4$	$7.5 \cdot 10^4$	culturable bac- teria	Personal sampler	[Lee et al., 2006a]	soy bean harvesting

[2005] who performed their experiments in urban, rural and coastal regions. Bovallius et al. [1978a] performed their experiments in Sweden with a 6-stage cascade impactor, Shaffer and Lighthart [1997] conducted their experiments in Oregon, USA, also with a 6-stage cascade impactor and Harrison et al. [2005] did experiments with a Hi-Vol sampler in the UK. Bovallius et al. [1978a] and Shaffer and Lighthart [1997] determined the concentration of viable bacteria, whereas Harrison et al. [2005] measured the total bacterial concentration. The total bacterial concentration includes both, viable and non-viable, bacteria.

As can be seen in figure 1.1, the total concentrations found (*i.e.* the data of Harrison et al. [2005]) are at least one order of magnitude higher than the culturable concentrations. This finding is in agreement with the work of Lighthart [1973], Wilson and Lindow [1992], Tong and Lighthart [1997], Lighthart [1997], Tong and Lighthart [1999]. When experimental data from different authors are compared it should be taken into account whether the target bacteria are viable or not. In this study the differences in the sampling devices are neglected, but even when the same sampler

Table 1.5:

Experimental data for concentrations of airborne bacteria in coastal/marine/desert areas

Average (geom) mean	Concentration (m^{-3})		Sample	Sampler	Reference	Source of bacteria
	lower limit	upper limit				
63 245 103	50	700	culturable bac- teria	impaction (by suc- tion) on filter	[Fulton and Mitchell, 1966]	
	0	560	culturable bac- teria	Anderson 6 stage cascade impactor	[Bovallius et al., 1978a]	
			culturable bac- teria	Anderson 6 stage cascade impactor	[Bovallius et al., 1978b]	
	91	116	culturable bac- teria	Anderson 6 stage cascade impactor	[Shaffer and Lighthart, 1997]	
	0	$1.5 \cdot 10^4$	total bacteria	single particle flu- orescence counter	[Seaver et al., 1999]	
	0	350	culturable bac- teria	impaction on filter	[Griffin et al., 2001]	
	$1.8 \cdot 10^4$	$1.6 \cdot 10^5$	total bacteria	impaction on filter	[Griffin et al., 2001]	
$1 \cdot 10^5$	2890	13,900	total bacteria	Hi-Vol sampler with PM10 inlet	[Harrison et al., 2005]	<i>Erwinia herbicola</i> release
			total bacteria	single particle flu- orescence counter	[Seaver et al., 1999]	
			total bacteria	single particle flu- orescence counter	[Seaver et al., 1999]	
$1.2 \cdot 10^4$			total bacteria	single particle flu- orescence counter	[Seaver et al., 1999]	<i>B. at- rophaeus</i> release

is used, rather big differences are found. For the experiments of Bovallius et al. [1978a] and Shaffer and Lighthart [1997], a 6-stage cascade impactor was used. The average concentrations found for the different locations match quite well for those two research groups. However, the data of Bovallius et al. [1978a] seems to fluctuate more than those of Shaffer and Lighthart [1997], as is indicated by the error bars. It should be noted that the larger fluctuation as observed by Bovallius et al. [1978a] could be due to the fact that for these data the upper and lower limit are presented, while for the data of Shaffer and Lighthart [1997] the upper and lower limit of the 95% confidence interval are used.

When the culturable bacterial concentrations at the different locations are compared, the same trend is found (figure 1.1). The bacterial concentration is the highest in urban regions, followed by rural regions and

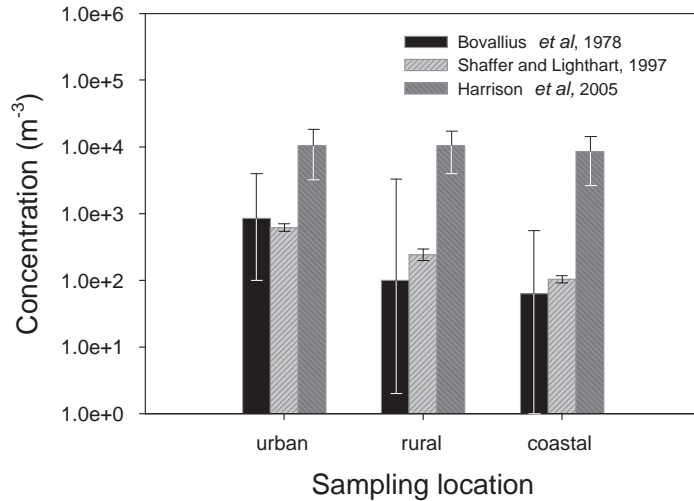


Figure 1.1:

Concentrations of airborne bacteria at urban, rural and coastal sampling locations. Data are after Bovallius et al. [1978a], Shaffer and Lighthart [1997] who determined the culturable bacteria concentrations and after Harrison et al. [2005] who measured the total bacteria concentration. The error bars represent the upper and lower limit of the measurements, the upper and lower limit of the 95% confidence interval and the standard deviations, respectively

the concentrations found at coastal sites is the lowest. A certain part of the 'air-mass' at a coastal site has been subject to long range transport. During this transport the airborne bacteria are exposed to UV-radiation and different temperatures, which is lethal for most of the bacteria and decreases the viable concentration. [Di Giorgio et al., 1996, Tong and Lighthart, 1997]. The high culturable concentrations found in urban regions are a result of human activities and traffic. Traffic causes turbulence resulting in resuspension of dust. [Di Giorgio et al., 1996, Bovallius et al., 1978a]. A source of bacteria in rural areas is the vegetation in those areas. Leaves of plants contain bacteria that are released into the air [Lighthart, 1984, Lindemann and Upper, 1985]. Harvesting activities also cause a

release of bacteria [Lighthart, 1984, Tong and Lighthart, 1999].

The total bacterial concentrations (data after Harrison et al. [2005]) are more constant over the different locations, indicating that despite the decrease in viability of the bacteria, the total bacterial concentrations do not seem to be affected by the sampling location.

1.3.2 Bacteria concentrations in urban areas

The data obtained for concentrations of bacteria at urban sampling locations are represented in a graphical way in figure 1.2. To obtain this graph, the data describing the ‘background’ concentration are treated separately from the data obtained from point and area sources. The data in the column ‘Average/(geometric) mean’ from table 1.1 is sorted from low to high. The same is done for the data in the columns ‘upper limit’ and ‘lower’ limit. This sorting of the data automatically implies that the concentration ranges are separated, meaning that the author who found the lowest lower limit is different from the one who found the lowest upper limit³. Since this evaluation intends to define a general bacterial ‘background’ concentration, the separation is justified. In addition the x-axis, which actually represents the experimental studies, is not defined. The Average/(geometric) mean values are plotted in such a way that they fall in between the upper and lower limits found. To avoid confusion, the data for the ‘background’ concentrations are plotted on the left part of the graph and the concentrations at point or area sources are placed on the right side of the graph.

In figure 1.2 it can be seen that the concentration of culturable bacteria ranges from approximately $1 \cdot 10^1$ to $4 \cdot 10^3$ *cfu/m*³ (*cfu* = colony forming unit). The total bacterial concentration ranges from $3 \cdot 10^3$ to $1.7 \cdot 10^4$ bacteria per *m*³. These values are one order of magnitude higher than the culturable concentration and are similar to the earlier found result (see figure 1.1).

Since the data compared are taken at different times and time intervals, it is worth to note that Pady and Kramer [1967] and Shaffer and Lighthart [1997] found a diurnal variation with high concentrations in the morning

³For example: for the urban location Mancinelli and Shulls [1978] and Pastuszka et al. [2000] found the lowest lower limit and the lowest upper limit was obtained by Shaffer and Lighthart [1997].

and evening, while Di Giorgio et al. [1996] report that the time of sampling did not affect the bacterial concentration. This difference is probably caused by the fact that Di Giorgio et al. [1996] measured the diurnal variation on different times on successive days, while Pady and Kramer [1967] and Shaffer and Lighthart [1997] determined the diurnal variation at different times on the same day. The method used by Pady and Kramer [1967] and Shaffer and Lighthart [1997] is better, since the day-to-day variation is excluded.

Seasonal variations are found, with the highest concentrations in summer and fall and the lowest concentrations are found in winter [Bovallius et al., 1978a, Matthias-Maser et al., 1995, Di Giorgio et al., 1996, Pastuszka et al., 2000], whereby Matthias-Maser et al. [1995] only found the seasonal variation for the bigger ($d_p > 0.4 \mu\text{m}$) particles, which are the particles likely to contain the bacteria.

The culturable concentration found by Bauer et al. [2002] at a point source (wastewater treatment plant) varies from $1 \cdot 10^2$ to $2.4 \cdot 10^4 \text{ cfu}/\text{m}^3$. Although the upper limit is above the ‘background’ concentration, most of the values found by Bauer et al. [2002] fall within in the background range. Thus, a detection of such a point source of bacterial aerosol particles, based on an increase in concentration, seems to be impossible in urban areas.

1.3.3 Bacteria concentrations in residential areas

The obtained data for concentrations of bacteria at suburban and residential sampling locations are represented in a graphical way in figure 1.3, in a similar way as done for the urban location. The culturable concentration for this type of sampling location varies from approximately $5 \cdot 10^1$ to $6.6 \cdot 10^3 \text{ cfu}/\text{m}^3$. This range is comparable to the concentration range at urban sites. The values for the (mean) total concentration is $1.5 \cdot 10^6$ and $1.9 \cdot 10^6 \text{ bacteria}/\text{m}^3$ which is three orders of magnitudes higher than the culturable concentration.

Jones and Cookson [1983] investigated the diurnal and seasonal effects on the concentration in a typical suburban area. No effect of the time of the day on the concentration was found. Jones and Cookson [1983] determined the diurnal variation on several days, as Di Giorgio et al. [1996] did for the urban locations, thereby including the day-to-day variation. The time of the year was an important determinant of viable particle

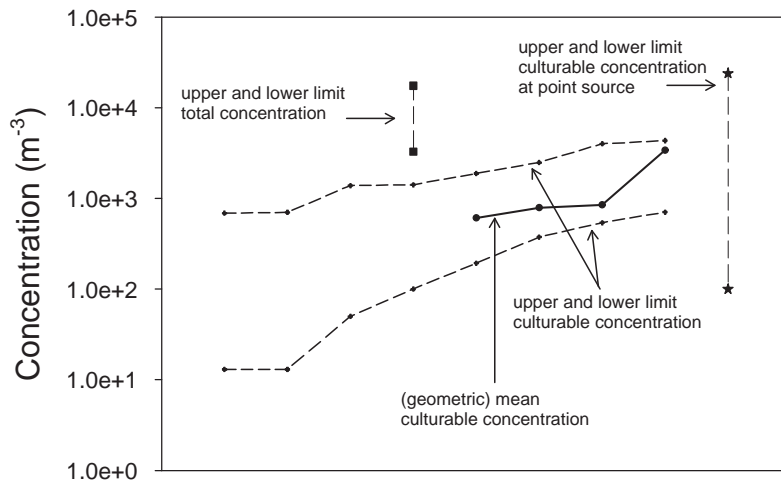


Figure 1.2:
Culturable and total concentrations of airborne bacteria at urban sites

concentrations. Comparable to the urban sites, the highest concentrations were found in summer and fall and the lowest concentration in winter [Jones and Cookson, 1983].

Teschke et al. [2001], Zucker and Müller [2004] and Lee et al. [2006b] determined the culturable concentrations in suburban regions of *Bacillus thuringiensis*, Gram negative bacteria and *Actinomyces* (a Gram positive bacteria, ubiquitous in soil) respectively. Logically, these concentrations are lower than the total concentrations. When the found concentrations for these bacteria species are summed, simulating a 'real air mass composition' the concentration range falls within the background range. This indicates that non-selective instruments (*i.e.* instruments in which the total culturable fraction is determined) do not underestimate the 'real' culturable concentration.

A point source (wastewater treatment plant) for the release of bacteria in a residential neighborhood is reported by Fannin et al. [1985]. The culturable concentration range is $5 \cdot 10^1$ to $4 \cdot 10^2$ *cfu/m^3* and falls within the 'background' concentration. The influence of an area source of bac-

terial particles is studied by Teschke et al. [2001], who investigated the influence of aerial spraying for the eradication of the gypsy moth. For the eradication the biological pesticide *Bacillus thuringiensis* was used and the concentration of this species was monitored. The culturable concentration of this specific species was found to be ranging from $1.6 \cdot 10^2$ to $2.4 \cdot 10^2$ *cfu/m³*, also falling within the ‘background’ concentration. The concentrations were measured within the spraying zone and the presented values are the highest values, which are found 2-3 hours after aerial spraying. It can be concluded that detection of a point of area source of bacterial particles in residential areas is not possible based on an increase in concentration. The values found by Teschke et al. [2001] for one specific bacterial species originating from an area source are similar to the total culturable concentrations from the point source of Fannin et al. [1985]. This example illustrates the influence of the type of source (point or area source) on the concentration. From a waste water treatment plant, several bacteria species are passively released into the air, while with active, aerial spraying usually only one type of bacteria is aerosolized. In the first case the bacterial concentration will only be increased over a certain (small) distance from the source and in the case of an area source an increase in bacterial concentration will be found over a much bigger area.

1.3.4 Bacteria concentrations in rural areas

Figure 1.4 shows the concentrations of bacteria at rural sites. The culturable concentration for these sampling locations ranges from approximately 0 to $8 \cdot 10^5$ *cfu/m³*⁴. The variation is much higher than found for the (sub)urban sampling locations. The concentration range, as reported by Tanner et al. [2005] for a class of bacteria, the coliforms, is within the concentration range for the culturable fraction of the bioaerosols. For the total bacteria concentration also a wide range is found, varying from $4.2 \cdot 10^3$ to $5.0 \cdot 10^6$ bacteria per *m³*.

Daily variations in the viable particle concentration at rural sites were observed by Lindemann and Upper [1985], Lighthart and Shaffer [1995] and Tong and Lighthart [1999], with a low concentration at dawn, grad-

⁴In figure 1.4 and figure 1.5 the value 0 is not plotted, because of the logarithmic scale of these graphs

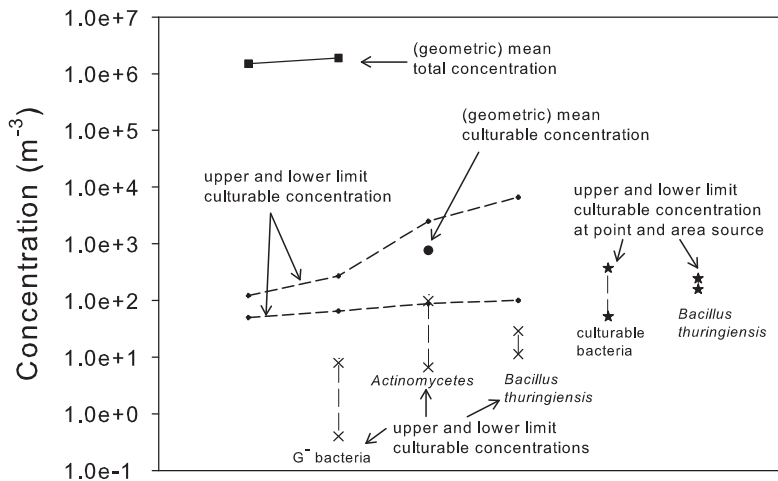


Figure 1.3:
Culturable and total concentrations of airborne bacteria at suburban sites

ually increasing at sunrise and reaching a maximum in the late afternoon. The peak in the afternoon is explained by convective warming and increased winds that would entrain plant debris and soil particles with attached microbes into the atmosphere [Lighthart and Mohr, 1994].

Seasonal variations in the microbial concentrations are found by Bovallius et al. [1978a], Di Giorgio et al. [1996], Tong and Lighthart [2000] and Harrison et al. [2005] in contrary to Fulton and Mitchell [1966] and Matthias-Maser et al. [2000], who did not find a seasonal variation. In the studies in which a seasonal trend was observed, the highest concentrations were found in summer and the lowest concentrations in winter. The summer maximum might be due to the large local sources of dense plant population (with a large surface area for bacteria), harvesting activities and dry and dusty soil conditions, which can be subject to vertical air fluxes created by solar heating of the ground that transports the released bacteria into the atmosphere.

The study carried out by Harrison et al. [2005] included some identi-

1.3 Results and Discussion

fication of the bacterial aerosol particles. While the total concentration shows seasonal dependency, some of the different species do not follow this general trend. The concentration of *Bacillus* was found to be high in summer and winter and the highest concentrations for *Pseudomonas* were found in winter and spring [Harrison et al., 2005]. A possible explanation for the high concentrations of *Bacillus* in summer is the resistance for UV-radiation of *Bacillus* spores, assuming that the *Bacillus* is cultured from spores rather than from vegetative cells. Other, non-sporulating bacteria are more sensitive for UV-radiation [Tong and Lighthart, 1997]. The high concentration in winter for *Bacillus* can also be explained by the sporulation of this bacterial species. The thick spore wall and the presence of the so-called SASP's (Small Acid Soluble Proteins) protect the core of the spore against temperature effects [Setlow, 2007].

As stated above, Matthias-Maser et al. [2000] did not find any significant seasonal influence on the *number* concentration of bioaerosols. However, the *volume* concentration was affected by the seasons, with the highest values in spring and summer. This means that the distribution has changed such that by equal numbers of aerosol particles the mean size has increased. Matthias-Maser et al. [2000] identified the bigger particles in spring and summer as pollen and spores. Also Tong and Lighthart [2000] observed seasonal influence on the particle size. The particle diameter in summer was much higher than in autumn and winter. A possible reason for the bigger diameter in summer is that in summer multiple culturable bacteria are released as aggregates and that in autumn and winter the aerosol consists of single culturable bacteria.

Point and area sources in rural areas include animal confinements [Lee et al., 2006a], land applications of biological pesticides and harvesting activities. In the right part of figure 1.4 the concentrations found at such point and area sources are presented. The culturable concentrations range from $2 \cdot 10^3$ to $1 \cdot 10^8$ *cfu/m*³, partly overlapping the 'background' concentrations. Confusingly, the mean culturable values that are found are 2 to 3 orders of magnitudes higher than the lower and upper limits found. For the total microbial concentration a value of $1 \cdot 10^7$ per *m*³ is found, which is strikingly lower than the mean culturable concentration. The 'background data' (presented in the left part of figure 1.4) also shows this overlap between culturable and total concentration. The concentration of *Bacillus anthracis* originating from dead carcasses (point source) is stud-

ied by Turnbull et al. [1998] and has a value of $1.2 \cdot 10^{-1}$ to $2.1 \cdot 10^1 \text{ cfu}/\text{m}^3$. The concentrations were measured to a maximum of 18 meters downwind the source. Much higher concentrations, $1.7 \cdot 10^4$ to $2.6 \cdot 10^4$ are found for culturable *Actinomyces* by Lee et al. [2006a], due to soy bean harvesting (area source). The measurements by Lee et al. [2006a] were performed on top of the combine that performed the soy bean harvesting. Again can be concluded that the effect of a point source on the bacterial concentration is almost negligible, while an area source has a much larger effect. In addition, when measurements are performed around a point source, the effect of distance from the source on the concentration should be taken into account.

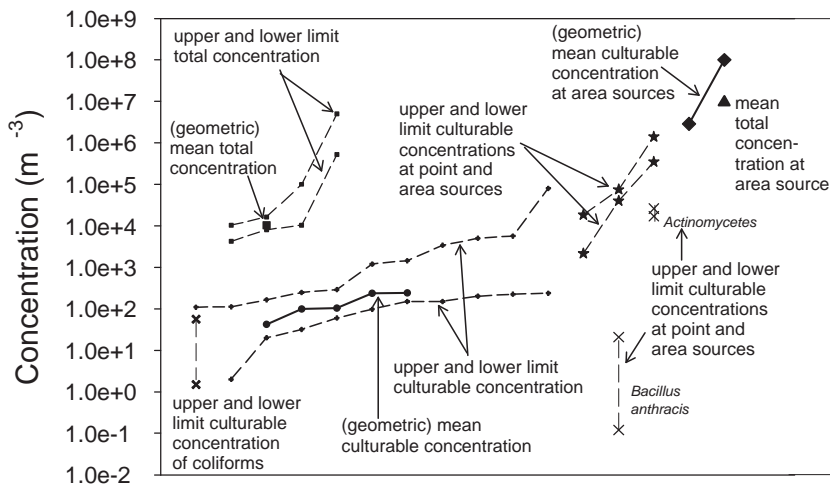


Figure 1.4:
Culturable and total concentrations of airborne bacteria at rural sampling locations

1.3.5 Bacteria concentrations at coastal sites

Figure 1.5 shows the concentrations of bacteria at coastal sites. The culturable concentration for these areas ranges from approximately 0 to 7

1.3 Results and Discussion

10^2 cfu/m³. The total bacteria concentration varies from 0 to $1.6 \cdot 10^5$ bacteria per m³.

Harrison et al. [2005] investigated the composition of marine influenced air masses and found greater diversity of bacteria than in air masses that were transported over land. The bacteria found at the coastal sampling locations might have been subject to long-range transport and might originate from terrestrial sources and released into the atmosphere by dust storms [Bovallius et al., 1978b, Harrison et al., 2005]. Seaver et al. [1999] investigated the bacterial concentration after a release of *Erwinia herbicola* and after a release of *Bacillus atrophaeus* spores with their single particle fluorescence counter. After the bacterial releases Seaver et al. [1999] observed an increase in the concentration of bioaerosols, even 800 m downwind of the source. Although an increase in concentration was observed by their specific instrument, the values found are in the range of the background concentration, as can be seen in figure 1.5. Also for the coastal sampling site is demonstrated that detection of a point of area source (of a specific type of bacteria) is not possible based on an increase in (total) concentration. One remark has to be made: the measurements by Seaver et al. [1999] were done in the desert, under conditions with low particle concentrations. In this work the desert measurements are included in the coastal sampling locations, since the values of the concentrations are similar.

1.3.6 A comparison of the found background concentrations

If the ‘background’ concentration ranges for the different sampling locations are compared the widest concentration range for the culturable bacteria is observed at the rural sampling locations, followed by the urban and residential locations. The culturable concentration range at the coastal site is the smallest. The concentration range is defined as the difference between the highest and lowest concentration found; the highest number resembles the widest range. Comparing the total bioaerosol concentration ranges for the different sampling locations, the widest range is also observed at the rural sampling locations, followed by the coastal sites and the smallest variation is observed in the cities. Note that for

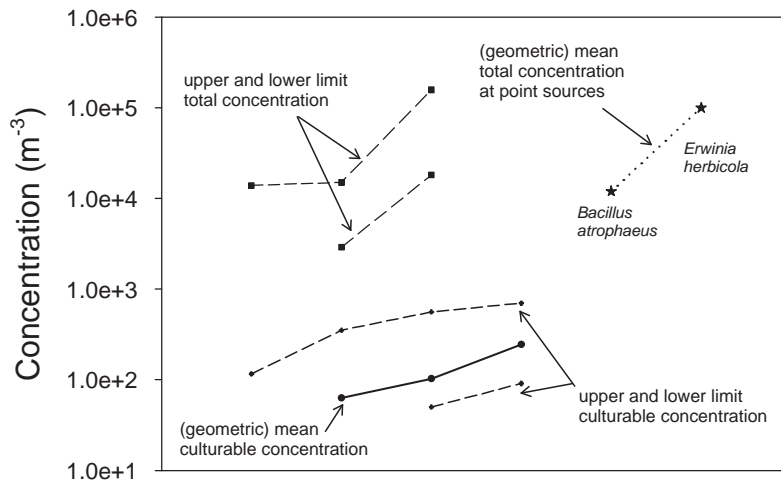


Figure 1.5:
Culturable and total concentrations of airborne bacteria at coastal sampling locations

the suburban locations only one mean value was found, and therefore is neglected in the above ranking of the sampling locations.

From figure 1.1 it was derived that the highest culturable concentrations were found in cities. The difference of this evaluation compared to figure 1.1 can be explained by the fact that the data used for figure 1.1 are only from two authors: Bovallius et al. [1978a] and Shaffer and Lighthart [1997], while the data in this evaluation are from much more authors and represent an average of more studies, which is likely to approach the 'real' bacterial concentration values better. Comparison of the 'absolute' total bacteria concentrations per sampling location results in the following order: rural ($5 \cdot 10^6$), coastal ($1.6 \cdot 10^5$) and urban ($1.7 \cdot 10^4$). The data of Harrison et al. [2005] represented in figure 1.1 indicated that there was no effect of the sampling location on the total microbial concentration. This finding is contradicted by the above mentioned 'absolute' values of the total concentration. Again, the data in figure 1.1 are from one author and

the obtained ‘absolute’ values represent an average of more studies. The variability in absolute bacteria concentrations and concentration ranges per sampling location complicates the definition of a bacteria ‘background’ concentration.

1.4 Bioaerosol sampling instrumentation

The evaluated experimental studies are performed with several instruments. In the foregoing the only distinction that is made for the instruments, is viable versus non-viable sampling. Other instrumental factors as sampling efficiency and the particle size range, as well as the principles of operation are neglected in the evaluation, but are briefly discussed here.

Most of the samplers evaluated in this study are based on the impaction principle (the cascade impactor, the wing impactor and a slit impactor). Impaction is used to separate a particle from the gas stream based on the inertia of the particle. Another bioaerosol sampling method is filtration, in which the particles are collected on a filter medium, which is adapted for the subsequent analysis method. Bioaerosol sampling can also be done with an impinger, whereby the particles are collected in a liquid medium which is subsequently used for further analysis [Lighthart and Mohr, 1994]. Principally impinging also relies on impaction.

Except for multistage cascade impactors and filtration, the above mentioned samplers do not provide information on the particle size. The design of the instrument determines the ‘cut-off’ size and therefore the size range of the sampled particles is also determined. The particle size can provide additional information regarding the composition of the bacterial particles as is shown by Matthias-Maser et al. [2000] and Tong and Lighthart [2000]. The sampling efficiency of the bioaerosol samplers, defined as ratio of the measured concentration to the real concentration, also depends on the design of the instrument and on the way the samplers are operated. Design parameters include the flow rate as well as the sizes of inlet and nozzles etc. The operating parameters include the position of the instrument: facing upwind or downwind, the sampling height, etc.

An advantage of the biosamplers utilizing impaction, filtration and impingement is that the instrument can be adapted for the target bacteria, by choosing a suitable culture medium or the right subsequent analysis.

Since fungal spores are also in the air, usually a growth medium is chosen that does not allow culturing of these fungal spores. An example of the right subsequent analysis is staining, which is usually performed on a gel that contains a dye. The gel is subsequently analyzed by a microscope for instance. A disadvantage of these instruments is that the samplers are not capable of on-line analysis. Instruments capable of on-line bioaerosol analysis are described by Seaver et al. [1999], Pinnick et al. [1995] and Pan et al. [2003]. These instruments utilize the fluorescing properties of biological aerosol particles. The aerosol particles are irradiated with UV-light and the emitted fluorescence is recorded. In chapter 3 the principle of fluorescence preselection, here used as a preselection method, is discussed in more detail. Since all types of biological particles emit fluorescent light under UV-irradiation, the total bioaerosol concentration is determined and specific species can not be detected.

1.5 Design criteria for sensing instruments

The criteria defined in the report of the National Research Council of the United States for detection systems to provide rapid warning in case of a biological attack are focused on the capabilities of the instruments. They are: detection of a broad range of biological agents, a small response time and a very low false alarm rate [National Research Council, 2005]. Although the NRC recommends that studies need to be conducted evaluating concentrations of bacterial aerosols and their variability on relevant time scales, no requirements are defined for the absolute values of concentrations the sensing system should be able to measure.

As is shown in this work the atmospheric bacteria concentrations are highly variable per sampling location as well as within one sampling location. This requires an instrument that can handle the absolute values and concentration ranges as reported in the tables 1.1, 1.2, 1.3 and 1.5. As an illustration, the concentrations found at the rural locations are highly variable and have a high ‘absolute’ concentration. Factors as time of the day, the season, the presence of harvesting activities are the cause of the high and variable rural concentration.

As is correctly mentioned by the NRC, the sensing system should have identification or classification capabilities, since a detected increase in bac-

teria concentration, does not automatically imply an attack. For instance, *Bacillus thuringiensis* is used as an insecticide for crops but is closely related to *Bacillus anthracis*, the cause of the infectious disease anthrax. Another requirement for a sensing system is the possibility to measure and classify the total range of bioaerosol particles, since the non-bacteria particles, as viruses, toxins, or pollen, can also be used in a biological attack.

Based on the performed evaluation it is suggested to add two more aspects to the design criteria of the NRC. A sensing instrument should be able to measure (high) absolute concentrations as well as wide concentration ranges. In addition, the instrument should be capable of identification (or classification) of the whole range of bioaerosol particles.

If the above mentioned requirements are taken into account, the aerosol MALDI mass spectrometer, as developed at Delft University of Technology and described in this work could fulfil most of the requirements for a sensing system capable of rapid warning. With the aerosol MALDI mass spectrometer the *total* bioaerosol concentration out of any atmospheric aerosol can be measured, utilizing fluorescence preselection, which is described in chapter 3. For the analysis of the bioaerosols MALDI mass spectrometry is used. This technique is described in chapter 4. The analysis of known bacterial aerosol samples is described in chapter 5. MALDI mass spectrometry is a method that allows identification of a sample. The particle sizes and concentrations of the aerosol particles can be determined by aerodynamic sizing (described in chapter 2). A foreseen limiting factor will be very high (absolute) particle concentrations, since the detection and classification of a single particle requires a time of 200-300 μs in the mass spectrometer. The total response time, including sample preparation (which is most time consuming), of the aerosol MALDI mass spectrometer is 1 minute, which is according to the requirements of the NRC.

1.6 Conclusions

A number of experimental studies on the determination of the concentration of bacteria particles in the atmosphere is evaluated. In this evaluation, different instruments were used and the different sampling efficiencies of those instruments is neglected, together with the different (optimal) par-

ticle size range of the instruments. Also the particle size, the diurnal and seasonal effects on the concentration were neglected.

A distinction between the culturable concentration and the total concentration of aerosolized bacteria is made. The culturable concentration is only a very small fraction of the total microbial concentration and therefore underestimates the real bacterial concentration. If the effects of airborne bacteria on human health are the goal of an experimental study, the total concentration of bioaerosols is the right parameter to look at, since non-culturable bioaerosol particles may also have adverse health effects.

The sampling location (urban, suburban, rural or coastal) is a determining factor for the viable concentrations of bacteria measured as well as for the concentration range that is covered. The concentration values obtained are highly variable. This variability complicates comparison of the experimental studies as well as the definition of a biological 'background' concentration. Some of the evaluated experimental studies considered the effect of a point or area source on bacterial concentrations. The evaluated point and area sources were often not detectable by an increased concentration. Thus, it is not possible to detect a biological attack based on an increase or change in concentration. Therefore, identification of the aerosol particles is required.

Based on this evaluation is suggested to extend the design criteria defined by the NRC for detection systems to provide rapid warning in case of a biological attack with two more criteria. Sensing instruments should be able to measure high absolute concentrations as well as wide concentration ranges, and the instruments should have the capability to measure and identify the total range of bioaerosol particles.

Based on this evaluation, the question if a biological attack can be measured, recognized and identified, is answered negatively, for the time being. With the currently available instruments it is impossible to measure and identify a biological attack within a short time range. On-line measuring techniques are required to meet the design criteria as defined by the NRC.

Chapter 2

Instrumental Improvements for Bioaerosol Mass Spectrometry

Showing respect to the Lord will make
you wise, and being humble will bring
honor to you

(Proverbs 15.33)

This chapter starts with the history and the previous improvements of the aerosol mass spectrometer. Then the newly implemented improvements and principles to make the instrument suitable for bioaerosol analysis are given, including a description of the current aerosol mass spectrometer. Analysis with protein containing aerosols is performed to show the effect of the improvements. Some attention is paid to the aerosol generation (particle size range and concentration) to be able to generate bioaerosol particles with typical sizes and concentrations in a controllable way. The chapter ends with a discussion about the suitability of IR-MALDI mass spectrometry for the aerosol mass spectrometer.

Parts of this chapter are submitted for publication in *KONA Powder and Particle* number 26 in 2008.

2.1 Introduction

In 1988 Marijnissen et al. [1988] proposed an instrument for on-line aerosol analysis in which size determination, laser-induced fragmentation and time-of-flight mass spectroscopy were combined. In that decade the chemical analysis of single particles just gained interest [Noble and Prather, 2000]. For instance, an experimental instrument for the chemical analysis of single particles based on vaporization of the particles and subsequent analysis of the fragments by mass spectrometry had been reported [Sinha et al., 1982, Sinha, 1984, Sinha et al., 1984]. The novelty in the proposed apparatus of Marijnissen et al. [1988] was the combination of particle sizing and laser fragmentation for *Time-of-Flight* mass spectrometry. A schematic diagram of the instrument of Marijnissen et al. [1988] is given in figure 2.1

Throughout the following years a substantial amount of work and research has been carried out to achieve the current performance of the aerosol mass spectrometer. The current aerosol mass spectrometer can be divided into three sections: the aerosol beam generator, the particle sizing and detection section and the mass spectrometer. For on-line analysis a fourth section can be distinguished: sample preparation, which is located before the aerosol beam generator.

In this chapter an overview of previous improvements of the mass spectrometer, improvements implemented in this work and a description of the current instrument are given. Another part of this chapter describes the aerosol generation, which is improved for bioaerosol analysis. Finally, the suitability of IR-MALDI is discussed. The implemented improvements are all based on the application or applicability for bioaerosol analysis.

2.2 Previous improvements on the aerosol mass spectrometer

Kievit [Kievit, 1995, Kievit et al., 1996] investigated particle introduction into the instrument and designed and characterized the aerosol beam generator. The aerosol beam generator is the interface which transports the aerosol particles from atmospheric pressure to the working pressure (10^{-6} mbar) of the mass spectrometer. The particle beam is formed when the

2.2 Previous improvements on the aerosol mass spectrometer

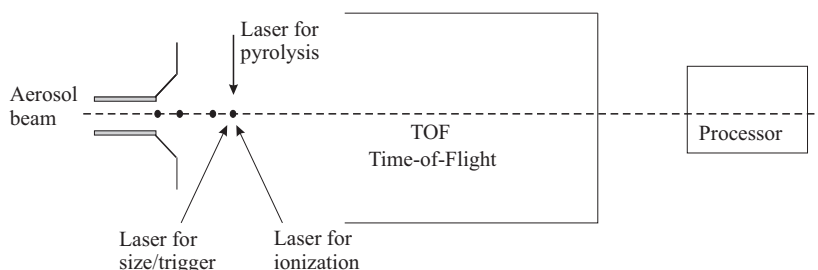


Figure 2.1:

Schematic drawing of the instrument for on-line aerosol analysis as proposed by Marijnissen et al. [1988]

aerosol is expanded into a space with lower pressure through a critical orifice. If the pressure ratio across the orifice is smaller than 0.5 the gas reaches supersonic velocity. The difference in inertia of the particles and the gas molecules causes the actual formation of the beam, since the particles cannot follow the gas stream lines and move straight reaching the size dependent terminal velocity. Once captured in the beam, the aerosol particles can be transported to the analysis section: into the ion source of the mass spectrometer. The final configuration was a three-stage vacuum system to generate an aerosol beam with low divergence and high transmittance. A schematic diagram of the aerosol beam generator according to the design of Kievit is given in figure 2.2a.

Weiss [Weiss et al., 1997, Weiss, 1997] described the aerodynamic sizing principle for the instrument, which was installed by late Dr. Grootveld. The aerodynamic sizing principle was adapted from Prather et al. [1994] who were the first implementing such a sizing system in an aerosol mass spectrometer. Earlier attempts to relate scatter intensity to particle size by Kievit [Kievit, 1995, Kievit et al., 1996] were not successful as the size measurements were not precise. Aerodynamic sizing relies on the particle-size-dependent velocity, after passing the aerosol beam generator. Aerodynamic sizing was implemented by adding a beam displacement prism in the optical system, which is still present in the current optical system as can be seen in figure 2.7. Besides aerodynamic sizing, Weiss [1997] replaced the flash lamp pumped Nd:YAG laser for an Excimer laser. Excimer lasers can be triggered much faster due to the shorter delay time

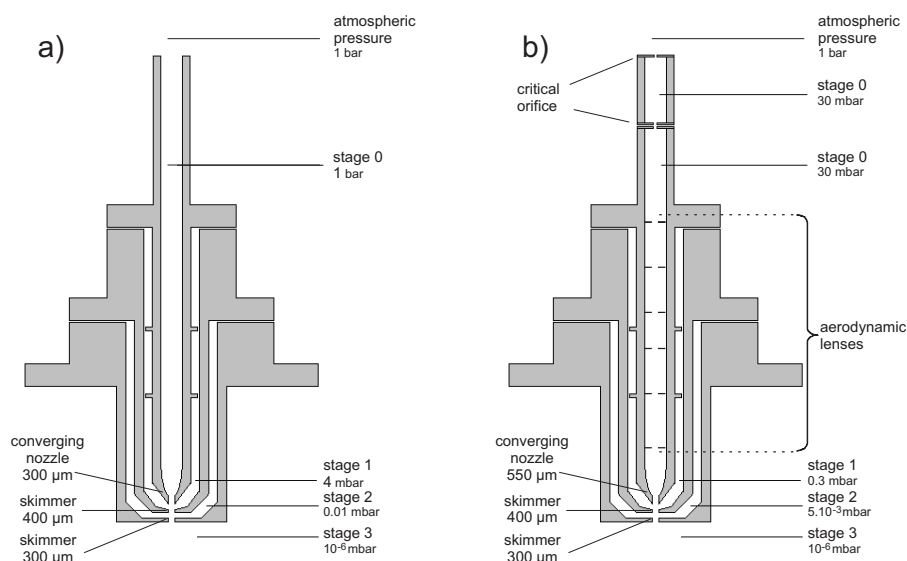


Figure 2.2:

Configurations of the aerosol beam generator according to a) the design of Kievit [Kievit, 1995, Kievit et al., 1996] and b) to the (current) design of Van Wuijckhuijse [2003]. (not to scale)

between trigger input and radiation output and are therefore better suited for this application. In addition with an Excimer laser multiple wavelengths can be applied. Weiss [1997] also implemented a new triggering circuit for fast triggering, based on the design of Nordmeyer and Prather [1994], who were the first to implement such a triggering circuitry in an aerosol mass spectrometer. Software to acquire and process the data from the oscilloscope was also developed by Weiss [1997].

Kievit [Kievit, 1995, Kievit et al., 1996] and Weiss [Weiss et al., 1997, Weiss, 1997] did mass spectrometric analysis on aerosol particles consisting for instance of sodium chloride, potassium chloride, ammonium sulfate, ascorbic acid, polystyrene latex, anthracene, uranium oxide, cerium oxide, soot, and on more complex molecules like cannabis and the protein gramicidin S.

Weiss [1997] already suggested the mass spectrometric method MALDI (matrix-assisted laser desorption/-ionization) as an option to extend the

2.2 Previous improvements on the aerosol mass spectrometer

mass range of the aerosol mass spectrometer. A detailed description of the MALDI technique can be found in chapter 4. MALDI mass spectrometry allows the ionization of high molecular mass molecules and is widely used for the analysis of more complex molecules, even for the analysis of whole bacteria cells and cell extracts [Lay, 2001, Fenselau and Demirev, 2001, van Baar, 2001]. The relatively high laser power applied in laser desorption/ionization (LDI) (which was used by Kievit [Kievit, 1995, Kievit et al., 1996] and Weiss [Weiss et al., 1997, Weiss, 1997]) results in the break-up of these high molecular weight molecules [Posthumus et al., 1978]. MALDI superseded LDI and accomplishes a softer ionization [Karas and Hillenkamp, 1988], due to the presence of a matrix compound. The matrix compound absorbs the ionizing laser light and subsequently causes ionization of intact high mass molecules. Stowers et al. [2000] extended the aerosol mass spectrometer with a flow cell to condense a matrix material onto the aerosol particles to allow MALDI mass spectrometry. With the implementation of MALDI mass spectrometry Stowers et al. [2000] were able to detect a surface protein of *Bacillus atrophaeus*, from an aerosol containing this bacterium.

The work done by Van Wuijckhuijse [2003], included further optimization of the aerosol beam generator. Another critical orifice and pumping stage were added on top of the aerosol beam generator as designed by Kievit [1995]. A schematic diagram of the aerosol beam generator according to the design of van Wuijckhuijse is given in figure 2.2b. As can be seen in figure 2.2b the pressure distribution of both designs is different. Lower pressure in stage 0 of the design of Van Wuijckhuijse allowed implementation of aerodynamic lenses to increase sampling efficiency. With aerodynamic lenses, the particle beam width at the ionization spot was reduced from 606 μm to 74 μm for 0.99 μm glass spheres. Besides modification of the aerosol beam generator, Van Wuijckhuijse [2003] and Stowers et al. [2006] also implemented particle selection by fluorescence. This particle selection process is described in detail in chapter 3. All mass spectrometric analysis performed by Van Wuijckhuijse [2003] was MALDI mass spectrometry, and included the analysis of protein aerosol particles like gramicidin S, insulin, cytochrome C and myoglobin. Also aerosol particles consisting of vegetative cells of the bacteria *Escherichia coli*, *Erwinia herbicola* and of spores of *Bacillus atrophaeus*, premixed with a MALDI matrix, were analyzed. On-line analysis, whereby aerosol parti-

cles of *Bacillus atrophaeus* were coated with the matrix picolinic acid was also performed, as is reported by Stowers et al. [2000]. The mass spectra obtained by van Wuijckhuijse [Van Wuijckhuijse, 2003, Van Wuijckhuijse et al., 2005] covered a mass range up to 20,000 Dalton and were of reasonable quality. This was achieved by optimizing the system for quality, by the implementation of a high voltage ion source, ion focusing by means of an Einzel lens (to focus the ions) and by implementing deflection plates.

2.3 Latest improvements of the aerosol mass spectrometer

In the present work, the improvement and optimization of the aerosol mass spectrometer for bioaerosol analysis continued. The latest improvements of the aerosol mass spectrometer conducted in this work are implementation of a new high-voltage ion source, delayed extraction and the possibility to monitor the alignment of the particle beam and laser beams. In the following, each novelty is explained in detail.

2.3.1 New high voltage ion source

After successful detection, fragmentation and ionization of an aerosol particle, the ions formed are accelerated in the ion source toward the detector plate at the end of the flight tube. The ions reach the detector with mass and charge dependent arrival times. This is referred to as Time-of-Flight mass spectrometry. A Time-of-Flight mass spectrometer consists of a source-extraction region, a drift region and a detector (see figure 2.4). In the source extraction region the ions formed are accelerated to the same final kinetic energy:

$$\frac{1}{2}mv^2 = eV \quad (2.1)$$

where m is the mass of the ions (kg), v the velocity of the ions (m/s), e the elementary charge ($1.6 \cdot 10^{-19} C$) and V the acceleration voltage. There is no electrical field in the drift region and the ions formed cross the drift region with a velocity proportional to the square root of the mass of the

2.3 Latest improvements of the aerosol mass spectrometer

ions,

$$v = \sqrt{\frac{2eV}{m}}. \quad (2.2)$$

The flight time (t) of the ions through the drift region of length L is then:

$$t = \sqrt{\frac{m}{2eV}}L. \quad (2.3)$$

Ions of high molecular mass will have a lower velocity (equation 2.2) and a longer flight time (equation 2.3) than low mass ions. The ions with sufficient velocity will have a detectable impact on the detector plate and can be recorded by a digital oscilloscope, for instance [Cotter, 1997]. The detector in the aerosol mass spectrometer is a microchannel plate (MCP) detector. It consists of two microchannel plates and an anode mounted in a chevron configuration as is shown in figure 2.3. The microchannels

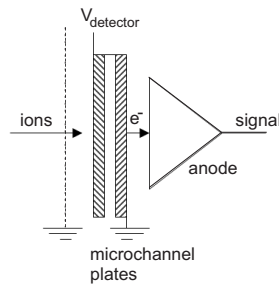


Figure 2.3: Schematic drawing of a microchannel plate detector

are angled with respect to the surface of the plate. The two microchannel plates are positioned in such a way that the angled channels are rotated 180° from each other producing a v-like shape. Each microchannel is a continuous-dynode electron multiplier, in which the multiplication takes place under the presence of a strong electric field. When an ion impacts and enters a channel, it hits the wall of the channel due to the angle of the channel. The ion impact starts a cascade of electrons that propagate through the channel, amplifying the original signal. In a chevron-MCP the electrons that exit the first plate start the cascade in the next plate. The electrons exiting the MCP are detected on the anode by measuring the

current. An earth grounded grid is mounted two cm before the first microchannel plate. The detector is operated at the detector voltage and the resulting potential difference between the earth grid and the microchannel plate causes a post-source acceleration of the ions to give a larger impact on the detection microchannel plate.

The resolution of a simple Time-of-Flight mass spectrometer is low. Cotter [1997] distinguishes three factors that contribute to the low resolution: the temporal distribution, the initial kinetic energy distribution and the spatial distribution. The temporal distribution includes the differences in time of ion formation and the device dependent spread of ion detection: the length of the drift region for example. Ions with the same mass, formed with a time difference of δt in the source, will enter the drift region with time difference δt and arrive at the detector with a time difference of δt . Increasing the length of the flight tube of the mass spectrometer, thereby increasing the flight time t of the ions, increases the resolution, which is determined by $t/2\delta t$.

The initial kinetic energy distribution is a result of the initial velocity distribution, along the time-of-flight axis of the ions. Ions with an initial velocity component will arrive earlier at the detector than ions with the same mass-to-charge ratio with no initial velocity component along the time-of-flight axis of the ions. Ions with an initial velocity component opposite to the flight direction will arrive even later, resulting in tailing of the peak and decreasing the resolution. Generally, the effects of the initial kinetic energy distribution is minimized by operating the ion source at high acceleration voltages. The difference between the smallest and largest initial velocities decreases in relation to the final velocity due to the acceleration.

Spatial distributions are due to the different positions of ion formation within the source, resulting in different travel distances in the source-extraction region and resulting in ions with a kinetic energy distribution. Ions formed closer to the detector will enter the drift region sooner but have a lower velocity and arrive at the detector later than ions formed further away from the detector. At a certain distance in the drift region the two above-mentioned ions catch up with each other. This distance is known as the space-focus plane and is independent of the ion mass and starting position. The space-focus plane is located close to the source-extraction region.

2.3 Latest improvements of the aerosol mass spectrometer

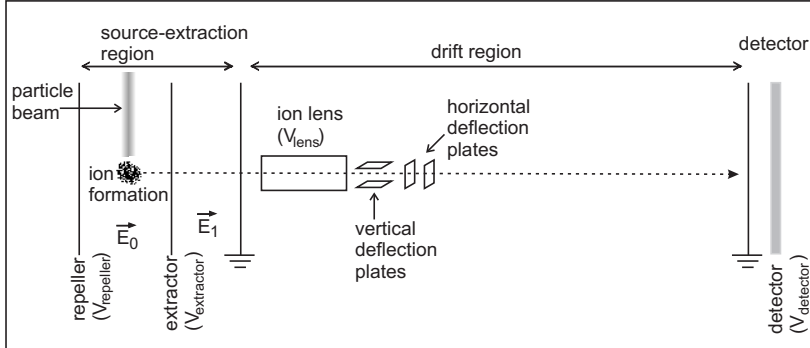


Figure 2.4:

Schematic drawing of the ion source in the aerosol time-of-flight mass spectrometer

In the aerosol mass spectrometer, the ions formed have a spatial distribution, since ionization takes place between the repeller and extractor (within the E_0 -region, see figure 2.4) at locations along the particle beam width. After irradiation, an ion cloud is formed. A way to minimize the effect of the spatial distribution is to use a dual stage extraction source. The aerosol mass spectrometer is equipped with such a source, implemented by Van Wuijckhuijse [2003]. A dual stage extraction source consists of two extraction regions, of which the second extraction field (E_1) is much higher than the first extraction region (E_0), *i.e.* where the ions are formed. In figure 2.4 a schematic drawing of a time-of-flight mass spectrometer with a dual extraction source is given. In a dual stage source the location of the space-focus plane is moved further away from the source-extraction region, allowing the placement of the detector at the space-focus plane [Cotter, 1997]. Another method to decrease the effect of spatial distributions on the mass resolution is time-lag focusing (also known as delayed extraction) as introduced by Wiley and McLaren [1955] [Colby and Reilly, 1996]. The implementation of delayed extraction is described in section 2.3.2.

A method to increase the mass spectrometric range and performance of the instrument is to operate the ion source at higher voltages. The ion source as described by Van Wuijckhuijse [2003] was operated at typical re-

pellor and extractor voltages of 18 kV and 12.5 kV respectively. Voltages of such magnitudes are also utilized in commonly used MALDI mass spectrometers like the Biflex III from Bruker Daltonics (Bremen, Germany), for instance. In cooperation with this company an ion source was designed for a maximum acceleration voltage of 35 kV on the repeller plate. The higher voltages decrease the effect of initial kinetic energy distributions (velocity focusing). In addition, the distances between the repeller, extraction and ground plate were optimized for space and velocity focusing. The distance between the repeller and first extraction plate is 9 mm and the distance between the first and second (grounded) extraction plate is 3 mm, which is based on calculations performed by van Wuijckhuijse and by Bruker Daltonics (Bremen, Germany). Typical values of extraction fields are 500 kV/m and 8000 kV/m respectively. The newly designed ion source is implemented in this work and all mass spectrometric analysis is performed with this new design.

The work by Van Wuijckhuijse [2003] included the implementation of an Einzel lens (ion lens) and horizontal deflection plates into the aerosol mass spectrometer. The ion lens focuses the ions to allow more ions to impact on the detector plate, thereby increasing the ion signal. The deflection plate is used to steer the focused ion beam onto the detector in case the ion beam deviates from the center line: ion-source - detector plate. The voltages of the deflection plates are adjusted to obtain high ion signals on the detector, while preparing the instrument for 'real' measurements. In this work vertical deflection plates are implemented and applied in addition to the horizontal deflection as used by Van Wuijckhuijse [2003].

2.3.2 Delayed extraction

One ultimate goal of the research project is classification of bacteria particles based on their MALDI mass spectra. Therefore, the mass spectra should have a reasonable quality regarding their signal-to-noise ratio, mass accuracy and resolution. Time-of-flight mass spectrometers have a limited mass resolution due to several factors including the velocity and spatial distributions of the ions. The effect of the velocity and spatial distributions is minimized by implementation of the design of the new dual stage ion source, as discussed above in 2.3.1. Another way to minimize the effect of spatial and velocity distribution can be accomplished by affecting

2.3 Latest improvements of the aerosol mass spectrometer

the way the ions are extracted. In this work, delayed extraction is implemented to improve the resolution of the mass spectra. In the delayed extraction mode acceleration of the ions formed takes place after a set delay time. During this delay time no electric field exists in the region the ions are formed (E_0 in figure 2.4). Ions with the same mass-to-charge ratio distribute themselves in the field free region according to their initial kinetic energy. After the delay time, the voltage of the first extractor plate ($V_{extractor}$) is pulsed down, causing the extraction field. When the extraction field is applied the ions with high initial kinetic energy will arrive at the detector at the same time as the ions with less initial kinetic energy, resulting in a high resolution [Cotter, 1997]. A disadvantage of delayed extraction is the mass dependency [Wiley and McLaren, 1955, Brown and Lennon, 1995]. The displacement of the ions in the delay time according to the initial kinetic energy is dependent on the mass of the ions ($E_{kin} = \frac{1}{2}mv^2$), resulting in a loss in space-focusing. Optimizing the voltage of the extraction pulse can correct for the loss in space-focusing, as is demonstrated by Whittall and Li [1995] and Dai et al. [1996b], who obtained high resolution spectra for a wide mass range (2 to 20 kDalton) at a fixed delay time. For the analysis of bacteria aerosol particles with the aerosol mass spectrometer, mass spectra of a broad mass range are required, whereby the ions originate from a single ionization and extraction event (*i.e.* single particle analysis). Therefore an optimum combination of delay time and extraction voltage has to be found. In this work the optimum combination of the delay time and the extraction voltage is adjusted for each experiment: the delay time is set first, followed by the adjustment of the extraction voltage.

2.3.3 Particle beam alignment

Another prerequisite for high quality aerosol mass spectra is good alignment of the laser beams and the alignment of the particle beam with respect to the laser beam. In addition, a good alignment increases the efficiency of the instrument. To control the alignment, a digital camera (Canon, Powershot A95) was mounted onto the apparatus, 90° to forward scattering (see figure 2.6). By applying a long shutter time it is possible to visualize the aerosol beam and to check the alignment of the lasers and the particle beam. The theoretical laser beam alignment is given in

figure 2.5a. The aerosol beam is visible in the photographs in figure 2.5 as two light-colored horizontal bars. On those locations the particle beam is illuminated by the 632/532 nm detection laser beams¹. The photograph in figure 2.5b was taken when there were no particles present. The photograph in figure 2.5c shows an incorrect alignment. The perpendicular line through the illuminated spots of the particle beam has a diagonal direction. On the thin vertical line, 0.5 mm below the second detection spot, the ionization spot is located (not visible on the photographs). The ionization spot is approximately 300 x 500 μm . With the alignment as shown in figure 2.5c, very few of the detected particles will be hit by the ionization laser, thereby decreasing the efficiency of the instrument. The photograph in figure 2.5d shows a correct alignment. The perpendicular line through the illuminated spots of the particle beam is almost vertical and therefore the detected particles will be intercepted by the ionization laser beam.

With the procedure developed to check the alignment of the particle and the laser beams the approximate position of the ionization laser beam can be derived. When the position of the ionization spot is known, the optimization of the deflection voltages is more easily achieved. Note that the function of the deflector plates is to guide the ion beam onto the detector plate to increase the ion signal. Experience with the aerosol mass spectrometer has learned that the alignment changes over time, when operating the instrument, resulting in less efficient particle detection. When a decrease in efficiency is observed the developed procedure to check the alignment can be applied to investigate whether this decrease in efficiency is caused by the alignment or not. Advantageous in this case is that checking the alignment can be done in situ, without shutting down and restarting the instrument, which takes several hours before the instrument is operational again. To summarize, the developed procedure to check the alignment of the laser beams and the particle beams increases the efficiency of the aerosol mass spectrometer and helps to obtain good quality mass spectra.

¹Figure 2.5a also shows the location of the 266-nm laser beam, utilized for the fluorescence preselection as described in chapter 3.

2.3 Latest improvements of the aerosol mass spectrometer

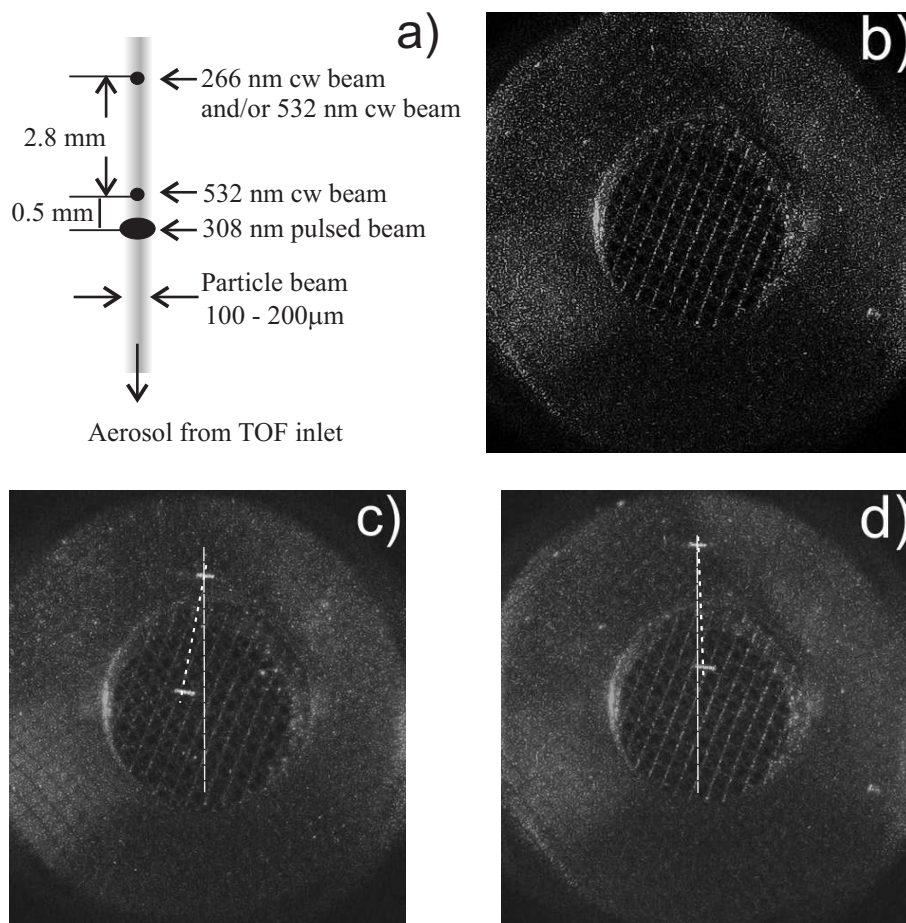


Figure 2.5:
Visualization of the aerosol beam. a) a schematic drawing of theoretical alignment of the lasers and particle beam; b) no particles are present; c) the aerosol beam with improper alignment; d) the aerosol beam with correct alignment, passing through the center of the ion source

2.4 Calibration of the aerosol mass spectrometer

For the transformation of the time-of-flight spectra into a mass spectra the aerosol mass spectrometer needs to be calibrated. For calibration the following equation is used [Van Wuijckhuijse, 2003]:

$$\frac{m}{ze} = \left(\frac{t - c_2}{c_1} \right)^2 \quad (2.4)$$

where m is the ion mass, z the number of elementary charges, e the elementary charge, t the flight time of the ion and c_1 and c_2 the calibration constants. The physical meaning of the constant c_2 is the time between the triggering of the ionization laser and the actual formation of the ions. During the ionization process mostly singly charged ions are formed, but also multiple charged ions can be formed, which is the reason why z is used in equation 2.4. Instrumental parameters as the applied acceleration and extraction voltages and the length of the flight tube are included in c_1 .

In practice, usually an aerosol containing particles of the protein insulin is used for calibration of the aerosol mass spectrometer. If the sample to be analyzed (or calibrated) consists of an other protein, then that protein is used for calibration. To determine the flight time t of an ion with a certain m/z value, several spectra are recorded and summed. From this summed spectrum the time of the specific ion is determined using the program MassSpecViewer (ContinuIT BV, Houten, The Netherlands). To solve equation 2.4 only the flight times (and m/z values) of two ions is required. Depending on the mass range of interest and the detectability of the peaks the doubly charged insulin ion ($m/2z$ is 2867.5 Dalton) and the protonated dimer ($2m/z$ is 11467 Dalton) or the combination of the main protonated peak (m/z is 5734 Dalton) and the dimer were used. Note that m is here the mass of the insulin molecule. Calibration experiments were performed with the same matrix material as used for the analyte, since different matrix have different initial velocities [Berkenkamp et al., 2002].

2.5 Description of the current aerosol mass spectrometer

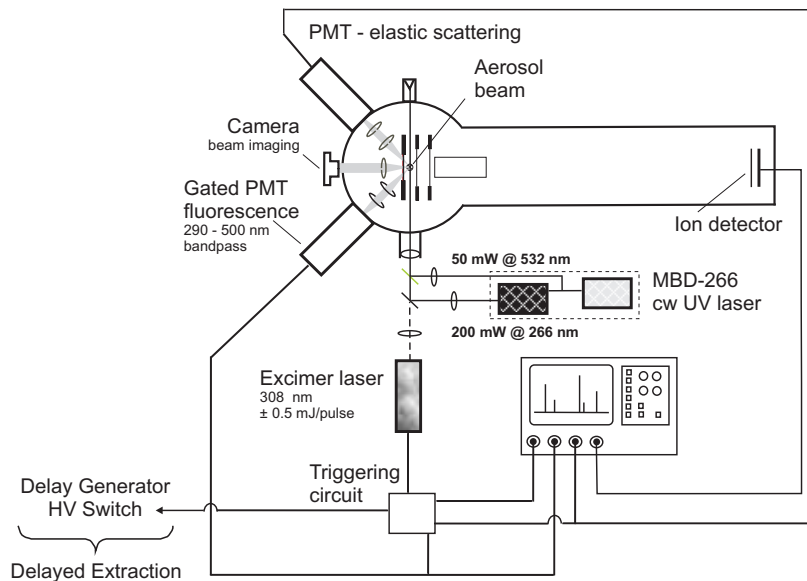


Figure 2.6:

Schematic diagram of the current aerosol mass spectrometer. In this arrangement the particle sizing and detection is accomplished with the 532 nm cw laser beams

2.5 Description of the current aerosol mass spectrometer

In figure 2.6 a schematic diagram of the current aerosol mass spectrometer, including the above described improvements (section 2.3) is given and is described as follows.

Aerosol is sucked into the instrument at a flow rate of 0.6 l/min through four differentially pumped chambers by a network of vacuum pumps. The pressure in the first section can be regulated and holds aerodynamic lenses which, together with the subsequent nozzle and two skimmers, act to generate a focused particle beam. The width of the beam was measured by Van Wuijckhuijse [2003] at the location of the ionization laser focus (approximately 50 mm below the second skimmer) to be around 100 μm . The pressure in the ionization chamber is maintained at approximately

10^{-6} mbar.

The aerodynamic size of individual particles is obtained by measuring the transit time between two continuous laser beams, realized by splitting a randomly polarized, continuous wave (cw), laser beam (532 nm) (MBD-266 laser Coherent Inc., Santa Clara, USA) into two beams with a beam displacement prism. The resulting 532 nm laser beams, focused to 75 μm spots, are 2.8 mm apart in a direction perpendicular to the particle trajectory.

In the ion source region the particles are accelerated as a function of their aerodynamic diameter up to velocities as high as 250 m/s. A photomultiplier tube (PMT, Thorn EMI, Middlesex, UK; Type 9202B), located 45° relative to forward scattering, records elastic scattering from particles intersecting the detection (632/532 nm) laser beams. The transit time is a measure for the aerodynamic size of the particle. Weiss [1997] derived a relationship between the transit time, particle size and particle density for the applied aerosol beam generator. The aerodynamic particle sizing is calibrated with monodisperse aerosols of polystyrene latex particles (Duke Scientific Corp, Palo Alto, CA, USA) in the size range of 0.24 to 5 μm . The density difference of natural aerosol particles and the latex particles is neglected. Note that assumption can result in an attributed particle size which is deviating from the real particle size. The alignment of the lasers can be monitored using a digital camera (Canon, Powershot A95) mounted at 90° relative to forward scattering. The particle detection according to the method described above is referred to as 'one color triggering' since both detection beams have the same wavelength: 532 nm.

Preselection of the biological fraction out of the total aerosol is accomplished by collecting fluorescence emitted from the biological particles. A part of the 532 nm cw-beam of the MBD-266 laser is deflected and goes into the external doubler, where a 266 nm laser beam is generated (see also figure 2.7). The 266 nm cw laser beam is utilized for fluorescence preselection [Van Wuijckhuijse, 2003, Van Wuijckhuijse et al., 2005, Stowers et al., 2006] and is described in chapter 3. The 266 nm cw laser beam intercepts the particle beam at the same spot as the top 532 nm laser beam. The emitted fluorescence is recorded on a gated UV-sensitive photomultiplier tube (Electron Tubes Ltd., Ruislip, UK; Model 9235QB at 135° relative to forward scattering. A wave pass filter allowing light between 290 and 500 nm is placed in front of the photomultiplier tube. The method of

2.5 Description of the current aerosol mass spectrometer

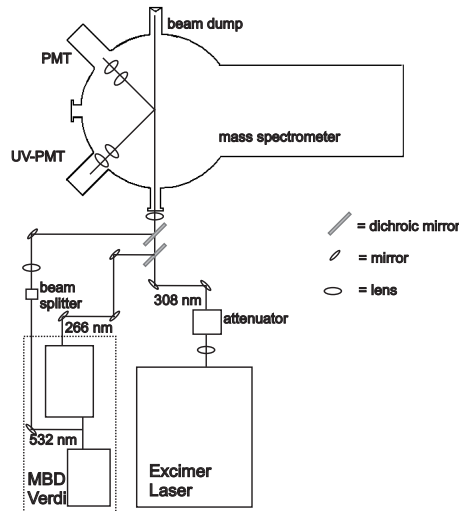


Figure 2.7:

The arrangement of the optical components for particle detection. The optical components for particle selection by fluorescence are also included

particle sizing and selection, as described above is referred to as ‘two color triggering’. In figure 2.7 the arrangement of the optical components and the laser paths is given.

The time between the PMT output pulses is also used to trigger the 308 nm Excimer ionization laser (ATL Lasertechnics, Friedrichstal, Germany; Model EC50), which is focused at 0.5 mm below the second detection beam. The Excimer laser with a nearly flat top beam profile and pulse-width of 3 ns accomplishes desorption, fragmentation and ionization of the aerosol particles. The UV laser spot area is approximately $300 \times 500 \mu\text{m}$ and the laser fluence is adjusted for MALDI analysis, typically to values of approximately 1.5 J/cm^2 . As a result of the particle size dependent triggering and proper alignment, over 95% of all particles intersecting both cw beams are intercepted by the ionization laser beam to generate ions. The particle detection efficiency of the instrument was measured by comparing the particle concentration (using a particle counter) outside

the instrument with the number of particles detected by the aerosol mass spectrometer during a certain time period at a fixed suction flow rate. The total sampling efficiency (*i.e.* the fraction for which a mass spectrum is generated) of the instrument is 1-5 %.

Positive ions, produced in the ionization process, are accelerated in a two-stage ion source toward a microchannel plate (MCP) detector that records the mass-dependent arrival time of the ions. The length of the flight tube is 1.5 m. As already discussed in section 2.3.1 and 2.3.2 the acceleration of the ions can be accomplished in two ways: continuous and delayed extraction. In continuous extraction mode the voltage potential on the repeller plate is set to 35 kV and the voltages of the extractor plate, the ion lens and detector are adjusted to obtain maximum signal on the ion detector, typically in the order of 28 kV, 13 kV and 2 kV respectively. In delayed ion extraction the voltages of the repeller and extractor plate are set to 35 kV. After a delay of 450 ns after ionization the voltage potential on the first extractor plate is pulsed down to voltages of 30 to 25 kV to accelerate the ions. The voltages of the ion lens, deflector plates and detector are adjusted to obtain maximum response.

A 500 MHz digital oscilloscope (LeCroy, Chestnut Ridge, NY, USA; Model 9354CL) is used to sample the signals from the PMT and the MCP detector and to send the spectrum output to a personal computer via a GPIB interface; the data are then further processed by a data system developed in-house. Thus, the instrument provides the aerodynamic size, fluorescence characteristics (see chapter 3) and a mass spectrum for all analyzed particles. Particles in the size range 0.2 to 10 micrometers can be analyzed with this system, however, the triggering circuitry can be adjusted to select a range of aerodynamic particle sizes or can be set to detect suitably sized particles with a fluorescence emission in the specified wavelength range.

In table 2.1 the adjustable instrumental parameters are given, together with the typical settings. Also the effects and function of the parameters is given. When the instrument is adjusted the parameters are adjusted such that optimal signal is obtained on the detector. An optimal signal refers to intense and narrow peak(s). Note that adjusting the parameters to obtain optimal ion signal is an iterative process, meaning that each parameter influences the other.

2.6 Performance of the aerosol mass spectrometer

Table 2.1:

Adjustable parameters, typical settings and their effects and functions, of the aerosol mass spectrometer

Parameter	Typical values	Effect/Function
particle transit time	10-60 μ s	particle size range of the detected particles and generation of trigger signal
type of triggering	1 color or 2 color	non-bioaerosol or bioaerosol particles
repeller voltage	30-35 kV	acceleration of the ions (velocity focusing)
extractor voltage	25-30 kV	extraction of the ions (velocity focusing)
lens voltage	10-17 kV	focusing the ion beam
deflector voltages	-500 to +500 V	guiding the ion beam onto detector
detector voltage	1.5-2 kV	ion detection
extraction delay time	450 ns	extraction of the ions (space and velocity focusing)

2.6 Performance of the aerosol mass spectrometer

The implemented improvements (described in detail in section 2.3) were done to optimize the aerosol mass spectrometer for bioaerosol analysis. For the analysis of bioaerosols mass spectra with a good quality are required. Among the quality aspects is the resolution (over a wide mass range) of the peaks. In this section the effect of the new ion source on the resolution of mass spectra of proteins is investigated. For complex aerosol particles such as bacteria, which contain a tremendous amount of different molecules in low amounts, an instrument with high sensitivity (also a quality aspect) is required. In this section the sensitivity of the aerosol mass spectrometer is also discussed.

2.6.1 Improved resolution

The effect of the implementation of the new ion source on the resolution of the mass spectra is shown in figure 2.8. The experiments were performed with aerosol particles consisting of insulin and the MALDI matrix PMC (a proprietary made compound, order number 0145GM02, kindly provided by TNO Defence, Security and Safety, Rijswijk, The Netherlands). The analyte and matrix were dissolved in a mixture of water and acetonitrile (70/30 v/v) with 0.1% TFA. In figure 2.8a a typical mass spectrum of a single aerosol particle is presented as a reference. Figure 2.8b shows the

effect of the implementation of the new ion source: the mass resolution, calculated as $t/2\delta t$, increases from 40 to 600. Note that the mass scale of figure 2.8a and b is different. The increase in mass resolution points to a considerable initial kinetic energy distribution of he ions. The new ion source, in which the repeller is operated at a voltage of 35 kV, decreases the effect of the initial distribution of kinetic energy of the ions (velocity focusing) and thus the resolution increases. Due to the velocity focusing the sodium adduct of the insulin ion is clearly visible. In figure 2.8c the

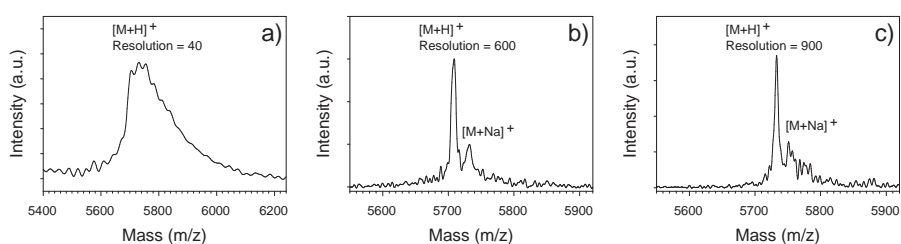


Figure 2.8:

Single particle MALDI mass spectra of insulin, a) before the implementation of the new ion source, b) after the implementation of the new ion source and c) after the changing the distance between the repeller and the first extraction plate and between the first and second extractor plate

effect of space and velocity focusing by changing the distance between the repeller and first extractor plate and between the first and second extractor plate (ground plate) is given. When the obtained resolutions from figure 2.8b and c are compared it can be seen that the additional space and velocity focusing increases the resolution of a single particle spectrum up to 900. It is concluded that the implementation of the new ion source has improved the performance of the mass spectrometer.

An example of the increased mass resolution due to the implementation of delayed extraction is given in figure 2.9. The experiments were performed with the same insulin aerosol particles as in the experiment for figure 2.8. First continuous ion extraction was applied, immediately followed by the experiment in which the ion extraction was delayed to analyze the aerosol particles. Thus, the experimental conditions were the

2.6 Performance of the aerosol mass spectrometer

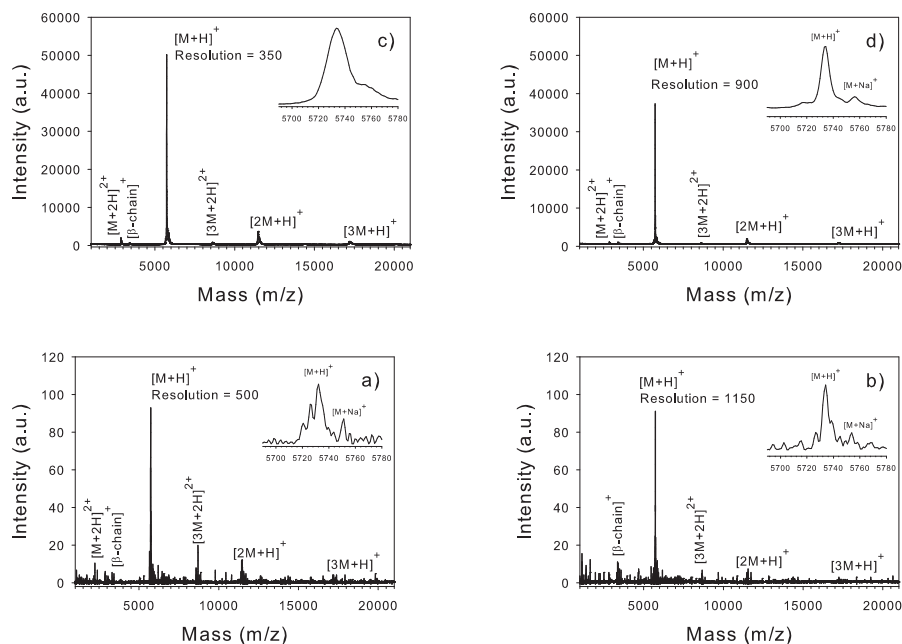


Figure 2.9:

MALDI mass spectra of insulin particles), a) a single particle mass spectrum obtained with continuous extraction and b) with delayed extraction; c) a summation of 1000 particles obtained with continuous extraction and d) with delayed extraction. The insets show the main protonated peak

same, except for the different ion extraction methods. Figure 2.9a and 2.9b show typical single particle mass spectra and figure 2.9c and fig:ceded are mass spectra of a summation of 1000 particles. The resolution of the spectra is calculated ($m/\Delta m$, where Δm is the full width at half maximum (FWHM)) for the main protonated insulin peak, at 5734 Dalton. For the single particle spectra resolutions of 500 (continuous extraction) and 1150 (delayed extraction) are obtained. A similar result is obtained for the summed mass spectra: the resolution of 900, obtained with delayed extraction (figure 2.9d) is higher than the resolution with continuous extraction,

which is 350 (figure 2.9c). The insets in figure 2.9 show the appearance of the main protonated insulin peak at 5734 Dalton. The resolution of the summed spectrum (figure 2.9c in continuous extraction mode is too low, to separate the sodium adduct. In the single particle mass spectrum (figure 2.9a the sodium adduct can be distinguished. The insets for the spectra in delayed extraction mode show, next to main protonated peak, a peak attributed to the sodium adduct.

Figure 2.10 shows the spread in the peak positions for continuous and delayed extraction mode for the protonated insulin molecule (5734 Dalton) and the dimer (11467 Dalton). As can be seen is the spread for both ions in the delayed extraction mode lower than in the continuous extraction mode. Also can be observed that the spread for the higher mass ion increases for both extraction modes, causing a lower resolution at higher mass. The decrease in resolution for higher masses is known for time-of-flight mass spectrometers. The lower resolution in delayed extraction mode is caused by the used delay time, which is mass dependent. The delay time is optimized for the single molecule and therefore contributing to a wider range of peak positions of the dimer.

In common time-of-flight mass spectrometry usually a summation or an averaged spectrum is obtained, but the strength of the aerosol mass spectrometer is the capability of single particle analysis. This capability requires single shot spectra with high resolution. Single particle mass spectra require a high resolution to allow identification of the single aerosol particle. In addition high resolution single particle spectra will contribute to a high resolution of the averaged spectrum. In aerosol mass spectrometry both types of resolutions can be applied, namely the single particle (single shot) resolution and the ‘overall’ resolution of multiple spectra together. The values of the resolution obtained from figure 2.9 are overall resolutions.

The single particle resolution is investigated for the same aerosol as in figure 2.9. The values for the single particle resolution are obtained with a procedure developed in MatLab, which is described in section 4.7.2. Figure 2.11 shows the frequency distributions of the single shot resolutions of the main protonated peak in both extraction modes. Note that the values of the resolution are not the same as in figure 2.9, due to the method the resolution is calculated. Although the absolute values are different when compared to figure 2.9, the behavior (the trend) will not change. As can

2.6 Performance of the aerosol mass spectrometer

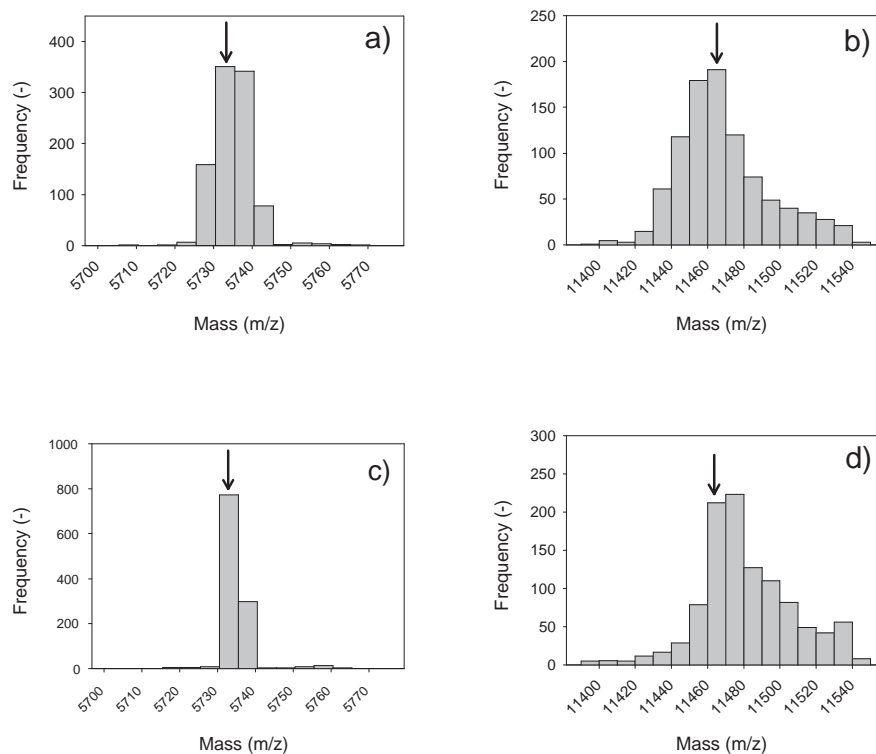


Figure 2.10:

Histograms of the peak positions of 1000 single particle spectra. a) the protonated insulin molecule in continuous extraction mode, b) the protonated dimer in continuous extraction mode, c) the protonated insulin molecule in delayed extraction mode and d) the protonated dimer in delayed extraction mode. The black arrows indicate the anticipated positions of the molecules

be seen in figure 2.11 the values for resolution in continuous extraction mode are almost a factor 2 lower than the resolutions found in delayed extraction mode. Note that the values for the resolution of single particle spectra as well as for the summed spectra are not equal to the resolutions found in standard MALDI TOF mass spectrometry, which are one order of magnitude larger.

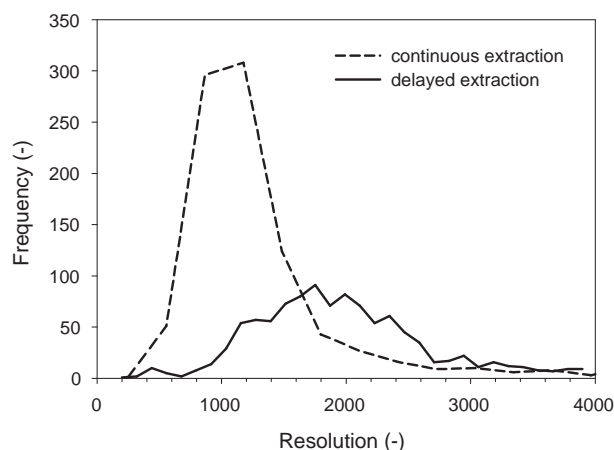


Figure 2.11:

Frequency distributions of single shot resolutions of the main protonated peak in continuous and delayed extraction mode

2.6.2 Isotopic resolution

Another way to examine the effect of the increased mass resolution due to the implementation of delayed extraction and the new design of the ion source is to investigate the presence of isotopes. For this purpose an aerosol was produced from a solution containing the neuropeptide substance P (1347 Dalton) and the matrix PMC (a proprietary made compound, order number 0145GM02, kindly provided by TNO Defence, Security and Safety, Rijswijk, The Netherlands). The delay time was optimized for the mass of this neuropeptide. In figure 2.12 a mass spectrum of a sin-

2.6 Performance of the aerosol mass spectrometer

gle particle and a mass spectrum of 50 particles is given. Figure 2.12a is the mass spectrum of a single particle. The inset shows the appearance of the main protonated peak, in which different peaks, with a mass difference of 1 Dalton, can easily be discriminated. The peaks are attributed to the isotopes, since the pattern is corresponding to the isotope distribution observed in nature from this protein². To the author's knowledge an aerosol MALDI mass spectrum with isotopic resolution has never been reported in literature.

The mass spectrum in figure 2.12b is a summation of the mass spectra of 50 aerosol particles. Again, the inset shows the resolution of the main protonated peak. The different isotopes, as obtained for a single aerosol particle, are not that clearly separated. The resolution for a single particle is optimized by a high acceleration voltage and by delayed extraction is visible, but due to the particle beam width, the place of ionization is not the same for each particle, resulting in a lower overall resolution. The spread in ionization spots can be decreased by reducing the particle beam width or by decreasing the diameter of the detection laser beams. The first method requires a well designed aerodynamic lens system, according to the design of Wang and McMurry [2006] for instance. In the second option, reducing the diameter of the detection laser beams, the sampling efficiency will decrease, since only a small fraction of the particle beam will be intercepted by the ionization laser beam for mass spectrometric analysis.

Again is concluded that the implementation of the new ion source and delayed extraction have improved the resolution of single particle mass spectra. A high single particle resolution is required for the identification of single aerosols. The obtained single particle resolution indicates the applicability of the aerosol mass spectrometer for the analysis of bacteria containing particles. Taking into account that biomarker molecules have masses in the range 4-20 kDalton, resolutions for these complex samples should be such that molecules with 20 Dalton mass difference can be distinguished from each other. This requires a mass resolution of 200 to 1000.

²The isotope distribution was obtained from <http://prospector.ucsf.edu/prospector/4.27.1/cgi-bin/msForm.cgi?form=msisotope>

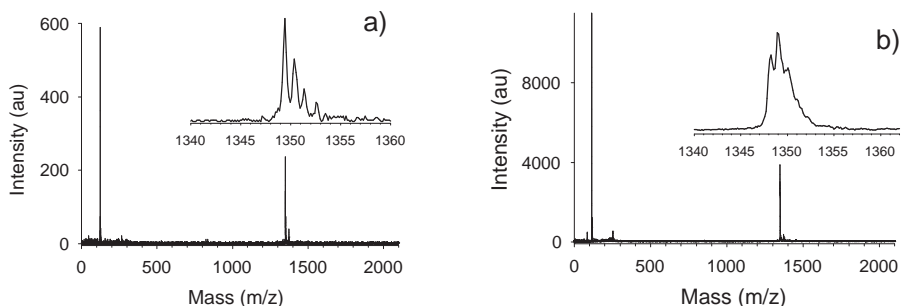


Figure 2.12:

MALDI mass spectra of aerosol particles consisting of the neuropeptide substance P and the matrix PMC; a) single particle spectrum and b) summation of 50 aerosol particles. The inset shows the protonated peak

2.6.3 Sensitivity limit

Identification of bacteria based on their MALDI spectra requires a very sensitive instrument. Madigan et al. [2000] estimates the protein content of vegetative bacterial cells. The total number of protein molecules per cell is estimated to be 2.4 million and the number of different proteins is estimated to be around 1900. Assuming that all proteins are present in equal amounts, the average amount of molecules per protein per cell will be in the order of 10^3 . The required sensitivity for an instrument capable of identification of bacteria is, based on the above mentioned example, thus in the order of 1 zeptomole (10^{-21} mole).

The sensitivity of the aerosol MALDI mass spectrometer is determined with an aerosol produced from a solution containing the protein insulin (5733 Dalton) and the matrix 2,5-dihydroxy benzoic acid (DHB). The molar ratio of matrix to analyte in the solution was gradually increased to 50,000:1, by serial dilution. The solutions were aerosolized and the resulting aerosol particles are assumed to have the same matrix to analyte ratio as the original solution, assuming a homogeneously mixed solution. Up to a matrix to analyte ratio of 50,000:1 peaks caused by insulin ions were appearing in the mass spectra. A similar experiment was performed with an aerosol of the neuropeptide substance P (1347 Dalton) with the matrix

2.6 Performance of the aerosol mass spectrometer

PMC (a proprietary made compound, order number 0145GM02, kindly provided by TNO Defence, Security and Safety, Rijswijk, The Netherlands). The molar ratio of matrix to analyte for this sample was increased by serial dilution to a maximum of 300,000:1. At these molar ratios the detection efficiency was about 5%, meaning that from only 5% of the detected and ionized particles a signal of the protein was seen in the spectra. For the calculation of the detection efficiency the procedure described in section 4.7.2 (peak occurrence) is used. Shortly, in this procedure the mass spectra are scanned on the presence of a peak in a user-defined mass range.

For the highest matrix to analyte ratio the size range of the detected particles was changed from the whole detection range (0.2 to approximately 5 μm) to the size range with an average aerodynamic diameter of 0.26 μm . In figure 2.13 an average spectrum of 30 0.26- μm insulin containing particles at a matrix to analyte ratio of 50,000:1 is given.

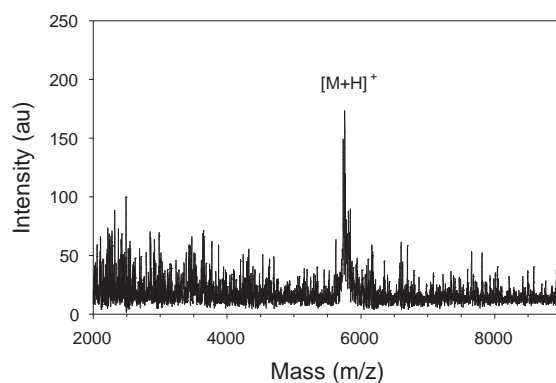


Figure 2.13:

MALDI mass spectrum of 0.26 μm aerosol particles consisting of insulin (5733 Dalton) and DHB in a matrix to analyte ratio of 50,000:1

Russell et al. [2005] determined the sensitivity limit of their BAMS system (Bioaerosol mass spectrometry) and used the following equation to calculate the number of analyte molecules per particle, assuming spherical,

homogeneously mixed particles:

$$N_{Analyte} = \frac{4}{3}\pi r^3 \left(\frac{\rho}{MW_{matrix}} \right) \left(\frac{moles_{Analyte}}{moles_{matrix}} \right) N_A \quad (2.5)$$

with:

$$r = \frac{d_A}{2\sqrt{\rho}} \quad (2.6)$$

in which $N_{Analyte}$ is the number of analyte molecules per particle, r the particle radius (cm), ρ the particle density (assumed to be the density of the matrix, which is 1.44 g/ml for DHB and 1.32 g/ml for PMC), MW_{matrix} the molecular weight of the matrix (which is 154 g/mole for DHB and for PMC the value of 140 g/mole is used³), N_A Avogadro's number and d_A the aerodynamic diameter. Note that equation 2.6 is not right. The aerodynamic particle size is defined as the diameter of a spherical particle with a density 1000 kg/m³ that has the same settling velocity as the particle. Therefore, formally the ratio of the densities should be used [Hinds, 1999]:

$$r = \frac{d_A}{2\sqrt{\frac{\rho}{\rho_0}}} \quad (2.7)$$

in which ρ_0 is the standard particle density of 1 g/ml. Since the ratio of the densities has the same value as the density of the matrix only, the calculated values of Russell et al. [2005] are correct.

Russell et al. [2005] report for their instrument a sensitivity limit of 14 zeptomole. The obtained sensitivity of 14 zeptomole by Russell et al. [2005] equals approximately 8400 molecules. When the BAMS system of Russell et al. [2005] would be applied for the analysis of bacteria particles, only a few ubiquitous types of proteins would be detected, covering a very small fraction of the protein content of a cell, assuming that the contribution of the different proteins is not equal.

The sensitivity limit of the aerosol mass spectrometer is also calculated applying equation 2.5 for the performed experiments with insulin and substance P. The number of analyte molecules is 600 molecules per particle

³The exact molecular weight of this matrix can not be given for confidentiality reasons.

2.7 Multicomponent aerosol analysis with the aerosol mass spectrometer

for the insulin experiment and 180 molecules per particle for the substance P experiment, corresponding to 1 and 0.3 zeptomole. This sensitivity limit is lower than the amount of molecules per protein per cell and meets the sensitivity criterion defined above (1 zeptomole). The target mass range for the classification of bacteria particles by their proteins is from 2 to 25 kDalton [Fenselau and Demirev, 2001]. Therefore the sensitivity limit of the aerosol mass spectrometer is defined as 1 zeptomole, since the protein insulin has a mass that falls within the proposed mass range for classification, whereas the mass of the peptide substance P is outside the target mass range.

The improvements of the mass spectrometer are all based on the idea to utilize the instrument for bioaerosol analysis. In the foregoing the sensitivity of the instrument is derived and meets the criterion for an instrument that should be capable of identification of vegetative cells. However, the sensitivity was derived based on experiments with a simple aerosol, containing solely insulin. Similar experiments are required with multicomponent aerosol particles and also with bacterial aerosol particles.

2.7 Multicomponent aerosol analysis with the aerosol mass spectrometer

The implemented improvements described in section 2.3 were inspired by the suitability of the aerosol mass spectrometer for the analysis of bioaerosol particles. The following describes the application of the aerosol mass spectrometer on internally and externally mixed aerosol⁴, to investigate the applicability of the instrument for mass spectrometric analysis over a broad mass range and to investigate the discriminative power of the aerosol mass spectrometer.

⁴Internally mixed aerosol refers to an aerosol of which the individual aerosol particles are composed of more than one analyte and an externally mixed aerosol contains aerosol particles composed of analyte mixed with aerosol particles composed of another analyte(s).

2.7.1 Internally mixed aerosol

To investigate the capability of the instrument to separate protein molecules over a broad mass range an experiment was performed using an internally mixed aerosol of the proteins insulin (5733 Dalton), ubiquitin (8565 Dalton) and cytochrome C (12360 Dalton) premixed with the matrix sinapinic acid, with the protein ratio 2:5:5, respectively. This protein ratio was chosen, since with an equimolar ratio the intense insulin signal obscured the presence of other ions. The matrix to the total amount of analytes was 500:1. The solution was nebulized with a capillary tube nebulizer (Meinhard Glass Products, Golden, CO, USA, Model TR-30-A1). The experiment was performed in the delayed extraction mode. The obtained mass spectrum of 1000 particles is shown in figure 2.14, in which monomers of the different proteins as well as clusters of the different protein molecules can be identified. The presence of the analyte species in the single particle spectra is not the same for each spectrum. The spectra-to-spectra variation is ruled out by the summation of multiple spectra. In the (summed) mass spectrum in figure 2.14 different peaks up to a mass of approximately 21 kDa, could be identified. This is the mass range proposed by Fenselau and Demirev [2001] (4-20 kDa) to contain the biomarkers for classification of bacteria. Note that the peak at 21 kDa is caused by a cluster of ubiquitin and cytochrome C. The fact that the three analyte molecules appear in several charged states, as well as in combination with each other, is good in this experiment to demonstrate the analysis over a wide mass range of the instrument. On the other hand for complex mixtures of unknown composition, the appearance of the molecules in several forms is not favored, since it will complicate the identification procedure. Optimization of the applied laser energy can decrease the fragmentation of the molecules [Van Wuijckhuijse et al., 2005] and the choice of the sample composition plays also a role in the detection of ions (see also chapter 4). The resolution of the peaks in the in figure 2.14 is 250-100 for the mass range 5-12.5 kDa. This resolution is not as high as obtained in figure 2.9, which might be due to not complete optimal settings of the instrument. As a consequence of the obtained resolutions 12,5 kDa molecules with 20 Dalton mass difference can not be discriminated from each other. However, this spectrum is also an example showing the applicability of the MALDI method for aerosol analysis. The single components over a wide

2.7 Multicomponent aerosol analysis with the aerosol mass spectrometer

mass range out of a mixture are clearly separated, with is to be expected when knowing the obtained resolutions in figure 2.9.

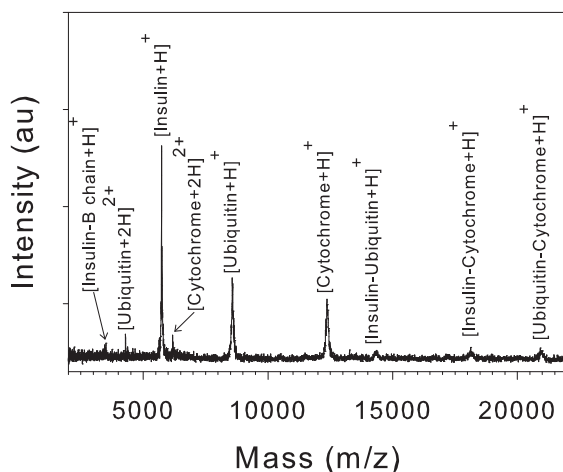


Figure 2.14:

MALDI mass spectrum of 1000 internally mixed aerosol particles containing insulin, ubiquitin and cytochrome C (molar ratio 2:5:5) pre-mixed with sinapinic acid

2.7.2 Externally mixed aerosol

The individual compounds in a complex aerosol particle can be identified as is shown in section 2.7.1. The capability to discriminate different types of aerosol particles is demonstrated with an externally mixed aerosol. The aerosol particles were either composed of insulin (5733 Dalton) with the matrix PMC (a proprietary made compound, order number 0145GM02, kindly provided by TNO Defence, Security and Safety, Rijswijk, The Netherlands) or composed of cytochrome C (12360 Dalton) with the matrix PMC. The aerosol particles were produced with a Collison 6-jet nebulizer (BGI Inc, Waltham, MA, USA). First, the insulin particles were produced and stored in an aerosol chamber. Then the nebulizer was cleaned

quickly, but thoroughly and the cytochrome particles were produced. A protonated insulin molecule has a mass of 5734 Dalton and the protonated dimer has a mass to charge ratio corresponding to 11467 Dalton. A protonated cytochrome C molecule has a mass of 12361 Dalton and a doubly charged molecule has a mass to charge ratio corresponding to 6181 Dalton. The mass difference between a protonated insulin ion and a doubly charged cytochrome C molecule is 447 Dalton and the mass difference between a protonated insulin dimer and an cytochrome C ion is 893 Dalton. With the obtained mass resolutions in figure 2.9b the mass differences are that big that discrimination of the two types of particles should be easily achieved.

In figure 2.15 MALDI spectra of six subsequent particles are given. The subsequent particles are identified as is indicated in the spectra. Based on this experimental example can be stated that the discriminative power of the instrument is sufficient to distinguish different protein particles with mass differences of approximately 500 Dalton in the 5-6 kDa range and with 1000 Da mass difference in the 11-12 kDa mass range. However, for the discrimination of bacteria particles smaller mass differences have to be measured. When the resolution values obtained with the internally mixed aerosol (figure 2.14) are evaluated, molecules with a mass difference of 125 Da at a mass of 12.5 kDa can be distinguished. Thus, the resolution values are too low to discriminate biomarker molecules, since for that mass resolutions of 200 to 1000 are required. Also, for the classification of bacteria particles more peaks are required, as is for example shown by Fenselau and Demirev [2001].

2.8 Particle generation and characterization

For *on-line* analysis of (bio)aerosol particles, the quality of the mass spectra generated with the aerosol MALDI mass spectrometer is, next to the instrumental performance, also dependent of the particle size and concentration. In the on-line analysis the particles need to be coated with a matrix material. The method for on-line coating is discussed in 4.6.3. The amount of matrix per particle is dependent on the particle size (surface area) and the concentration. Sufficient matrix material needs to be deposited on the particles to allow proper ionization of the analyte molecules.

2.8 Particle generation and characterization

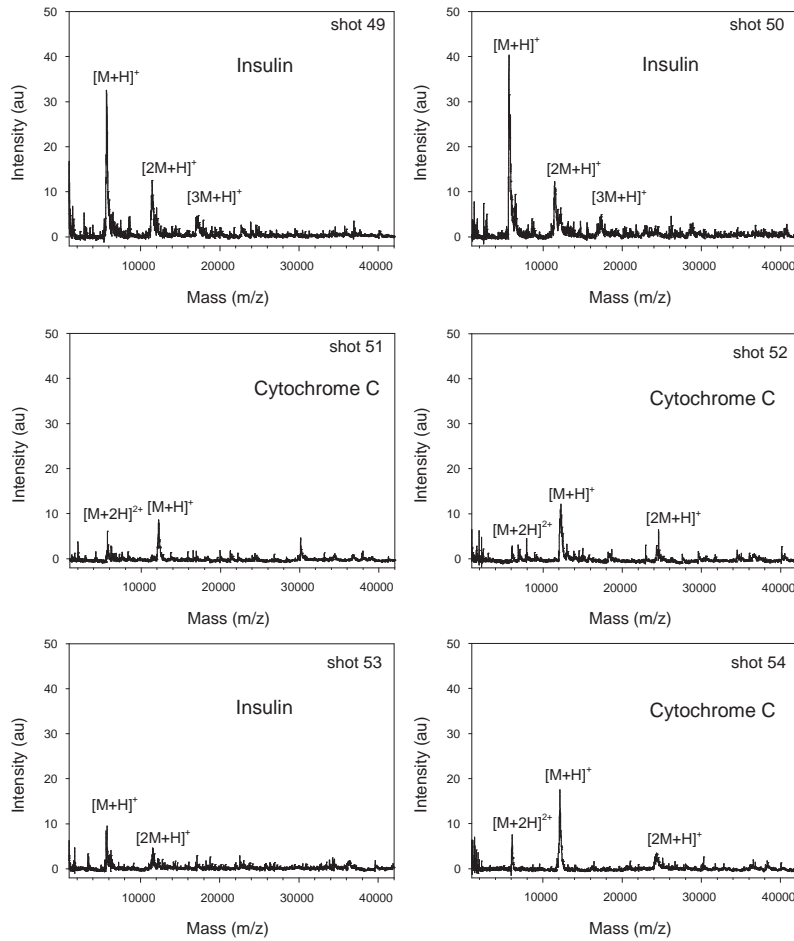


Figure 2.15:
MALDI mass spectra of 6 subsequent shots from an externally mixed aerosol containing insulin and cytochrome C particles

To control the particle size and concentration of the aerosol to be analyzed, a particle generation and characterization system is developed. The developed system is intended for investigation and characterization of the on-line coating process; a fieldable instrument will measure directly from the atmosphere.

The particle generation and characterization system consists of an aerosol chamber of 250 liters on which several nebulizers can be mounted. The nebulizers used are a Collison 6-jet nebulizer (BGI Inc, Waltham, MA, USA), a capillary tube nebulizer (Meinhard Glass Products, Golden, CO, USA, Model TR-30-A1) and an ultrasonic nebulizer (Sono-Tek Corporation, NY, USA, Model 8700-35). The particle size and concentration can be measured with an aerodynamic particle sizer (APS, TSI Inc, MN, USA, model 3321) or with an ELPI (electrical low pressure impactor) (Dekati Ltd, Tampere, Finland). The developed system allows the use of a virtual impactor. A virtual impactor acts to concentrate the particles bigger than the cut-off size of the impactor into a smaller volume. With a virtual impactor the capacity of the instrument increases, making the instrument suitable for outdoor analysis.

The used nebulizer determines the final particle size distribution of the aerosol. To demonstrate the influence of the choice of the (type of) nebulizer on the particle size distribution an experiment was performed with an aerosol of vegetative cells of *Erwinia herbicola*. Prior to nebulization, the bacterial samples were washed three times by centrifuging the solution at 4000 rpm for 5 minutes; each time the supernatant was removed and the bacteria pellets formed were then resuspended in deionized water. An amount of 500 μ l of the bacterial suspension was either nebulized with the capillary tube nebulizer or with the ultrasonic nebulizer. The particle size distribution was measured for 10 minutes with the ELPI, starting at the moment of nebulization. The obtained average particle size distribution is given in figure 2.16.

As can be seen in figure 2.16 different particle size distributions are generated with different nebulizers. With the capillary tube nebulizer a lot of very small particles (< 150 nm) are produced. These particles are not detected by the aerosol mass spectrometer, which has a lower detection limit of approximately 240 nm. The size of a single vegetative cell is 0.6-0.7 μ m (determined by scanning electron microscopy, data not shown) and therefore most of the produced small particles do not contain

2.8 Particle generation and characterization

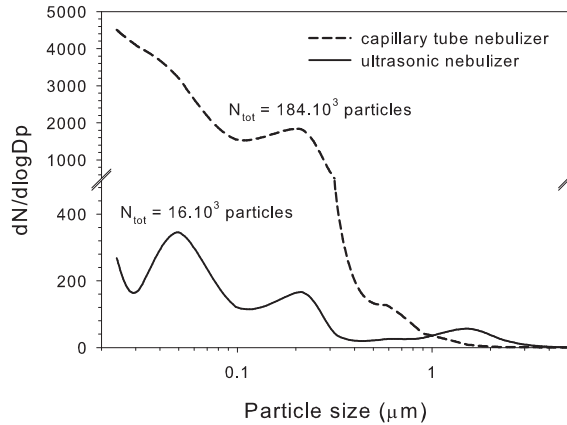


Figure 2.16:

Particle size distribution of an aerosol of *Erwinia herbicola* produced with a capillary tube nebulizer (dashed line) and with an ultrasonic nebulizer (solid line). Both aerosols are produced from the same solutions

any cell. The amount of particles produced with the ultrasonic nebulizer is an order of magnitude lower. The shape of the particle size distribution is trimodal, as is a typical particle size distribution of atmospheric air [Hinds, 1999]. Very small particles (< 150 nm) are also generated, but the amount is less.

The total number of particles produced by the two nebulizers is different, since the initial droplet size of the two nebulizers is not the same. The mean droplet size of the capillary tube nebulizer is $12 \mu\text{m}$ versus $60 \mu\text{m}$ of the ultrasonic nebulizer⁵. A bigger initial droplet (from a solution with the same concentration) will result in a bigger particle when the solvent has evaporated than a smaller initial droplet. An advantage of bigger aerosol particles is the bigger amount of material available for ionization and subsequent mass spectrometric analysis. This is especially the case for bacteria-containing aerosol particles, since a bacterium consists of many

⁵Initial droplet sizes are taken from the product information from www.meinhard.com and www.sono-tek.com respectively

different molecules in very low concentrations. Thus, for the analysis of bacteria containing aerosols the usage of the ultrasonic nebulizer is favored.

In figure 2.17 a scanning electron microscopic (SEM) image of an aerosol particle consisting of spores of *Bacillus atrophaeus* is given. SEM analysis was performed at TNO Defence, Security and Safety, Rijswijk, The Netherlands. The aerosol was produced with the ultrasonic nebulizer from an unwashed solution. After aerosolization the particles were collected by impaction on a SEM-grid. The aerosol particle shown in figure 2.17 is a cluster of multiple spores together with some material originating from the spore solution.

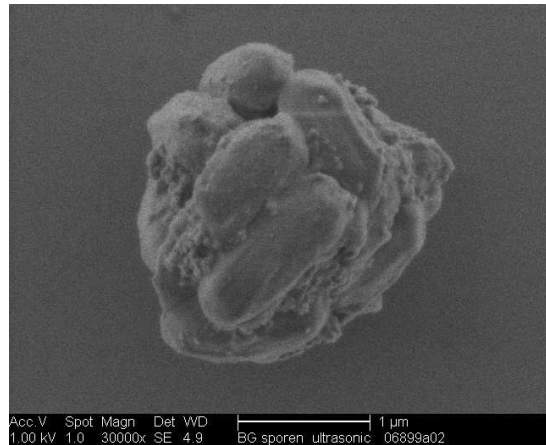


Figure 2.17:

SEM-image of an aerosol particle of spores of *Bacillus atrophaeus* produced with the ultrasonic nebulizer

Besides monitoring the particle size distribution the particle concentration can also be monitored. An example of the particle concentration over the course of half an hour is given in figure 2.18. The aerosol was the same *Erwinia herbicola* aerosol as in figure 2.16. Particles were produced by nebulizing 500 μl every 7-8 minutes and the concentration was measured for 1 second every 10 seconds by the ELPI. The concentration for all the measured particles is given together with the particle concentration of particles bigger than 0.7 μm . The latter fraction are the particles likely

2.8 Particle generation and characterization

to contain vegetative cells.

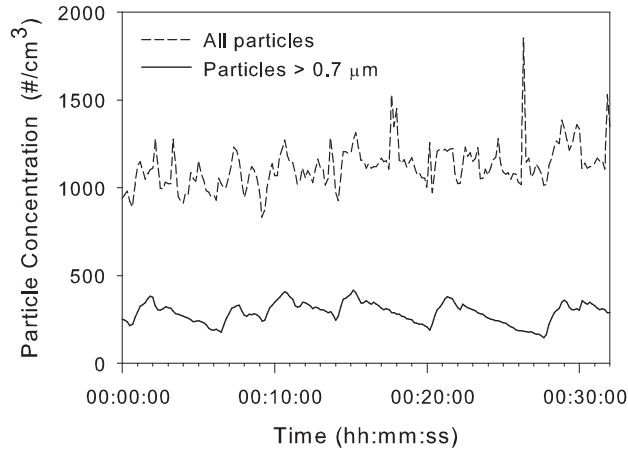


Figure 2.18:

The change of the particle concentration over the course of 30 minutes for all particles (dashed line) and particles bigger than $0.7 \mu\text{m}$ (solid line)

Figure 2.18 shows that the total particle concentration is highly variable over the course of the experiment. This might be caused by the way the measurement is performed: taking a ‘point’ measure of 1 second every 10 seconds. It is rather likely that the total particle concentration is constant. The particle concentration of the bigger fraction of the aerosol is less constant, since the moments on which the particles are generated are visible, by an increase in concentration. The subsequent decrease in concentration of the bigger particles is due to the sedimentation of the bigger particles.

From the figures 2.16 and 2.18 can be seen that the amount of small and very small particles is rather big. This fraction of small particles do not contain bacterial cells and might therefore interfere in the aerosol mass spectrometer. The fraction of small particles can be separated from the aerosol by a virtual impactor. A virtual impactor also concentrates the bigger particles in a smaller volume, which allows the instrument to be

used for environmental studies.

In the on-line MALDI analysis in which the aerosol particles are coated with a matrix by the evaporation-condensation principle, a constant particle concentration will result in a constant amount of matrix per particle (assuming an excess of matrix material available). With the developed particle generation system it is possible to keep the particle concentration rather constant, prohibiting a regular particle generation. The performed experiments with on-line coating, as described in chapter 4 and 5 are performed while monitoring the particle size and concentration with the developed particle generation and characterization system.

2.9 Applicability of IR-MALDI for bioaerosols

MALDI mass spectrometry has since its invention in the late 80s of the last century [Karas et al., 1987, Karas and Hillenkamp, 1988, Tanaka et al., 1988] been associated with pulsed UV-lasers. In 1990 Overberg et al. [1990][Overberg et al., 1991] reported the use of an IR-laser for MALDI analysis of proteinaceous material, following the work of Posthumus et al. [1978], who used a pulsed IR-laser for mass spectrometric analysis of involatile, thermally labile biomolecules. In the following the advantages and disadvantages of IR-MALDI as compared to UV-MALDI is discussed, followed by the discussion of a possible implementation of an IR-laser for the aerosol mass spectrometer.

The poor shot-to-shot reproducibility due to large variations in laser energy per pulse of IR-lasers, used to be the main factor prohibiting a wider utilization of IR-MALDI. This shot-to-shot instability seems to have decreased to the level of UV-lasers by the manufacturers of IR-lasers [Berkenkamp et al., 1997]. In general IR-MALDI is regarded as a softer desorption method.

As compared to UV-MALDI, IR-MALDI can be applied for the same analysis, although for the analysis of proteins and peptides UV-MALDI performs better [Dreisewerd et al., 2003]. With IR-MALDI better results are obtained for the analysis of large and labile compounds like DNA-molecules, since the degree of metastable ion fragmentation is much lower in IR-MALDI [Berkenkamp et al., 1998]. Metastable ion fragmentation is fragmentation that occurs in the source-extraction region (see figure 2.4)

2.9 Applicability of IR-MALDI for bioaerosols

when the ions are accelerated. The fragment ions enter the drift region with a velocity which is not proportional to the square root of the mass (see equation 2.2). The flight times of the fragments are intermediate to the molecular ions and the 'real' fragments, resulting in tailing of the main ion peak (toward the low mass side) and an increase in baseline noise [Cotter, 1997].

Other drawbacks reported for IR-MALDI, like the high sample consumption per laser pulse [Overberg et al., 1990, Cramer et al., 1996, Berkenkamp et al., 1997] does not hold for aerosol MALDI, since only one laser pulse is used per particle. As a matter of fact the high sample consumption will only be beneficial if this results in the formation of more ions. Sadeghi et al. [1997] obtained spectra with high resolution and low signal-to-noise ratio for a single shot, indicating that IR-MALDI would be very suitable for aerosol MALDI. A major advantage of IR-MALDI for on-line aerosol analysis would be the wide range of possible matrix materials, including simple liquids as water and glycerol. The use of liquid matrices in IR-MALDI has been reported to give better reproducible spectra than when solid state matrices were used [Berkenkamp et al., 1997, Caldwell and Murray, 1998]. The poor reproducibility of the solid state matrix materials was attributed to the heterogeneous matrix crystal layers.

The wavelengths of the lasers utilized in IR-MALDI research are around 3 μm (Er:YAG, 2.94 μm and Er:YSGG, 2.79 μm , tunable OPO systems 2.6-4.0 μm) [Overberg et al., 1990, Caldwell et al., 1997, Sadeghi et al., 1997, Berkenkamp et al., 1997, Niu et al., 1998, Caldwell and Murray, 1998, Sheffer and Murray, 1998, Berkenkamp et al., 1998, Schleuder et al., 1999, Cramer and Burlingame, 2000, Feldhaus et al., 2000, Lawson and Murray, 2000, Menzel et al., 2001, Berkenkamp et al., 2002, Menzel et al., 2002] 5-6 μm (the Free Electron Laser) [Cramer et al., 1996, 1997] and 10.6 μm (CO₂-laser) [Overberg et al., 1991, Menzel et al., 1999, Jackson and Murray, 2001, Berkenkamp et al., 2002]. At the different wavelengths the way the laser energy is absorbed by the matrix is different. The energy deposition at 3 μm results from vibrational excitation of O-H, C-H en N-H stretching modes of the IR-matrices. Between 5.5 and 6.5 μm the energy is absorbed by C=O stretch vibrations. Molecular excitation at 10 μm proceeds via the O-H deformation and C-O stretching modes.

Most experience in IR-MALDI has been obtained for the 3 μm wavelength range. This wavelength could also be used for the aerosol mass spec-

trometer. The Er:YAG and the Er:YSGG laser are so-called Q-switched lasers. These lasers utilize the light of a conventional flash lamp that is transformed to the right wavelength by a crystal. The lasers are equipped with a Q-switch. The Q-switch-material has non-linear characteristics, which causes a gradual build-up of energy in the laser medium. When the quality factor Q, defined as the ratio of stored energy over dissipated energy, is increased a burst of light occurs.

The implementation of IR-MALDI in the aerosol mass spectrometer, requires an IR-laser that can be triggered. As is shown by Kievit [1995] and Weiss [1997] the random external triggering of a Q-switched Nd:YAG laser (model HY1200, Lumonics Ltd. Rugby, UK) was not an efficient process. When the standard external trigger mode would be used it would have taken 180 μ s from an external trigger pulse to radiation output. Kievit [1995] and Weiss [1997] designed a different external trigger mechanism. The flash lamps were triggered in a fixed repetition rate of 10 Hz. A trigger signal (when a particle is detected) opens the Q-switch. The available time for the opening of the Q-switch is only 40 μ s per flash. When no particles were detected, the system had to wait for the next flash. The trigger efficiency of the system was determined to be $4 \cdot 10^{-4}$ in this operation mode.

Together with Bioptic Lasersysteme AG (Berlin, Germany) a similar, but more efficient trigger scheme was designed for a possible implementation of an IR-laser. As in the design of Kievit [1995] and Weiss [1997] the flash lamps will flash continuously at a fixed repetition rate, to keep the temperature and energy level of the flashes and the crystals stable. In contrary to the design of Kievit [1995] and Weiss [1997] two external trigger signals are required. The first trigger signal (the passage of a particle by the first detection beam) will generate a 'super pulse' of the flash lamp. This 'super pulse' can occur independently of the frequency of the flash lamps and will 'prepare' the Q-switch. A second trigger signal (the passage of the particle through the second detection beam) will open the Q-switch. The opening of the Q-switch will take place $140 \pm 40 \mu$ s after the first trigger signal. A schematic drawing of the trigger scheme is given in figure 2.19.

Due to the generation of the 'super pulse' the flash frequency of the flash lamp has no influence on the trigger efficiency. The trigger efficiency of this configuration is only dependent on the (delay) time between the first

2.9 Applicability of IR-MALDI for bioaerosols

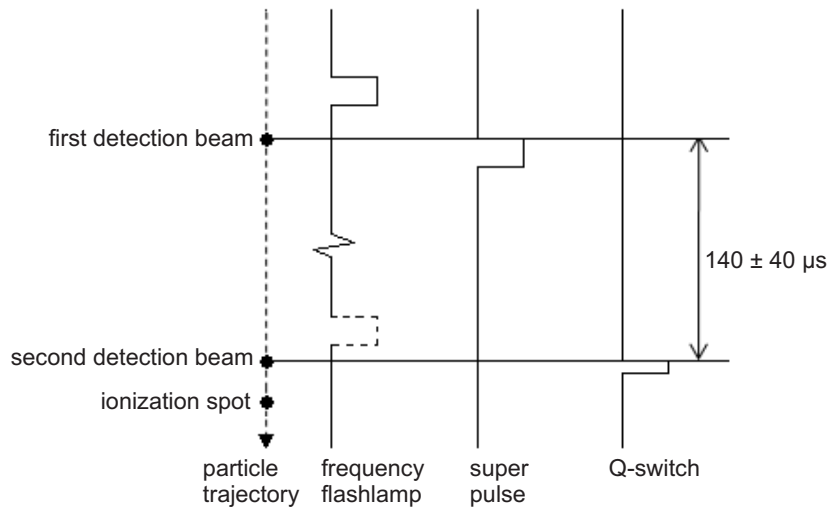


Figure 2.19: Schematic drawing of the trigger scheme for the IR-laser

trigger and the radiation output of the laser, which is $140 \pm 40 \mu\text{s}$. Around $7 \cdot 10^3$ particles per second can be detected with this triggering scheme (For comparison: the delay time of the Excimer laser is $1 \mu\text{s}$, resulting in the detection of $1 \cdot 10^6$ particles per second). The sampling efficiency of the aerosol mass spectrometer will decrease drastically by the implementation of an IR-laser.

An aerosol particle with a velocity of 250 m/s will travel a distance of $3.5 \pm 1 \text{ cm}$ in the response time of $140 \pm 40 \mu\text{s}$. The vacuum chamber of the mass spectrometer has to be modified with an extra port to allow detection and ionization. In addition, due to the uncertainty of $80 \mu\text{s}$, the ionization can take place over a length of 2 cm , requiring a beam diameter of the same length at the ionization spot.

The low sampling efficiency, the modification of the vacuum chamber, the IR-laser beam diameter and the not outstanding performance of IR-MALDI as compared to UV-MALDI are the reasons that IR-MALDI is not implemented.

2.10 Conclusions

The aerosol mass spectrometer has been developed into an aerosol MALDI mass spectrometer over the course of several years. The working principle of the instrument is divided into three steps: particle detection, particle selection and the analysis of the particles using mass spectrometry. Previous improvements in the design of the aerosol beam generator and in the particle detection (and selection) have resulted in an instrument with a better sampling and higher detection efficiency. Improvements implemented in this work are inspired by the idea to make the aerosol mass spectrometer suitable for bioaerosol analysis. The newly implemented improvements: the design of a repeller and an extractor plate and delayed extraction, have resulted in the capability to obtain mass spectra of single bioaerosol particles. Thus, the improvements which are already known to work in standard MALDI TOF mass spectrometry also improved the performance of the aerosol MALDI TOF mass spectrometer. The resolution was taken as a measure for the quality of the spectra, whereby the single shot resolution and overall resolution are distinguished. The single shot resolution increased from 1000 to 2000 and the resolution of summed mass spectra increased from 350 to 900. Isotopic resolution was obtained for a low mass peptide on single particle level. The sensitivity limit of the instrument is determined to be 1 zeptomole, which is sufficient for the analysis of bacteria particles. The observed peaks in the spectra have resolution values of 100 up to a mass range of 12.5 kDa and peaks are detected up to a mass of 21 kDa. This mass range is sufficient to allow the discrimination of bacteria particles. The discriminative power of the instrument is demonstrated with an externally mixed aerosol. It was found that with the aerosol mass spectrometer different protein particles with a mass difference of approximately 500 Dalton in the 5-6 kDa range and with 1000 Da mass difference in the 11-12 kDa mass range can be distinguished. The obtained resolutions, however, allow a discrimination of molecules with 125 Dalton mass difference at a mass of 12. kDalton.

The influence of other parameters on the quality of the mass spectra, like particle size and concentration, can be monitored with the developed particle generation system.

The aerosol mass spectrometer under investigation utilizes UV-MALDI mass spectrometry. The feasibility of IR-MALDI is investigated, since for

2.10 Conclusions

IR-MALDI more types of matrix materials can be used, including liquids. The triggering of an IR-laser requires a longer time than the triggering of the UV-laser. Therefore, implementation of an IR-laser will result in a less efficient apparatus. In addition, no outstanding performance of IR-MALDI above UV-MALDI is reported in literature.

Chapter 3

Particle Selection by Fluorescence

But the gate to life is very narrow. The road that leads there is so hard to follow that only a few people find it

(Matthew 7.14)

In this chapter it is described how only the biological fraction of an aerosol is selected for mass spectrometric analysis. The need for a pre-selection step is discussed, followed by the principle and implementation of the fluorescence preselection. Experiments with bacterial samples and measurements with an atmospheric aerosol are reported. The chapter ends with the analysis of the fluorescence signals of soot particles to determine if their omnipresence can obstruct the preselection of bioaerosol particles.

Parts of this chapter are published in 2007 in *Particle & Particle Systems Characterization* [Kleefsman et al., 2007]

3.1 Introduction

As is discussed in chapter 1 a fraction of the atmospheric aerosol particles has a biological origin. The total bioaerosol fraction includes viable and non-viable bacteria pollen, spores, algae, fungi, viruses, proteins, skin fragments, and more. The size of these bioaerosol particles ranges from a few tens of nanometers even to millimeters. The size of the bacterial bioaerosol particles can vary from $0.5 \mu\text{m}$ to $20\text{-}30 \mu\text{m}$, occurring as single cells or as clusters of cells [Hinds, 1999].

In chapter 2 it is described how the aerosol mass spectrometer has been optimized with respect to mass resolution and mass range. Furthermore, it was observed that only 1-5% of the total aerosol concentration sampled by the instrument results in a mass spectrum. Since only a fraction of the atmospheric load of particles is bacteria, a sensitive instrument is required.

Stowers et al. [2006] assumed for the sensitivity of a biological detector, the detection of one agent-containing particle per liter of air (ACPLA) within five minutes. In a report of the Department of Defense of the United States [of Defense, 2003] about the 'Chemical and Biological Defense Program' (to ensure that the Department of Defense has a world class defense capability that addresses all current and future threats to war fighter and homeland security missions) several examples for sensing instruments are given with different sensitivities. The values typically range from 10-100 ACPLA. To ensure a good detection of these agent containing particles, in the following example a sensitivity of 1 ACPLA to be detected in 5 minutes will be used.

In the aerosol mass spectrometer the particles are analyzed by mass spectrometry. The mass spectra can be used for identification of the particles. Assuming an identification capability of the instrument on the order of 50 % (meaning that 50% of the analyzed agent containing particles is correctly identified as a pathogen), 10 particles need to be detected within 5 minutes, to be sure that there is an attack and minimize the chance for a false alarm.

With an efficiency of the instrument of 1% 1000 agent containing particles have to be introduced into the mass spectrometer to detect those 10 particles, which corresponds to 1000 liter. This volume has to be analyzed in 5 minutes. The suction flow rate of the instrument is 0.6 lpm, and thus a particle concentrator with concentration factor of 330 is required.

3.1 Introduction

Common virtual impactors have this concentration factor or better.

In chapter 1 the concentration ranges of biological particles at different locations is presented. In the following example the concentration values of urban areas will be used, since these areas are likely to be target areas in case of a biological attack. A typical load of (culturable) biological particles in urban areas ranges from $1 \cdot 10^2$ to $4 \cdot 10^3$, with an average value of $1 \cdot 10^3$ bacteria per m^3 (see table 1.1 and figure 1.2). In the following the upper limit of 4000 bacterial particles per m^3 (4 per liter) will be used to represent a worst case scenario.

With the assumption that the agent containing particles are mixed with the background concentration, the foregoing example, with 1000 liter implies the processing of 4000 biological particles with the 1000 agent containing, *i.e.* a total of 5000 spectra are to be generated in 5 minutes. This corresponds to a sampling rate of 17 Hz for the mass spectrometer. Because the particles are not introduced equidistance in time the minimum sampling rate should be 50 Hz to have a reliable detection rate. Note that the assumptions in the foregoing example are worst case: the upper limit of the urban bacterial concentrations has been used, the assumed identification capacity is rather low and the lowest value for the instrument efficiency has been used. It is expected that a real sampling rate will be in the order of 10-50 Hz. These sampling rates are on the edge of the sampling rate of aerosol mass spectrometer, which is assumed to be 10-20 Hz.

The above mentioned example is based on the biological fraction of a total aerosol. Matthias-Maser et al. [2000] found that the biological fraction of a total aerosol is 20%. Thus to monitor all aerosol particles a sampling rate of 250 Hz is required. This sampling rate is not achievable with the present aerosol mass spectrometer. To avoid that the system is mainly processing non-bacteria particles a preselection step based on the fluorescing properties of biological particles is implemented in the aerosol mass spectrometer [Stowers et al., 2006]. The The fluorescing properties are caused by the excitation of the amino acid tryptophan, which is present in all biological aerosol particles. The fluorescence preselection step was inspired by the work done by Pinnick et al. [1995, 1998], Hairston et al. [1997], Pan et al. [1999].

In this chapter the principle of fluorescence is explained and how the fluorescence preselection is implemented in the system. The suitability of

the fluorescence preselection is investigated with known aerosols as well as with an unknown aerosol. Interference on the preselection by soot particles is also investigated.

3.2 Fluorescence principle

Biological material is known to contain fluorophores. Fluorophores are molecules that can be excited by absorbing a photon. During the excitation an electron moves up to a energy level, higher than its ground state. In the excited singlet state the electron in the excited orbital is paired to a second electron in the ground state orbital. When the electron subsequently relaxes from the excited state to the ground state it emits a photon. The emitted light has lower energy than the absorbed photon, resulting in light with longer wavelength than the excitation light. This emission is called fluorescence. For biological materials the largest fluorescent signals have been obtained with UV-radiation [Pinnick et al., 1995]. The fluorophores present in bacteria are the amino acids tryptophan, tyrosine and phenylalanine (excitation maximum 270-300 nm), reduced nicotinamide adenine dinucleotides (NADH, NADPH) (excitation maximum 340 nm) and flavin compounds (FAD, FADH, riboflavin, flavoproteins) (excitation maximum 450 nm). The fluorescence characteristics of bacteria particles when irradiated with one of the above mentioned wavelengths are not organism specific. Therefore, fluorescence emission is not suitable for bacteria discrimination [Pinnick et al., 1998, Van Wuijckhuijse, 2003, Stowers et al., 2006]. A more powerful approach is a multiple wavelength excitation. Sivaprakasam et al. [2004] demonstrate that with 266 and 355 nm excitation, combined in one instrument, aerosol particles consisting of proteins, vegetative cells or spores could be distinguished based on their (combined) fluorescence emission characteristics. Nevertheless, bacterial species could not be discriminated by Sivaprakasam et al. [2004]. The fluorescence emission can be used as a trigger criterion for more specific analysis, such as mass spectrometric analysis. Another example of an instrument that uses fluorescence emission as a selection criterion for further, more specific analysis is reported by Pan et al. [2004]. In their instrument the emission of fluorescence triggers a puffer to physically separate the bioaerosols from the remaining aerosols.

3.3 Experimental

To utilize the aerosol mass spectrometer for only the fraction of bioaerosols, the original optical configuration, as discussed in section 2.5 and figure 2.6, has been supplemented, with an UV-laser and optics to allow the collection of emitted fluorescence after excitation [Van Wuijckhuijse, 2003, Stowers et al., 2006]. In this configuration (referred to as ‘two color triggering’) the particle beam is intercepted by a continuous wave 266 nm laser beam (Coherent Inc., Santa Clara, USA) at the same spot as the top 632/532 detection beam. A pulsed UV-laser would have the disadvantage of the need of an additional triggering system and that together with the limited number of triggering events per unit time, would result in a less intense fluorescence signal, which would also depend on the time of the laser pulse. With a continuous laser beam the fluorophores can be excited multiple times during the time the particle is present in the laser beam.

For the collection of the emitted fluorescence a lens system and a gated UV-sensitive photomultiplier tube (Electron Tubes Ltd., Ruislip, UK; Model 9235QB) with a wave pass filter allowing light between 290 nm and 600 nm at 135° relative to forward scattering are mounted. The lens system consists of a plano convex fused silica lens ($f/1.6$), mounted inside the vacuum chamber to collimate the fluorescence. Outside the vacuum chamber another planoconvex lens ($f/6$) focuses the light onto the sensitive area of the PMT. The gating time (from ‘on’ to ‘off’) of the PMT is set at 1 μ s, to avoid any collection of the 308-nm laser light of the Excimer laser. This gating time is also the collection time of the fluorescence by the PMT, but fluorescence is only emitted during the residence time of the particle within the laser beam. The laser beam diameter is 75 μ m and for a particle with a velocity of 250 m/s, the residence time is 0.3 μ s.

With this dual beam set-up, fluorescence emission is added as an additional triggering criterion for the ionization laser, so that particles that fluoresce are selected by the system for further investigation by mass spectrometry. A schematic diagram of the instrument, including the fluorescence preselection is given in figure 2.6.

3.4 Size selection and fluorescence preselection

To demonstrate the principle of the fluorescence preselection an aerosol containing vegetative cells of the bacterium *Escherichia coli* was analyzed. To produce this aerosol vegetative cells of *Escherichia coli* K12 XL1 blue were cultured and harvested at TNO Defence, Security and Safety, Rijswijk, the Netherlands. Prior to nebulization, the bacterial samples containing 10^9 cfu/ml in growth medium, were washed three times by centrifuging the solution at 4000 rpm for 5 minutes; each time the supernatant was removed and the bacteria pellets, formed during centrifuging, were then resuspended in deionized water to approximately 10^9 cfu/ml. The final suspension was nebulized with a capillary tube nebulizer (Meinhard Glass Products, Golden, CO, USA, Model TR-30-A1). The aerodynamic size and the fluorescence characteristics above a preset threshold of the particles were measured. The fluorescence threshold was set to be just above the noise of the PMT, so that all the recorded fluorescence was emitted by the aerosol particles. Figure 3.1 is a histogram of data obtained using the ‘two color’ detection from the *E. coli* aerosol. The size range of the particles with fluorescence intensity above the preset threshold is approximately 1-3 μm , which indicates that the particles contain one to a few bacteria cells. The fluorescence intensity range measured is narrow, indicating that a homogeneous aerosol was produced. The histogram in figure 3.1 shows that fluorescence can be used as a trigger criterion to preselect the biological particles from an aerosol.

The capability of the instrument for particle sizing and fluorescence preselection is also demonstrated by the analysis of an aerosol containing spores of *Bacillus atrophaeus*. The aerosol was produced by dispersing *Bacillus atrophaeus* spores (provided by TNO Defence, Security and Safety, Rijswijk, The Netherlands) at $1.8 \cdot 10^5$ cfu/mg, mixed with small silica particles as a desiccant, with a DeVilbiss powder disperser (Model 175) into an aerosol chamber. The particles that emitted fluorescence above the preset threshold are presented in a particle size/fluorescence histogram in figure 3.2. The irradiation time of 0.3 μs is significantly longer than typical pulsed laser fluorescence measurements and allows analysis of particles containing single cells using a relatively small solid angle of fluorescent light collection. The detected particles are present over a wide size range and same size particles exhibit fluorescence with intensities over a wide

3.4 Size selection and fluorescence preselection

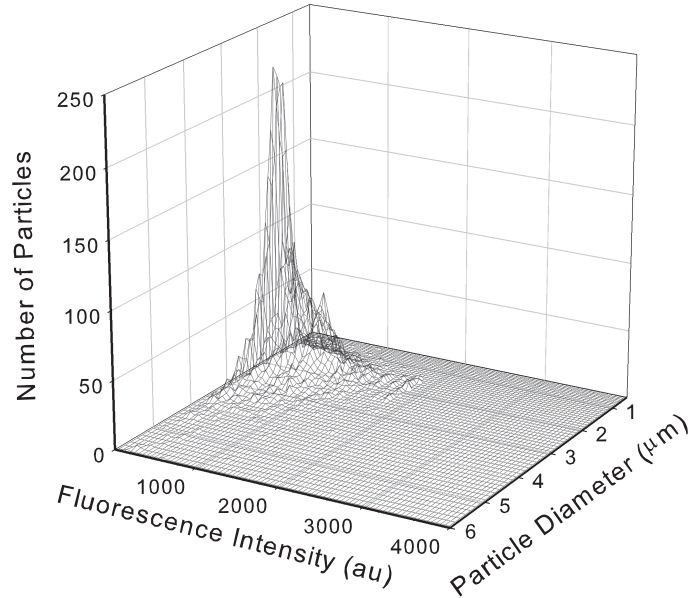


Figure 3.1:

Histogram of particle size and fluorescence intensity obtained from an aerosol containing *Escherichia coli*

range. Frequently the fluorescence intensity resulted in a maximum output current (saturation) of the photomultiplier. This occurs even for particles in the size range between 1 and 2 μm ; there is no apparent correlation between the size and the emitted fluorescence. The different fluorescence intensity for same size particles can be due to several factors, including the laser beam profile, and the morphology and composition of each particle. The difference due to the particle morphology and composition might be caused by the way the spores were produced. When the spores were grown, they are freeze-dried together with the growth medium they are in. During the freeze drying process some cells are destroyed. Silicon oxide particles are added to improve the flowability of the sample. The aerosol particles as produced with the nebulizer do not necessarily exist of whole cells, but might contain parts of the growth medium and silicon

oxide as well. To avoid the mass spectrometric analysis of small particles that hardly contain any bacterial information, an additional criterion, the particle size, is used. Since, the presence of emitted fluorescence is used only as a trigger criterion in our instrument, no qualitative measurements using the ‘two color triggering’ are carried out.

When figure 3.1 and 3.2 are compared, it can be seen that the mean particle diameter and fluorescence intensity are different for the two types of aerosol. This difference can be caused due to the fact that two different organisms are used. Another explanation can be the washing of the *Escherichia coli* cells. The cells are washed with deionized water. Due to the difference in osmotic pressure the cells might swell, resulting in bigger aerosol particles. Due to the washing the cells might have lost some fluorophores, resulting in less intense fluorescence signal. Again is shown that the particle fluorescence information, together with the particle size, serves as a preselection step, to reserve the instrument for only those aerosol particles that might contain bacteria.

3.5 Fluorescence properties of atmospheric air

Atmospheric air was analyzed to test the fluorescence preselection on an unknown aerosol and to determine the contribution of bioaerosols to the total atmospheric aerosol concentration. Atmospheric air was analyzed over the course of an evening (3 hours) when there was minimal human activity. The windows of the laboratory were opened and the only entrance to the room was closed. A bank of fume hoods opposite the windows ventilated the room. The suction rate of the 6 fume hoods together was approximately $30\text{ m}^3/\text{min}$, resulting in approximately 4 air exchanges per hour in the laboratory. A virtual impactor (MSP Corp, Shoreview, MN, USA; Model 4240) with an inlet flow rate of 270 l/min was connected to the aerosol inlet of the mass spectrometer to concentrate the air. The virtual impactor acts to concentrate particles in the range of 1 to 10 μm , with a 50% cutoff at 1.0 μm and a concentration factor of 450. The aerodynamic size and fluorescence characteristics of all the particles were measured.

Figure 3.3a shows a histogram of all the data collected over 3 hours from atmospheric aerosol, and figure 3.3b shows that fraction of the same

3.5 Fluorescence properties of atmospheric air

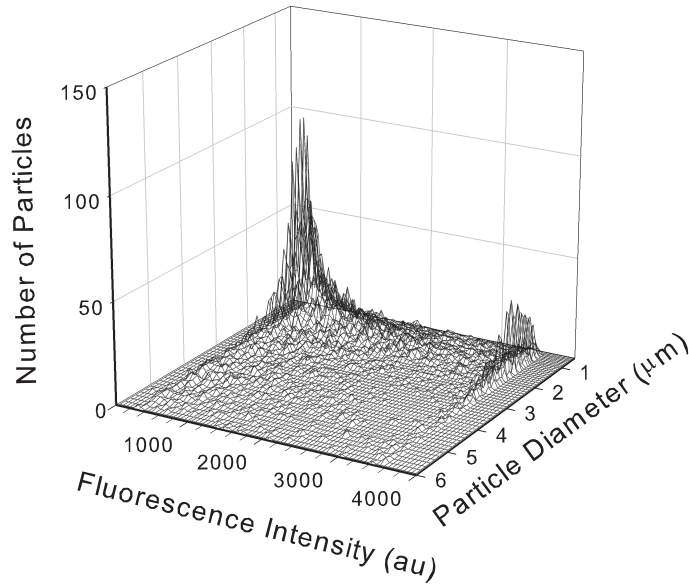


Figure 3.2:

Histogram of particle size and fluorescence intensity obtained from aerosol containing spores of *Bacillus anthropheaus*

aerosol that had fluorescence above a preset threshold. The majority of the sampled atmospheric aerosol particles is small (1 to 2 μm) and shows no or very little fluorescence (figure 3.3c). Particles around 2 μm were the most common of the fluorescing particles, with over half of the 3- μm particles emitting significant fluorescence (figure 3.3d). The size of the fluorescing particles is in the same order as shown in figures 3.1 and 3.2. One can be reasonably sure that these particles might contain bacteria. Since this experiment was performed to demonstrate the fluorescence pre-selection, no mass spectrometric analysis is performed on the atmospheric air particles. The fraction of the particles that show significant fluorescence is 23% of the total measured particles. This number corresponds for example with the 20% found by Matthias-Maser et al. [2000], who measured the total atmospheric bioaerosol concentration in a rural area. The total bioaerosol concentration of the atmospheric air was calculated using

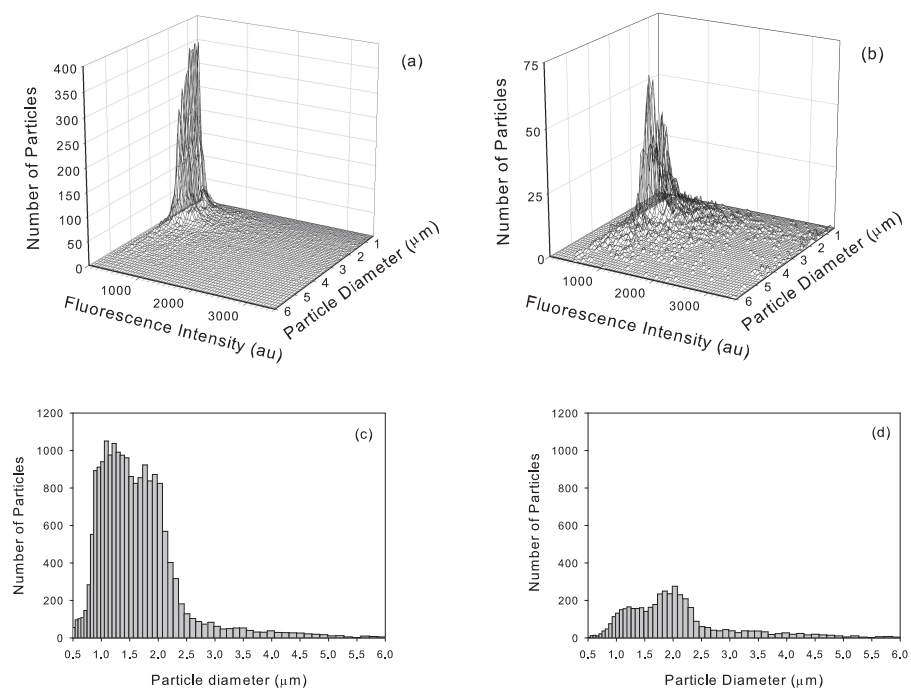


Figure 3.3:
Histograms of particle size and fluorescence intensity obtained from atmospheric aerosol, a) all collected particles and b) the fluorescing particles. Particle number distribution of c) all the collected atmospheric particles and d) the fluorescing particles

the following variables: 4300 fluorescing particles were detected in 3 hrs, a sampling efficiency of 1%, a flow rate of 0.6 lpm and a concentration factor of 450 due to use of the virtual impactor. The total concentration was 10^4 bioaerosols per m^3 . This number corresponds to the total microbial concentration range found in urban and rural areas, see figure 1.2 and 1.4.

3.6 Fluorescence properties of soot

It is known that other than biological particles can produce fluorescence signals that are similar to those of the bioaerosols [Pinnick et al., 1995]. For instance, Merola et al. [2001] have investigated the fluorescence behavior of exhaust diesel soot particles, when irradiated with UV-laser light. They found that diesel soot emitted fluorescence, with strong fluorescence bands at 300 and 400 nm. Pan et al. [2003] investigated the possible masking effects of diesel soot on their single particle fluorescence spectrometer and found that supermicrometer particles exhibit significant fluorescence. The excitation wavelength used by Pan et al. [2003] was 266 nm and the masking effects of diesel soot they found, might also be present in the aerosol mass spectrometer. Therefore, the possible interference of soot particles on the fluorescence preselection in the aerosol mass spectrometer is investigated.

A direct injection, 3-cylinder diesel engine (Lister-Petter LPW-3), fueled with a summer quality diesel, was used to produce soot particles. Soot particles were collected in an aerosol chamber of 25 liters from the exhaust pipe of the engine. Then the filled aerosol chamber was quickly transported to the laboratory and the chamber was connected to the instrument. The experiment was performed twice. In the first experiment the size and fluorescence characteristics of all the sampled particles were measured and in the second experiment the size and fluorescence characteristics of only the fluorescing particles were measured. The sampling time in both experiments was 70 minutes.

Figure 3.4a shows the particle size histogram resulting from the first experiment, in which the size and fluorescence of all the sampled particles were measured. Figure 3.4b shows the particle size histogram of the second experiment, in which the size and fluorescence of only the fluorescing particles were measured. The particle size histogram of all the

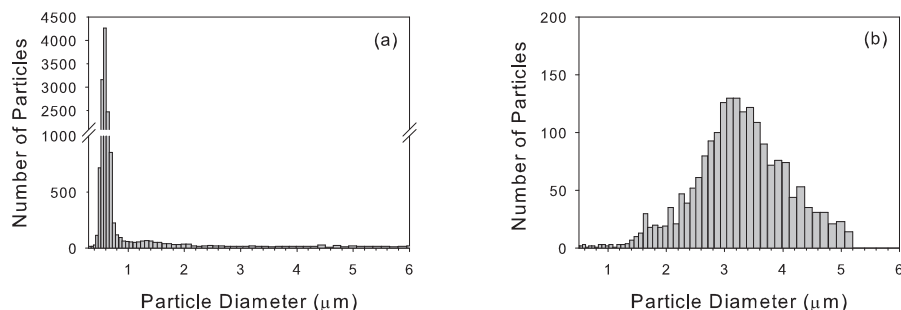


Figure 3.4:

Particle number distributions of the collected soot particles. a) All sampled particles and b) fraction of the particles with fluorescence above preset threshold

detected particles (figure 3.4a) has a mode of $0.6 \mu\text{m}$ aerodynamic diameter, but contains a significant tail toward larger particles. The vast majority of the soot particles do not emit fluorescence above the preset threshold of the PMT. However, the second experiment in which only the fluorescing particles were measured, only the large particles, proves that primarily in the 2 to $5 \mu\text{m}$ size range, emitted significant fluorescence as can be seen in figure 3.4b. The 2 to $5 \mu\text{m}$ -particles were also detected in the first experiment. These particles are probably due to coagulation of small soot particles in the aerosol chamber [Schnell et al., 2004]. Pan et al. [2003] discussed that the fluorescing particles they measured were a result of coagulation, due to the experimental circumstances: collection of the soot samples in an enclosed aerosol chamber. This coagulation is less likely in a ‘normal’ atmosphere, because of the immediate dilution. A small fraction of soot aerosol has the size and fluorescence properties of bacteria-containing particles, as can be seen in figure 3.5 and must be discriminated by mass spectrometry analysis. Thus, soot particles are seen as a small but possible source of interference.

3.7 Comparison of size and fluorescence of different aerosols

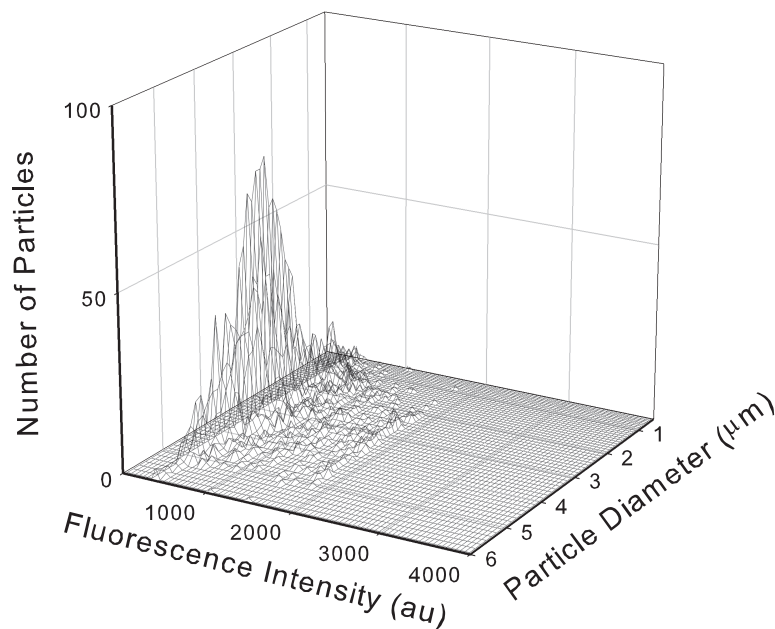


Figure 3.5:

Histogram of particle size and fluorescence intensity obtained from the fluorescing fraction of the soot aerosol

3.7 Comparison of size and fluorescence of different aerosols

The implementation of fluorescence preselection was initially meant to use the emitted fluorescence as a selection criterion. As is already mentioned in section 3.2 the fluorescence characteristics of bacteria particles are not species specific. However, in the following is investigated if the emitted fluorescence in combination with the size could provide additional information about the composition of an aerosol.

In figure 3.6 the size and the (integrated) fluorescence intensity of 80% of the aerosol particles of *Escherichia coli* (derived from figure 3.1), of *Bacillus atrophaeus* (derived from figure 3.2) and diesel soot (derived from

figure 3.5 are given.

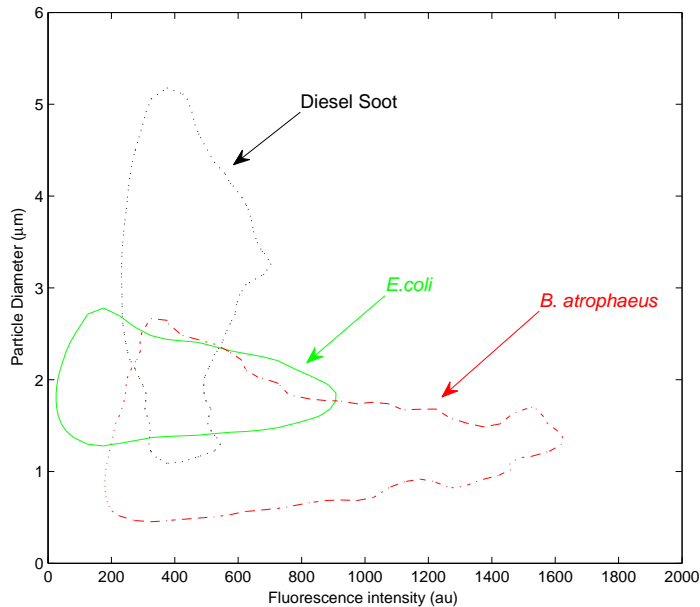


Figure 3.6:

Contour plots of particle size versus fluorescence intensity for *Escherichia coli*, *Bacillus atrophaeus* and diesel soot

As can be seen in figure 3.6 the area covered by *Escherichia coli* is almost completely overlapped by the areas covered by *Bacillus atrophaeus* and diesel soot. Also can be seen that the fluorescence threshold of the UV-PMT used in the experiment with *Escherichia coli* (see section 3.4) was lower than used in the experiments of the other two aerosols. This could be due to a different intensity of 266 nm laser beam in the different experiments. The overlapping indicates that the combination of size and emitted fluorescence of *Escherichia coli* is not a distinctive feature for this type of bacterium.

The area that is covered by *Bacillus atrophaeus* is characterized by a wide range of fluorescence intensities and a rather small size range. The

3.8 Conclusions

area that is covered by diesel soot is characterized by a low fluorescence intensity and a wide size range. When measuring an aerosol composed of these three particle types solely, the obtained size and fluorescence information could provide some additional information about the composition of the aerosol particle, or could be used as a confirmation for the mass spectrometric analysis. However, the additional information and/ or confirmation can be obtained only if the fluorescence intensity is high or when the particles are large. For all intermediate cases the combination of size and fluorescence provides no additional information. In addition a slightly different laser intensity might already cause a different fluorescence signal, indicating that the value of the fluorescence intensity is not a robust characteristic. It is expected that the size and fluorescence characteristics of more types of bacterial aerosol particles will overlap the characteristics of the above mentioned bacterial species, and that different aerosols can not be distinguished by using the combination of size and fluorescence.

A more powerful approach to use the size and fluorescence as additional information is the use of multiple wavelength excitation, which is demonstrated by Sivaprakasam et al. [2004]. With the combined fluorescence characteristics aerosol particles consisting of proteins, vegetative cells or spores could be distinguished. However, bacterial species could not be discriminated using the multiple wavelength excitation [Sivaprakasam et al., 2004]. Thus, it might be possible to obtain additional information about the composition of an aerosol using size and (multiple wavelength) fluorescence information, but discrimination based on these two parameters is rather unlikely. Therefore, the emitted fluorescence is used only as a trigger criterion in the current mass spectrometer.

3.8 Conclusions

A selection step, based on fluorescence has been implemented to increase the sensitivity of the instrument. The capability to select the bioaerosol fraction out of an aerosol based on the fluorescence emission has been demonstrated with a pure aerosol containing *Escherichia coli* and with an mixed aerosol consisting of *Bacillus atropheus* and silicon oxide. The obtained particle size and fluorescence histogram of the mixed aerosol showed a similar fluorescing behavior, as obtained from the pure aerosol.

Chapter 3 Particle Selection by Fluorescence

The silicon oxide particles were not detected in the mixed aerosol. Similar fluorescence emission characteristics were also obtained when an unknown aerosol, atmospheric air, was analyzed. Approximately 20% of the analyzed atmospheric aerosol particles were identified to be biological. The original concentration of these particles was calculated to be in the order of 10^4 bioaerosol particles m^3 , corresponding with the concentration ranges found in chapter 1. The experiments proved that with the implementation of fluorescence preselection bioaerosols particles are selected from non-bioaerosol particles. The result is that the mass spectrometer can be reserved for the fluorescing particles to perform mass spectrometric analysis.

The interference of diesel soot particles on the applied preselection was investigated. A minor fraction of the diesel aerosol had the size and fluorescence characteristics of bacteria. However, this interfering fraction is expected to be easily discriminated by mass spectrometry.

The combination size and fluorescence information is investigated to provide additional information about the composition of an aerosol. It was found that this combination is not distinctive to discriminate different bacterial aerosols. An additional UV-laser with a different wavelength, to excite other fluorophores would offer the possibility to obtain additional information about the composition of an aerosol particle. Obviously this second excitation has to take place before mass spectrometric analysis. Another possibility is to divide the wavelength range of the emitted fluorescence into two parts and to plot the total fluorescence intensities of each wavelength range against each other. However, complete classification or identification, up to species or strain level is not possible with only fluorescence, therefore the fluorescence signal is only used as a trigger criterion in this work.

Chapter 4

Effect of Sample Preparation and Composition in Aerosol MALDI

You may think you have won your case
in court, until your opponent speaks

(Proverbs 18.17)

This chapter about the sample preparation in MALDI mass spectrometry starts with the history and principles of standard MALDI mass spectrometry. The matrix materials, sample compositions and methods for sample preparations are discussed. Then the sample preparation methods used in aerosol MALDI, the premixed method, the impaction and evaporation/condensation method and the on-line coating method are reported. The main part of this chapter describes the effect of sample composition on the appearance of the mass spectra. The effect of fifteen matrix-solvent combinations on the formation of ions, the peak areas and the variability of the peak areas is discussed.

4.1 Introduction

The first use of a laser in mass spectrometry was demonstrated by Honig in 1963 and in 1968 Vastola and Pirone [1968] demonstrated the applicability of laser mass spectrometry on organic compounds [Lubman, 1990]. The samples to be analyzed were irradiated with short laser pulses (nsecs to psecs) of high intensity (up to $\pm 10^8$ W/cm²) in vacuum. This technique is called LDI (Laser Desorption/Ionization). Due to the laser irradiation a fast heating of the substrate is induced and ions are emitted thermionically from the hot center of the sample. Intact molecules at lower temperatures, outside the hot center are vaporized. The length and rate of the heating, as well as the type of molecule, determine whether the molecules will evaporate or thermally degrade. The latter happens at longer irradiation times and higher irradiance power.

In 1978 Posthumus et al. [1978] used LDI to analyze bio-organic molecules. He found hardly any degradation of a polypeptide of ~ 800 Dalton, in contrary to nucleotides, which did show extensive break-up. The analysis of higher molecular mass peptides resulted in extensive fragmentation.

It was not before the mid 80s of the 20th century that easy and quick mass spectrometric detection of peptides and proteins (*i.e.* high molecular mass biomolecules) became reality. In 1987 Karas et al. [1987] reported the use of a matrix compound for the analysis of non-volatile compounds. The idea was adapted from the good results obtained by using a liquid matrix (glycerol) for fast atom bombardment (FAB)/secondary ion mass spectrometry (SIMS) for the analysis of non-volatile organic compounds. In 1988 Karas and Hillenkamp [1988] and Tanaka et al. [1988] independently published mass spectra of proteins up to molecular masses of 100,000 Dalton, using a mixture of cobalt powder (with a particle size of 300 Ångstrom), dispersed in glycerol (Tanaka et al. [1988]) and nicotinic acid (Karas and Hillenkamp [1988]) as the matrix materials. Not long after that, this new technique in mass spectrometry became known as 'MALDI' (matrix-assisted laser/desorption ionization). The invention of MALDI initiated the 'quest' for matrix-compounds, but until now no universal matrix compound has been found.

In this chapter the different MALDI matrix materials and sample preparation methods as used in standard MALDI mass spectrometry are discussed. Also the ionization and desorption processes are discussed. The

main part of this chapter handles about the sample preparation methods in aerosol MALDI and the effect of the sample preparation on the mass spectra. Therefore, the effect of matrix material and solvent composition on ion signals is determined. For this analysis a computational program was developed. Details, background thoughts and procedures of this program are discussed and concludes with recommendations for the matrix-solvent choice.

4.2 MALDI mechanisms: desorption and ionization

In the MALDI technique the matrix has several functions. The matrix material serves as the primary and highly efficient absorber of the laser irradiation. Upon radiation the matrix molecules break down rapidly and expand into the gas phase while carrying along intact analyte molecules. In this reactive plume the matrix promotes the ionization of the analyte molecules [Cotter, 1997]. The ion formation is suggested to be the result of two mechanisms: primary and secondary ion formation. Both types of ions are observed in the mass spectra [Zenobi and Knochenmuss, 1998].

The ‘primary’ ions are generated from neutral molecules in the sample and are often matrix-derived species. The ions are formed by multiphoton ionization, thermal ionization and excited-state proton transfer [Zenobi and Knochenmuss, 1998]. The ‘secondary’ ions are the ions formed by non-primary processes and involve analyte ions. Molecular dynamic simulations performed by Zhigilei et al. [2003] show that the MALDI plume is a result of a very rapid solid-to-gas phase transition, whereby material is ablated from the surface of the sample into the gas phase.

Secondary ion formation can occur when a MALDI plume containing primary ions exist. In the plume matrix-matrix reactions occur, providing intermediates that can protonate analytes. Also matrix-analyte reactions occur in which the charge of the matrix is transferred to the analyte molecule. A third mechanism for the ionization of analyte molecules is the gas-phase cationization. The cations are usually not added to the sample, but originate from ubiquitous sodium and potassium impurities in the sample [Zenobi and Knochenmuss, 1998].

Karas et al. [2000] investigated the reason why mostly singly charged ions are detected in MALDI mass spectrometry and proposed that the MALDI-ions are survivors of a possibly highly efficient ionization and that only singly charged ions have a chance of surviving.

Currently, the principle and mechanisms of MALDI is still under investigation by several research groups. Simulations and experimental data are combined with matrix properties to understand the processes in MALDI [Mirza et al., 2004b, Breuker et al., 2003, Knochenmuss and Zenobi, 2003, Erb et al., 2006, Meier et al., 2007, Chang et al., 2007].

4.3 MALDI matrices

4.3.1 MALDI matrix compounds

As the name of the MALDI (matrix-assisted laser desorption/ionization) technique implies a matrix compound is used for the analysis. Since the introduction of the technique, several matrix compounds, each with their own characteristics are reported. In the following an historic overview of the most important, commonly used matrix materials is given.

The inventors of MALDI (Karas and Hillenkamp [1988] and Tanaka et al. [1988]) used two completely different matrix materials. The use of ultrafine cobalt powder by Tanaka et al. [1988] was supposed to enhance the speed of sample heating, due to following characteristics of the fine particles, as compared to bulk material: high photo-absorption, low heat capacity, and extremely large surface area per unit volume, resulting in the easy formation of molecular ions. This type of matrix has not been extensively exploited in the field of MALDI mass spectrometry. Some papers are published in which pencil lead (graphite) has been used as a MALDI matrix, also for the analysis of biological material [Li et al., 2005, Black et al., 2006]. The matrix material nicotinic acid as used by Karas and Hillenkamp [1988] was suggested to control the coupling of laser energy into the condensed phase, to initiate chemical reactions between excited-state and ground-state matrix and/ or analyte molecules, and to control the disintegration of the condensed phase, resulting in a 'soft-desorption' of the analyte molecules. The matrix material nicotinic acid is seen as the first one belonging to the organic matrix materials.

4.3 MALDI matrices

In 1989 Beavis and Chait [1989b,a] did a survey for matrix materials using cinnamic acid derivatives, whereby they introduced sinapinic (SA), ferulic (FA) and caffeic (CA) acid as new matrix compounds. A non-cinnamic derivative matrix material, was introduced in 1991 by Strupat et al. [1991] namely, 2,5-dihydroxybenzoic acid (DHB). So far, only solid state organic matrices were used¹. In 1991 Zhao et al. [1991] introduced the first liquid matrix: nitrobenzyl alcohol (NBA), shortly followed by Chan et al. [1992] and Cornett et al. [1993] who also used liquid matrices. Cornett et al. [1993] included also coumarin as a solid state matrix material in their study. An extensive study on coumarin dyes as MALDI matrix materials was done by Perera et al. [1994] in 1994.

More investigations of Beavis et al. [1992] resulted in 1992 in the introduction of another cinnamic derivative as a matrix material: α -cyano-hydroxycinnamic acid. In 1993 a group of basic matrix materials (derivatives of pyrimidine and pyridine as well as benzene derivatives containing basic amino groups) was studied by Fitzgerald et al. [1993]. The best results for the analysis of biological material were obtained with two substituted nitropyridines.

Other reported matrix materials are: benzoic acid derivatives [Juhász et al., 1993, Karas et al., 1993, Bashir et al., 2003], picolinic acid [Tang et al., 1994] and substituted acetophenones [Zhu et al., 1996], but no significant better performance as compared to the more common matrix materials, was reported for picolinic acid, the benzoic acid derivatives and the substituted acetophenones.

Another class of organic MALDI matrix materials is the group of mercaptobenzothiazoles, first introduced in 1997 by Xu et al. [1997]. The successful usage of substituted derivatives of the mercaptobenzothiazoles is reported by Raju et al. [2001] and Mirza et al. [2004a].

Nowadays, the cinnamic acid derivatives ferulic acid, sinnapinic acid and α -cyano-hydroxycinnamic acid and the non-cinnamic acid derivatives dihydroxybenzoic acid and mercaptobenzothiazole are the solid state matrix materials that are commonly used in MALDI mass spectrometry. Although the search for a universal MALDI matrix compound has not been given up, it seems to be a non-feasible goal. In figure 4.1 the chemi-

¹The solvent glycerol, as used by Tanaka et al. [1988] is not regarded as a matrix material here, since the 'matrix-effect' was attributed to solid state cobalt powder.

cal structures of the most common solid state matrix materials are given in the order of historical introduction as described above. Since the application of MALDI mass spectrometry for aerosol analysis is quite a young field of research, no specific ‘aerosol matrices’ are reported. Therefore, the commonly used solid state matrices are used for aerosol MALDI in this work, but also by other researchers: *e.g.* by Beeson et al. [1995], Russell et al. [2005], Harris et al. [2006], Jackson et al. [2004].

In this work the matrix PMC (a proprietary made compound, order number 0145GM02, kindly provided by TNO Defence, Security and Safety, Rijswijk, The Netherlands) is often used. For confidentiality reasons the only information that can be given about this compound is that it has a mass range of 100-160 Dalton and it sublimates at atmospheric pressure.

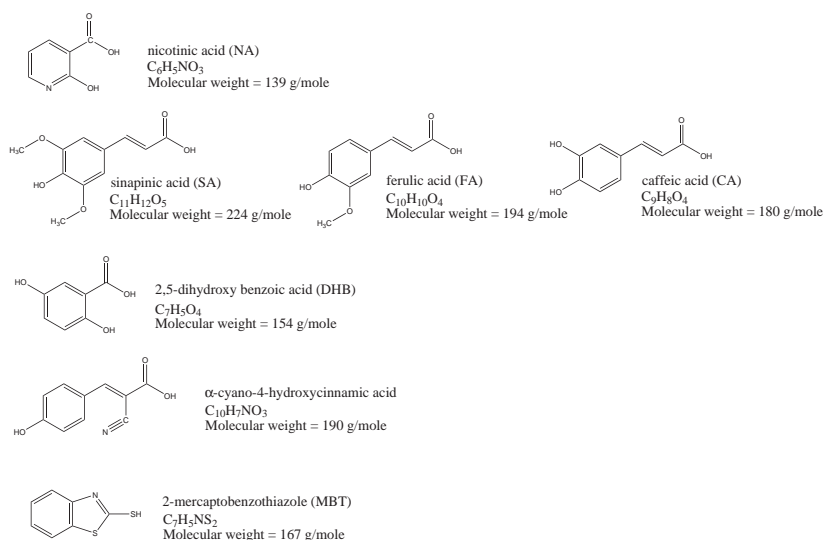


Figure 4.1: Chemical structures of common MALDI matrix materials

4.3.2 MALDI matrix properties

There are several properties that determine the utility of a material as a MALDI matrix. The selection criteria in the first systematic survey for matrix materials by Beavis and Chait [1989b] next to the requirement

for strong absorption at the excitation wavelength (266 nm) were: the solubility in aqueous solutions and a low boiling/ sublimation point [Beavis and Chait, 1989b]. The presence of the matrix, implies that it should co-exist with the analyte in the condensed phase. It should be capable to absorb laser energy and to transfer this energy to the analyte molecules via ion or molecule interactions [Fitzgerald et al., 1993]. This translates itself to four requirements, which are defined by Juhasz et al. [1993] for the matrix

- miscibility with the analyte in the solid phase and soluble in the solvent used during the sample preparation
- high molecular extinction coefficient at the chosen irradiation wavelength
- a low heat of sublimation
- proper chemical composition: the protonation of the analyte might be due to the presence of OH and/ or NH bonds in the matrix compound². The analyte is protonated via ion or molecule interactions in the gas phase

Perera et al. [1994] added to the above mentioned functions that a matrix material should protect the analyte molecules against thermal degradation, and that the performance of the matrix compound should not be affected by impurities such as salts or detergents that might be present in the sample solution.

The above mentioned requirements and functions are derived for standard MALDI mass spectrometric analysis and are also applicable in aerosol MALDI, since most of the functions and requirements deal with the desorption/ionization processes in the mass spectrometer. Those processes are the same for both types of MALDI. The difference between standard and aerosol MALDI is the area-to-volume ratio, which is in aerosol MALDI larger. The larger area in aerosol MALDI is expected to result in a better contact and mixing between analyte and matrix molecules and therefore less matrix material might be needed.

²When the ionization of the analyte is caused by cation or anion attachment the presence of OH or NH bonds is not necessary

4.4 MALDI sample composition

As in cooking the ingredients of a dish determines the taste, the ingredients in a MALDI sample determines the outcome of an analysis. Depending on the target analyte(s) a matrix is chosen. For the analysis of peptides and small proteins, the matrix α -cyano-hydroxycinnamic acid is often used. Due to the tendency for multiple protonation it is less suitable for proteins [Beavis et al., 1992]. Sinapinic acid and ferulic acid are commonly used for the analysis of proteins. The cinnamic acid derivatives are tolerant for contaminants like salts or detergents [Beavis et al., 1992, Beavis and Bridson, 1993] but have the (minor) disadvantage of adduct formation and the formation of background ions in the low mass range [Beavis et al., 1992]. The matrix 2,5-dihydroxy benzoic acid (DHB) was found to give hardly any adduct formation and was very tolerant for contaminants [Strupat et al., 1991], but has the disadvantage of a low signal-to-noise ratio for high mass proteins [Karas et al., 1993]. An advantage of DHB is the suitability of this material for the analysis of carbohydrates and oligonucleotides [Karas et al., 1993, Fitzgerald et al., 1993].

Next to the choice of matrix material, the solvent in which the analyte and matrix are dissolved affects the quality of the spectra. The effect of the solvent composition and the presence of detergents on the common MALDI analysis of proteins is studied by Cohen and Chait [1996], Börnsen et al. [1997], Sze and Chan [1998], Loo and Loo [2007] for instance. Several combinations of water and organic solvents as methanol, ethanol, propanol, acetonitrile, tetrahydrofuran were investigated. One observed effect of the solvent composition is the influence on the rate of the co-crystallization of matrix and analyte. When a slow crystallization procedure was applied, high mass components were detected, in contrary to a rapid crystallization process where the formation of low mass ions was favored [Cohen and Chait, 1996]. Note that the solvent composition is not the only factor influencing the crystallization, the sample preparation method (see section 4.5) is also a determining factor for the crystallization process.

Commonly used recipes include the use of an acid, usually trifluoroacetic acid (TFA) in an amount of 0.1-1% of the total sample weight or volume. The role of the acid addition is not fully understood. One of the reasons is to reduce the effect of contaminants as salts, detergents

4.5 Standard MALDI sample preparation methods

or buffers [Kussman et al., 1997], suggesting that TFA acts as a proton donor by lowering the pH of the sample. A second reason for the addition of TFA is to enhance the solubility of proteins [Börnson et al., 1997, Loo and Loo, 2007]. Cohen and Chait [1996], who added formic acid, found an effect of the pH on the presence of ions. At pH values lower than 1.8 mostly ions with masses bigger than 2 kDalton were detected, whereas at pH values higher than 2.3 ions smaller than 2 kDalton were present in the mass spectra. Experiments performed by Loo and Loo [2007] show that different acids produce spectra with a different subset of proteins, when the same protein mixture is analyzed. In this work the effect of the pH is not investigated, usually an acid concentration of 0.1% TFA was used.

4.5 Standard MALDI sample preparation methods

Besides the discovery of MALDI matrix materials, also different methods for the sample preparation have been reported. The chosen procedure to prepare the sample, next to the chosen matrix material, determines the outcome of the experiment. During the sample preparation the analyte and matrix need to co-crystallize to allow proper ionization and detection of the analyte molecules. Commonly used sample preparation methods are the dried-droplet method, the fast evaporation method, the slow evaporation method and the crushed-crystal method, each resulting in different crystals. The above mentioned sample preparation methods are discussed in the following.

The way the samples were prepared at the time the MALDI technique was introduced is still the most common method used in MALDI mass spectrometric analysis. This method is called the dried-droplet method. In this method a solution containing dissolved matrix molecules is mixed with a small amount of a solution containing the analyte molecules. The matrix is usually dissolved in mixtures of water and organic materials, like acetonitrile, methanol, ethanol or higher alcohols. The organic solvents serve to dissolve the matrix material. The analyte is usually dissolved in water. Aliquots of the resulting solutions are spotted onto a MALDI target. After evaporation of the solvent the sample is ready to be analyzed.

Advantages of this methods are the easiness, the high tolerance for contaminants such as salts and buffers, and the suitability to use this method for all kind of (mixed) samples. The main drawback of this sample preparation method is the inhomogeneous distribution of the analyte molecules in the matrix crystals. In some cases where sinapinic acid or dihydroxybenzoic acid are used, higher concentrations of the analyte molecules were found in the outer edge of the dried spot and high concentrations of salts were found in the center of the sample spot [Strupat et al., 1991, Dai et al., 1996a]. This results in the presence of the so-called ‘hot spots’ or ‘sweet spots’, for which have to be searched through the sample spot.

A method to obtain a homogeneous distribution of the analyte molecules within the matrix crystal is the slow evaporation method [Beavis and Bridson, 1993, Cohen and Chait, 1996]. Large, analyte doped matrix crystals are grown under near equilibrium conditions, which can be used immediately in the ion source. The main advantage of this method is that the crystals have more defined starting conditions which is useful for fundamental MALDI ionization studies.

Another way to avoid the segregation and inhomogenization of the analyte molecules, is to let the solvent evaporate very quickly by vacuum drying, the fast evaporation method. In the fast evaporation method the different molecules cannot rearrange themselves within the sample. Due to the fast evaporation smaller crystals are formed, resulting in an improved mass accuracy and resolution. In some cases this method has been applied with success but has not become a real standard method, because of the need for additional vacuum equipment. Another way to increase the evaporation rate of the solvent is using a very volatile solvent, as is introduced by Vorm et al. [1994]. They pre-coated the MALDI target plate with the matrix in a volatile solvent like acetone. After solvent evaporation a small amount of the analyte solution is deposited onto this matrix layer, whereby complete solubilization of the matrix crystals should be avoided (if complete solubilization of the matrix crystals takes place the matrix molecules would rearrange themselves and the effect of fast evaporation has disappeared, and the method would be similar as the dried droplet method). The sample is ready for analysis when the solvent of the analyte has been evaporated. Dai et al. [1996a] studied the distribution of the analytes in MALDI matrices, prepared with the preparation method of Vorm et al. [1994] with confocal fluorescence microscopic imaging and

4.6 Aerosol MALDI sample preparation methods

found a more homogeneous distribution of the analyte throughout the sample surface than samples prepared with the dried droplet method.

The crushed-crystal method was introduced by Xiang et al. [1994] and has been successfully applied for the analysis of proteins and oligonucleotides by Dai et al. [1996b]. In the crushed-crystal method a droplet of a solution, only containing the matrix, is applied on the MALDI target. After solvent evaporation the deposit is crushed with a glass slide or rod. Excess particles are removed and a droplet of a solution containing both, matrix and analyte, is applied on top of the crystals. A thin film is formed, which can be immersed in water to remove contaminants and involatile solvents. The crushed crystal method allows the growth of protein doped crystals in the presence of high concentrations of involatile solvents without any purification. As compared to the dried-droplet method where the droplet surface is the preferred site for initial crystallization, the crushed-crystal method results in a shift of crystal nucleation from the air/liquid interface to the surface of the substrate, by the smeared matrix crystals. The films produced are therefore more uniform than dried droplet deposits, regarding the ion production and spot-to-spot reproducibility. The crushed-crystal method is labor intensive, which is seen as a major drawback of this method.

Combinations of sample preparations are also suggested, but are not widely applied. An example is the overlayer method (also known as the two-layer method) [Vorm et al., 1994, Jørgensen et al., 1998, Dai et al., 1999]. It involves the use of fast solvent evaporation to form a layer of small matrix crystals, followed by deposition of a mixture of matrix and analyte solution on top of the crystal layer (as in the sample matrix deposition step of the crushed-crystal method). The second solution should not dissolve the matrix crystals, otherwise the method is similar to the dried-droplet method.

4.6 Aerosol MALDI sample preparation methods

The sample preparation methods as described in 4.5 are methods used for standard MALDI mass spectrometric analysis. The standard mass spec-

trometers are equipped with a MALDI target holder to introduce the samples into the instrument. The samples are prepared on the MALDI targets before the mass spectrometric analysis. Similarly, in aerosol MALDI the sample preparation also has to take place before the introduction into the mass spectrometer. Whereas the standard sample preparation techniques are off-line, with aerosol MALDI both off-line and on-line analysis can be performed. In off-line aerosol analysis the matrix and analyte are brought in contact with each other in a separate process, before nebulization and introduction of the sample (then consisting of analyte and matrix) in the mass spectrometer. In on-line aerosol analysis the matrix is added to the aerosol on-line: in the same process-step the mass spectrometric analysis is performed. A few aerosol sample preparation techniques are utilized and developed in this work and include the premixed method, the crushed-crystal method, the impaction and condensation/evaporation method and the on-line coating method. The applied and (further) developed methods are discussed in the following.

4.6.1 Aerosol production by premixing

The easiest way to prepare the samples for aerosol MALDI is the premixed method. This method is very similar to the dried-droplet method for standard MALDI analysis and is also an off-line sample preparation technique. This method of sample preparation is a common method for aerosol MALDI (see the work Murray and Russell [1994], Beeson et al. [1995] for instance) and often applied in the work described here. In the premixed method aerosol particles are produced from a solution containing the matrix and analyte in proper ratios. Typically, in standard MALDI the analyte to matrix ratios are in the order of 10^{-4} to 10^{-5} for proteins and increasing with increasing analyte mass. It is suggested that the analyte to matrix ratios should be such that the 'normal' crystal structure of the matrix lattice is preserved [Wang et al., 1993, Dreisewerd, 2003]. The analyte-matrix ratios in aerosol MALDI are in the order of 10^{-2} and also increasing with increasing mass [Murray and Russell, 1994, Beeson et al., 1995]. The lower amount of matrix needed in the case of aerosol MALDI indicates the better contact and mixing between matrix and analyte molecules, due to the large area-to-volume ratio for aerosol MALDI. A necessity for the premixed method to ensure the right analyte to matrix

4.6 Aerosol MALDI sample preparation methods

ratio is that the matrix and analyte have to be completely dissolved in the solution. The work performed by Russell and Beeson [1996] included also sample preparation recipes in which the matrix was not completely dissolved. Their usage of the intended analyte-matrix ratio might not be correct. The solution containing the matrix and analyte is nebulized and the aerosol particles formed are assumed to consist of homogeneously mixed analyte and matrix molecules. During the rapid solvent evaporation within in a few seconds [Hinds, 1999] the analyte molecules co-crystallize with the matrix molecules. Subsequently, the resulting aerosol particles are introduced into the aerosol mass spectrometer.

4.6.2 Aerosol production by the crushed-crystal method

Another off-line method to prepare the samples for aerosol mass spectrometry is the crushed-crystal method. This method is not completely similar to the crushed-crystal method as is used for standard MALDI, it is more a sophisticated premixed method. The crushed-crystal method is a method developed and tested in this work. In the crushed-crystal method for aerosol MALDI a solution containing matrix and analyte in a proper ratio, is poured into a Petri dish and vacuum dried. After complete solvent evaporation the remaining solids are ground and subsequently nebulized with a DeVilbiss powder disperser (Model 175). This method to prepare samples for aerosol MALDI has been successfully applied for the analysis of bacteria containing aerosol particles [Kleefsman et al., 2007] (see also 5.2).

4.6.3 On-line coating of aerosols

Aerosol MALDI offers the possibility for on-line single particle analysis. The on-line analysis requires an on-line sample preparation of the aerosol particles. Stowers et al. [2000] and Van Wuijckhuijse et al. [2005] described the use of a evaporation/condensation flow cell to condense a MALDI matrix onto the aerosol particles. The flow cell consists of an evaporation section and a condensation section. The evaporation section contains the matrix material and is externally heated. When the aerosol pass the evaporation section it is contacted with the matrix vapor. The gas stream will be saturated with the matrix compound. In the following

condensation section the aerosol is (gradually) cooled to create supersaturation to accommodate particle growth. The condensation of the matrix should be a heterogeneous nucleation process to avoid the creation of new particles, composed of only matrix material. Heterogeneous condensation takes place at a supersaturation of a few percent. To avoid homogeneous nucleation a careful temperature adjustment of the evaporation section as well as the condensation section is required. A requirement for this preparation method is that only matrix materials with a high vapor pressure and that do not decompose at increased temperature can be used. Matrix materials with a low vapor pressure can be used when the coating device is operated at lower pressures, as is reported by van Wuijckhuijse [Van Wuijckhuijse, 2003, Van Wuijckhuijse et al., 2005]. The on-line sample preparation method as reported by Stowers et al. [2000] and Van Wuijckhuijse et al. [2005] is further developed and applied in this work.

As is discussed in 4.4 some samples require the addition of an acid, to enhance the ion signal. Another reason to add acid is to extract proteins from the interior of bacterial cells and is discussed in 5.1. An acid can be applied using the evaporation/condensation principle, provided that the acid is condensible. The acid trichloroacetic acid (TCA) has been applied using the evaporation/condensation principle. Another acid like the commonly used trifluoroacetic acid (TFA) for instance, is too volatile and requires an other method to be applied on-line. Since TFA is liquid at room temperature, it can be added to the aerosol using a syringe pump operated at very low flow rates. At the moment the TFA is introduced into the gas stream it evaporates and is mixed with the aerosol, just before the on-line addition of the matrix. Then the aerosol enters a cooled session and the matrix and acid molecules condense onto the aerosol particles. Note that for evaporation/condensation a pure acid, and not an aqueous solution, is required, since the acid dissociates in aqueous solution, and thus condensation of the acid is not possible.

The quality of the mass spectra depends on several instrumental and experimental factors. The instrumental factors are discussed in chapter 2. Experimental factors include the choice of matrix material (see section 4.3) and solvent (see section 4.4). The ratio of analyte to matrix is also an experimental factor that determines the detection of the analyte ions. In the case of on-line coating a layer of matrix is created onto an analyte-core. Therefore, it is hard to control or determine the analyte to matrix ratio,

4.6 Aerosol MALDI sample preparation methods

since the amount of matrix deposited onto a particle is also dependent on the particle concentration and the particle size. A way to determine if there is enough matrix deposited onto the particles is measuring the particle size before and after coating whereby the matrix layer thickness can be calculated, as is done by Jackson and Murray [2002]. As is known from common MALDI experiments, the laser penetration depth into the sample is 50-200 nm [Dreisewerd, 2003]. There is no reason that the laser penetration depth in aerosol MALDI samples is different. If it is assumed that ions are created only over the penetration depth, a too thin matrix layer will result in extensive break-up of the target molecules, since the analyte to matrix ratio is too small. A too thick matrix layer will result in the formation of only matrix ions, since the target molecules are not 'reached', since they further away in the core of the aerosol particle. Thus, the matrix layer required for proper aerosol MALDI analysis should be in the range of the laser penetration depth.

To determine the particle growth an experiment is performed with an aerosol containing vegetative cells of *Erwinia herbicola*. The bacteria were cultured and harvested at TNO Defence, Security and Safety, Rijswijk, the Netherlands. Prior to nebulization, the bacterial samples containing 10^9 cfu/ml (determined by optical density at 260 nm), were washed three times by centrifuging the solution at 4000 rpm for 5 minutes; each time the supernatant was removed and the bacteria pellets were then resuspended in deionized water to approximately 10^9 cfu/ml. The solution was nebulized with a ultrasonic nebulizer (Sono-Tek Corporation, NY, USA, Model 8700-35). The operating frequency of this nebulizer is 35 kHz, which is lower than the frequency used for sterilization, which is typically 70-200 kHz. The aerosol particles were coated on-line with the matrix PMC (a proprietary made compound, order number 0145GM02, kindly provided by TNO Defence, Security and Safety, Rijswijk, The Netherlands). The particle size before coating and after coating at different matrix temperatures was determined, using both: one-color and two-color detection. In this case the two-color detection was used to check if particles consisting mainly of matrix molecules were formed. The particles referred to include particles consisting solely of matrix and formed by homogeneous nucleation as well as particles with a very thick matrix layer. These particles will not fluoresce in contrary to the matrix-coated bacteria-containing particles. The obtained particle number distribution obtained with one-color

detection is recalculated into a particle volume distribution. Particle volume distribution are chosen, to be able to see the effect on the particle size at a matrix temperature of 125 °C. The calculated particle volume distributions are given in figure 4.2.

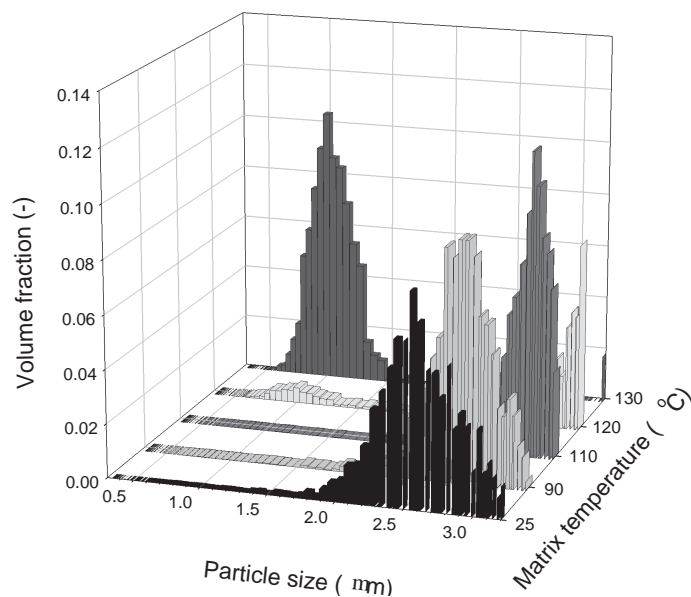


Figure 4.2:

Particle size distributions of *Erwinia herbicola* containing aerosol particles on-line coated with the matrix PMC at different temperatures

The particle volume distribution obtained with the matrix at room temperature (25°C) is the initial particle volume distribution with a mean particle size of $2.45 \pm 0.55 \mu\text{m}$ (standard deviation). At this temperature all the measured particles were fluorescing. At a matrix temperature of 90°C all the measured particles did fluoresce but the mean particle size has moved to $2.58 \pm 0.47 \mu\text{m}$, indicating a growth of $0.13 \mu\text{m}$, and thus a thickness of the matrix layer around the particles of 65 nm. At a temperature of 110°C the mean particle size was $2.91 \pm 0.44 \mu\text{m}$, indicating that a growth is obtained of $0.46 \mu\text{m}$, which is corresponding to a layer thickness of 230 nm. Note that the standard deviation is decreasing at

4.6 Aerosol MALDI sample preparation methods

increasing temperature. This is caused by the ‘Kelvin-effect’ from which can be derived that the particle growth rate is dependent on the particle size. Smaller initial particles experience a rapid growth while the growth of larger particles is slower. Further increase of the matrix temperature to 120°C leads to a bimodal distribution with mean particle sizes of $0.89 \pm 0.15 \mu\text{m}$ and $3.15 \pm 0.17 \mu\text{m}$. The smaller particles either originate from homogeneous nucleation or are initially very small particles produced at the nebulization process (see also section 2.8) and are grown into the detectable size range of the aerosol MALDI mass spectrometer. Only the fraction consisting of the bigger particles has fluorescing properties. Increasing the matrix temperature to 130°C results in a volume distribution with a peak at $0.96 \pm 0.25 \mu\text{m}$. Almost none of these particles emitted fluorescence, indicating that these particles do not contain bacterial material. In addition, the initial particle size in this experiment was $2.45 \mu\text{m}$, which is another reason to assume that the $0.96 \mu\text{m}$ particles are not biological. In this experiment the optimal matrix temperature to coat the particles with a sufficient amount of matrix is between 90 and 110 °C. At these temperatures the matrix layer was between 65 and 230 nm, which is corresponding with the laser penetration depth of 50-200 nm Dreisewerd [2003].

The on-line coating method has been successfully applied for the analysis of proteins and is also used for the analysis of bacteria containing aerosol particles (see section 5.4). In all the performed experiments with on-line coating, the particle growth is monitored by determining the particle size distribution of the aerosol before and after on-line addition of the matrix.

4.6.4 Aerosol analysis by impaction and matrix evaporation/condensation

A semi on-line method to analyze aerosol particles with the aerosol MALDI mass spectrometer is the impaction and evaporation/condensation method. The method is inspired on the work performed by Kim et al. [1998]. In their developed method the matrix material and analyte are mixed in the solid state. This mixed powder is put in a vacuum reservoir (0.01 Torr) at 100°C and sublimates and crystallizes on the sample plate, which is put

above the sample. Van Wuijckhuijse [2003] reports the use of this method (referred to as the co-evaporation technique) for the matrix ferulic acid. The method of Kim et al. [1998] and Van Wuijckhuijse [2003] is further developed into the impaction and evaporation/condensation method and is applied in this work.

For the impaction and evaporation/condensation method applied in this work analyte aerosol particles (proteins or bacteria) are generated and impacted on a MALDI target with a home-made impactor setup. The pressure in the impactor is adjusted to impact particles in the size range of interest. The used pressures in the impactor were slightly below atmospheric pressure. Subsequently, solid matrix material, placed in a Petri dish, is heated to temperatures that evaporation starts. The MALDI target is removed from the impactor setup and is put a certain distance above the heated Petri dish while externally cooled. The matrix material condenses onto the MALDI target covering the impacted sample spot. The condensation process is carried out at atmospheric pressure. After sufficient matrix material is condensed onto the spot, the MALDI target is analyzed using a standard MALDI Mass Spectrometer (Biflex III, Bruker Daltonics, Bremen, Germany). The standard MALDI analysis was performed at TNO Defence, Security and Safety, Rijswijk, The Netherlands. The matrix materials used for this method were ferulic acid (FA) and PMC (a proprietary made compound, order number 0145GM02, kindly provided by TNO Defence, Security and Safety, Rijswijk, The Netherlands).

As is stated in section 4.6.3 the MALDI analysis of some samples requires the addition of an acid. With the impaction and evaporation/condensation method, the acid can be added to the analyte solution, or applied on-line (see section 4.6.3) onto the aerosol particles. The impaction and evaporation/condensation allows the investigation of the on-line sample preparation: the acid-addition, for instance, on its own, since the on-line sample preparation is disconnected from the matrix addition.

The work performed by Kim et al. [2005] is rather similar to the impaction and evaporation/condensation method, with this difference that they impact the bioaerosol particles either on a MALDI target, pre-coated with matrix, or on a bare target on which a droplet of a matrix containing solution is applied. Kim et al. [2005] did not include any on-line sample preparation.

The semi on-line sample preparation method has been used for the anal-

4.6 Aerosol MALDI sample preparation methods

ysis of protein and bacteria containing aerosol particles (see also section 5.3).

In figure 4.3 aerosol mass spectra of the protein insulin (5733 Dalton) with the matrix PMC are given, prepared with the premixed method, the on-line coating method and the impaction and evaporation/condensation method. In the spectra of figure 4.3 the main protonated peak is the dominant peak, neglecting the matrix peaks at the beginning of the mass spectrum. Only in the spectrum prepared with the on-line coating method (figure 4.3b) the doubly charged ion is visible. The dimer is not formed during the ionization of aerosol particles produced with the impaction and evaporation/condensation method ((figure 4.3c). In this figure also a wide background-signal attributed to the matrix is obtained. Together with the absence of the dimer molecule, this might indicate the presence of too much matrix material. Addition of the matrix with the impaction and evaporation/condensation method is hard to control, which can result in the addition of too much matrix as is shown in (figure 4.3c). Figure 4.3 shows that with the used and developed sample preparation methods good to reasonable quality spectra are obtained.

4.6.5 On-line coating of aerosols using electrospray

On-line coating of aerosol particles using the evaporation/condensation principle as discussed in section 4.6.3 is possible for a limited number of MALDI matrices. Commonly used matrices as sinapinic acid and 2,5-dihydroxy benzoic acid do not evaporate but decompose at elevated temperatures. Therefore, these matrix materials are not suitable for on-line coating with the evaporation/condensation method.

To allow the use of more matrix materials for the on-line analysis of aerosol particles, an alternative coating method based on electrospray is investigated. In this method it is advantageous to charge the aerosol particles and coat the (charged) aerosol particles with oppositely charged matrix-containing droplets using bipolar coagulation [Borra et al., 1999]. The particles were charged in a positive unipolar corona charger according to the design of Büscher et al. [1994]³ Electrospray or ElectroHydroDy-

³The charging efficiency efficiency of aerosol chargers can be determined using the method proposed by Kleefsman and Van Gulijk [2008].

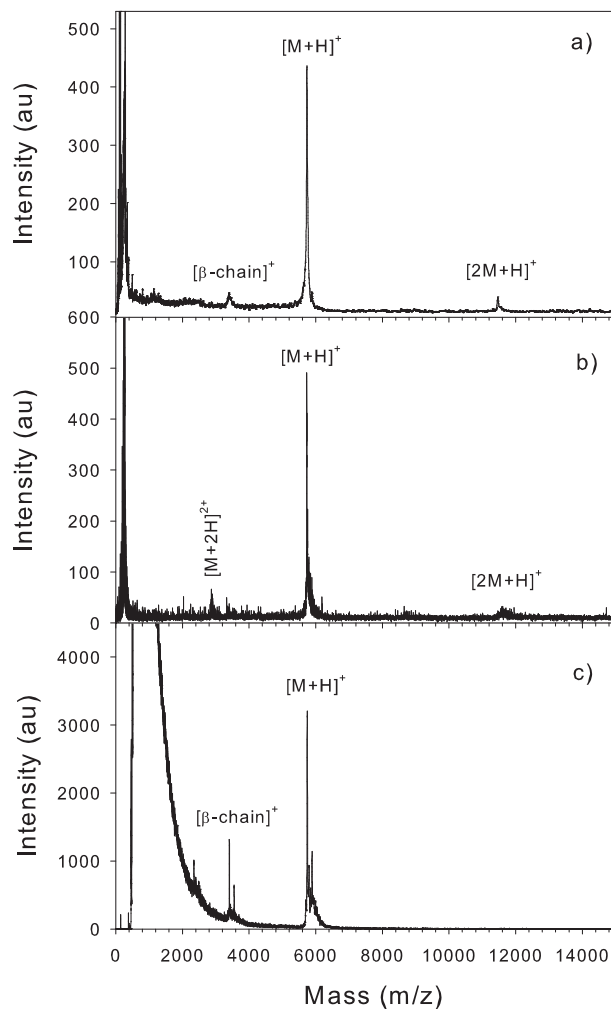


Figure 4.3:
Aerosol mass spectra of insulin and the matrix PMC, prepared with a) the premixed method, b) the on-line coating method, including on-line addition of TFA and c) the impaction and evaporation/condensation method. The spectra are summations of 50 single particle spectra for a) and b) and a summation of 200 shots for spectrum c)

4.6 Aerosol MALDI sample preparation methods

Electric Atomization (EHDA) is an atomization method based on electrical forces. In electrospray a liquid is supplied to a nozzle at a low flow rate. At the end of the nozzle a droplet is formed. Applying an electric field over this droplet induces free charge in the liquid surface, which results in electrical stresses. The stresses transform the droplet in a conical shape. At the cone apex a liquid jet with a high charge density occurs. This jet will break up into highly charged droplets with a narrow size distribution [Hartman et al., 1999]. The droplets generated by the EHDA method have a high electric charge.

To investigate the coating process the difference in size distribution of the aerosol particles before and after electrospray-coating were measured. Aerosol particles containing vegetative cells of *Erwinia herbicola* were generated with a capillary tube nebulizer (Meinhard Glass Products, Golden, CO, USA, Model TR-30-A1). The generated aerosol particles were charged in a positive unipolar corona charger according to the design of Büscher et al. [1994]⁴ The charged aerosol particles were coated by electrospraying with droplets from solutions of 10 mg/ml sinapinic acid in 50/50 (v/v) mixture of water and acetonitrile. The liquid was pumped through a nozzle with inner diameter 0.25 mm at flow rates of 2 and 8 ml/hr. A potential difference of 9.5 kV was applied between the nozzle and the counter electrode. A schematic diagram of the electrospray setup is given in figure 4.4. The surface tension and the conductivity of the matrix solution were determined and were used to calculate the diameter of the matrix droplets exiting the nozzle according to the scaling laws derived by Hartman et al. [1999]. The calculated matrix droplet size varied from 1.21 to 1.31 μm .

The particle size distributions of the bacteria were measured with an Electrical Low-Pressure Impactor (Electrical Low-Pressure Impactor, Dekati Ltd., Finland) before and after electrospray-coating. Figure 4.5 shows the obtained particle size distributions.

The mean particle size (\pm standard deviation) before electrospray-coating lies at $0.58 \pm 0.83 \mu\text{m}$. This size is different than reported in section 4.6.3 and due to the different nebulizer used in the electrospray experiment. The measured size here indicates that particles consist of single bacte-

⁴The charging efficiency of aerosol chargers can be determined using the method proposed by Kleefsman and Van Gulijk [2008].

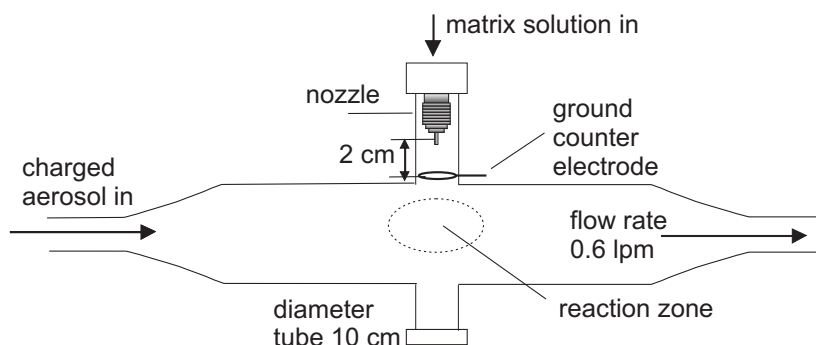


Figure 4.4:

Schematic drawing of the electro spray set-up used to coat aerosol particles of *Erwinia herbicola* with the matrix sinapinic acid

rial cells. At an electro spray flow rate of 2 ml/hr the mean particle size has shifted to the right to $0.66 \pm 0.78 \mu\text{m}$. The mean particle size at an electro spray flow rate of 8 ml/hr is $0.71 \pm 0.63 \mu\text{m}$. The mean layer thickness of the coating was determined to be 50 and 65 nm for 2 and 8 ml/hr respectively, thereby neglecting that the mean particle size from 2 and 8 ml/hr are not significantly different from each other at a confidence interval of 95%. However, The mean particle sizes at these flow rates are significantly different from the blank sample. The obtained matrix layers are close to the minimum penetration depth of the ionization laser [Dreisewerd, 2003]. However, the matrix layer could be increased by using multiple electro sprays in series. When the right matrix layer can be obtained then electro spray coating can be used as an alternative coating method for the on-line analysis of aerosol particles.

4.7 The effects of sample composition in Aerosol MALDI

In section 4.4 is the effect of sample composition on the mass spectra in standard MALDI mass spectrometry discussed. In aerosol MALDI the effect of solvent composition is investigated by Beeson et al. [1995], Russell and Beeson [1996]. Experiments performed in this work seemed to indicate

4.7 The effects of sample composition in Aerosol MALDI

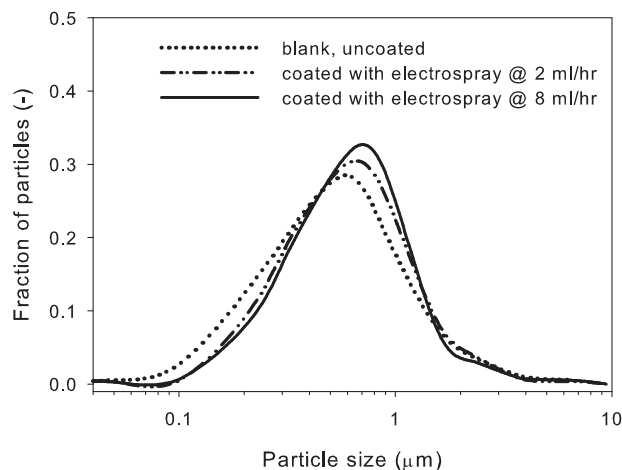


Figure 4.5:

Particle size distributions of *Erwinia herbicola* containing aerosol particles on-line coated by use of electro spray with the matrix SA

that the effect of matrix material is less important in aerosol MALDI as compared to standard MALDI. To investigate this hypothesis, as well as the effect of the solvent composition on the mass spectra, several combinations of matrix and solvents are analyzed. The effects of matrix materials and solvents on the ion-detection in common MALDI mass spectrometry are compared with the observed effects in aerosol MALDI mass spectra. The effects on the presence of ions, the peak area and the spectra to spectra variation are investigated. The spectra to spectra variation is seen as a possible problem in bioaerosol analysis. Several criteria are developed to quantify this variation, based on the reproducibility of the spectra. The results are described for different combinations of matrix materials and solvents. The matrix materials chosen are commonly used matrices in standard MALDI mass spectrometry and solvents with different volatilities are used to simulate different evaporation rates. The conclusion from this investigation lead to a better choice of sample composition in aerosol MALDI mass spectrometry.

4.7.1 Aerosol generation

Aerosol particles were generated from solutions of analyte compounds pre-mixed with matrix using a Collison 6-jet nebulizer (BGI Inc, Waltham, MA, USA). The flow rate through the nebulizer was set at 5 L/min, with approximately 0.6 L/min pulled into the instrument; the carrier gas was filtered air. The aerosol was dried in a diffusion drier packed with silica gel. The protein bovine insulin (Sigma Aldrich Chemie BV, Zwijndrecht, The Netherlands) was dissolved either in water/acetonitrile (7:3 v/v) -referred to as WATFA- or in butanol/water/acetonitrile (5:5:2 v/v/v) -referred to as BWA- or in ethylene glycol -referred to as EG- to a concentration of 1 mg/ml. The acid trifluoro acetic acid was added to the solutions to a concentration of 0.1 % to dissolve the protein. The matrix materials sinapinic acid (SA), ferulic acid (FA), 2,5-dihydroxy benzoic acid (DHB) and 2-mercaptobenzothiazole were purchased from Sigma Aldrich (Sigma Aldrich Chemie BV, Zwijndrecht, The Netherlands). The matrix PMC (a proprietary made compound, order number 0145GM02) was kindly provided by TNO Defence, Security and Safety, Rijswijk, The Netherlands. The matrix materials were dissolved in the analyte solutions to an analyte to matrix molar ratio of 1:400. The solutions were sonicated until the matrix material was dissolved completely. The instrument was adjusted such that aerosol particles with an aerodynamic diameter of 0.8 to 1.2 μm were selected for mass spectrometric analysis.

4.7.2 Data analysis

For each matrix-solvent-combination a subset of at least 1000 spectra was analyzed. Several methods for mass spectra analysis do exist and are commonly applied. The major difference as compared to standard mass spectra analysis is that in aerosol MALDI only 1 mass spectra is taken from each particle, while in standard MALDI more spectra are taken together. In addition, the peaks in the single particle MALDI spectra are quite narrow. Another fact in aerosol MALDI that requires a different approach for the analysis of the mass spectra is the variation of the calibration constants from particle to particle (see also section 2.4. In the following the different steps in the analysis procedure for single particle spectra are explained.

4.7 The effects of sample composition in Aerosol MALDI

The time-of-flight spectra of single aerosol particles are recorded with a digital oscilloscope and are transferred to a personal computer using data acquisition software via a GPIB interface. The data received from the oscilloscope are in binary format and are also stored in this format. With the in-house developed acquisition software the mass spectra are converted to wav-files, as described by Weiss [1997]. The procedure is only used for the analysis of the spectra. The graphical presentation of the mass spectra in this work is accomplished with an externally developed program: MassSpecViewer, by ContinuIT BV (Houten, The Netherlands). The program MassSpecViewer is based on the data processing software developed by Weiss [1997], but is more user-friendly.

The wav-files are the input for the spectra analysis procedure. The first step in the procedure is the conversion of the wav-files into MatLab vector arrays and ascii formats. In this step the spectra are inverted, if necessary. Depending on the analysis to be performed the time-of-flight spectra are converted into mass spectra. Necessary inputs for this step are the calibration constants (see also section 2.4), which can be determined manually for a subset of spectra or can be calculated (by this procedure) for each spectrum separately. If the latter option is chosen, it is optional to convert the time-of-flight spectra to mass spectra. For the manually determination of the calibration constants the program MassSpecViewer was used. To be able to compare and analyze the spectra, the spectra are preprocessed. In this step the background of a spectrum is estimated and subtracted from the spectrum and the peaks are detected, and fitted to Gaussian peaks. For the determination of the background it is assumed and verified that the mass spectrum is a constant background with peaks (positive) on top of it. The y-values (*i.e.* intensity) of the mass spectra consist of a maximum of 256 bins, which is limited by the AD-converter on the oscilloscope. This results in a rather low resolution, *i.e.* a small number of bins, containing the noise signals. Therefore the background level and its standard deviation is determined with the Maximum Likelihood Method using direct computation. The results from the Maximum Likelihood Method were confirmed, firstly by independent estimates in areas where there were no peaks. Secondly, by the fact that always the same noise level was found across various mass spectra. Thirdly, visual inspection confirmed the goodness-of-fit. In addition, the Maximum Likelihood Method was also beneficial for the peak detection. A peak is defined when

the y-value of a data point is 4 times higher than the noise. To avoid that ‘spikes’ (noise intrinsic to the device) are interpreted as peaks, a peak should be at least 2 data points wide. A data point corresponds to a time of 2 ns, indicating that the minimum peak width is 4 ns. Common flight times of protein molecules are in the order of several μs , so this minimum peak width has a negligible effect on the resolution of a peak in a single particle mass spectrum. Another criterion that had to be fulfilled was that on the left and on the right side of the peak the y-value should be less than 4 standard deviations from the constant bias, over a distance of 3 peak widths.

The Gaussian peak fitting is based on three parameters: the peak position, the peak width and the peak height. These fitted parameters are the peak characteristics and are used for comparing multiple spectra.

The developed procedure allows to scan for presence of peaks within certain mass ranges. Note that for this scanning the defined mass range needs to be converted into the right time scale, using the calibration constants belonging to the spectrum (see also section 2.4). The mass ranges that will be scanned needs to be defined and need to be the mass range at the base of the peak. The developed procedure also allows to analyze multiple spectra files, with different calibration constants. For the analysis of multiple spectra from multiple data files, the spectra need to be aligned. Therefore the spectra are analyzed on the time scale. Alignment of the spectra is accomplished by removing the time off-set: c_2 (see equation 2.4).

From the peaks detected in the defined mass ranges the following characteristics are obtained:

- The presence of the peak; in order words: is the expected peak indeed detected in the defined mass range.
- The position of the peak. This is the position on the time scale of the detected peak.
- The mass of the peak. The mass is calculated using the detected peak position and the defined calibration constants.
- The width of the peak: FWHM (Full Width at Half Maximum).
- The area of the peak. From the area and the width of a peak the height (intensity) is derived

4.7 The effects of sample composition in Aerosol MALDI

- The amount of peaks in the defined mass range. Due to for instance metastable ion fragmentation (see also section 2.9), some of the created fragments might have flight times close to the real ion, resulting in more peaks within the defined mass range. For the determination of the peak position and for the calculation of the peak width, peak area and resolution, the position of the most intense peak is chosen.
- The resolution. Depending on the domain of the spectra to be analyzed (time or mass) the resolution R is defined as $m/\Delta m \approx t/2\Delta t$, with m the peak position, Δm at FWHM (full width at half maximum), t the peak position and Δt at FWHM [Lubman, 1990].

The peak characteristics of multiple spectra are combined to determine the mean, median and standard deviation of the above mentioned items (except for the amount of peaks in the defined mass range). Also the geometric mean and geometric standard deviation of the peak characteristics are determined. The geometric mean and geometric standard deviations have the advantage that they are comparable across different experiments.

The variability of the data is determined by the geometric standard deviation. To verify that no outliers are seriously affecting this measure, a comparison was made with a robust measure for the spread, the median absolute deviation (MAD). The MAD is calculated using the inter quartile range (IQR). The IQR is equal to the difference between the third and first quartiles and is expected to include about half of the data, and to exclude the outliers. The IQR is divided by 1.349 to calculate the MAD. When the ratio MAD to the standard deviation was >0.5 and <2 (more or less resembling the 95% confidence interval), then the estimates from the data are less affected by outliers. Note that this test is not a standard statistical test.

To determine whether the obtained data are log-normal distributed, the Jarque-Bera test (JB-test) was performed at a level of significance of 0.05%. The Jarque-Bera test is a 2-sided goodness-of-fit test suitable for situations where a fully-specified null distribution is not known, and its parameters must be estimated. The JB test includes the shape of the data distribution. As a matter of fact the JB-test serves as a verification of the method. If more peaks are included, the data would not have a log-normal distribution. Next to the statistical measures the presence, defined as the

number of spectra containing the target peak divided by the total number of evaluated spectra, is determined.

For the evaluation of the effect of sample composition on the ion signal of insulin, the presence, the peak area and the variability of the peak area of the following peaks were determined: the doubly charged molecule (m/z corresponding to 2867.5 Dalton), the β -chain, which is a fragment product of insulin (3401 Dalton), the protonated peak (5734 Dalton), the sodium-adduct (5756 Dalton), the doubly charged trimer (m/z corresponding to 8600.5 Dalton), the singly charged dimer (11467 Dalton) and the singly charged trimer (17201 Dalton). The mass ranges defined for these peaks are ± 30 , ± 35 , ± 10 , ± 10 , ± 95 , ± 118 and ± 180 Dalton respectively. With these mass ranges, which is the mass range at the base of the fitted Gaussian peak, the absolute minimum resolution, defined as $m/\Delta m$, of each peak will be approximately 100, except for the protonated main peak and the sodium adduct, for which it will be 600. The smaller mass range chosen for these two peaks is to keep those two peaks separated, meaning that a sodium adduct will not be regarded as the main protonated peak. Note that the above-mentioned resolutions refer to the resolutions of single peaks in single particle spectra.

4.7.3 Results and Discussion

Figure 4.6 shows typical, averaged aerosol mass spectra of insulin with the matrix ferulic acid (FA) in the solvent water/acetonitrile 7:3 v/v (WATFA)(figure 4.6a), with sinapinic acid (SA) in ethylene glycol (EG) (figure 4.6b), with dihydroxy benzoic acid (DHB) in WATFA (figure 4.6c) and PMC (a proprietary made compound) in butanol/water/acetonitrile in (BWA) (figure 4.6d). The appearance of the mass spectra is different for the different matrix-solvent combinations. The intensities of the main protonated peak is different, with the highest intensity obtained for insulin with PMC and BWA (figure 4.6d). For the combination FA-WATFA (figure 4.6a) several peaks are observed, while for the combination DHB-WATFA (figure 4.6c) only two peaks are observed. The applied laser energy for the FA-WATFA combination might have been a little too high, causing fragmentation of the insulin molecule, into the α -chain and β -chain. These fragment molecules are observed in FA-WATFA spectrum ((figure 4.6a). The noise level for the FA-WATFA combination (figure

4.7 The effects of sample composition in Aerosol MALDI

4.6a) and for the DHB-WATFA (figure 4.6c) combination is decreasing with increasing mass, while the noise level for the combinations SA-EG (figure 4.6b) and PMC-BWA (figure 4.6d) are more constant, with a high relative noise level for the combination SA-EG. The choice of matrix material and solvent is demonstrated to influence the mass spectra in common MALDI mass spectrometry. The mass spectra in figure 4.6 show that the sample composition in aerosol MALDI is also a determining factor for appearance of the final mass spectrum.

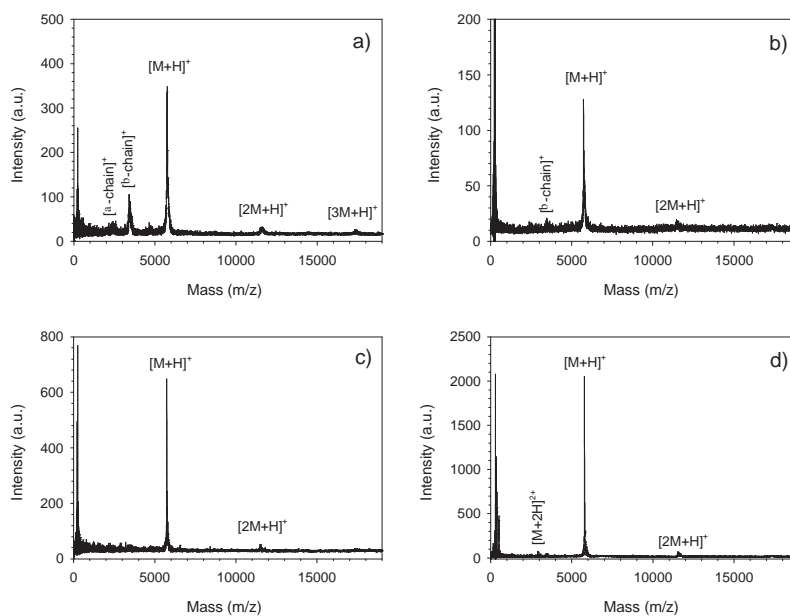


Figure 4.6:

Average aerosol mass spectra of 50 insulin particles in different matrix-solvent combinations, a) ferulic acid in water/acetonitrile (FA-WATFA); b) sinapinic acid in ethylene glycol (SA-EG); c) dihydroxy benzoic acid in water/acetonitrile 0.1% TFA (DHB-WATFA) and d) the TNO proprietary made compound in butanol/water/acetonitrile (PMC-BWA)

Some background thoughts regarding the data analysis procedure

The influence of sample composition on single particle basis is investigated for each of the investigated matrix-solvent combinations, using the developed procedure described before. With the procedure the peaks are detected when the signal-to-noise ratio (S/N) exceeds a defined threshold value. The threshold in this evaluation is chosen to be 4, whereby the noise is defined as the mean noise of the whole spectrum. In principle, a S/N of 2 is sufficient to discriminate a peak from the noise. Despite that the background estimation with the Maximum Likelihood Method has been proven to be successful, a minimum S/N of 4 excludes detection of peaks caused by any instrumental noise, the so-called 'spikes'.

Another assumption in the procedure is the determination of the peak domain, which is in this work based on the peak width. The peak domain is in this work defined by a zero intensity at a distance of 3 times the peak width at both sides of the peak. As stated above a minimum peak width is 2 data points wide (which is one of the criteria a peak has to fulfill). Thus the minimum peak domain is 14 data points wide, corresponding to 28 ns. Depending on the mass, different isotopes of a peak are regarded as 1 peak in this way. Since the chosen mass ranges for the target peaks are much wider this detailed peak information is lost. Except for the defined mass ranges for the main protonated peak and the sodium adduct, the chosen mass range for the other target peaks is that wide that alkali-adducts are identified to be the target peak causing a decreased resolution and misidentification.

The S/N and the definition of the peak domain do affect the derived peak characteristics. In the investigation of the effect of sample composition on the mass spectra, the same assumed values of S/N (≥ 4) and peak domain (± 3 times the peak width) are used. Therefore the comparison of these spectra is justified.

For each target peak the presence, the geometric mean of the peak area and the geometric standard deviation of the peak area (σ_{g-Area}) is determined. The presence of the peak is a measure for the ability of ion-formation of that ion from a particle. The geometric standard deviation is chosen since the distribution of areas on a logarithmic scale tends to be normal. The geometric standard deviation has the added advantage to be easily interpretable and is dimensionless. For all the matrix-solvent

4.7 The effects of sample composition in Aerosol MALDI

combinations the spread in the data distributions of the σ_{g-Area} -values was not affected seriously by outliers. Therefore no spectra are rejected. The hypothesis that the data distribution of the σ_{g-Area} -values was log-normal was valid for 10% of the matrix-solvent combinations, indicating that the data distributions can not simply be described by a log-normal distribution alone. However, the general feature of being a distribution skewed to the right was valid for all the investigated cases.

Effect of sample composition on ion formation - the presence of the detected ions

The presence of each of the peaks, for each matrix solvent combination is given in figure 4.7. The order of the solvents is from volatile (WATFA) to low volatility (EG). The solvents are expected to have an influence on the crystallization rate.

As can be seen in figure 4.7 the main protonated peak (5734 Dalton) was for all the investigated matrix-solvent combinations the most 'present' ion, directly followed by the sodium adduct (5756 Dalton), except for the combination PMC-EG where the dimer (11467 Dalton) is the second most present ion. The presence of the main protonated peak varies from 76-97% for the investigated matrix-solvent combinations. In other words, the formation of these ions is the easiest, which is to be expected, since the particles exist of this analyte molecule. The sodium in the adduct ion is very likely to originate from contaminants in the sample as well as being taken up from the atmospheric air. The high values of the protonated main peak and the sodium adduct also indicate that the instrumental conditions were suitable for the detection of the insulin-ion. For example, if the laser energy was too high, fragmentation of the ion would have occurred, causing a high presence of the fragments: the α - chain and β -chain.

The total ion formation, which is determined by adding the presence of each of the detected ions, is the lowest from the combinations DHB-BWA and DHB-EG. Apparently the formation of ions from these matrix-solvent combinations is more difficult than for the other matrix-solvent combinations.

In MALDI the analyte molecules (should) co-crystallize with the matrix molecules, under solvent evaporation. In common MALDI slow and fast evaporation sample preparations are used, both to enhance the ion signal

Chapter 4 Effect of Sample Preparation and Composition in Aerosol MALDI

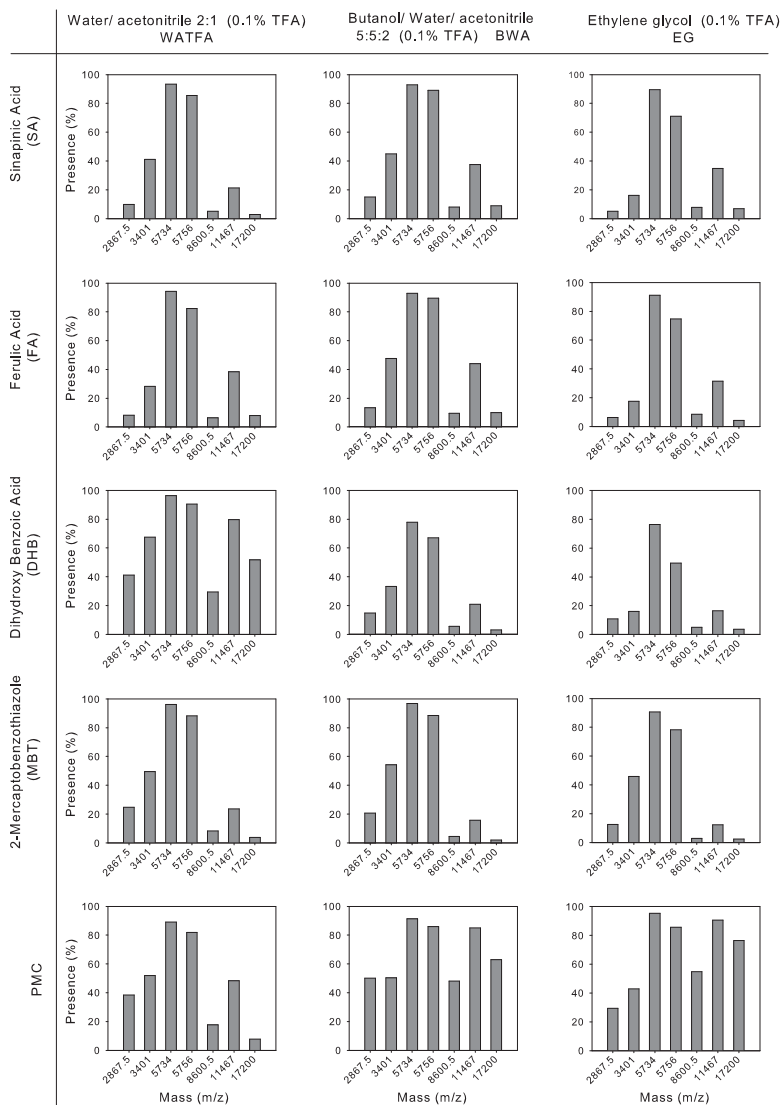


Figure 4.7: The effect of different matrix and solvent combinations on the detection of different ions in insulin-containing aerosol mass spectra. The volatility of the solvents is decreasing when reading from left to right

4.7 The effects of sample composition in Aerosol MALDI

and the quality of the spectra (see also section 4.5). One of the factors determining the rate of the co-crystallization process is the volatility of the solvent. A possibility to influence the evaporation rate is the choice of the solvent. In this work solvents with different volatilities are used and thus is tried to simulate different crystallization rates. Experiments with the solvent glycerol/ethylene glycol (1:9 v/v) (data not shown) were also performed, but required high laser energies and much higher detector voltages for ion detection, than the other investigated solvents. It is assumed that the aerosol particles from the glycerol-containing solution were not dry and that the crystallization process was not finished at the moment of analysis. Since the laser energies applied in the experiments with the solvent EG alone are similar to the laser energies applied for the other solvents, it was assumed that the particles from EG-solutions were dry and completely crystallized.

From figure 4.7 can be concluded that for the matrices DHB and PMC the volatility of the solvent has an influence on the ion formation. For the matrix DHB the most ions are formed from particles originating from the most volatile solvent (WATFA), *i.e.* at an assumed (very) fast crystallization rate. A decrease in solvent volatility results in the formation of less ions: the amount of ions formed from the EG-containing solutions is slightly lower than the amount of ions originating from BWA.

Opposite effects are found for the matrix PMC. For this matrix the most ions are formed from particles originating from less volatile solvents, *i.e.* from BWA and EG. Strikingly, a further decrease in volatility (EG) does not increase the ion formation. Thus, the ion formation in aerosol MALDI is for the matrices DHB and PMC affected by the volatility of the solvent

The presence of the different ions for the matrices SA, FA and MBT, is the same for each of the investigated solvents. Therefore, the solvent is not affecting the ion formation in aerosol MALDI, indicating that the choice solvent is not a determining factor in the ion formation in aerosol MALDI for the matrices FA, SA and MBT.

In literature several investigations into the co-crystallization process of matrix and analyte in standard MALDI mass spectrometry have been reported and several (sometimes contradicting) mechanisms have been proposed

Strupat et al. [1991] and Karas et al. [1993] have investigated the inclu-

sion of analyte molecules in the matrix DHB. They found that the matrix and analyte crystallized at the rim of the sample spot. The crystals at the rim are the first crystals that are created, since the solvent evaporates the fastest from the rim.

Mansoori and Johnston [1996] proposed a different method for the crystallization process of droplets containing DHB. They postulate that the analyte is distributed at the surface of the droplet. As the droplet dries, matrix crystals are formed in the core of the droplet, incorporating analyte molecules. The droplet surface remains enriched with analyte molecules. When the solvent evaporation is complete, the surface analyte molecules are deposited on the dry particle surface, which makes them available for ionization [Mansoori and Johnston, 1996]. It is questionable whether this mechanism allows for proper use of the matrix-analyte charge transfer to generate (sufficient) intact analyte molecules.

As found by Strupat et al. [1991] and Karas et al. [1993] as well as by Xiang et al. [1994] the analyte and present contaminants are separated during the crystallization process, due to the fast evaporation at the rim. Since contaminants might influence the ion signal (ion-suppression) the separation is advantageous. Strupat et al. [1991], Karas et al. [1993], Xiang et al. [1994] assumed that during slow evaporation the analyte molecules at the surface diffuse toward the core, and more analyte molecules are incorporated in the matrix crystals. The layer of analyte which is deposited on the surface during this evaporation, might be less rich in analyte molecules under slow crystallization conditions. Next to that, the contaminants are rearranging during the crystallization process, whereby analyte, contaminants and matrix molecules co-crystallize, which might result in ion-suppression. In the performed experiments here, this separation is assumed to be affected by decreasing the volatility of the solvent, which should result in lower ion signal according to Strupat et al. [1991], Karas et al. [1993], Xiang et al. [1994]. However, a decrease in ion signal is not observed when changing the volatility of the solvent, which makes this assumption less possible for aerosol MALDI.

It is suggested by Russell and Beeson [1996], who investigated the effect of sample composition in aerosol MALDI, that the ion signal is a result of the competition between solvent volatility and solvent polarity. Solvent polarity refers to the hydrophobic or hydrophilic character of the solvent. The solvent polarity is not determined in this work, so the suggestion

4.7 The effects of sample composition in Aerosol MALDI

could not be verified in this work.

Cohen and Chait [1996] proposed that in a slow crystallization process the analyte molecules get the opportunity to partition between the solvent and the matrix crystals. Since the equilibrium between analyte molecules in the solvent and in the crystal is changed slowly, more high mass of the molecules are incorporated in the matrix crystal, resulting in the appearance of high mass molecules in the mass spectra. In rapid crystallization higher mass molecules do not have sufficient time to establish an equilibrium between the analyte molecules in the solvent and crystals. Thus only low mass ions are incorporated in the matrix crystals, which results in the appearance of low mass ions in the mass spectra, according to Cohen and Chait [1996]. However, in aerosol MALDI such a difference is not found, since no shift toward the higher mass for the ion presence is found in figure 4.7, except for PMC.

Next to the effect of solvent volatility on ion formation in aerosol MALDI, the effect of the different matrices on the ion formation can also be deduced from figure 4.7. The presence of the high mass ions from the MBT aerosol particles is slightly lower than from aerosol particles containing the cinnamic acid derivatives SA and FA (valid for all the investigated solvents). In addition, the presence of the low mass ions is higher than for the matrices SA and FA. Xu et al. [1997], who introduced this matrix, also found that MBT favors the ionization of peptides and low mass proteins. Therefore, MBT could be the matrix of choice in aerosol MALDI for the detection of low mass ions, whereas with the matrices SA and FA a wider mass range is covered. The cinnamic acid derivatives are known to cause adduct formation [Juhasz et al., 1993]. In figure 4.7 the presence of the adducts for SA and FA is not significantly higher than for the other matrix materials. It is not clear whether the observed adduct formation originates from the matrix material or if the alkali ions are taken up from the air.

The widest mass range, with high presence values of each peak is covered by the matrix PMC. However, this matrix is also subject to multiple charging of the ions, as is indicated by the high presence of the doubly charged single molecule (2867.5 Dalton) as well by the high presence of the doubly charged trimer (8600.5 Dalton). Although a wide mass range is covered, the presence of a single molecule in different forms might complicate identification of more complex mixtures.

To summarize, the ion formation is only influenced by the crystallization rate (choice of solvent) in the case of aerosol particles of the matrices DHB and PMC. The solvent has no effect on the ion formation when the matrices SA, FA and MBT are used. The chosen type of matrix material is also affecting the ion formation in aerosol MALDI, whereby MBT favors the formation of low mass ions and the widest mass range is covered with the matrix PMC. Several investigations into the interaction between matrix and analyte molecules during the co-crystallization process are reported in literature, with contradicting explanations.

Effect of sample composition on ion formation - the size of the peak areas

The ion formation can also be evaluated by determining the peak area. The peak area is a measure for the total amount of ions formed during ionization. Figure 4.8 shows the geometric mean of the peak areas, for each of the investigated matrix-solvent combinations. For the PMC-combinations the highest values for the peak areas are found. From figure 4.8 can be concluded that the matrix PMC allows proper and efficient ionization of the target insulin molecules and the ion formation is independent of the solvent volatility.

As for the presence of the ions, the biggest peak areas are found for the main protonated peak, directly followed by the peak areas found for the sodium adduct, which is another indication for suitable instrumental conditions.

From figure 4.8 the ratio of the geometric mean of the peak area of the main protonated peak to the other peaks can be deduced. The ratio of the peak area of the main protonated peak to the other peaks in the spectrum is much higher for the combinations DHB-WATFA, MBT-WATFA and all PMC-combinations than for the other investigated combinations. It seems that for these combinations the formation of a protonated insulin molecule is favorable, since a lot of these ions are formed. To obtain aerosol mass spectra with a high ion signal over a broad mass range, *i.e.* to obtain a detailed finger print, PMC would be the matrix material of choice, using a solvent that allows slow crystallization.

4.7 The effects of sample composition in Aerosol MALDI

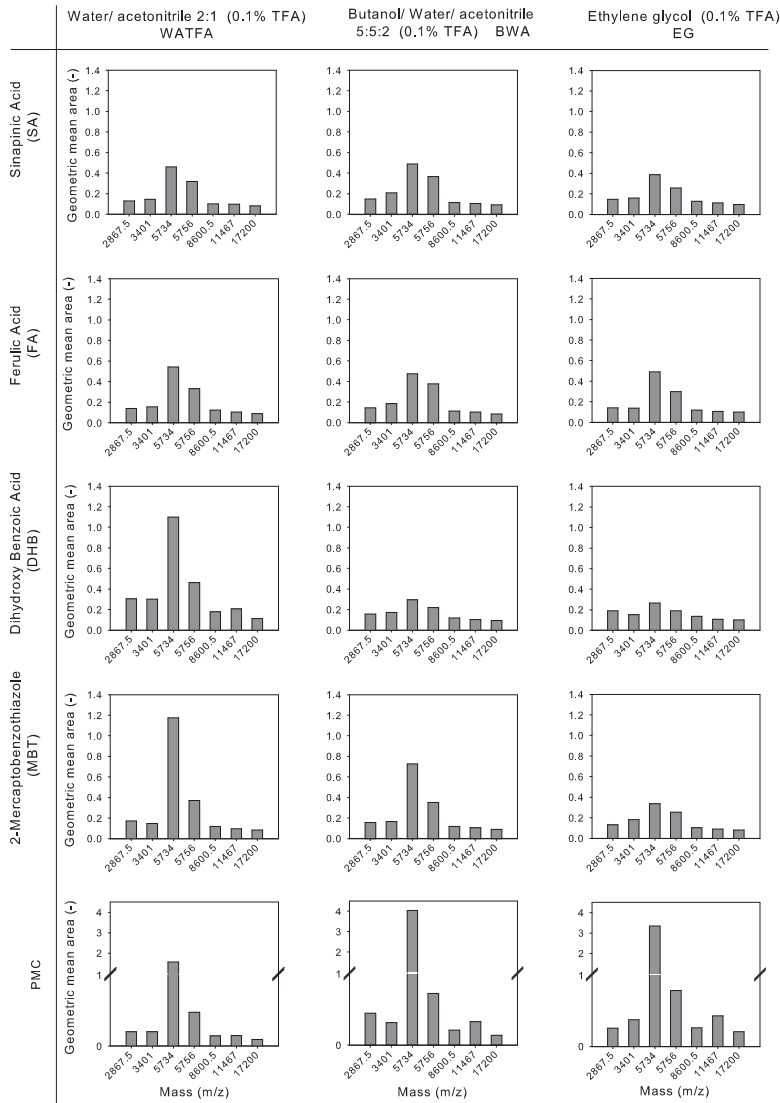


Figure 4.8:
The effect of different matrix and solvent combinations on the geometric mean peak area of the different ions in mass spectra of insulin-containing aerosols

Effect of sample composition on ion formation - the variability of the peak areas

The applicability of aerosol MALDI mass spectrometry is dependent on the reproducibility, which is the spectra to spectra variation (actually differences in the ionization process from particle to particle). The spectra to spectra variation is investigated by determining the geometric standard deviation (σ_{g-Area}) of the peak areas of each matrix-solvent combination. The σ_{g-Area} is a dimensionless number allowing a justified comparison of the peak areas. The geometric standard deviation of the peak areas is given in figure 4.9.

The highest values for σ_{g-Area} are found for the DHB-WATFA combination and all the PMC combinations. Similar result was found for the peak areas. For the σ_{g-Area} hardly an effect of the solvent was found for the PMC-combinations, neither for the other investigated combinations. The crystallization rate (choice of solvent) in aerosol MALDI for insulin samples is not affecting the spectra to spectra variation. When the σ_{g-Area} of the other matrix materials (thus excluding DHB-WATFA and the PMC combinations) are compared no differences are observed. For aerosol MALDI these matrix materials cause the same spectra to spectra variation, which makes them robust matrix materials for aerosol MALDI.

Concluding remarks on effects of sample composition in aerosol MALDI

The effect of sample composition on the ion formation is investigated. The effect on the presence of ions is evaluated as well as the effect on the peak area and the variability of the peak area. The volatility of the solvents is expected to affect the crystallization rate. No general trend was found for the different volatilities (crystallization rate). It proves that the ion formation is mostly influenced by the choice of matrix material. Based on the presence of the peaks the matrix MBT seems to be the right matrix for the detection of ions smaller than 6 kDalton in aerosol MALDI. However, the peak areas and the found σ_{g-Area} do not support this finding, since the values found for these parameters are respectively not much higher or lower than for the other investigated matrix-solvent combinations. The matrix materials SA, FA and DHB perform similar in

4.7 The effects of sample composition in Aerosol MALDI

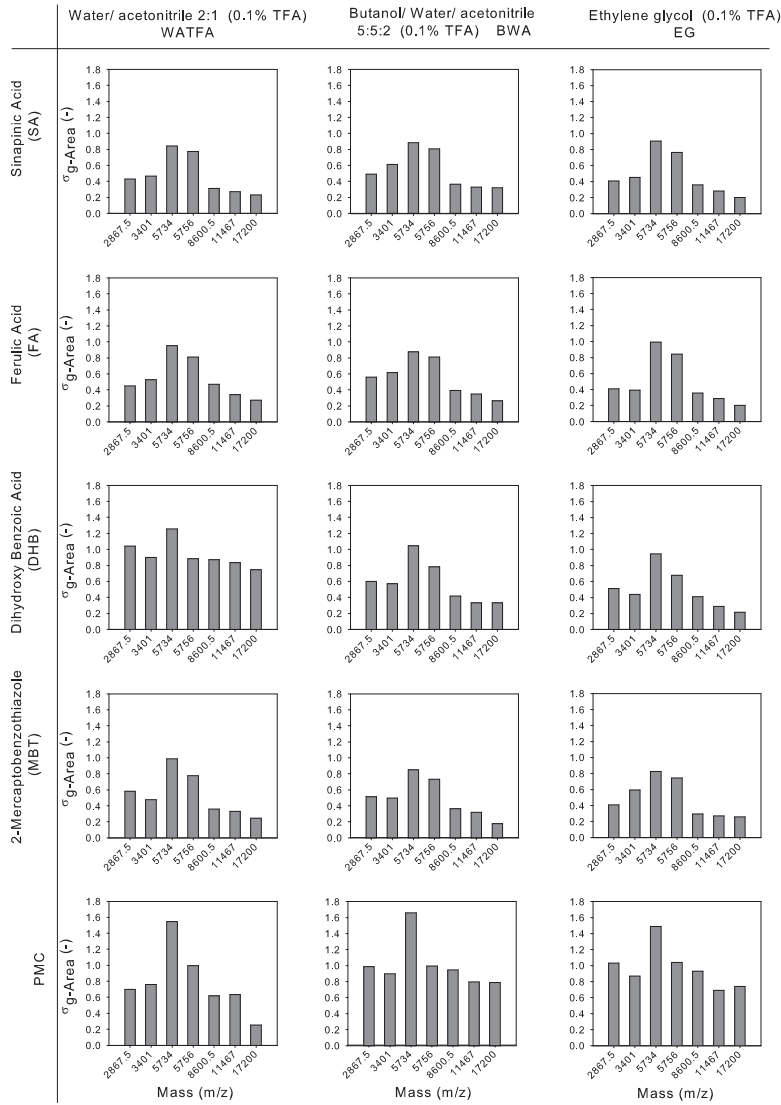


Figure 4.9:

The effect of different matrix and solvent combinations on the geometric standard deviation (σ_{g-Area}) of the peak area of the different ions in mass spectra of insulin-containing aerosols

aerosol MALDI, since the presence, the peak area and the σ_{g-Area} are not affected by the type of solvent. With the matrix PMC a high ion-presence is found over a wide mass range and also the peak areas are high. Thus, the formation of ions is efficient for this matrix. On the other hand, the highest spectra to spectra variation, as expressed by σ_{g-Area} , is found for PMC. Although the spectra to spectra variation might be high for the matrix PMC, peaks with a low intensity are detected with the developed analyzing procedure. The detection of a peak is important, since the identification of a bacterial aerosol particle will be based on the fingerprint *i.e.* the presence of a number of peaks, of such a particle. The performance of the matrix PMC makes it a suitable matrix for the analysis of aerosols. Finally, aerosol MALDI has been shown to be a quite robust analyzing method regarding the formation of ions: effects of sample composition are less pronounced than reported in literature for standard MALDI mass spectrometry. Since in standard MALDI mass spectrometry no analysis is done on single spectra, but always on multiple spectra together, no quantitative comparison between standard and aerosol mass MALDI mass spectrometry can be made.

4.8 Conclusions

The application of the MALDI technique for on-line analysis of aerosol particles, implies the introduction of the aerosol MALDI sample preparation methods. In this work aerosol particles are generated and prepared using one of the following methods: the premixed method, the crushed crystal method, the on-line coating method by either the evaporation-condensation principle or electrospray and the impaction and evaporation/condensation method. Except for the premixed method, the aerosol sample preparation methods are developed in this work. The effect of the sample preparation method on the mass spectra has been demonstrated with insulin aerosol particles, prepared with the premixed method, the impaction and evaporation/condensation method and the on-line coating method by evaporation-condensation. The obtained mass spectra have a different appearance, but the insulin-ions were detected. The on-line coating method with electrospray has only been examined by determining the particle growth. The obtained growth of the particles of approximately

4.8 Conclusions

60 nm is within the range of the penetration depth of the ionization laser and therefore it is concluded that electrospray coating could be used to apply the matrix onto the aerosol particles. Also was found that the analyte to matrix ratio needed in aerosol MALDI is 2-3 orders of magnitudes lower (10^2) as compared to standard MALDI, indicating a better contact between analyte and matrix molecules.

The effect of the sample composition on the ion formation in aerosol MALDI is investigated. For each of fifteen matrix-solvent combinations at least 1000 single particle spectra are analyzed with a developed analyzing procedure. It was found that the effect of matrix material is more pronounced than the effect of the solvent on the ion formation. The effects of the matrix on the spectra are rather similar as found in standard MALDI mass spectrometry, indicating similar interactions between analyte and matrix in both types of MALDI. The investigation also revealed that the matrix PMC is the matrix of choice for the analysis of biological aerosols. In addition, PMC can also be used in the on-line coating method based on evaporation/condensation. The developed procedure for the analysis of single particle spectra has been demonstrated to be very useful.

Chapter 5

Detection of Bacteria by Aerosol MALDI Mass Spectrometry

Our Lord, by your wisdom you made so many things; the whole earth is covered with your living creatures

(Psalms 104.24)

This chapter reports the analysis of bacteria containing aerosol particles. First a historic overview of MALDI mass spectrometry for bacteria analysis is given, as well as a short history on single particle mass spectrometry. Then, the analysis of bacteria containing aerosol particles with the aerosol mass spectrometer using three different sample preparation methods is described. The influence of matrix material, the comparability with standard MALDI mass spectrometry and the differentiation of bacterial aerosol particles by means of ribosomal protein related signals is demonstrated with the off-line, crushed-crystal sample preparation method. The impaction and evaporation/condensation method, was applied to investigate the on-line sample preparation and was found not to be suitable for bacterial analysis. Finally, the mass spectra obtained with on-line analysis of bacterial aerosols are discussed.

5.1 Introduction

Mass spectrometric analysis of biological compounds was first reported in the 1980s, due to the introduction of new ionization techniques at that same time. Until then, the analysis of biological material was restricted by its thermolability and limited volatility. The new ionization techniques included fast atom bombardment, plasma desorption and laser desorption/ionization (LDI) [van Baar, 2001]. With the introduction of matrix-assisted laser desorption/ionization (MALDI) in 1988 it became possible to analyze biological material up to molecular masses of 100,000 Dalton by mass spectrometry. MALDI mass spectrometry is now a common (off-line) routine for the analysis of bacteria [van Baar, 2001, Fenselau and Demirev, 2001, Lay, 2001].

Detection and identification of pathogenic and non-pathogenic bacterial cells by MALDI TOF MS is reported by Krishnamurthy et al. [1996]. They derived genus, species and strain-specific biomarkers and were able to distinguish pathogenic bacteria from the corresponding non-pathogenic species. The analysis performed by Krishnamurthy et al. [1996] involved lysis of the cells during the sample preparation. The identification of whole and intact bacterial cells by direct MALDI TOF MS is reported by Krishnamurthy and Ross [1996] and Holland et al. [1996]. In both studies the tested bacteria could be discriminated and identified. The mass spectra published by Krishnamurthy and Ross [1996] and Holland et al. [1996] covered a mass range up to 20 kDalton. Welham et al. [1998] reported the characterization of various whole cell microorganisms. Their reproducible fingerprint mass spectra covered a mass range up to 40 kDalton and contained more peaks than reported before [Welham et al., 1998]. The discrimination of whole cell bacteria on strain level, was reported by Arnold and Reilly [1998], who could distinguish 25 *Escherichia coli* strains. Identification on strain level of whole and intact cells is also reported by Demirev et al. [2001] for *Helicobacter pylori*, by Vargha et al. [2006] for *Arthrobacter* and by Hettick et al. [2006] for mycobacteria, for instance. In appendix A the above mentioned studies are summarized according to the bacteria analyzed. For a more complete overview of performed MALDI mass spectrometric analysis on bacteria is referred to van Baar [2001].

The development of MALDI TOF mass spectrometry for bacterial anal-

5.1 Introduction

ysis also involved the development of algorithms and proteomic approaches to identify the microorganisms based on the mass spectra [Arnold and Reilly, 1998, Demirev et al., 1999, Pineda et al., 2000, Jarman et al., 2000, Demirev et al., 2001, Pineda et al., 2003, Warscheid and Fenselau, 2004, Keys et al., 2004, Demirev et al., 2005, Chen et al., 2008]. This identification is complicated, since spectra produced from identical strains and under controlled experimental conditions are rarely completely identical [Wang et al., 1998]. In addition, the bacteria respond rapidly to minor changes in their environment thereby changing the protein content [Lay, 2000]. Thus, for identification the detection of species-specific and strain-specific biomarkers, which are insensitive to the environments the bacteria have been in. Another approach could be pattern recognition of peaks occurring in the spectra of types of bacteria, which is done for instance by Fergenson et al. [2004] and Chen et al. [2008].

Proposed biomarkers that are strain and species-specific are the ribosomal proteins for vegetative cells [Arnold and Reilly, 1999, Ryzhov and Fenselau, 2001] and the so-called SASP's (small acid soluble proteins) for spores [Hathout et al., 1999, 2003, English et al., 2003]. *Bacillus* and *Clostridium* species are able to sporulate, when the circumstances are not favorable for cell growth and cell divisions. A spore is a dormant stage for these species. The SASP's play a major role in the survival of the spores, since they protect the DNA of the spore against degradation by UV-radiation for instance. The SASP's are also a pool for the build-up of new proteins when the spores germinate [Setlow, 2007]. In the case of vegetative cells the ribosomes are involved in the surviving and reproduction of the bacteria. Ribosomes consist of RNA-molecules and proteins and are involved in the protein synthesis of the cells [Arnold and Reilly, 1999, Wittmann, 1982]. The ribosomes have been subject to evolutionary studies [Wittmann, 1982] and it is found that the gene-sequences are conserved throughout the time, making them excellent biomarkers.

The proposed biomarkers are bound inside the bacterial cells and need to be extracted. The ribosomal proteins are bound within the ribosomes and the SASP's are located in the spore interior, which is surrounded by a thick spore wall. Successful SASP-extraction using acid treatment is reported by Hathout et al. [2003], Swatkoski et al. [2006] The extraction of the ribosomal proteins is also achieved by acid treatment, usually under less severe conditions as applied for the SASP-extraction. The vegeta-

tive cells are already lysed being dissolved in an acidified organic solution [Ryzhov and Fenselau, 2001]. The proposed biomarkers (ribosomal proteins and SASP's) could also serve as biomarkers in aerosol MALDI. Later in this chapter the on-line sample preparation to extract these biomarkers from single aerosol particles is discussed.

The above-mentioned MALDI MS analysis of bacteria from literature has been performed off-line and onto bulky materials. *Rapid* detection and identification of aerosolized bacteria is seen as one of today's challenges [Kuske, 2006].

The real-time analysis of the chemical composition of airborne particulate matter by mass spectrometry was introduced in 1973 by Davis. The technique, aerosol mass spectrometry, has been evolved since then [Noble and Prather, 2000]. With the developed real-time single particle mass spectrometers in the decades 1970 to 1990 mostly organic and inorganic particles were detected. However, Sinha et al. [1984] [Sinha et al., 1985] were the first that reported the analysis of single bacterial aerosol particles by laser pyrolysis and mass spectrometry of three bacterial species. The three test bacteria could be discriminated based on the peaks in an average mass spectrum of several thousand particles. The peaks in the mass spectra covered a mass range up to 300 Dalton [Sinha et al., 1985].

At the Lawrence Livermore National Laboratory an on-line bioaerosol mass spectrometer (BAMS) is developed. The applied mass spectrometric technique is LDI (Laser Desorption/Ionization) Time-of-Flight mass spectrometry. This technique requires no reagents and mass spectral signatures of individual spores are reported [Steele et al., 2003, Srivastava et al., 2005]. Fergenson et al. [2004] were able to discriminate individual spore particles of either *Bacillus thuringiensis* or *Bacillus atrophaeus*, based on the presence or absence of only one peak. The mass spectrometric range that is covered with LDI is approximately up to 200 Dalton. Due to this small mass range very sophisticated algorithms are required for identification, especially on strain level, prohibited that the strains can be distinguished at this mass range. In addition, most of the peaks detected can be attributed to molecules as glucose, which presence is influenced by the environment the particles were in and are common to any bacteria species

A more powerful approach for on-line bioaerosol analysis is aerosol MALDI mass spectrometry, as employed by Murray and coworkers [Jackson

5.1 Introduction

and Murray, 2002, Jackson et al., 2004, Kim et al., 2005], at Oak Ridge National Laboratory [Harris et al., 2005a,b, 2006] and in Delft [Stowers et al., 2000, Van Wuijckhuijse, 2003, Van Wuijckhuijse et al., 2005, Kleefsman et al., 2007]. Murray and coworkers reported the on-line MALDI TOF MS analysis of proteinaceous material, whereby the particles were coated in-flight with the matrix nitrobenzyl alcohol [Jackson et al., 2004]. Good results were only obtained from an aerosol containing an *Escherichia coli* strain with a semi on-line method. In this method the bacteria particles were impacted on a MALDI target plate, which was precoated with matrix. This MALDI target plate was subsequently analyzed in a standard MALDI mass spectrometer [Kim et al., 2005]. The researchers at Oak Ridge use an ion trap mass spectrometer and have reported the on-line detection of proteins and peptides, applying the matrix by evaporation and condensation onto the aerosol particles [Harris et al., 2005a, 2006]. So far, no on-line analysis of bacteria containing aerosol particles is reported by the researchers from Oak Ridge National Laboratory. On-line analysis of bacteria containing aerosols by aerosol MALDI is only reported from Delft [Stowers et al., 2000, Van Wuijckhuijse, 2003, Van Wuijckhuijse et al., 2005]. Stowers et al. [2000] reported the on-line aerosol MALDI analysis of spores of *Bacillus atrophaeus* and found repetitively a peak at a mass of 1224 Dalton, which was attributed to a part of peptidoglycan. The work done by Van Wuijckhuijse [2003], Van Wuijckhuijse et al. [2005] included on-line aerosol MALDI analysis of spores of *Bacillus atrophaeus* and of vegetative cells of *Escherichia coli*. The obtained mass spectra covered a mass range up to 10 kDa. However, the S/N-ratio of the spectra was low and the spectra were hard to reproduce.

In the foregoing chapters the working principles and the (improved) performance of the aerosol mass spectrometer are discussed. The aerosol mass spectrometer has been optimized for the analysis of bacteria containing aerosols. For the analysis of single bacterial aerosol particles, the mass spectra should cover a wide mass range and should have high single shot mass resolution. The mass spectrometer also needs to be very sensitive to detect individual components from a complex mixture. These goals have been (partially) achieved. The aerosol mass spectra obtained cover a mass range up to 20 kDa, the single particle resolution at 5-6 kDa is more than 1000 and the sensitivity of the aerosol mass spectrometer is 1 zeptomole for the analysis of aerosols containing a single protein component (see also

chapter 2). The effect of sample preparation methods and sample composition was evaluated from a series of experiments. The sample preparation method influences the number and heights of the peaks in the mass spectra, but the target molecules are always detected. The effect of matrix material is rather similar as in standard MALDI mass spectrometry, but almost no effect of the solvent was found (see also chapter 4).

In this chapter the analysis of aerosol particles containing bacteria with the aerosol MALDI mass spectrometer is discussed. The effect of sample preparation on the detectability of such aerosols (bioaerosols) is investigated. Final goal is to confirm the on-line detection of bioaerosols in comparison with the crushed-crystal method. Therefore, bacteria particles are analyzed with three sample preparation methods: The crushed-crystal method, the impaction and evaporation/condensation method and the on-line coating method. The results are discussed separately. With the crushed-crystal method aerosols of *Erwinia herbicola*, *Escherichia coli* and *Bacillus atrophaeus* are analyzed. An aerosol containing *Erwinia herbicola* was analyzed with the impaction and evaporation/condensation method. On-line bioaerosol analysis is performed on aerosols containing *Escherichia coli* and *Bacillus atrophaeus*.

5.2 Crushed-crystal sample preparation method for bacterial analysis

In the crushed-crystal method for aerosol MALDI a solution containing matrix and the bacteria, is poured into a Petri dish and vacuum dried. After complete solvent evaporation the remaining solids are ground and subsequently nebulized with a DeVilbiss powder disperser (Model 175). This method is discussed in more detail in section 4.6.2. This method is similar to the dried droplet method in standard MALDI mass spectrometry. Vegetative cells of *Escherichia coli* K12 XL1-blue, *Escherichia coli* M15, *Erwinia herbicola* and spores of *Bacillus atrophaeus* ATCC9372 were grown and harvested at TNO Defence, Security and Safety, Rijswijk, the Netherlands. The bacterial samples with a concentration of 10^9 cfu/ml were washed three times by centrifuging the solution at 4000 rpm for 10 minutes; each time the supernatant was removed and the bacteria pellets

5.2 Crushed-crystal sample preparation method for bacterial analysis

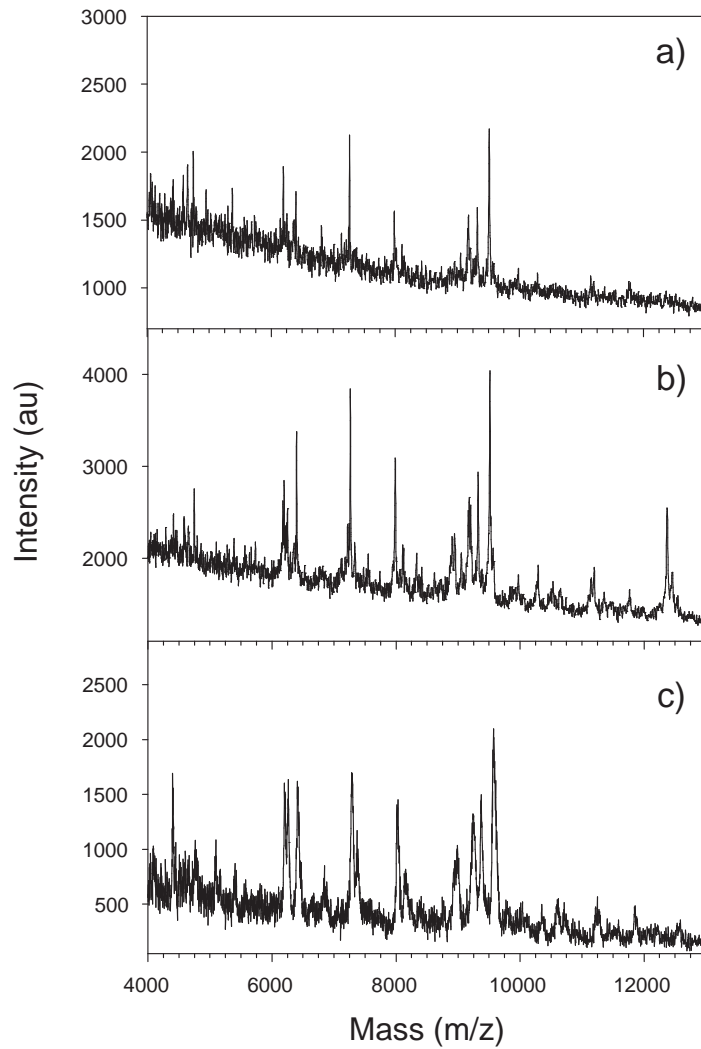


Figure 5.1:

Mass spectra of *Erwinia herbicola* produced with the crushed-crystal method; a) summed aerosol mass spectrum of 2000 aerosol particles with the matrix PMC, b) summed aerosol mass spectrum of 2000 aerosol particles with the matrix sinapinic acid and c) mass spectrum with the matrix sinapinic acid, obtained with a standard MALDI mass spectrometer

formed, were then resuspended in deionized water. Matrix solutions of 20 mg/ml of sinapinic acid (SA) and PMC (a proprietary made compound, order number 0145GM02, kindly provided by TNO Defence, Security and Safety, Rijswijk, The Netherlands) were prepared in water/acetonitrile 3:7 (v/v) 0.2% TFA for the vegetative cells, and with 10% TFA for the spores. Same amounts of the bacteria solution and matrix solution were poured into a Petri dish, so that the final matrix concentration was 10 mg/ml in $\sim 7:3$ (v/v) water/acetonitrile 0.1% TFA (or 5% TFA for the spores). The solutions were vacuum dried overnight and the ground solids were stored at 4-7°C till analysis. The aerosol mass spectrometer was calibrated before each experiment using a premixed aerosol of insulin (or known contaminations were used for the calibration of the mass spectra, see section 5.2.3). Two-point calibration was done using the main protonated insulin peak (m/z 5734 Dalton) and the dimer (m/z 11467 Dalton). The instrument was set such that particles with an aerodynamic size larger than 0.7 μm were selected for mass spectrometric analysis.

In the following sections experiments performed with the crushed-crystal method are described. With aerosol particles containing *Erwinia herbicola* the effect of the matrix material on the aerosol mass spectra is investigated. Also a comparison with a standard MALDI mass spectrum is made. An aerosol containing *Escherichia coli* is used to investigate the reproducibility of the aerosol mass spectrometer. This bacterium is also used to make a comparison with a standard MALDI mass spectrum. To investigate the discriminative power of the aerosol mass spectrometer two different strains of *Escherichia coli* were analyzed and identification/discrimination is done by peak identification. Bacterial spores of *Bacillus atrophaeus* are also analyzed and the effect of the sample preparation on the appearance of the spores is investigated by SEM-analysis.

5.2.1 *Erwinia herbicola*

Effect of matrix material in aerosol MALDI

To investigate the influence of the matrix material on the mass spectrum, aerosol samples of the same culture of *Erwinia herbicola* with the matrix PMC and with sinapinic acid were produced and analyzed. The mass spectra, averaged over 2000 particles are given in figure 5.1. Figure 5.1a

5.2 Crushed-crystal sample preparation method for bacterial analysis

shows the mass spectrum from the aerosol with the matrix PMC, and figure 5.1b shows the mass spectrum with sinapinic acid as matrix material. The most intense peaks are observed in both spectra, except for the peak at approximately m/z 12,400 Dalton, which is only observed in the SA-spectrum (figure 5.1b). The peaks from the spectrum with sinapinic acid (figure 5.1b) are more intense than from the the aerosol with PMC as the matrix (figure 5.1a).

The effect of the matrix material on the analysis of whole bacterial cells is investigated by Williams et al. [2003] and Ruelle et al. [2004]. Their samples were prepared with the dried droplet method [Williams et al., 2003, Ruelle et al., 2004] and with the overlayer method [Ruelle et al., 2004]. In both studies was found that the use of a different matrix resulted in different spectra. Williams et al. [2003] found no reproducible trend with respect to signal intensity for the matrices α -cyano-hydroxycinnamic acid and sinapinic acid. It was only concluded that different ions were detected with both matrices. Ruelle et al. [2004] found that the matrix α -cyano-hydroxycinnamic acid gave more intense peaks than the matrix ferulic acid. From the spectra shown in figure 5.1 it can also be seen that the matrix influences the signal intensity. These strong effects were not observed in the experiments performed in this work with the matrix materials PMC and SA, as used in the crushed-crystal method.

Aerosol MALDI versus standard MALDI MS

For comparison the same culture of *Erwinia herbicola* was analyzed on a standard MALDI mass spectrometer (Biflex III, Bruker Daltonics, Bremen, Germany). The analysis was performed at TNO Defence, Security and Safety, Rijswijk, The Netherlands. The matrix material used was sinapinic acid, in water/acetonitrile 7:3 (v/v) 0.1% TFA and the sample was prepared with the dried droplet method (see also section 4.5). The principle of the dried droplet method: mixing matrix and analyte solutions followed by drying, is rather similar to the principle of the crushed-crystal method. In this way differences caused by a different sample preparation are minimized. The obtained mass spectrum is given in figure 5.1c and is referred to as the standard spectrum. The peak observed at m/z of approximately 12,400 Dalton in the aerosol spectrum (figure 5.1b) is not present in the standard spectrum (figure 5.1c). Further comparison

of the standard spectrum and the aerosol spectrum with sinapinic acid, reveals different intensities of some of the peaks. In general for this experiment, the standard mass spectrum is similar to the two aerosol mass spectra, with this remark that the resolution (defined as $m/\Delta m$, and here the overall resolution) for the aerosol mass spectra is better compared to the resolution obtained from the standard spectrum presented here. Note that resolutions of 10,000-25,000 have been reported for standard MALDI analysis.

From this experiment with *Erwinia herbicola* can be concluded that the mass spectra from a complex aerosol particle prepared with the crushed-crystal method cover a mass range up to 12.5 kDa. This is less than the mass range up to 20 kDa proposed by Fenselau and Demirev [2001] to contain the biomarkers for the identification of bacteria. The resolutions found in figure 5.1a are around 300 for the peaks at m/z 6.2 kDa at m/z 9.5 kDa and at m/z 12.4 kDa. These resolutions are comparable to the value reported by Ruelle et al. [2004], for m/z of 9.1 kDa which was obtained in the analysis of bacterial samples with standard MALDI mass spectrometry.

To summarize, in this experiment the matrix material used had only influenced the signal intensity of the mass spectra. The resolutions of around 300 obtained with the aerosol mass spectrometer are comparable to the resolutions obtained for bacterial samples analyzed with standard MALDI mass spectrometry. The mass spectra cover a mass range up to 12.5 kDalton.

5.2.2 Escherichia coli

Reproducibility of the aerosol MALDI mass spectrometer

The reproducibility of the mass spectra is investigated with two cultures of *Escherichia coli* M15. The time between the two experiments was 19 days, and for both experiments a fresh, overnight grown culture was used. The matrix material used was sinapinic acid. The aerosol mass spectra are given in figure 5.2.

In the two mass spectra in figure 5.2 the peaks with a high intensity occur in both spectra, except for the peak at m/z of approximately 9730 Da, which is much more intense in figure 5.2b. The opposite is the case

5.2 Crushed-crystal sample preparation method for bacterial analysis

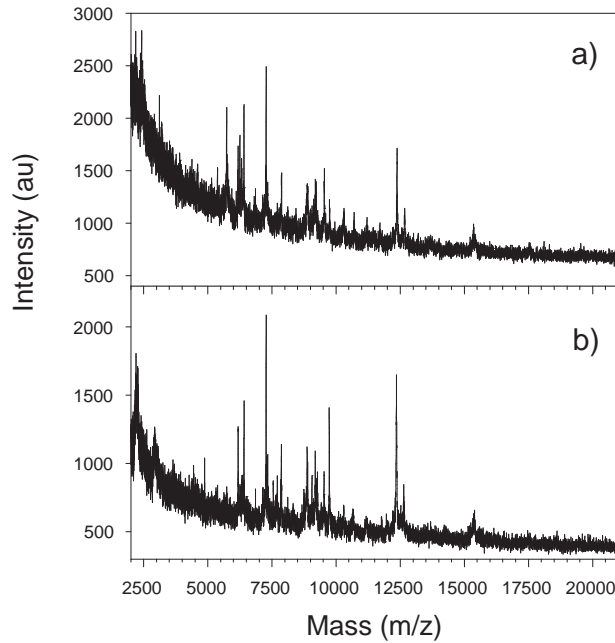


Figure 5.2:

Mass spectra of *Escherichia coli* M15 produced with the crushed-crystal method; a) summed aerosol mass spectrum of 2000 aerosol particles and b) summed aerosol mass spectrum of 2000 aerosol particles prepared and analyzed 19 days later, from a fresh culture

for the peak at m/z of approximately 5750 Da. Low intensity peaks are highly variable and are not discussed.

The reproducibility of bacterial spectra collected on different days is for common MALDI investigated by Saenz et al. [1999]. In their study hardly any differences in the spectra were observed for the replicate analysis of *Escherichia coli* and *Bacillus atrophaeus* spores, which were the two species investigated. Generally, the observed differences by Saenz et al. [1999] are only the different intensities of the same peaks at the different days.

The observed differences in peak intensity in figure 5.2 might be due to slightly different circumstances the cells have been in. These differences

could be the growth phase, and the bacterial concentrations. More intensive research could be performed with samples taken at different times in the growth curve, at different bacterial concentrations and with different growth media to explain the observed differences. In addition, the identity of the peaks needs to be revealed to investigate the above-mentioned effects. From the mass spectra shown in figure 5.2 can be concluded that bacterial aerosol particles prepared by the crushed-crystal method can be analyzed with the aerosol mass spectrometer.

Aerosol MALDI versus standard MALDI MS

A comparison between the performance of the aerosol MALDI mass spectrometer and a standard MALDI mass spectrometer is already demonstrated with an aerosol of *Erwinia herbicola* in figure 5.1. To strengthen this finding similar experiments were performed with an aerosol of *Escherichia coli* M15 and with an aerosol of *Escherichia coli* K12 XL1 blue. The samples with the matrix sinapinic acid were prepared with the crushed-crystal method. Aliquots of the same cultures of these *Escherichia coli* strains were also analyzed on a common MALDI mass spectrometer (Biflex III, Bruker Daltonics, Bremen, Germany) at TNO Defence, Security and Safety, Rijswijk, The Netherlands. For this analysis the matrix used was sinapinic acid and the samples were prepared with the dried droplet method. The aerosol and the standard mass spectra for *Escherichia coli* M15 are given in figure 5.3 and the mass spectra for *Escherichia coli* K12 XL1 blue are given in figure 5.4.

The aerosol spectra and the standard spectra in figure 5.3 and 5.4 look rather similar but there are some differences. Most of the peaks observed in the aerosol spectra occur also in the standard spectrum, but with different intensities. As was seen in figure 5.1 the resolution of the aerosol spectra is again better than for the standard spectra. From this experiment is also concluded that the aerosol MALDI mass spectrometer has a similar performance as a standard MALDI mass spectrometer.

Discrimination on strain level by peak identification

The mass spectra in figure 5.3 and 5.4 are from two different strains of the bacterium *Escherichia coli*. To investigate the discriminative power of the

5.2 Crushed-crystal sample preparation method for bacterial analysis

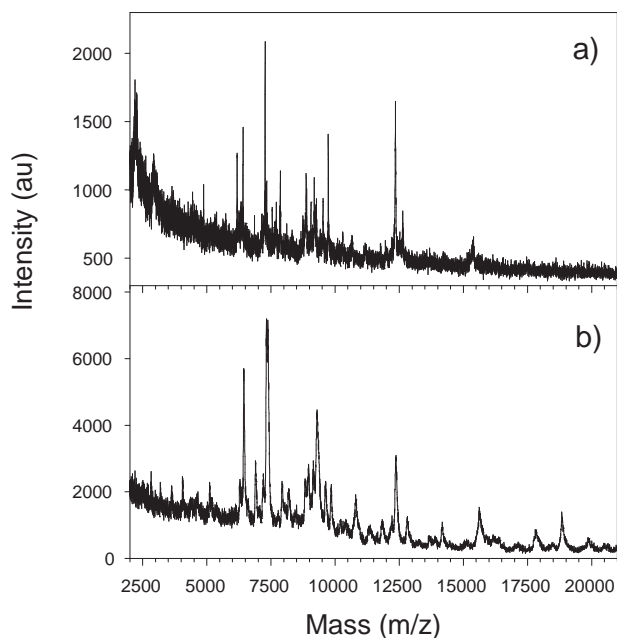


Figure 5.3:

Mass spectra of *Escherichia coli* M15 with the matrix sinapinic acid; a) summed aerosol mass spectrum of 2000 aerosol particles produced with the crushed-crystal method and b) mass spectrum obtained with a standard MALDI mass spectrometer

aerosol MALDI mass spectrometer on strain level, the obtained spectra of the two *Escherichia coli* strains are compared in figure 5.5. At a first glance the aerosol mass spectra of the two *Escherichia coli* strains are similar. In both spectra peaks at the same m/z are observed, sometimes with a different intensity.

To be able to distinguish the two *Escherichia coli* strains, the m/z -values of the observed peaks in the mass range 4-16 kDalton in the aerosol spectra are identified, using an externally developed computer program: MassSpecViewer (ContinuIT BV, Houten, The Netherlands). The peaks in the standard MALDI mass spectra are identified with the software of the MALDI mass spectrometer. The peaks are listed in table 5.1. Such

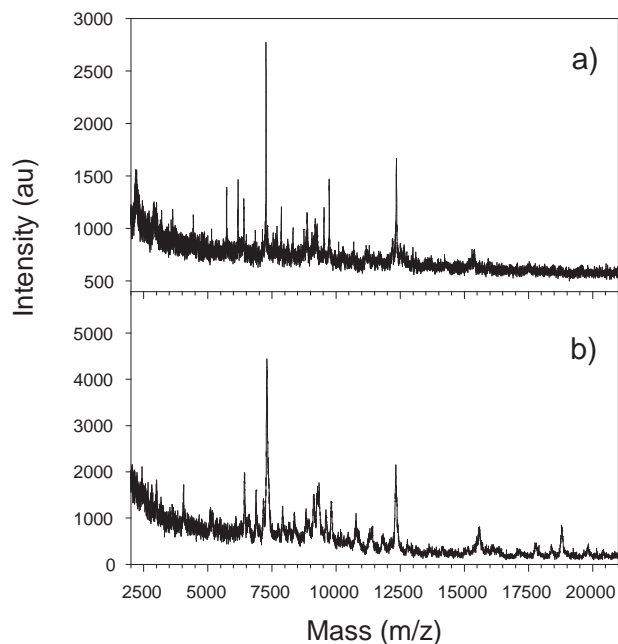


Figure 5.4:

Mass spectra of *Escherichia coli* K12 XL1 blue with the matrix sinapinic acid; a) summed aerosol mass spectrum of 2000 aerosol particles produced with the crushed-crystal method and b) mass spectrum obtained with a standard MALDI mass spectrometer

peak lists can be used for protein database searches for the identification of bacteria.

Ribosomal proteins are proposed to be biomarkers suitable for identification of bacteria [Arnold and Reilly, 1999, Ryzhov and Fenselau, 2001]. Pineda et al. [2003] published a data analysis method for the identification of intact microorganisms by MALDI mass spectrometry. With this data analysis method Pineda et al. [2003] generated databases that contain biomarker masses, derived from ribosomal protein sequences, instead of being derived from mass spectral fingerprints. A database containing the proteomic and model-derived ribosomal protein biomarkers is available at www.pinedalab.jhsph.edu/microOrgID/index.pl. The

5.2 Crushed-crystal sample preparation method for bacterial analysis

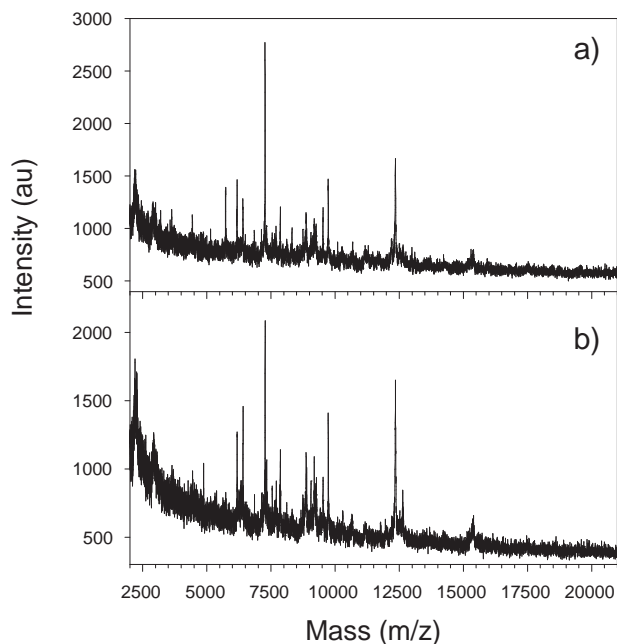


Figure 5.5:

Aerosol mass spectra of two strains of *Escherichia coli*, with the matrix sinapinic acid and produced with the crushed-crystal method; a) summed aerosol mass spectrum of 2000 aerosol particles of *Escherichia coli* K12 XL1 blue and b) summed aerosol mass spectrum of 2000 aerosol particles of *Escherichia coli* M15

database contains the masses of the ribosomal proteins of *Escherichia coli*. The peaks from the spectra in figure 5.3 and 5.4 are compared with the masses of the ribosomal proteins of *Escherichia coli* taken from www.pinedalab.jhsph.edu/microOrgID/index.pl.

In table 5.1 possible matches of the observed peaks with a ribosomal protein are given. In table 5.1 peaks that have the same mass are placed at one line. The maximum allowed mass difference between the peaks was 50 Dalton up to 5 kDalton, 75 Dalton for peaks at masses between 5 and 10 kDalton and 100 Dalton for peaks with a mass higher than 15 kDalton. Peaks with a mass higher than 16 kDalton are not identified,

since they only occur in the spectra obtained with standard MALDI mass spectrometry.

In the following first the peak lists obtained with standard MALDI mass spectrometry of the two *Escherichia coli* strains are compared with each other and discussed. Then the peak lists obtained with aerosol MALDI mass spectrometry are compared and discussed. The third comparison made is between the peak lists of standard and aerosol MALDI for each *Escherichia coli* strain separately. Finally the identification of peaks as ribosomal proteins is discussed and a comparison with the work of Ryzhov and Fenselau [2001] is made.

The total number of peaks (27) detected in the standard mass spectrum of *Escherichia coli* M15 hardly differs from the total number of peaks (28) in the standard spectrum of *Escherichia coli* K12 XL1 blue. The number of peaks that is detected is dependent on the sensitivity of the method used for peak detection, as well as the criteria (*e.g.* S/N ratio) used. In addition, the method used to obtain the peak list is different for aerosol and standard MALDI. Therefore, the difference in number of peaks is not discussed. In table 5.1 can be seen that 4 peaks of the standard MALDI spectrum of *Escherichia coli* M15 do not occur in the standard spectrum of *Escherichia coli* K12 XL1 blue, and 5 peaks of the *Escherichia coli* K12 XL1 blue spectrum do not occur in the standard spectrum of *Escherichia coli* M15. More research is required to determine whether the observed peaks are reproducible for those two strains of *Escherichia coli*. Reproducibility is defined as the re-occurrence of the peaks at different circumstances like growth medium, age of the bacterial cells. If the observed peaks are reproducible, those two strains can be distinguished by standard MALDI mass spectrometry.

In the aerosol mass spectra of *Escherichia coli* M15 and *Escherichia coli* K12 XL1 blue, respectively 23 and 22 peaks are observed. Again, the difference in number of peaks is not discussed. There are two peaks in the *Escherichia coli* M15 spectrum, that are not present in the spectrum of *Escherichia coli* K12 XL1 blue. In the aerosol spectrum of *Escherichia coli* K12 XL1 blue there is one peak not detected in the aerosol spectrum of *Escherichia coli* M15. As compared to the results of standard MALDI, the number of different peaks (9 versus 4 in aerosol MALDI), is lower in aerosol MALDI. More research in the reproducibility of the peaks in aerosol MALDI is required. Only, then can be confirmed if those two

5.2 Crushed-crystal sample preparation method for bacterial analysis

Table 5.1:

Peaks detected in the mass spectra of *Escherichia coli*, figures 5.3 and 5.4

<i>Escherichia coli</i> M15 standard MALDI	<i>Escherichia coli</i> K12 XL1 blue standard MALDI	<i>Escherichia coli</i> M15 aerosol MALDI	<i>Escherichia coli</i> K12 XL1 blue aerosol MALDI	Ribosomal proteins derived from www.pinedalab.jhsph.edu/microOrgID/index.pl
4062	4056			
4622		4439	4437	
5113	5097 5172	4872	5146	RS22 (5095) ¹
		5049 5732 6182	5729 6177	
6447	6293 6431	6411	6406	RL30 (6410) ¹
6902	6883	6856	6852	¹
7203	7174			
7356	7306			
	7748	7272	7268	RL29 (7273) ¹
7941	7918	7870	7866	RL31 (7871) ¹
8200	8178 8372	8326	8322	RS21 (8368) ¹
8484				
8840	8872	8872	8865	RS18 (8855) ¹
8961				
9162	9131	9187	9185	RS16 (9190) ¹
9301	9305			
9631	9607	9533	9526	RS20 (9553) ¹
9847	9814	9734	9735	¹
	10062	10099	10099	RS15 (10137)
10210	10189			
10401	10430	10331 10680	10353 10681	RL25 (10693) ¹
10811	10775			
		11175	11180	RL24 (11185) or RL23 (11199)
11343	11381			
11846	11829	11775	11764	
12215				
12373	12332	12354 12641	12352 12648	
12819	12780			RL18 (12769)
13689	13642			
14178	14146	14226	14225	
15634	15582	15587	15592	

¹ These peaks are also observed by Ryzhov and Fenselau [2001]

Escherichia coli strains can be discriminated by aerosol MALDI mass spectrometry.

When the peak lists of the standard and aerosol mass spectra are compared, more differences are identified than is directly visible from the spectra (figure 5.3 and 5.4). The standard mass spectrum of *Escherichia coli* M15 contains 16 peaks that are not observed in the aerosol mass spectrum. However, in the aerosol mass spectrum of *Escherichia coli* M15 there are 12 peaks detected, which are not seen in the standard spectrum. In the case of *Escherichia coli* K12 XL1, there are 15 peaks from the standard spectrum that are not present in the aerosol spectrum. In the aerosol spectrum of this strain 8 peaks are not detected in the standard spectrum.

Apparently different molecules are ionized and detected with the two mass spectrometric methods, which can be due to the sample preparation method. In general, in the aerosol spectra more peaks are found that possibly can be correlated with ribosomal proteins than in the standard spectra, as can be seen in table 5.1. If the observed peaks really can be identified as to be related to ribosomal proteins, then aerosol MALDI mass spectrometry has a high potential to identify good method to identify *Escherichia coli* and other bacteria in bioaerosols. Obviously if peaks that can not be correlated with ribosomal proteins turn out to be species or strain specific, they could also be used for the identification of bacteria.

As is demonstrated by Ryzhov and Fenselau [2001] who analyzed *Escherichia coli* K12, their observed reproducible peaks could be identified as proteins from the interior of the bacterial cell. Since the sample composition used in this experiment is the same as in the experiments of Ryzhov and Fenselau [2001], it is rather likely that the peaks observed in the spectra in figure 5.3, 5.4 and 5.5 also originate from the cell interior. Half of the reproducible peaks observed by Ryzhov and Fenselau [2001] could be identified as ribosomal proteins. The identified ribosomal proteins in this work are also observed by Ryzhov and Fenselau [2001] except for the RS15, RL24/RL23 and RL18, which are not detected by Ryzhov and Fenselau [2001]. Note that RL18 in this work was only detected with standard MALDI mass spectrometry. Since the ribosomal proteins are detected in this work and by Ryzhov and Fenselau [2001], which makes them robust markers, identification of vegetative cells by ribosomal proteins could also be achievable in aerosol MALDI mass spectrometry if the observed peaks

5.2 Crushed-crystal sample preparation method for bacterial analysis

(see table 5.1) prove to be reproducible.

5.2.3 *Bacillus atrophaeus*

Aerosol MALDI analysis on bacterial spores

The analysis and identification of spores require a different sample composition and thus a different sample preparation. To extract the SASP's, which are proposed as biomarkers for the identification of spores [Hathout et al., 1999, 2003, English et al., 2003], a strong acidic solution is used, to allow solubilization of the SASPs, *i.e.* to accommodate the SASP-extraction. To investigate the capability of the aerosol MALDI mass spectrometer for spore analysis and identification, an aerosol of *Bacillus atrophaeus* spores with the matrix sinapinic acid was produced with the crushed-crystal method and subsequently analyzed. The matrix solution contained 10% TFA, to allow SASP-extraction from the spores. In figure 5.6 an averaged aerosol mass spectrum of 500 particles (figure 5.6a) and a single shot spectrum (figure 5.6b) are given.

Whiteaker et al. [2004] investigated the most abundant SASP's of *Bacillus atrophaeus*¹. The SASP's identified by Whiteaker et al. [2004] were SASP-1 (m/z 7069), SASP-2 (m/z 7333) and γ -SASP (m/z 8890). Those SASP's are also found in this experiment and are accordingly labeled in the mass spectra in figure 5.6.

In the averaged spectrum (figure 5.6a) a peak with a mass of 5734 Dalton is observed. This peak is identified as the protein insulin. The appearance of the peak is probably due to inadequate cleaning, or due to contamination of the matrix with the protein (both caused by the author). In this case the contamination has been used as an internal calibrant.

The spore containing aerosol can be identified based on the appearance of the SASP's in the summed mass spectrum (figure 5.6a), which makes the aerosol MALDI mass spectrometer suitable for the analysis of bacterial spores. However, the shot to shot variability should be taken into account, as is demonstrated in the single particle spectrum (figure 5.6b). This spectrum shows only two SASP-peaks. With the applied sample

¹*Bacillus atrophaeus* is also known as *Bacillus globigii* or as *Bacillus subtilis* var. *niger*

preparation method multiple mass spectra of single aerosol particles need to be analyzed to identify the aerosol.

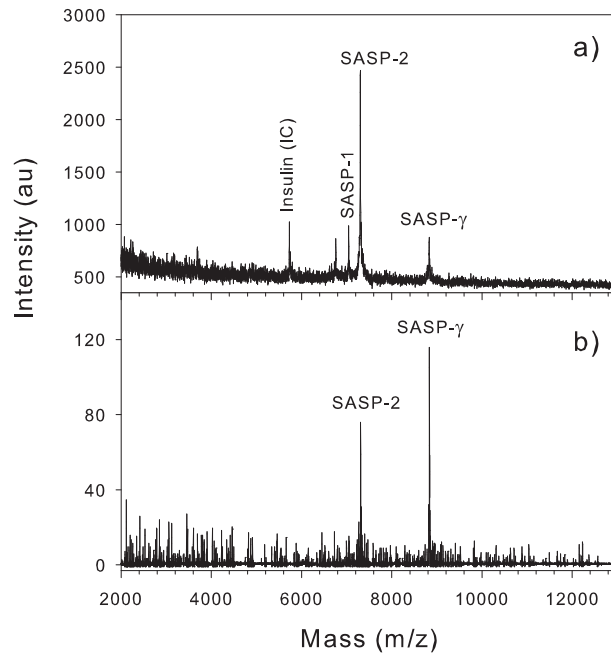


Figure 5.6:

Aerosol mass spectra of *Bacillus atrophaeus* spores, with the matrix sinapinic acid and produced with the crushed-crystal method; a) summed aerosol mass spectrum of 500 aerosol particles and b) a single particle mass spectrum

The effect of the sample preparation on the appearance of the spores

The SASP's are extracted from the spores by acid treatment. The effect of the acid treatment on the appearance and physiological state of the spores is not known. As suggested by Whiteaker et al. [2004] the spore coat might be completely disrupted or the proteins are solubilized from

5.2 Crushed-crystal sample preparation method for bacterial analysis

the inner region, whereby the spore coat is probably partially disrupted. Whiteaker et al. [2004] performed Scanning Electron Microscopy (SEM) analysis of the spores before and after the acid treatment. Their SEM images show that the spore coat is not disrupted and that the spores shrank as a result of the acid treatment. Therefore, Whiteaker et al. [2004] concluded that the proteins are solubilized from the cell interior. A critical remark regarding this conclusion has to be made: it might be possible that during the acid treatment holes are created in the spore coat, which are not visible on the SEM images, since they might be located in the folds. However, to investigate the effect of the acid treatment on the spores in the crushed-crystal method, SEM analysis is performed, following the work of Whiteaker et al. [2004]. SEM analysis was performed at TNO Defence, Security and Safety, Rijswijk, The Netherlands. In figure 5.7 two photographs of the crushed-crystal aerosol particles are shown. On the photographs can be seen that multiple spores are attached to the matrix crystal. As can be seen in figure 5.7b, the spores seem to be intact and seem not affected by the acid treatment. Following the conclusion of Whiteaker et al. [2004], these SEM-images also indicate the solubilization of the SASP's. Due to the scale of SEM images possible holes in the spore coat are not visible.

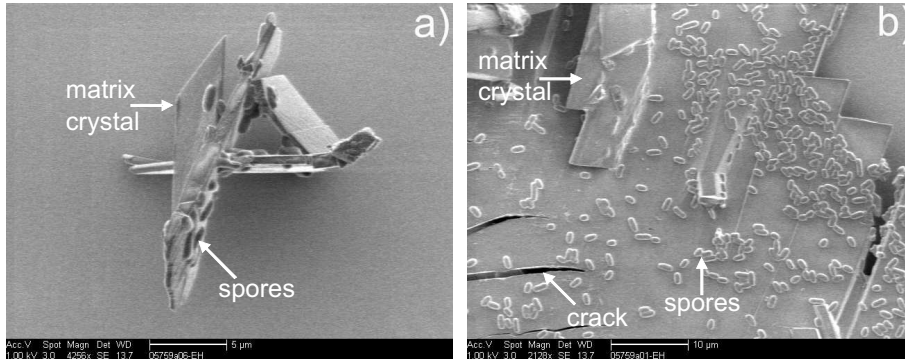


Figure 5.7:

SEM images of the *Bacillus atrophaeus* aerosol prepared with the crushed-crystal method

5.2.4 Concluding and summarizing remarks for aerosol MALDI on bacteria using the crushed-crystal method

The crushed-crystal method is an off-line sample preparation method and is used to demonstrate the applicability of the aerosol mass spectrometer for bacterial analysis. It is concluded that the aerosol MALDI mass spectrometer, and thus aerosol mass spectrometry is suitable for the analysis of vegetative and spore-forming bacterial samples. The obtained aerosol mass spectra covered mass range up to 16 kDa, which is lower than the maximum mass in the mass range (20 kDalton) proposed by Fenselau and Demirev [2001]. The resolution up to 12 kDa is 200-400. The choice of matrix material affects the signal intensity of the most intense peaks (see figure 5.1) and the presence of less intense peaks. Also is demonstrated that with aerosol MALDI mass spectrometry different strains of *Escherichia coli* can be discriminated (see figure 5.5). In the mass spectra peaks in the mass ranges of ribosomal proteins are observed. Aerosol MALDI mass spectrometric analysis is also performed with bacterial spores and peaks are present in the mass ranges of the proposed SASP biomarkers (see figure 5.6). The aerosol mass spectra from the spores contain only a few peaks, whereas several peaks are observed in the spectra of vegetative cells. This is in agreement with the nature of the samples: vegetative cells are alive and many (metabolic) processes are going on, resulting in the presence of several different molecules. Spores, in contrary, are in a dormant stage and are less rich in composition.

5.3 Semi on-line analysis of bacteria-containing aerosols

Introduction and goal of semi on-line analysis

Now it has been demonstrated that it is possible to analyze off-line prepared bacterial samples with the aerosol MALDI mass spectrometer, the *on-line* analysis of bacterial aerosols is only dependent on the on-line sample preparation. In principle in the on-line sample preparation the same 'circumstances' as in the off-line sample preparation method should be

5.3 Semi on-line analysis of bacteria-containing aerosols

achieved. In other words, the extraction of the ribosomal proteins, in the case of vegetative cells, and the SASP's, in the case of spores, needs to happen in-flight together with the matrix coating. The on-line matrix coating of the aerosols is discussed in section 4.6.3.

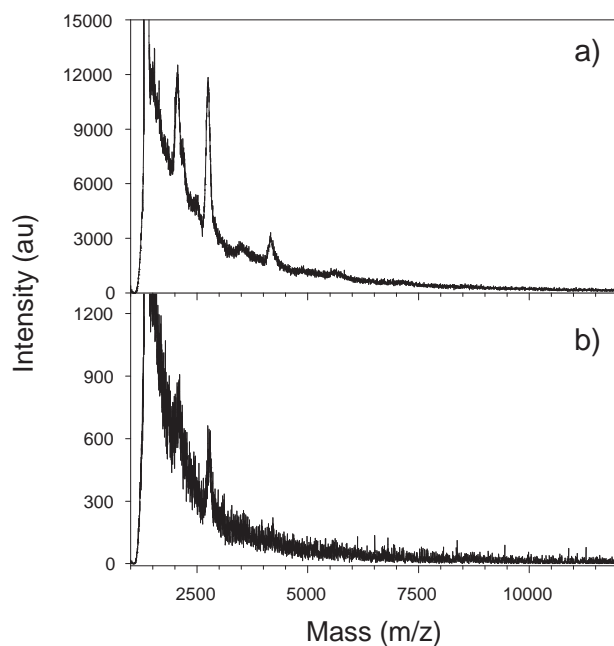


Figure 5.8:

Mass spectra of *Erwinia herbicola* exposed to the water and acid treatment and obtained using the impaction evaporation/condensation method, with the matrix PMC; a) summed mass spectrum of 200 shots and b) summation of 10 shots at 1 location at the impaction spot (see text for more explanation)

To investigate only the effect of on-line acid addition (to extract ribosomal proteins and SASP's) the impaction and evaporation/condensation method is developed, which is described and successfully applied for proteinaceous aerosol analysis in section 4.6.4. The principle of the method is that the sample preparation (acid extraction) is obtained on-line while

the matrix is added to the sample afterwards (off-line). The necessity of the acid treatment is discussed, followed by the implementation of on-line acid addition in the aerosol mass spectrometer, using the results obtained with the impaction and evaporation/condensation method.

Experimental

In the impaction and evaporation/condensation method, the aerosol particles are impacted on a MALDI target plate using a home-made impactor setup. The pressure in the impactor is adjusted to impact particles in the size range of interest. The used pressures in the impactor were slightly below atmospheric pressure.

An aerosol consisting of vegetative cells of *Erwinia herbicola* was generated with an ultrasonic nebulizer (Sono-Tek Corporation, NY, USA, Model 8700-35). Prior to nebulization the bacterial solution with a concentration of 10^9 cfu/ml in growth medium was washed three times by centrifuging the solution at 4000 rpm for 5 minutes. Each time the supernatant was removed and the bacteria pellets formed were then resuspended in deionized water. Subsequently, solid matrix material (PMC), placed in a Petri dish, was heated to temperatures that evaporation starts. Then the MALDI target was removed from the impactor setup and was put a certain distance above the heated Petri dish under externally cooling. The matrix material condensed onto the MALDI target covering the impacted sample spot. The condensation process was carried out at atmospheric pressure. After sufficient matrix material was condensed onto the spot, the MALDI target was analyzed using a standard MALDI Mass Spectrometer (Biflex III, Bruker Daltonics, Bremen, Germany) at TNO Defence, Security and Safety, Rijswijk, The Netherlands.

Results and Discussion - Acid treatment

The extraction of the biomarkers in standard MALDI mass spectrometry occurs by acid treatment. The necessity of acid treatment for the analysis of vegetative cells in aerosol MALDI is demonstrated in the following experiment with *Erwinia herbicola*.

The mass spectrum obtained with the standard MALDI mass spectrometer of this sample did not contain any peak, except for matrix related

5.3 Semi on-line analysis of bacteria-containing aerosols

material in the low mass range. The impacted spot was then recrystallized (on the MALDI target plate) with a small amount of the solvent water/acetonitrile (7:3 v/v). Subsequent mass spectrometric analysis resulted in a mass spectrum with a few humps in the m/z range of 1-2 kDalton. Recrystallization of the impaction spot with the solvent water/acetonitrile (7:3 v/v) with 0.1% TFA, resulted in a mass spectrum with a similar quality as the mass spectrum in figure 5.1c. Experiments performed by Kim et al. [2005], who impacted an aerosol of *Escherichia coli* on a MALDI target pre-coated with matrix, resulted in a mass spectrum only after the addition of an acidic solvent. Based on the results of Kim et al. [2005] and obtained in this work, it is suggested that in the recrystallization with an acidic solvent the material from the cell interior is released and that the released molecules co-crystallize with the matrix material.

Implementation of on-line acid addition

For the implementation of on-line acid addition the flow cell used for the on-line addition of matrix was extended with two more sections. In the extended flow cell the aerosol particles enter first a section in which the acid TFA is applied, using a syringe pump at a flow rate of 0.4 ml/hr. Due to the volatility of TFA the liquid evaporates immediately when entering the aerosol stream. The aerosol is further drawn into the matrix section. Note that when the impaction and evaporation/condensation is applied, no matrix material is placed in the flow cell. Then the aerosol enters the solvent-addition section where solvent is present in a reservoir. The solvent-addition section is externally heated to create a vapor. The aerosol stream is mixed with the vapor of the solvent (water for these experiments). The acid and solvent sections are externally heated, to temperatures of 60°C and 75°C respectively. Exiting the evaporation sections the aerosol enters the condensation section. In the condensation section the temperature decreases gradually and it is assumed that acidified droplets containing the bacterial cells are formed, and that protein extraction occurs until the droplets have evaporated. The pH was measured from droplets that were collected at the end of the condensation zone, and were found to be acidic (pH 1). After the condensation section the aerosol enters a diffusion dryer in which the droplets are dried.

The working principle of the extended flow cell was tested with an aerosol of *Erwinia herbicola*. The aerosol particles were exposed to the water and acid treatment (at the settings mentioned above) and subsequently impacted on a MALDI target. The matrix PMC was condensed onto the MALDI target and the MALDI target was subsequently analyzed in the MALDI mass spectrometer. The mass spectra shown in figure 5.8 were obtained.

Figure 5.8a is a mass spectrum of 200 laser shots, across the impacted spot. At each location the laser fired 10 times (*i.e.* 10 mass spectra) and the sample was moved to fire another set of 10 shots at a different location. Figure 5.8b is an example of such a set of 10 shots. In the summed spectrum (figure 5.8a) 3 peaks were found at m/z -values of approximately 2070, 2750 and 4160 and a bump is observed at m/z of 5600. The peaks at m/z 2070 and 2750 are also visible in figure 5.8b. The peaks are not well resolved: the overall resolutions ($m/\Delta m$) of the peaks are 9, 21 and 16 respectively, indicating that the on-line sample treatment was not as optimal as obtained with the crushed-crystal method, where much higher resolutions were obtained (the peak at m/z 9515 Dalton in figure 5.1b has a resolution of 170 for instance). But, when the impaction spot was recrystallized with a droplet containing water/acetonitrile (7:3 v/v), a similar mass spectrum as shown in figure 5.1c was obtained.

The good results obtained after recrystallization of the impaction spot with a solvent indicates that during this solvent evaporation the condensed matrix material co-crystallizes with the extracted analyte molecules. It is suggested that the matrix molecules partially or completely dissolve when the solvent is added and mixing of the analyte and matrix molecules occur. When the solvent starts to evaporate the matrix and analyte molecules co-crystallize. Thus, adding a matrix layer around the analyte, as obtained in the impaction and evaporation/condensation method, is not sufficient. Mixing of matrix and analyte molecules is necessary. To create this mixing *on-line* the droplets (in the condensation section) should contain also matrix material. Thusm the aerosol particles need to be exposed first to an acid vapor, then to a matrix vapor, followed by exposure to the solvent vapor. Then the created droplets will consist of acid, matrix and solvent. During the evaporation of the droplets the matrix molecules can co-crystallize with the extracted analyte molecules. The development and implementation of this on-line mixing is described in the next section.

5.4 On-line analysis of bacterial aerosols

To conclude, the impaction and evaporation/condensation method is not further investigated since this method is not suitable for (semi) on-line bacterial analysis. The required mixing and co-crystallization of analyte and matrix do not occur in this method.

5.4 On-line analysis of bacterial aerosols

On-line bacterial aerosol requires subsequent exposure to vapors of acid, matrix and solvent, to allow mixing and co-crystallization of the matrix and analyte molecules. An aerosol containing vegetative cells of *Escherichia coli* and an aerosol containing spores of *Bacillus atrophaeus* are analyzed using the on-line coating method and are described in the following.

5.4.1 On-line analysis of *Escherichia coli*

An aerosol containing vegetative cells of *Escherichia coli* K12 XL1 blue was generated with an ultrasonic nebulizer (Sono-Tek Corporation, NY, USA, Model 8700-35). Prior to nebulization the bacterial solution was washed three times by centrifuging the solution at 4000 rpm for 5 minutes; each time the supernatant was removed and the bacteria pellets formed, were then resuspended in deionized water. The aerosol particles were drawn into the flow cell where the acid TFA was added with a flow rate of 0.4 ml/hr at 65°C. Then the particles entered the section in which a vapor of the matrix PMC was present. This matrix section was heated to 115°C. After that the aerosol was exposed to a water vapor, created by heating the water section to 70°C. The aerosol was further drawn into the condensation section in which droplets were formed and were subsequently drawn into the drying section, to remove the water. Finally the particles were sucked into the instrument to be preselected and analyzed by mass spectrometric analysis.

In figure 5.9a a summed on-line aerosol mass spectrum of 250 particles of this aerosol is given. In this spectrum four peaks with m/z of approximately 1420, 2140, 2880 and 3620 are present. The resolution of these peaks ($m/\Delta m$) was determined for the first three peaks and was for these peaks the same: 16. The same culture of *Escherichia coli* was also

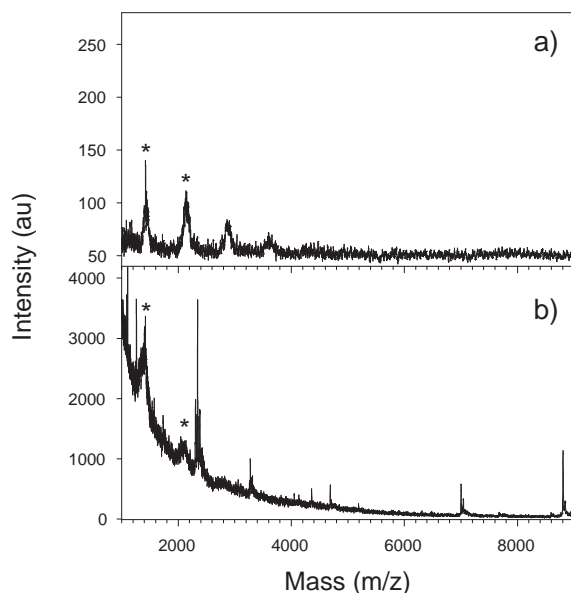


Figure 5.9:

Mass spectra of *Escherichia coli* with the matrix PMC; a) obtained by on-line analysis with the aerosol MALDI mass spectrometer, summation of 250 particles; b) obtained from the same culture of *Escherichia coli* and matrix with a standard mass spectrometer. The asterisks indicate the corresponding peaks in both spectra

analyzed on a common MALDI mass spectrometer (Biflex III, Bruker Daltonics, Bremen, Germany) at TNO Defence, Security and Safety, Rijswijk, The Netherlands. For this analysis the matrix used was also PMC and the samples were prepared with the dried droplet method. The obtained mass spectrum is given in figure 5.9b. The two corresponding peaks in both mass spectra are marked with an asterisk.

The choice of matrix material has been demonstrated to have an influence on the signal intensity when the crushed-crystal method is used, and thus the effect of the matrix material for on-line analysis was investigated. Since the used coating method allows the use of only a few matrix materials, the matrix ferulic acid is used, following the work performed at Oak

5.4 On-line analysis of bacterial aerosols

Ridge National Laboratory [Harris et al., 2005a,b, 2006], and compared with the matrix PMC. In figure 5.10 on-line aerosol mass spectra of *Escherichia coli* with the matrix PMC (figure 5.10a) and ferulic acid (figure 5.10b) are given.

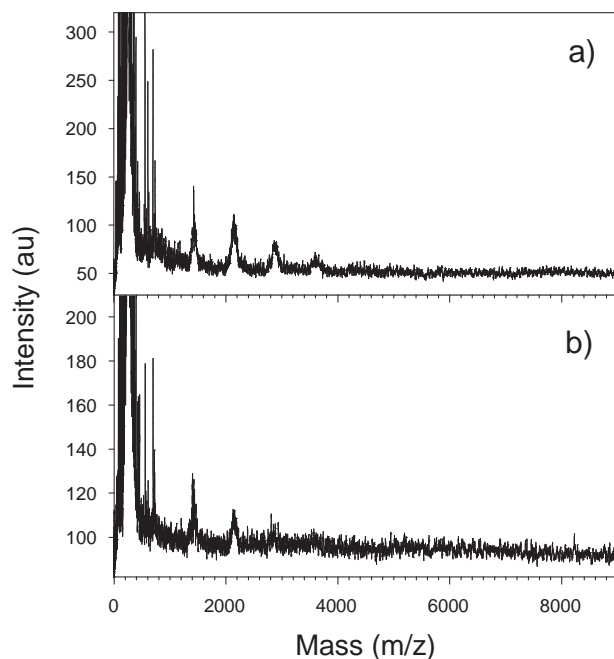


Figure 5.10:

On-line aerosol mass spectra of 250 *Escherichia coli* particles with a) the matrix PMC and b) with the matrix ferulic acid

The peaks observed in figure 5.10a are also observed in the ferulic acid spectrum (figure 5.10b) at m/z 1410, 2140 and 2860 respectively, except for the peak at m/z 3620, which is not identified in the ferulic acid spectrum. The intensity of the peaks in the ferulic acid spectrum is lower than in the PMC spectrum. The same effect was observed when using the crushed-crystal method. The resolution ($m/\Delta m$) of the peaks at m/z 1410, 2140 in the ferulic acid and PMC spectrum is determined and are

14 and 18 respectively. Thus, on-line aerosol MALDI mass spectra of bacterial aerosols can be obtained, but the mass range and resolution have to be improved for successful classification and identification of bacteria in natural aerosols.

5.4.2 On-line analysis of *Bacillus atrophaeus*

Since vegetative cells are rather complex particles, due to the presence of many types of proteins within one cell, a bacterial species with a less complex content is investigated with the on-line analysis. Less complex bacterial species are spores. Spores contain a few types of SASP's (species specific) and are abundant within the spore core [Whiteaker et al., 2004]. Thus, on-line analysis is performed with an aerosol of spores of *Bacillus atrophaeus* and the matrix PMC. The obtained mass spectrum is presented in figure 5.11. In the spectrum two distinct peaks at m/z of approximately 1070 and 2160 are observed, together with a bump at 3250. The resolution of the first two peaks is 21 and 18. At the m/z values of SASP-1 (7069) and SASP-2 (7333) which are marked with an asterisk in figure 5.11, some activity is observed, which could be attributed to the SASP's.

Earlier performed on-line aerosol MALDI analysis on spores of *Bacillus atrophaeus* by Van Wuijckhuijse [2003] resulted in mass spectra with a single peak at m/z 1225. This peak was found when the matrix materials picolinic acid and sinapinic acid were used. The identity of this peak was investigated with liquid chromatography/electrospray mass spectrometry (LC/EC-MS/MS). It was found that the mass of the peak represented a part of the *Bacillus atrophaeus*' peptidoglycan. Peptidoglycan, also known as mureine, is a polymer consisting of sugars and amino acids and is part of the plasma membrane. However, the peak at m/z 1225 was not well resolved when the matrix ferulic acid was used.

The mass spectra in figure 5.11 do not show a peak at m/z 1225. This absence might be explained by the fact that in this experiment a different matrix material is used, PMC (a proprietary made compound, order number 0145GM02, kindly provided by TNO Defence, Security and Safety, Rijswijk, The Netherlands). On the other hand, in the experiments with the crushed-crystal method (see section 5.2.1) the obtained mass spectra with the matrices sinapinic acid and PMC were almost similar for the most intense peaks. The results obtained in the previous chapter (section

5.4 On-line analysis of bacterial aerosols

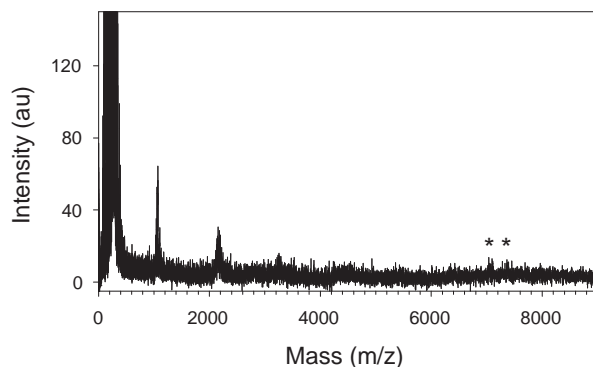


Figure 5.11:

On-line aerosol mass spectrum of 200 particles of *Bacillus atrophaeus* with the matrix PMC. The asterisks indicate the m/z of SASP-1 and SASP-2

4.7) demonstrated that these two types of matrix perform rather similar: the same ions were detected when these matrix material were used. The mass of the peak in figure 5.11 (m/z is 1070) is outside the range that is investigated in section 4.7 and it is possible that the matrices sinapinic acid and PMC behave different in ionization of very low mass ions. It is recommended to investigate the observed peaks in figure 5.11 further by techniques such as LC/EC-MS/MS to retrieve the identity of the observed peaks.

5.4.3 Discussion on on-line bioaerosol MALDI MS

As can be seen from figure 5.9, 5.10 and 5.11 the peaks observed do not cover the wide mass range which has been demonstrated in chapter 2 with aerosols consisting of a single protein. In section 5.2 the analysis of bacteria containing aerosols is described with the off-line crushed-crystal method. The mass spectra obtained with these aerosols did cover a mass range up to 16 kDa. The values for the resolution of the peaks, determined from figure 5.9, 5.10 and 5.11 are much lower as obtained with protein containing aerosols (chapter 2) and with the off-line prepared bacterial

aerosols. Since it has been demonstrated in section 5.2 that it is possible to obtain good quality mass spectra from bacterial samples, the absence of the high mass peaks in the on-line spectra must be caused by non-instrumental factors, like the on-line sample preparation.

In section 5.3 is discussed that addition of a solvent to the impacted aerosol spot resulted in better quality spectra. The solvent addition on the impaction spot indicates that during the solvent evaporation the matrix can co-crystallize with the molecules. This co-crystallization seems to be essential for MALDI analysis. Co-crystallization is tried to be achieved on-line by creating acidic droplets that contain matrix and extracted analyte molecules. A reason why the extracted analyte molecules are not detected could be a too short extraction time, meaning that the droplets dry too fast to provide sufficient extraction and mixing time. In the crushed-crystal method the extraction time is much longer and therefore the extracted analyte molecules are seen in the mass spectra. An additional complication in the on-line analysis, as compared to the crushed-crystal method, is the amount of matrix: it is not certain that the right amount of matrix is present to allow ionization of intact analyte molecules.

Another reason for the lower quality of the on-line aerosol mass spectra could be the solubility of the matrix. To achieve co-crystallization in the on-line analysis, the matrix and analyte should be mixed on a molecular scale. Therefore the matrix and the extracted biomarker molecules should be soluble in the solvent used. The solubility and dissolution rate of the matrix materials ferulic acid and PMC was determined in several solvents including water, acetonitrile, water/acetonitrile (7:3 v/v), ethanol, (iso)propanol and butanol (data not shown). It was found that the matrix materials are soluble in the solvents used in standard MALDI mass spectrometry, like water/acetonitrile (7:3 v/v) for instance. The matrix materials were hardly soluble in pure acetonitrile or water. Since water was used as the solvent for the on-line experiments, the low solubility of the matrix might have prevented molecular mixing of matrix and analyte.

To achieve the molecular mixing on-line standard MALDI solvents could be used. However, to create droplets containing multiple solvent components in the right composition by evaporation/condensation is very difficult. Thus, a single solvent is favorable. The vapor pressure and the boiling point of such a solvent, should be such that evaporation and condensation can be achieved. Solvents with a vapor pressure and boiling

point similar to water can be used in the developed flow cell. Several experiments have been carried out (data not shown) with the impaction and evaporation/condensation method to investigate possible solvents. Results obtained with isopropanol are rather promising. More experiments with this solvent in the aerosol mass spectrometer need to be performed.

5.5 Conclusions

The analysis of bacteria containing aerosol particles with the aerosol mass spectrometer using three different sample preparation methods is described. Bacteria spectra obtained with the crushed-crystal method covered a mass range up to 16 kDa and the resolution was 200-400 up to 12 kDa. Two different strains of vegetative cells could be discriminated. Experiments with the impaction and evaporation/condensation method revealed that for on-line analysis mixing and co-crystallization of analyte and matrix is required. The sample preparation section of the instrument was adapted to achieve this mixing and co-crystallization. On-line analysis of bacteria containing aerosol particles resulted in mass spectra with reproducible, but low resolution peaks up to 4 kDa. These results indicate that the on-line sample preparation is not yet optimal, which was caused by the used solvent. The matrix materials used were not soluble in water and thus mixing and co-crystallization of matrix and analyte molecules was not achieved. For practical reasons a single solvent is favorable for on-line aerosol MALDI and a promising solvent is isopropanol.

Chapter 6

Conclusions, Recommendations and Outlook

Day and night I went without sleep,
trying to understand what goes on in
this world. I saw everything God does,
and I realized that no one can really
understand what happens. We may be
very wise, but no matter how much we
try or how much we claim to know, we
cannot understand it all

(Ecclesiastes 8.16-17)

In this last chapter the conclusions of the performed work are summarized and recommendations for further improvements and experiments are given. The chapter ends with an outlook for possible applications of the aerosol mass spectrometer.

6.1 Summarized conclusions

In this section the main conclusions of the foregoing chapters are summarized. The goal of the thesis was the on-line detection of bacteria particles by means of aerosol MALDI mass spectrometry. The working principle of the aerosol MALDI mass spectrometer is divided into four steps: sample preparation, particle detection, particle selection and the identification of the particles based on their mass spectra. In the following the implemented improvements and obtained results for these four steps are given.

(On-line) sample preparation

The state of affairs before this research for the on-line sample preparation was the use of a flow cell in which matrix was added to the analyte particles. In this thesis is found:

- On-line addition of solely matrix is not enough to create bacteria spectra. It was found that on-line mixing and co-crystallization of matrix and analyte molecules is required. The flow cell for on-line sample preparation is extended and now the aerosol particles are subsequently exposed to a vapor of acid, a vapor of matrix and a vapor of solvent. The bacteria spectra obtained indicated that the sample preparation was not optimal, due to the solvent used. A promising solvent in which matrix and analyte both are soluble is isopropanol.
- Preliminary results were obtained with an alternative on-line sample preparation method: electrospray coating.
- A comparison of the different sample preparation methods that can be used in aerosol MALDI was made. The spectra had different appearances, but the target ions were detected.
- The effect of sample composition on the mass spectra is less pronounced as reported for standard MALDI mass spectrometry, revealed an evaluation of 15 matrix-solvent combinations for the protein insulin. In this investigation the premixed method was used, since only a few matrix materials can be used in the on-line coating method based on evaporation and condensation.

Particle detection

For this step this thesis built on the work done by Kievit [1995], Weiss [1997], Van Wuijckhuijse [2003]. The improvement made here for the particle detection is the implementation of a camera to monitor the alignment of the laser beams with respect to the particle beam.

Particle selection

Previous work in this step focused mainly on size determination and therefore particles could be selected on the basis of size. For the particle selection based on fluorescence from bioaerosols a gated UV-sensitive PMT was implemented, to allow subsequent mass spectrometric analysis. The fluorescence behavior of known and unknown aerosols was investigated.

- The analysis of an atmospheric aerosol revealed that 20% of the particles is possibly biological
- Soot particles are a possible source of interference on the preselection
- The fluorescence signals are not suitable to discriminate different bacteria particles, another identification step is required

Particle analysis by MALDI mass spectrometry

The performance of the mass spectrometer at the beginning of this research was a resolution of 40 at a mass of 5-6 kDalton. To discriminate bacteria particles by biomarker molecules the instrument should have a sensitivity of 1 zeptomole, mass spectra with a mass range up to 20 kDalton and with resolutions to distinguish a mass difference of 20 Dalton. The implementation of a new design high voltage ion source and delayed extraction resulted in:

- The resolution of single particle mass spectra is 2000 at 6 kDa
- The mass range covered is up to 21 kDa
- The sensitivity of the instrument is 1 zeptomole for a single component aerosol

- Analysis of aerosols containing multiple proteins resulted in resolutions of 250-100 at 6-12.5 kDa. This resolution is too low to discriminate biomarker molecules

An investigation into requirements for a sensing instrument to warn in case of a biological attack, revealed that such an instrument should be able to measure high absolute concentrations as well as wide concentration ranges. In addition, it should have the capability to measure and identify the total range of bioaerosol particles. It is suggested to add these two criteria to the design criteria of the NRC (National Research Council of the United States) for sensing instruments to warn in case of a biological attack which are: detection of a broad range of biological agents, a short response time and a very low false alarm rate.

Thus it is concluded that the current aerosol mass spectrometer does not meet the criteria as defined by the NRC, since the on-line sample preparation is not optimal and the resolution of the mass spectra is too low to discriminate biomarker molecules. However, the aerosol MALDI mass spectrometer is applicable for bacterial analysis when an off-line sample preparation method is used. It was demonstrated that different strains of *Escherichia coli* could be discriminated with aerosol MALDI mass spectrometry.

6.2 Recommendations

The goal of this work was to prove the suitability of the aerosol mass spectrometer for (on-line) analysis of single bioaerosol particles. This work has demonstrated that the aerosol mass spectrometer is instrumentally suitable for the analysis of biological aerosol particles. Also shown is that the performance of the instrument is not at all points optimal yet. For example, the performance of the mass spectrometer based on single particle level is better than when multiple particles are summed together (see section 2.6.2). In this section suggestions for further improvements for the aerosol mass spectrometer are presented and include instrumental improvements for particle sampling, other instrumental improvements and improvements for the sample preparation and composition.

6.2.1 Suggested improvements for aerosol sampling

The inlet flow rate of the aerosol mass spectrometer is 0.6 l/min. This is too low for an instrument to be used in the field. Thus the instrument requires a section in which particles are separated and concentrated into a smaller volume. In section 3.5 the use of a virtual impactor was described to increase the sampling volume. With a virtual impactor aerosol particles are concentrated into a smaller volume. The working principle of a virtual impactor is based on inertia. Despite that the efficiency of the used virtual impactor in section 3.5 (MSP Corp, Shoreview, MN, USA; Model 4240) is more than 50% for the particles with sizes between 1 and 5 μm , outside this size range, however, the concentration efficiency is low. Besides the restriction to the size range, the virtual impactor has a high energy consumption and the cut-off diameter is fixed. An option to overcome these disadvantages may be the use of a straight-through cyclone. In a straight-through cyclone the particle separation and concentration is based on centrifugal forces. With a virtual cyclone flow, length and diameter can easily be changed and hence the particle size range can easily be adapted. Some preliminary modeling and experimental work has been performed onto such a straight-trough cyclone [Nieuwmeyer, 2004]. Also some work was performed on a virtual cyclone based on corona wind [Khoury, 2006]. The working principle has been demonstrated, but the design and performance still need further investigation.

6.2.2 Instrumental improvements

The efficiency of the current aerosol mass spectrometer is 1-5%. The sampling efficiency could be increased by modifying the aerosol inlet. The example described in section 3.1 demonstrated that the efficiency of the inlet is a limiting step of the instrument. In the current instrument the expansion of the gas to 30 mbar and separation takes place simultaneously in stage 0 before the critical orifice (see figure 2.2b). Due to the turbulent character the separation of the gas and the particles can not be regulated. Controlling the separation and expansion can be achieved by implementation of a virtual impactor stage, operating at a pressure slightly below atmospheric pressure, before stage 0. The exiting, reduced flow of this virtual impactor stage can be subsequently expanded to 30

mbar by the critical orifice as in figure 2.2b. The implementation would only require the manufacturing of the virtual impactor stage, the expansion being achievable with the current configuration of the aerosol beam generator. Another method to improve the efficiency, as well as the resolution of the instrument is to implement a new aerodynamic lens system, according to the design of Wang and McMurry [2006]. With such a lens system the width of the particle beam can be reduced and the effect of the location of ionization will be reduced.

In the mass spectra presented in section 2.6.2, figure 2.12, isotopic resolution was clearly observed in the mass spectrum of a single particle. The resolution of the isotopes of the summed mass spectrum was lower. This difference is caused by the fact that different particles are ionized at slightly different positions in the ion source. Several options to obtain the single particle quality for summed mass spectra are possible. One option is to use an internal calibrant and align the mass spectra with such an internal calibrant. The internal calibrant should be present in each particle and each spectrum can be calibrated with this calibrant material. The calibrated spectra can be summed together and processed further for peak detection and identification. On-line analysis requires a calibrant material that has the right properties to be added by the evaporation/condensation principle, *i.e.* a low boiling point and a vapor pressure similar to that of the matrix material and the solvents used. In principle, the matrix material could be used as an internal calibrant. However, the obtained ‘matrix peaks’ are rather complex. Besides the monomers and polymers of the matrix molecules, also other peaks are detected. In addition, the flight time of low mass ions is less effected by a different flight distance (*i.e.* length of the flight tube) than high mass ions. It is preferable to use an internal calibrant with a similar mass as the molecules of interest.

Another option for aligning the spectra is to record the ionization location of each particle using a camera, similar to the work performed by Farquar et al. [2008]. In this way the exact flight distance of the ions from a single particle can be calculated. The aerosol mass spectrometer already has the option to implement a camera, so no physical modification of the instrument is required. Thus in addition of the mass spectrum a concomitant picture of the same aerosol particle could be obtained.

Regarding the preselection by fluorescence there are possibilities to obtain more information from the measured aerosol. In the current aerosol

6.2 Recommendations

mass spectrometer the emitted fluorescence is only used as a trigger criterion. As is discussed in section 3.2 an additional UV-laser could offer the possibility to obtain additional information (before mass spectrometric analysis) about the composition of an aerosol particle, by exciting different fluorophores. This information could be used as a confirmation of the obtained identification based on the mass spectrum. Implementation of another UV-laser requires modification of the instrument. Another possibility is to use the current UV-laser and photomultiplier tube, and divide the wavelength range of the emitted fluorescence. The obtained fluorescence intensities of these two wavelength ranges can be plotted against each other, to obtain more information of the possible composition of the aerosol particle, like Sivaprakasam et al. [2004] did.

A method to improve the mass resolution could be the use of a reflectron. In a reflectron the ions formed are turned around 180° at the point where the detector is in a linear TOF. The reflectron uses an electrostatic field to reflect the ion beam toward the detector. The more energetic ions penetrate deeper into the reflectron, and take a slightly longer path to the detector. Less energetic ions of the same charge and mass only will penetrate a short distance into the reflectron and take a shorter path the detector. The detector is placed at the focal point where ions of different energies focused by the reflectron reach the detector at the same time. An additional advantage to the reflectron arrangement is that twice the flight path is achieved in a given length of instrument. A reflectron can be relatively easily implemented in the aerosol mass spectrometer.

A method to obtain more information from a mass spectrum is tandem mass spectrometry. Tandem mass spectrometry, also known as MS/MS, involves multiple steps of mass spectrometry, with some form of fragmentation occurring in between the stages. For the aerosol mass spectrometer an additional time-of-flight mass spectrometer has to be added to obtain tandem TOF/TOF. In the first (the current) TOF-MS precursor ions are separated, and the second TOF-MS analyzes the product ions. With tandem mass spectrometry more information than only the mass of the ion can be obtained, since the ion is another time fragmented. Tandem mass spectrometry would simplify the identification of (bacterial) particles.

6.2.3 Improvements for the sample preparation

A shortcoming of the instruments used in the studies which are evaluated in chapter 1, is the fact that when the total concentration of bioaerosols was determined, no information about the viability of the bioaerosols is obtained. Some dyes known in microbiology are used to determine the viability of bacterial cells [Miyanağa et al., 2007]. Such dyes might be used in aerosol mass spectrometry to determine the viability state of the bacteria particles. Depending on the sample preparation method used, the dye could be added to the mixture to be aerosolized or the dye has to be added on-line. Beneficial of such a dye is that its presence also can be used to calibrate the spectra, *i.e.* as an internal calibrant. The addition of such a ‘viability’-dye can be especially useful in experiments with the crushed crystal method, to perform more extensive research in the reproducibility of the peaks as observed in chapter 5. There the suggestion was made to perform experiments with bacterial aerosols at different stages in the growth curve and different growth media. It is rather likely that an internal calibrant and/or a ‘viability’-dye are not suitable for the on-line analysis, since the properties of these materials should allow evaporation and condensation. The method described in section 4.6.3 to coat the particles by means of electrospray would be more suitable for addition of such materials. In electrospray coating the only requirement is the solubility of the materials in the used solvent. In addition, the concentration of the materials to be added can be more easily controlled, when compared to evaporation and condensation. It is recommended to investigate the on-line coating method by means of electrospray further.

The obtained mass spectra from on-line bacterial analysis (chapter 5) did not cover the mass range as obtained with an off-line sample preparation method. It was concluded that the applied on-line sample preparation method is not optimal. In the on-line sample preparation method extraction, mixing and co-crystallization of analyte and matrix molecules has to take place. This requires a solvent in which matrix and analyte are soluble. Preliminary solubility experiments indicate that isopropanol could be such a solvent. A more extensive investigation of possible solvents and the solubility (rate) in these solvents is required.

6.3 Outlook

The development of the aerosol mass spectrometer for the detection of biological particles was initiated for defensive purposes: to warn in case of a biological attack. The implemented, instrumental improvements have led to a better and a more sensitive instrument, which can generate mass spectra of (size-)selected bioaerosol particles. Good results are obtained from aerosol samples when prepared off-line and subsequently analyzed.

The performance of the current aerosol mass spectrometer with respect to the on-line analysis is limited to allow immediate use for this defensive purpose, as well as for all other purposes (see below) that require on-line analysis. It could be argued if the on-line analysis based on evaporation and condensation of the matrix ultimately will provide similar performance as obtained by the off-line aerosol analysis. This work demonstrates that addition of a matrix onto aerosol particles can be achieved. However, likewise extraction of biomarkers, mixing and co-crystallization of analyte and matrix molecules have to take place as well as to obtain mass spectra that can be used for identification. At the moment, much more research is required in the on-line sample preparation based solely on evaporation and condensation. Other methods to achieve on-line sample preparation, such as coating of aerosol particles by means of electrospray (preliminary results are presented in section 4.6.5) are certainly worthwhile to be further investigated. Beneficial of electrospray coating is the addition of all the necessary components in one step, whereby droplets are formed. If is assured that these droplets collide with the bioaerosol particles, by choosing a solvent with a low volatility, extraction, mixing and co-crystallization can take place in this droplet. It could be stated carefully that electrospray coating has a bigger chance for success than on-line coating based on evaporation and condensation.

When the aerosol MALDI mass spectrometer is capable of on-line, single bioaerosol particle analysis, the aerosol mass spectrometer can be employed for more civil purposes, next to the above mentioned military application. The instrument can be used in environmental monitoring, to investigate the effect of bioaerosols on air quality, for instance. In industry the aerosol mass spectrometer can be used to monitor hygienic production processes in pharmaceutical industries, for instance. If a certain product is contaminated, the production process can be stopped immediately. Thus

Chapter 6 Conclusions, Recommendations and Outlook

a lot of costs can be saved, since current monitoring depends on culturing. Culturing is time consuming and lasts several days before a contamination is known. At that time the whole batch has already been produced. One step further, the aerosol mass spectrometer can be used as a PAT-tool (Process Analytical Technology) within the frame work of Quality by Design. Quality by design is defined as a systematic scientific approach to product and process design and development [ICH, 2005], which is currently being employed in the pharmaceutical industry. The final goal of PAT-tools in this perspective is to assure final product quality. In the example of monitoring hygienic processes the aerosol mass spectrometer could function as such a PAT-tool.

An other area where the aerosol mass spectrometer can be used is in health care. In hospitals the air could be monitored on the presence of harmful, infectious bacteria. Proper counteractions can be taken with respect to the choice of antibiotics. A less obvious application of the aerosol mass spectrometer lies in the field of microbiology. The aerosol mass spectrometer allows analysis of bacterial cultures on a single cell basis. The effect and methods of all kind of (proteomic) processes within a single bacterium can be followed.

Appendix A

Overview of standard MALDI MS analysis on bacteria

In table A.1 the studies mentioned in chapter 5 are summarized. For a more complete overview of performed MALDI mass spectrometric analysis on bacteria is referred to van Baar [2001].

Appendix A Overview of standard MALDI MS analysis on bacteria

Table A.1: Overview of standard MALDI MS analysis on bacteria

Bacteria	Type of sample	Remark	Reference
<i>Acinetobacter</i> strains	whole cells		[Ruelle et al., 2004]
<i>Arthrobacter</i>	whole cells	discrimination on strain level	[Vargha et al., 2006]
<i>Bacillus</i> species	whole cells	discrimination between pathogenic and non-pathogenic strains	[Krishnamurthy and Ross, 1996]
<i>Bacillus atrophaeus</i>	whole spores	discrimination on species and strain level	[Hathout et al., 1999]
	whole cells		[Welham et al., 1998]
	cell lysates	discrimination between pathogenic and non-pathogenic strains	[Krishnamurthy et al., 1996]
<i>Brucella melitensis</i>	whole cells	discrimination between pathogenic and non-pathogenic strains	[Krishnamurthy and Ross, 1996]
	cell lysates	discrimination between pathogenic and non-pathogenic strains	[Krishnamurthy et al., 1996]
<i>Enterobacter cloacae</i>	whole cells		[Holland et al., 1996]
<i>Escherichia coli</i> strains	whole cells		[Holland et al., 1996]
	whole cells	discrimination on strain level	[Arnold and Reilly, 1998]
	whole cells		[Welham et al., 1998]
<i>Francisella tularensis</i>	whole cells		[Ryzhov and Fenselau, 2001]
	whole cells		[Williams et al., 2003]
	whole cells		[Ruelle et al., 2004]
	whole cells		[Krishnamurthy and Ross, 1996]
	cell lysates		[Krishnamurthy et al., 1996]
<i>Helicobacter pylori</i>	whole cells	discrimination on strain level	[Demirev et al., 2001]
<i>Klebsiella aerogenes</i>	whole cells		[Welham et al., 1998]
<i>Listeria innocua</i>	whole cells		[Williams et al., 2003]
Mycobacteria	whole cells	discrimination on strain level	[Hettick et al., 2006]
<i>Proteus mirabilis</i>	whole cells		[Holland et al., 1996]
<i>Pseudomonas</i> species	whole cells		[Welham et al., 1998]
	whole cells		[Holland et al., 1996]
	whole cells		[Ruelle et al., 2004]
<i>Salmonella enteritidis</i>	whole cells		[Ruelle et al., 2004]
<i>Salmonella thymurium</i>	whole cells		[Welham et al., 1998]
<i>Serratia marcescens</i>	whole cells		[Ruelle et al., 2004]
<i>Shingella flexneri</i>	whole cells		[Holland et al., 1996]
<i>Staphylococcus aureus</i>	whole cells		[Holland et al., 1996]
	whole cells		[Welham et al., 1998]
<i>Yersinia pestis</i>	whole cells		[Krishnamurthy and Ross, 1996]
	cell lysates		[Krishnamurthy et al., 1996]

List of Symbols

c_1	calibration constant (-)
c_2	calibration constant (-)
d_A	aerodynamic diameter (m)
E	electric field strength (kV/m)
e	elementary charge ($1.6 \cdot 10^{-19} C$)
L	length (m)
m	mass (kg)
MW	molecular weight ($g/mole$)
N_A	number of Avogadro ($6.02 \cdot 10^{23}$)
$N_{Analyte}$	number of analyte molecules (-)
r	particle radius (m)
ρ	particle density (g/m^3 , or $1 \cdot 10^{-6} g/ml$)
ρ_0	standard particle density ($1 \cdot 10^6 g/m^3$)
t	time (s)
V	voltage (V)
v	velocity (m/s) (
z	number of elementary charges (-)

Bibliography

- J.D. Allan, M.R. Alfarra, K.N. Bower, H. Coe, J.T. Jayne, D.R. Worsnop, P.P. Aalto, M. Kulmala, T. Hytylinen, F. Cavalli, and A. Laaksonen. Size and composition measurements of background aerosol and new particle growth in a Finnish forest during QUEST 2 using an Aerodyne Aerosol Mass Spectrometer. *Atmospheric Chemistry and Physics*, 6: 315–327, 2006.
- R.J. Arnold and J.P. Reilly. Fingerprint matching of *E. coli* strains with matrix-assisted laser desorption/ionization time-of-flight mass spectrometry of whole cells using a modified correlation approach. *Rapid Communications in Mass Spectrometry*, 12:630–636, 1998.
- R.J. Arnold and J.P. Reilly. Observation of *Escherichia coli* ribosomal proteins and their posttranslational modifications by mass spectrometry. *Analytical Biochemistry*, 269:105–112, 1999.
- S. Bashir, R. Mutter, and P.J. Derrick. Matrix-assisted laser desorption/ionization mass spectrometry with re-engineered 2,5-dihydroxybenzoic acid derivative. *The Analyst*, 128:1452–1457, 2003.
- M. Bauer, H. and Fuerhacker, F. Zibuschka, H. Schmid, and H. Puxbaum. Bacteria and fungi in aerosols generated by two different types of wastewater treatment plants. *Water Research*, 36:3965–3970, 2002.
- R.C. Beavis and J.N. Bridson. Epitaxial protein inclusion in sinapinic acid crystals. *Journal of Physics D: Applied Physics*, 26:442–447, 1993.
- R.C. Beavis and B.T. Chait. Cinnamic acid derivatives as matrices for ultraviolet laser desorption mass spectrometry of proteins. *Rapid Communications in Mass Spectrometry*, 3:432–435, 1989a.

Bibliography

- R.C. Beavis and B.T. Chait. Factors affecting the ultraviolet laser desorption of proteins. *Rapid Communications in Mass Spectrometry*, 3: 233–237, 1989b.
- R.C. Beavis, T. Chaudhary, and B.T. Chait. α -cyano-4-hydroxycinnamic acid as a matrix for matrix-assisted laser desorption mass spectrometry. *Organic Mass Spectrometry*, 27:156–158, 1992.
- M.D. Beeson, K.K. Murray, and D.H. Russell. Aerosol matrix-assisted laser desorption ionization: Effects of analyte concentration and matrix-to-analyte ratio. *Analytical Chemistry*, 67:1981–1986, 1995.
- S. Berkenkamp, C. Menzel, M. Karas, and F. Hillenkamp. Performance of infrared matrix-assisted laser desorption/ionization mass spectrometry with lasers emitting in the 3 μm wavelength range. *Rapid Communications in Mass Spectrometry*, 11:1399–1406, 1997.
- S. Berkenkamp, F. Kirpekar, and F. Hillenkamp. Infrared MALDI mass spectrometry of large nucleic acids. *Science*, 281:260–262, 1998.
- S. Berkenkamp, C. Menzel, F. Hillenkamp, and K. Dreisewerd. Measurement of mean initial velocities of analyte and matrix ions in infrared matrix-assisted laser desorption ionization mass spectrometry. *Journal of the American Society of Mass Spectrometry*, 13:209–220, 2002.
- C. Black, C. Poile, J. Langley, and J. Herniman. The use of pencil lead as a matrix and calibrant for matrix-assisted laser desorption/ionisation. *Rapid Communications in Mass Spectrometry*, 20:1053–1060, 2006.
- K.O. Börnsen, M.A.S. Gass, G.J.M. Bruin, J.H.M. von Adrichem, M.C. Biro, G.M. Kresbach, and M. Ehrat. Influence of solvents and detergents on matrix-assisted laser desorption/ionization mass spectrometry measurements of proteins and oligonucleotides. *Rapid Communications in Mass Spectrometry*, 11:603–609, 1997.
- J.P. Borra, D. Camelot, K.-L. Chou, P.L. Kooyman, J.C.M. Marijnissen, and B. Scarlett. Bipolar coagulation for powder production: micro-mixing inside droplets. *Journal of Aerosol Science*, 30:945–958, 1999.

- Å. Bovallius, B. Bucht, R. Roffey, and P. Ånäs. Three-year investigation of the natural airborne bacterial flora at four localities in Sweden. *Applied and Environmental Microbiology*, 35:847–852, 1978a.
- Å. Bovallius, B. Bucht, R. Roffey, and P. Ånäs. Long-range air transmission of bacteria. *Applied and Environmental Microbiology*, 35:1231–1232, 1978b.
- G. Brandi, M. Sisti, and G. Amagliani. Evaluation of the environmental impact of microbial aerosols generated by wastewater treatment plants utilizing different aeration systems. *Journal of Applied Microbiology*, 88:845–852, 2000.
- K. Breuker, R. Zhang J Knochenmuss, A. Stortelder, and R. Zenobi. Thermodynamic control of final ion distributions in MALDI: in-plume proton transfer reactions. *International Journal of Mass Spectrometry*, 226: 211–222, 2003.
- J.P. Brooks, B.D. Tanner, K.L. Josephson, C.P. Gerba, C.N. Haas, and I.L. Pepper. A national study on the residential impact of biological aerosols from the land application of biosolids. *Journal of Applied Microbiology*, 99:310–322, 2005.
- R.S. Brown and J.J. Lennon. Mass resolution improvement by incorporation of pulsed ion extraction in a matrix-assisted laser desorption/ionization linear time-of-flight mass spectrometer. *Analytical Chemistry*, 67:1998–2003, 1995.
- P. Büscher, A. Schmidt-Ott, and A. Wiedensohler. Performance of an unipolar square wave diffusion charger with variable Nt -product. *Journal of Aerosol Science*, 25:651–663, 1994.
- K.L. Caldwell and K.K. Murray. Mid-infrared matrix-assisted laser desorption ionization with a water/glycerol matrix. *Applied Surface Science*, 127-129:242–247, 1998.
- K.L. Caldwell, D.R. McGarity, and K.K. Murray. Matrix-assisted laser desorption/ionization with a tunable mid-infrared optical parametric oscillator. *Journal of Mass Spectrometry*, 32:1374–1377, 1997.

Bibliography

- T.-W.D. Chan, A.W. Colburn, and P.J. Derrick. Matrix-assisted laser desorption/ionization using a liquid matrix: Formation of high-mass cluster ions from proteins. *Organic Mass Spectrometry*, 27:53–56, 1992.
- W.C. Chang, L.C.L. Huang, Y.-S. Wang, W.-P. Peng, H.C. Chang, N.Y. Hsu, W.B. Yang, and C.H. Chen. Matrix-assisted laser desorption/ionization (MALDI) mechanism revisited. *Analytica Chimica Acta*, 582:1–9, 2007.
- P. Chen, Y. Lu, and P.B. Harrington. Biomarker profiling and reproducibility study of MALDI-MS measurements of *escherichia coli* by analysis of variance - principal component analysis. *Analytical Chemistry*, 80:1474–1481, 2008.
- S.L. Cohen and B.T. Chait. Influence of matrix solution conditions on the MALDI-MS analysis of peptides and proteins. *Analytical Chemistry*, 68: 31–37, 1996.
- S.M. Colby and J.P. Reilly. Space-velocity correlation focussing. *Analytical Chemistry*, 68:1419–1428, 1996.
- D.S. Cornett, M.A. Duncan, and I.J. Amster. Liquid mixtures for matrix-assisted laser desorption. *Analytical Chemistry*, 65:2608–2613, 1993.
- R.J. Cotter. *Time-of-Flight Mass Spectrometry; Instrumentation and Application in Biological Research*. Chemical Society, Washington, DC, USA, 1997.
- R. Cramer and A.L. Burlingame. Employing target modifications for the investigation of liquid infrared matrix-assisted laser desorption/ionization mass spectrometry. *Rapid Communications in Mass Spectrometry*, 14:53–60, 2000.
- R. Cramer, F. Hillenkamp, and R.F. Haglund. Infrared matrix-assisted laser desorption and ionization by using a tunable mid-infrared free-electron laser. *Journal of the American Society of Mass Spectrometry*, 7:1187–1193, 1996.
- R. Cramer, R.F. Haglund, and Hillenkamp F. Matrix-assisted laser desorption and ionization in the O-H and C=O absorption bands of aliphatic

- and aromatic matrices: dependence on laser wavelength and temporal beam profile. *International Journal of Mass Spectrometry and Ion Processes*, 169-170:51–67, 1997.
- Y. Dai, R.M. Whittal, and L. Li. Confocal fluorescence microscopic imaging for investigating the analyte distribution in MALDI matrices. *Analytical Chemistry*, 68:2494–2500, 1996a.
- Y. Dai, R.M. Whittal, L. Li, and S. Weinberger. Accurate mass measurements of oligonucleotides using a time-lag focussing matrix-assisted laser desorption/ionization time-of-flight mass spectrometer. *Rapid Communications in Mass Spectrometry*, 10:1792–1796, 1996b.
- Y. Dai, R. Whittal, and L. Li. Two-layer sample preparation: A method for MALDI-MS analysis of complex peptide and protein mixtures. *Analytical Chemistry*, 71:1087–1091, 1999.
- P.A Demirev, Y.-P. Ho, V. Ryzhov, and C. Fenselau. Microorganism identification by mass spectrometry and protein database searches. *Analytical Chemistry*, 71:2732–2738, 1999.
- P.A. Demirev, J.S. Lin, F.J. Pineda, and C. Fenselau. Bioinformatics and mass spectrometry for microorganism identification: Proteome-wide post-translational modifications and database search algorithms for characterization of intact *sch. pylori*. *Analytical Chemistry*, 73:4566–4573, 2001.
- P.A. Demirev, A.B. Feldman, P. Kowalski, and J.S. Lin. Top-down proteomics for rapid identification of intact microorganisms. *Analytical Chemistry*, 77:7455–7461, 2005.
- C. Di Giorgio, A. Krempff, Guiraud H., P. Binder, C. Tiret, and G. Dumenil. Atmospheric pollution by airborne microorganisms in the city of Marseilles. *Atmospheric Environment*, 30:155–160, 1996.
- K. Dreisewerd. The desorption process in MALDI. *Chemical Reviews*, 103: 395–425, 2003.

Bibliography

- K. Dreisewerd, S. Berkenkamp, A. Leisner, A. Rohlfig, and C. Menzel. Fundamentals of matrix-assisted laser desorption/ionization mass spectrometry with pulsed infrared lasers. *International Journal of Mass Spectrometry*, 226:189–209, 2003.
- R.D. English, B. Warscheid, C. Fenselau, and R.J. Cotter. *Bacillus* spore identification via proteolytic peptide mapping with a minaturized MALDI TOF mass spectrometer. *Analytical Chemistry*, 75:6886–6893, 2003.
- W.J. Erb, S.D. Hanton, and K.G. Owens. A study of gas-phase cationization in matrix-assisted laser desorption/ionization time-of-flight mass spectrometry. *Rapid Communications in Mass Spectrometry*, 20:2165–2169, 2006.
- K.F. Fannin, S.C. Vana, and W. Jakubowski. Effect of an activated-sludge waste-water treatment-plant on ambient air densities of aerosols containing bacteria and viruses. *Applied and Environmental Microbiology*, 49:1191–1196, 1985.
- G.R. Farquar, P.T. Steele, E.L. McJimpsey, C.B. Lebrilla, E.E. Tobias, H.J. Gard, M. Frank, K. Coffee, V. Riot, and D.P. Fergenson. Supramicrometer particle shadowgraph imaging in the ionization region of a single particle aerosol mass spectrometer. *Journal of Aerosol Science*, 39:10–18, 2008.
- D. Feldhaus, C. Menzel, F. Berkenkamp, S. and Hillenkamp, and K. Dreisewerd. Influence of the laser fluence in infrared matrix-assisted laser desorption/ionization with a 2.94 μm Er:YAG laser and a flat top beam profile. *Journal of Mass Spectrometry*, 35:1320–1328, 2000.
- C. Fenselau and P.A. Demirev. Characterization of intact microorganisms by MALDI mass spectrometry. *Mass Spectrometry Reviews*, 20:157–171, 2001.
- D.P. Fergenson, M.E. Pitesky, H.J. Tobias, P.T. Steele, G.A. Czerwieniec, S.C. Russell, C.B. Lebrilla, J.M. Horn, K.R. Coffee, A. Srivastava, S.P. Pillai, M-T.P. Shih, H.L. Hall, A.J. Ramponi, J.T. Chang, R.G. Langlois, P.L. Estacio, R.T. Hadley, M. Frank, and E.E. Gard. Reagentless

- detection and classification of individual bioaerosol particles in seconds. *Analytical Chemistry*, 76:373–378, 2004.
- M.C. Fitzgerald, G.R. Parr, and L.M. Smith. Basic matrices for the matrix-assisted laser desorption/ionization mass spectrometry of proteins and oligonucleotides. *Analytical Chemistry*, 65:3204–3211, 1993.
- S.K. Friedlander. *Smoke, Dust, and Haze - Fundamentals of Aerosol Dynamics*. Oxford University Press Inc., New York, New York, 2000.
- J.D. Fulton and R.B. Mitchell. Microorganisms of the upper atmosphere: II. microorganisms in two types of air masses at 690 meters over a city. *Applied and Environmental Microbiology*, 14:232–236, 1966.
- D.W. Griffin, V.H. Garrison, J.R. Herman, and E.A. Shinn. African desert dust in the Caribbean atmosphere: Microbiology and public health. *Aerobiologia*, 17:203–213, 2001.
- P.P. Hairston, J. Ho, and F.R. Quant. Design of an instrument for real-time detection of bioaerosols using simultaneous measurement of particle aerodynamic size and intrinsic fluorescence. *Journal of Aerosol Science*, 28:471–482, 1997.
- W.A. Harris, P.T.A. Reilly, and W.B. Whitten. MALDI of individual biomolecule-containing airborne particles in an ion trap mass spectrometer. *Analytical Chemistry*, 77:4042–4050, 2005a.
- W.A. Harris, P.T.A. Reilly, W.B. Whitten, and J.M. Ramsey. Transportable real-time single-particle ion trap mass spectrometer. *Review of Scientific Instruments*, 76:064102, 2005b.
- W.A. Harris, P.T.A. Reilly, and W.B. Whitten. Aerosol MALDI of peptides and proteins in an ion trap mass spectrometer: Trapping, resolution and signal-to-noise. *International Journal of Mass Spectrometry*, 258: 113–119, 2006.
- R.M. Harrison, A.M. Jones, P.D.E. Biggins, N. Pomeroy, C.S. Cox, S.P. Kidd, J.L. Hobman, N.L. Brown, and A. Beswick. Climate factors influencing bacterial count in background air samples. *International Journal of Biometeorology*, 49:167–178, 2005.

Bibliography

- R.P.A. Hartman, D.J. Brunner, D.M.A. Camelot, J.C.M. Marijnissen, and B. Scarlett. Electrohydrodynamic atomization in the cone-jet mode: Physical modelling of the liquid cone and jet. *Journal of Aerosol Science*, 30:823–849, 1999.
- Y. Hathout, P.A. Demirev, Y.-P. Ho, J.L. Bundy, V. Ryzhov, L. Sapp, J. Stutler, J. Jackman, and C. Fenselau. Identification of *Bacillus* spores by matrix-assisted laser desorption/ionization mass spectrometry. *Applied and Environmental Microbiology*, 65:4313–4319, 1999.
- Y. Hathout, B. Setlow, R.M. Cabrera-Martinez, C. Fenselau, and P. Setlow. Small, acid-soluble proteins as biomarkers in mass spectrometry analysis of *Bacillus* spores. *Applied and Environmental Microbiology*, 69:1100–1107, 2003.
- J.M. Hettick, M.L. Kashon, J.E. Slaven, Y. Ma, J.P. Simpson, P.D. Siegel, G.N. Mazurek, and D.N. Weissman. Discrimination of intact mycobacteria at the strain level: A combined MALDI-TOF MS and biostatistical analysis. *Proteomics*, 6:6416–6425, 2006.
- W. C. Hinds. *Aerosol Technology: Properties, Behaviour and Measurement of Airborne Particles*. John Wiley and Sons Ltd, Chichester, New England, 1999.
- R.D. Holland, J.G. Wilkes, J.B. Rafii, J.B. Sutherland, C.C. Persons, K.J. Voorhees, and J.O. Lay. Rapid identification of intact whole bacteria based on spectral patterns using matrix-assisted laser desorption/ionization with time-of-flight mass spectrometry. *Rapid Communications in Mass Spectrometry*, 10:1227–1232, 1996.
- ICH. International conference on harmonisation of technical requirements for registration of pharmaceuticals for human use, ICH harmonised tripartite guideline pharmaceutical development Q8. <http://www.ich.org/cache/compo/363-272-1.html>, November 2005.
- S.N. Jackson and K.K. Murray. Infrared matrix-assisted laser desorption/ionization of polycyclic aromatic hydrocarbons in a sulfolane matrix. *Rapid Communications in Mass Spectrometry*, 15:1448–1452, 2001.

Bibliography

- S.N. Jackson and K.K. Murray. Matrix addition by condensation for matrix-assisted laser desorption/ionization of collected aerosol particles. *Analytical Chemistry*, 74:4841–4844, 2002.
- S.N. Jackson, S. Mishra, and K.K. Murray. On-line laser desorption/ionization mass spectrometry of matrix-coated aerosols. *Rapid Communications in Mass Spectrometry*, 18:2041–2045, 2004.
- K.H. Jarman, S.T. Cebula, A.J. Saenz, C.E. Petersen, N.B. Valentine, M.T. Kingsley, and K.L. Wahl. An algorithm for automated bacterial identification using matrix-assisted laser desorption/ionization mass spectrometry. *Analytical Chemistry*, 72:1217–1223, 2000.
- B.L. Jones and J.T. Cookson. Natural atmospheric microbial conditions in a typical suburban area. *Applied and Environmental Microbiology*, 45:919–934, 1983.
- T.J.D. Jørgensen, G. Bojesen, and H. Rahbek-Nielsen. The proton affinities of seven matrix-assisted laser desorption/ionization matrices correlated with the formation of multiply charged ions. *European Mass Spectrometry*, 4:39–45, 1998.
- P. Juhasz, C.E. Costello, and K. Biemann. Matrix-assisted laser desorption ionization mass spectrometry with 2-(4-hydroxyphenylazo)benzoic acid matrix. *Journal of the American Society for Mass Spectrometry*, 4:399–409, 1993.
- M. Karas and F. Hillenkamp. Laser desorption ionization of proteins with molecular masses exceeding 10 000 Daltons. *Analytical Chemistry*, 60:2299–2301, 1988.
- M. Karas, D. Bachmann, U. Bahr, and F. Hillenkamp. Matrix-assisted ultraviolet laser desorption of non-volatile compounds. *International Journal of Mass Spectrometry and Ion Processes*, 78:53–68, 1987.
- M. Karas, H. Ehring, E. Nordhoff, B. Stahl, K. Strupat, F. Hillenkamp, M. Grehl, and B. Krebs. Matrix-assisted laser desorption/ionization mass spectrometry with additives to 2,5-dihydroxybenzoic acid. *Organic Mass Spectrometry*, 28:1476–1481, 1993.

Bibliography

- M. Karas, M. Glückmann, and J. Schäfer. Ionization in matrix-assisted laser desorption/ionization: singly charged molecules are the lucky survivors. *Journal of Mass Spectrometry*, 35:1–12, 2000.
- C.J. Keys, D.J. Dare, H. Sutton, G. Wells, M. Lunt, T. McKenna, M. McDowall, and H.N. Shah. Compilation of a MALDI-TOF mass spectral database for the rapid screening and characterisation of bacteria implicated in human infectious diseases. *Infection, Genetics and Evolution*, 4:221–242, 2004.
- E. Khoury. Corona wind bioaerosol concentrator. Master’s thesis, Delft University of Technology, 2006.
- O. Kievit. *Development of a laser mass spectrometer for aerosols*. PhD thesis, Delft University of Technology, 1995.
- O. Kievit, M. Weiss, P.J.T. Verheijen, J.C.M. Marijnissen, and B. Scarlett. The on-line chemical analysis of single particles using aerosol beams and time of flight mass spectrometry. *Chemical Engineering Communications*, 151:79–100, 1996.
- J.K. Kim, S.N. Jackson, and K.K. Murray. Matrix-assisted laser desorption/ionization mass spectrometry of collected bioaerosol particles. *Rapid Communications in Mass Spectrometry*, 19:1725–1729, 2005.
- S.H. Kim, C.M. Shin, and J.S. Yoo. First application of thermal vapor deposition method to matrix-assisted laser desorption ionization mass spectrometry: Determination of molecular mass of bis(p-methyl benzylidene) sorbitol. *Rapid Communications in Mass Spectrometry*, 12:701–704, 1998.
- W.A. Kleefsman and C. Van Gulijk. Robust method to compare aerosol chargers. *Journal of Aerosol Science*, 39:1–9, 2008.
- W.A. Kleefsman, M.A. Stowers, P.J.T. Verheijen, A.L. van Wuijckhuijse, Ch.E. Kientz, and J.C.M. Marijnissen. Bioaerosol analysis by single particle mass spectrometry. *Particle & Particle Systems Characterization*, 44:85–90, 2007.

- R. Knochenmuss and R. Zenobi. MALDI ionization: The role of in-plume processes. *Chemical Reviews*, 103:441–452, 2003.
- T. Krishnamurthy and P.L. Ross. Rapid identification of bacteria by direct matrix-assisted laser desorption/ionization mass spectrometric analysis of whole cells. *Rapid Communications in Mass Spectrometry*, 10:1992–1996, 1996.
- T. Krishnamurthy, P.L. Ross, and U. Rajamani. Detection of pathogenic and non-pathogenic bacteria by matrix-assisted laser desorption/ionization time-of-flight mass spectrometry. *Rapid Communications in Mass Spectrometry*, 10:883–888, 1996.
- M. Kulmala, P. Hari, A. Laaksonen, T. Vesala, and Y. Viisanen. Research unit of physics, chemistry and biology of atmospheric composition and climate change: Overview of recent results. *Boreal Environment Research*, 10:459–477, 2005.
- C.R. Kuske. Current and emerging technologies for the study of bacteria in the outdoor air. *Current Opinion in Biotechnology*, 17:291–296, 2006.
- M. Kussman, E. Nordhoff, H. Rahbek-Nielsen, S. Haebel, M. Rossel-Larsen, L. Jakobsen, J. Gobom, E. Mirgorodskaya, A. Kroll-Kristensen, L. Palm, and P. Roepstorff. Matrix-assisted laser desorption/ionization mass spectrometry sample preparation techniques designed for various peptide and protein analytes. *Journal of Mass Spectrometry*, 32:593–601, 1997.
- M.E. Lacey and J.S. West. *The air spora*. Springer, Dordrecht, The Netherlands, 2006.
- S.J. Lawson and K.K. Murray. Continuous flow infrared matrix-assisted laser desorption/ionization with a solvent matrix. *Rapid Communications in Mass Spectrometry*, 14:129–134, 2000.
- J.O. Lay. MALDI-TOF mass spectrometry and bacterial taxonomy. *Trends in Analytical Chemistry*, 19:507–516, 2000.
- J.O. Lay. MALDI-TOF mass spectrometry of bacteria. *Mass Spectrometry Reviews*, 20:172–194, 2001.

Bibliography

- R. Lee, K. Harris, and G. Akland. Relationship between viable bacteria and air pollutants in an urban atmosphere. *American Industrial Hygiene Association journal*, 34:164–170, 1973.
- S.A. Lee, A. Adhikari, S.A. Grinshpun, R. McKay, R. Shukla, and T. Reponen. Personal exposure to airborne dust and microorganisms in agricultural environments. *Journal of Occupational and Environmental Hygiene*, 3:118–130, 2006a.
- T. Lee, S.A. Grinshpun, D. Martuzevicius, A. Adhikari, C.M. Crawford, J. Luo, and T. Reponen. Relationship between indoor and outdoor bioaerosols collected with a button inhalable aerosol sampler in urban homes. *Indoor Air*, 16:37–47, 2006b.
- X. Li, M. Wilm, and T. Franz. Silicone/graphite coating for on-target desalting and improved peptide mapping performance of matrix-assisted laser desorption/ionization-mass spectrometry targets in proteomic experiments. *Proteomics*, 5:1460–1471, 2005.
- B. Lighthart. Survival of airborne bacteria in a high urban concentration of carbon monoxide. *Applied Microbiology*, 25:86–91, 1973.
- B. Lighthart. Microbial aerosols: estimated contribution of combine harvesting to an airshed. *Applied and Environmental Microbiology*, 47:430–432, 1984.
- B. Lighthart. The ecology of bacteria in the alfresco atmosphere. *FEMS Microbiology Ecology*, 23:263–274, 1997.
- B. Lighthart and A.J. Mohr, editors. *Atmospheric Microbial Aerosols - Theory and Applications*. Chapman & Hall, Inc., New York, New York, USA, 1994.
- B. Lighthart and B.T. Shaffer. Airborne bacteria in the atmosphere surface layer: Temporal distribution above a grass seed field. *Applied and Environmental Microbiology*, 61:1492–1496, 1995.
- J. Lindemann and C.D. Upper. Aerial dispersal of epiphytic bacteria over bean plants. *Applied and Environmental Microbiology*, 50:1229–1232, 1985.

Bibliography

- R.R.O. Loo and J.A. Loo. Matrix-assisted laser desorption/ionization-mass spectrometry of hydrophobic proteins in mixtures using formic acid, perfluorooctanoic acid, and sorbitol. *Analytical Chemistry*, 79: 1115–1125, 2007.
- D.L. Lubman, editor. *Lasers and Mass Spectrometry*. Oxford University Press, Inc, New York, New York, 1990.
- M. T. Madigan, J. M. Martinko, and J. Parker. *Brock Biology of Microorganisms*. Prentice Hall, Upper Saddle River, New Jersey USA., 9th edition, 2000.
- R.L. Mancinelli and W.A. Shulls. Airborne bacteria in an urban environment. *Applied and Environmental Microbiology*, 35:1095–1101, 1978.
- B.A. Mansoori and M.V. Johnston. Matrix-assisted laser desorption/ionization of size- and composition-selected aerosol particles. *Analytical Chemistry*, 68:3595–3601, 1996.
- J.C.M. Marijnissen, B. Scarlett, and P.J.T. Verheijen. Proposed online aerosol analysis combining size determination, laser-induced fragmentation and time-of-flight mass-spectroscopy. *Journal of Aerosol Science*, 19:1307–1310, 1988.
- S. Matthias-Maser and R. Jaenicke. Examination of atmospheric bioaerosol particles with radii $> 0.2 \mu\text{m}$. *Journal of Aerosol Science*, 25:1605–1613, 1994.
- S. Matthias-Maser and R. Jaenicke. The size distribution of primary biological aerosol particles with radii $> 0.2 \mu\text{m}$ in an urban/rural influenced region. *Atmospheric Research*, 39:279–286, 1995.
- S. Matthias-Maser, Peters K., and R. Jaenicke. Seasonal variation of primary biological aerosol particles. *Journal of Aerosol Science*, 26: S545–S546, 1995.
- S. Matthias-Maser, V. Obolkin, T. Khodzer, and R. Jaenicke. Seasonal variation of primary biological aerosol particles in the remote continental region of Lake Baikal/Siberia. *Atmospheric Environment*, 34: 3805–3811, 2000.

Bibliography

- M.A.R. Meier, N. Adams, and U.S. Schubert. Statistical approach to understand MALDI-TOFMS matrices: Discovery and evaluation of new MALDI matrices. *Analytical Chemistry*, 79:863–869, 2007.
- C. Menzel, S. Berkenkamp, and F. Hillenkamp. Infrared matrix-assisted laser desorption/ionization mass spectrometry with a transversely excited atmospheric pressure carbon dioxide laser at 10.6 μm wavelength with static and delayed ion extraction. *Rapid Communications in Mass Spectrometry*, 13:26–32, 1999.
- C. Menzel, K. Dreisewerd, S. Berkenkamp, and F. Hillenkamp. Mechanisms of energy deposition in infrared matrix-assisted laser desorption/ionization mass spectrometry. *International Journal of Mass Spectrometry*, 207:73–96, 2001.
- C. Menzel, K. Dreisewerd, S. Berkenkamp, and F. Hillenkamp. The role of laser pulse duration in infrared matrix-assisted laser desorption/ionization mass spectrometry. *Journal of the American Society of Mass Spectrometry*, 13:975–984, 2002.
- S.S. Merola, G. Gambi, C. Allouis, F. Beretta, A. Borghese, and A. DAlessio. Analysis of exhausts emitted by i.c. engines and stationary burners, by means of U.V. extinction and fluorescence spectroscopy. *Chemosphere*, 42:827–834, 2001.
- S.P. Mirza, N.P. Raju, S.S. Madhavendra, and M. Vairamani. 5-amino-2-mercapto-1,3,4-thiadiazole: a new matrix for the efficient matrix-assisted laser desorption/ionization of neutral carbohydrates. *Rapid Communications in Mass Spectrometry*, 18:1666–1674, 2004a.
- S.P. Mirza, N.P. Raju, and M. Vairamani. Estimation of the proton affinity values of fifteen matrix-assisted laser desorption/ionization matrices under electrospray ionization conditions using the kinetic method. *Journal of the American Society for Mass Spectrometry*, 15:431–435, 2004b.
- K. Miyanaga, S. Takano, Y. Morono, K. Hori, H. Unno, and Y. Tanji. Optimization of distinction between viable and dead cells by fluorescent

Bibliography

- staining method and its application to bacterial consortia. *Biochemical Engineering Journal*, 37:56–61, 2007.
- K.K. Murray and D.H. Russell. Aerosol matrix-assisted laser desorption ionization mass spectrometry. *Journal of the American Society for Mass Spectrometry*, 5:1–9, 1994.
- BMED National Research Council. *Sensor Systems for Biological Agents Attacks: Protecting Buildings and Military Bases*. National Academies Press, Washington, District of Columbia, USA, 2005.
- A. Nevalainen, J. Pastuszka, F. Liebhaber, and K. Willeke. Performance of bioaerosol samplers: Collection characteristics and sampler design considerations. *Atmospheric Environment*, 26A:531–540, 1992.
- A. Nieuwmeyer. Development particle concentrator for bioaerosol alarm. Master's thesis, Particle Engineering Research Center Florida, 2004.
- S. Niu, W. Zhang, and B.T. Chait. Direct comparison of infrared and ultraviolet wavelength matrix-assisted laser desorption/ionization mass spectrometry of proteins. *Journal of the American Society for Mass Spectrometry*, 9:1–7, 1998.
- C.A. Noble and K.A. Prather. Real-time single particle mass spectrometry: A historical review of a quarter century of the chemical analysis of aerosols. *Mass Spectrometry Reviews*, 19:248–274, 2000.
- T. Nordmeyer and K.A. Prather. Real-time measurement capabilities using aerosol time-of-flight mass spectrometry. *Analytical Chemistry*, 66: 3540–3542, 1994.
- Department of Defense. Chemical and biological defense program. volume i: Annual report to congress. Technical report, Department of Defense of the United States, 2003.
- A. Overberg, M. Karas, U. Bahr, R. Kaufmann, and F. Hillenkamp. Matrix-assisted infrared-laser (2.94 μm) desorption/ionization mass spectrometry of large biomolecules. *Rapid Communications in Mass Spectrometry*, 4:293–296, 1990.

Bibliography

- A. Overberg, M. Karas, and F. Hillenkamp. Matrix-assisted laser desorption of large biomolecules with a tea-co₂-laser. *Rapid Communications in Mass Spectrometry*, 5:128–131, 1991.
- S.M. Pady and C.L. Kramer. Diurnal periodicity in airborne bacteria. *Mycologia*, 59:714–716, 1967.
- Y.-L. Pan, V. Boutou, J.R. Bottiger, S.S. Zhang, J.-P. Wolf, and R.K. Chang. A puff of air sorts bioaerosols for pathogen identification. *Aerosol Science and Technology*, 38:598–602, 2004.
- Y.L. Pan, S. Holler, R.K. Cheng, S.C. Hill, R.G. Pinnick, S. Niles, and J.R. Bottiger. Single shot fluorescence spectra of individual micro-sized bio-aerosols illuminated by a 351 nm or 266 nm ultraviolet laser. *Optics Letters*, 24:116–118, 1999.
- Y.L. Pan, J. Hartings, R.G. Pinnick, S.C. Hill, J. Halverson, and R.K. Chang. Single-particle fluorescence spectrometer for ambient aerosols. *Aerosol Science and Technology*, 37:628–639, 2003.
- J.S. Pastuszka, U.K.T. Paw, D.O. Lis, A. Wlazło, and K. Ulfig. Bacterial and fungal aerosol in indoor environment in Upper Silesia, Poland. *Atmospheric Environment*, 34:3833–3842, 2000.
- I.K. Perera, S. Kantartzoglou, and P.E. Dyer. Coumarin dyes as matrices for matrix assisted UV laser desorption/ionization mass spectrometry. *International Journal of Mass Spectrometry and Ion Processes*, 137:151–171, 1994.
- S.D. Pillai and S.C. Ricke. Bioaerosols from municipal and animal wastes: background and contemporary issues. *Canadian Journal of Microbiology*, 48:681–696, 2002.
- F.J. Pineda, J.S. Lin, C. Fenselau, and P.A. Demirev. Testing the significance of microorganism identification by mass spectrometry and proteome database search. *Analytical Chemistry*, 72:3739–3744, 2000.
- F.J. Pineda, M.D. Antoine, P.A. Demirev, A.B. Feldman, J. Jackman, M. Longenecker, and J.S. Lin. Microorganism identification by matrix-assisted laser/desorption ionization mass spectrometry and model-

- derived ribosomal protein biomarkers. *Analytical Chemistry*, 75:3817–3822, 2003.
- R.G. Pinnick, S.C. Hill, P. Nachman, J.D. Pendleton, G.L. Fernandez, M.W. Mayo, and J.G. Bruno. Fluorescence particle counter for detecting airborne bacteria and other biological particles. *Aerosol Science and Technology*, 23:653–664, 1995.
- R.G. Pinnick, S.C. Hill, P. Nachman, G. Videen, G. Chen, and R.K. Chang. Aerosol fluorescence spectrum analyzer for rapid measurement of single micrometer-sized airborne biological particles. *Aerosol Science and Technology*, 28:95–104, 1998.
- M.A. Posthumus, P.G. Kistemaker, H.L.C. Meuzelaar, and Ten Noever de Brauw. Laser desorption-mass spectrometry of polar nonvolatile bio-organic molecules. *Analytical Chemistry*, 50:985–991, 1978.
- K.A. Prather, T. Nordmeyer, and K. Salt. Real-time characterization of individual aerosol particles using time-of-flight mass spectrometry. *Analytical Chemistry*, 66:1403–1407, 1994.
- N.P. Raju, S.P. Mirza, M. Vairamani, A.R. Ramulu, and M. Pardhasaradhi. 5-ethyl-2-mercaptothiazole as matrix for matrix-assisted laser desorption/ionization of a broad spectrum of analytes in positive and negative ion mode. *Rapid Communications in Mass Spectrometry*, 15:1879–1884, 2001.
- V. Ruelle, B. El Moualij, W. Zorzi, P. Ledent, and de E. Pauw. Rapid identification of environmental bacterial strains by matrix-assisted laser desorption/ionization time-of-flight mass spectrometry. *Rapid Communications in Mass Spectrometry*, 18:2013–2019, 2004.
- D.H. Russell and M.D. Beeson. Aerosol matrix-assisted laser desorption/ionization mass spectrometry. I.-effect of solvent on ion signal. *Journal of Mass Spectrometry*, 31:295–302, 1996.
- S.C. Russell, G. Czerwieńiec, C. Lebrilla, P. Steele, V. Riot, K. Coffee, M. Frank, and E.E. Gard. Achieving high detection sensitivity (14 zmol) of biomolecular ions in bioaerosol mass spectrometry. *Analytical Chemistry*, 77:4734–4741, 2005.

Bibliography

- V. Ryzhov and C. Fenselau. Characterization of the protein subset desorbed by MALDI from whole bacterial cells. *Analytical Chemistry*, 73: 746–750, 2001.
- M. Sadeghi, Z. Olumee, X. Tang, A. Vertes, Z. Jiang, A.J. Henderson, H.S. Lee, and C.R. Prasad. Compact tunable Cr:LiSAF laser for infrared matrix-assisted laser desorption/ionization. *Rapid Communications in Mass Spectrometry*, 11:393–397, 1997.
- A.J. Saenz, C.E. Peterson, N.B. Valentine, S.L. Gantt, K.H. Jarman, M.T. Kingsley, and K.L. Wahl. Reproducibility of matrix-assisted laser desorption/ionization time-of-flight mass spectrometry for replicate bacterial culture analysis. *Rapid Communications in Mass Spectrometry*, 13: 1580–1585, 1999.
- D. Schleuder, F. Hillenkamp, and K. Strupat. IR-MALDI-mass analysis of electroblotted proteins directly from the membrane: Comparison of different membranes, application to on-membrane digestion, and protein identification by database searching. *Analytical Chemistry*, 71:3238–3247, 1999.
- M. Schnell, C.S. Cheung, and C.W. Leung. Coagulation of diesel particles in an enclosed chamber. *Journal of Aerosol Science*, 34:1289–1293, 2004.
- M. Seaver, J.D. Eversole, J.J. Hardgrove, W.K. jr. Cary, and D.C. Roselle. Size and fluorescence measurements for field detection of biological aerosols. *Aerosol Science and Technology*, 30:174–185, 1999.
- P. Setlow. I will survive: DNA protection in bacterial spores. *Trends in Microbiology*, 15:172–180, 2007.
- B.T. Shaffer and B. Lighthart. Survey of culturable airborne bacteria at four diverse locations in Oregon: Urban, rural, forest, and coastal. *Microbial Ecology*, 34:167–177, 1997.
- J.D. Sheffer and K.K. Murray. Infrared matrix-assisted laser desorption/ionization using OH, NH and CH vibrational absorption. *Rapid Communications in Mass Spectrometry*, 12:1685–1690, 1998.

Bibliography

- M.P. Sinha. Laser-induced volatilization and ionization of microparticles. *Review of Scientific Instruments*, 55:886–891, 1984.
- M.P. Sinha, C.E. Giffina, D.D. Norrison, T.J. Estesb, V.L. Vilkerb, and S.K. Friedlander. Particle analysis by mass spectrometry. *Journal of Colloid and Interface Science*, 87:140–153, 1982.
- M.P. Sinha, R.M. Platz, V.L. Vilker, and S.K. Friedlander. Analysis of individual biological particles by mass spectrometry. *International Journal of Mass Spectrometry and Ion Processes*, 57:125–133, 1984.
- M.P. Sinha, R.M. Platz, S.K. Friedlander, and V.L. Vilker. Characterization of bacteria by particle beam mass spectrometry. *Applied and Environmental Microbiology*, 49:1366–1373, 1985.
- V Sivaprakasam, A. Huston, C. Scotto, and J. Eversole. Multiple UV wavelength excitation and fluorescence of bioaerosols. *Optics Express*, 12:4457–4466, 2004.
- A. Srivastava, M.E. Pitesky, P.T. Steele, H.J. Tobias, D.P. Fergenson, J.M. Horn, S.C. Russell, G.A. Czerwieniec, C.B. Lebrilla, E.E. Gard, and M. Frank. Comprehensive assignment of mass spectral signatures from individual *Bacillus atrophaeus* spores in matrix-free laser desorption/ionization bioaerosol mass spectrometry. *Analytical Chemistry*, 77:3315–3323, 2005.
- P.T. Steele, H.J. Tobias, D.P. Fergenson, M.E. Pitesky, J.M. Horn, G.A. Czerwieniec, S.C. Russell, C.B. Lebrilla, E.E. Gard, and M. Frank. Laser power dependence of mass spectral signatures from individual bacterial spores in bioaerosol mass spectrometry. *Analytical Chemistry*, 75:5480–5487, 2003.
- M.A. Stowers, A.L. van Wuijckhuijse, J.C.M. Marijnissen, B. Scarlett, B.L.M. van Baar, and Ch.E. Kientz. Application of matrix-assisted laser desorption/ionization to on-line aerosol time-of-flight mass spectrometry. *Rapid Communications in Mass Spectrometry*, 14:829–833, 2000.

Bibliography

- M.A. Stowers, A.L. van Wuijckhuijse, J.C.M. Marijnissen, Ch.E. Kientz, and T. Ciach. Fluorescence preselection of bioaerosol for single-particle mass spectrometry. *Applied Optics*, 45:8531–8536, 2006.
- K. Strupat, Karas. M., and F. Hillenkamp. 2,5-dihydroxybenzoic acid: a new matrix for laser desorption-ionization mass spectrometry. *International Journal of Mass Spectrometry and Ion Processes*, 111:89–102, 1991.
- S. Swatkoski, S.C. Russell, N. Edwards, and C. Fenselau. Rapid chemical digestion of small acid-soluble spore proteins for analysis of *Bacillus* spores. *Analytical Chemistry*, 78:181–188, 2006.
- E.T.P. Sze and T.-W. D. Chan. Formulations of matrix solutions for use in matrix-assisted laser desorption/ionization of biomolecules. *Journal of the American Society for Mass Spectrometry*, 9:166–174, 1998.
- K. Tanaka, H. Waki, Y. Ido, S. Akita, Y. Yoshida, and T. Yoshida. Protein and polymer analyses up to m/z 100 000 by laser ionization time-of-flight mass spectrometry. *Rapid Communications in Mass Spectrometry*, 2:151–153, 1988.
- K. Tang, N.I. Taranenko, S.L. Allman, C.H. Chen, L.Y. Cháng, and K.B. Jacobson. Picolinic acid as a matrix for laser mass spectrometry of nucleic acid and proteins. *Rapid Communications in Mass Spectrometry*, 8:673–677, 1994.
- B.D. Tanner, J.P. Brooks, C.N. Haas, C.P. Gerba, and I.L. Pepper. Bioaerosol emission rate and plume characteristics during land application of liquid class B biosolids. *Environmental Science and Technology*, 39:1584–1590, 2005.
- K. Teschke, Y. Chow, k. Bartlett, A. Ross, and C. van Netten. Spatial and temporal distribution of airborne *Bacillus thuringiensis* var. *kurstaki* during an aerial spray program for gypsy moth eradication. *Environmental Health Perspectives*, 109:47–54, 2001.
- Y. Tong and Lighthart. Solar radiation has a lethal effect on natural populations of culturable outdoor atmospheric bacteria. *Atmospheric Environment*, 31:897–900, 1997.

- Y. Tong and B. Lighthart. The annual bacterial particle concentration and size distribution in the ambient atmosphere in a rural area of the willamette valley, Oregon. *Aerosol Science and Technology*, 32:393–403, 2000.
- Y. Tong and B. Lighthart. Diurnal distribution of total and culturable atmospheric bacteria at a rural site. *Aerosol Science and Technology*, 30:246–254, 1999.
- Y. Tong, F. Che, X. Xu, M. Chen, B. Ye, and L. Jiang. Population study of atmospheric bacteria at the Fengtai district of Beijing on two representative days. *Aerobiologia*, 9:69–74, 1993.
- P.C.B. Turnbull, P.M. Lindeque, J. Le Roux, A.M. Bennett, and S.R. Parks. Airborne movement of anthrax spores from carcass sites in the Etosha National Park, Namibia. *Journal of Applied Microbiology*, 84: 667–676, 1998.
- B.L.M. van Baar. Characterisation of bacteria by matrix-assisted laser desorption/ionisation and electrospray mass spectrometry. *FEMS Microbiology Reviews*, 24:193–219, 2001.
- A.L. Van Wuijckhuijse. *Aerosol Time-of-Flight Mass Spectrometry - Approach to detect, select and identify Bioaerosols*. PhD thesis, Delft University of Technology, 2003.
- A.L. Van Wuijckhuijse, M.A. Stowers, W.A. Kleefsman, B.L.M. van Baar, Ch.E. Kientz, and J.C.M. Marijnissen. Matrix-assisted laser desorption/ionisation aerosol time-of-flight mass spectrometry for the analysis of bioaerosols: development of a fast detector for airborne biological pathogens. *Journal of Aerosol Science*, 36:677–687, 2005.
- M. Vargha, Z. Takáts, A. Konopka, and C.H. Nakatsu. Optimization of MALDI-TOF MS for strain level differentiation of *Arthrobacter isolates*. *Journal of Microbiological Methods*, 66:399–409, 2006.
- F.J. Vastola and A.J. Pirone. Ionization of organic solids by laser irradiation. *Advances in Mass Spectrometry*, 4:107–111, 1968.

Bibliography

- O. Vorm, P. Roepstorff, and M. Mann. Improved resolution and very high sensitivity in MALDI TOF of matrix surfaces made by fast evaporation. *Analytical Chemistry*, 66:3281–3287, 1994.
- B.H. Wang, K. Dreisewerd, U. Bahr, M. Karas, and F. Hillenkamp. Gas-phase cationization and protonation of neutrals generated by matrix-assisted laser desorption. *Journal of the American Society for Mass Spectrometry*, 4:393–398, 1993.
- X. Wang and P.H. McMurry. A design tool for aerodynamic lens systems. *Aerosol Science and Technology*, 40:320–334, 2006.
- Z. Wang, L. Russon, L. Li, D.C. Roser, and S.R. Long. Investigation of spectral reproducibility in direct analysis of bacteria proteins by matrix-assisted laser desorption/ionization time-of-flight mass spectrometry. *Rapid Communications in Mass Spectrometry*, 12:456–464, 1998.
- B. Warscheid and C. Fenselau. A targeted proteomics approach to the rapid identification of bacterial cell mixtures by matrix-assisted laser desorption/ionization mass spectrometry. *Proteomics*, 4:2877–2892, 2004.
- M. Weiss. *An On-line Mass Spectrometer for Aerosols - Development, Characterization and Applications*. PhD thesis, Delft University of Technology, 1997.
- M. Weiss, P.J.T. Verheijen, J.C.M. Marijnissen, and B. Scarlett. On the performance of an on-line time-of-flight mass spectrometer for aerosols. *Journal of Aerosol Science*, 28:159–171, 1997.
- K.J. Welham, M.A. Domin, D.E. Scannell, E. Cohen, and D.S. Ashton. The characterization of micro-organisms by matrix-assisted laser desorption/ionization time-of-flight mass spectrometry. *Rapid Communications in Mass Spectrometry*, 12:176–180, 1998.
- K.T. Whitby, B.Y.H. Liu, R.B. Husar, and Barsic N.J. The Minnesota aerosol analyzing system used in the Los Angeles smog project. *Journal of Colloid and Interface Science*, 39:136–164, 1972.

Bibliography

- J.R. Whiteaker, B. Warscheid, P. Pribil, Y. Hathout, and C. Fenselau. Complete sequences of small acid-soluble proteins from *Bacillus globigii*. *Journal of Mass Spectrometry*, 39:1113–1121, 2004.
- R.M. Whittal and L. Li. High-resolution matrix-assisted laser desorption/ionization in a linear time-of-flight mass spectrometer. *Analytical Chemistry*, 67:1950–1954, 1995.
- W.C. Wiley and I.H. McLaren. Time-of-flight mass spectrometer with improved resolution. *Review of Scientific Instruments*, 26:1150–1157, 1955.
- T.L. Williams, D. Andrzejewski, J.O. Lay, and S.M. Musser. Experimental factors affecting the quality and reproducibility of MALDI TOF mass spectra obtained from whole bacteria cells. *Journal of the American Society for Mass Spectrometry*, 14:342–351, 2003.
- M. Wilson and S.E. Lindow. Relationship of total viable and culturable cells in epiphytic populations of *Pseudomonas syringae*. *Applied and Environmental Microbiology*, 58:3908–3913, 1992.
- H.G. Wittmann. Components of bacterial ribosomes. *Annual Review of Biochemistry*, 51:155–183, 1982.
- F. Xiang, R.C. Beavis, and W. Ens. A method to increase contaminant tolerance in protein matrix-assisted laser desorption/ionization by the fabrication of thin protein-doped polycrystalline films. *Rapid Communications in Mass Spectrometry*, 8:199–204, 1994.
- N. Xu, Z.-H. Huang, J.T. Watson, and D.A. Gage. Mercaptobenzothiazoles: A new class of matrices for laser desorption ionization mass spectrometry. *Journal of the American Society for Mass Spectrometry*, 8:116–124, 1997.
- R. Zenobi and R. Knochenmuss. Ion formation in MALDI mass spectrometry. *Mass Spectrometry Reviews*, 17:337–366, 1998.
- S. Zhao, K.V. Somayajula, A.G. Sharkey, D.M. Hercules, F. Hillenkamp, M. Karas, and A. Ingendoh. Novel method for matrix-assisted laser mass spectrometry of proteins. *Analytical Chemistry*, 63:450–453, 1991.

Bibliography

- L.V. Zhigilei, Y.G. Yingling, T.E. Itina, T.A. Schoolcraft, and B.J. Garrison. Molecular dynamics simulation of matrix-assisted laser desorption-connections to experiment. *International Journal of Mass Spectrometry*, 226:85–106, 2003.
- Y.F. Zhu, C.N. Chung, N.I. Taranenko, S.L. Allman, S.A. Martin, L. Haff, and C.H. Chen. The study of 2,3,4-trihydroxyacetophenone and 2,4,6-trihydroxyacetophenone as matrices for dna detection in matrix-assisted laser desorption/ionization time-of-flight mass spectrometry. *Rapid Communications in Mass Spectrometry*, 10:383–388, 1996.
- B.-A. Zucker and W. Müller. Airborne endotoxins and airborne gram-negative bacteria in a residential neighborhood. *Water, Air, & Soil Pollution*, 158:67–75, 2004.

Samenvatting

Aërosol MALDI

massaspectrometrie voor de

analyse van bioaërosolen

In dit proefschrift wordt de ontwikkeling van de aërosol massaspectrometer voor de analyse van biologische deeltjes in de lucht beschreven. Een groot gedeelte van dit onderzoeksproject werd door TNO Defensie en Veiligheid gefinancierd, met als voornaamste doel een instrument te ontwikkelen die een biologisch aanval kan aantonen. Onder een biologische aanval wordt verstaan een aanval met ziekteverwekkers, waarvan de verspreiding plaatsvindt door bijvoorbeeld de lucht. Allereerst is een evaluatie gemaakt van in de literatuur beschreven studies, waarin de concentraties van bacteriën in de lucht werden gemeten. Het doel van deze evaluatie was om de noodzaak en criteria vast te stellen waaraan het instrument zou moeten voldoen. Uit de evaluatie kwam naar voren dat een biologische aanval niet kan worden herkend aan de hand van gemeten (totale) concentraties van aërosolen. De gemeten ‘achtergrond’ concentraties zijn erg variabel en een toename in de concentratie wordt vaak veroorzaakt door normale (menselijke) activiteiten, bijvoorbeeld het oogsten. Identificatie van de aërosolen is daarom vereist.

De NRC (National Research Council of the United States) heeft design criteria gedefinieerd voor instrumenten die snel moeten kunnen waarschuwen in het geval van een biologische aanval: het detecteren van een breed scala aan biologische agentia, een korte responstijd en het optreden van zeer weinige valse alarmen. Op basis van deze evaluatie wordt aanbevolen de design criteria van de NRC uit te breiden met twee nieuwe criteria. Instru-

Samenvatting

menten die een biologische aanval moeten kunnen meten, moeten in staat zijn hoge concentraties en een groot concentratiebereik te meten. Met de huidige apparatuur is het niet mogelijk om een biologische aanval op een korte tijdschaal te detecteren en te identificeren, daarom zijn on-line technieken nodig. De aërosol MALDI massaspectrometer wordt voorgedragen als een instrument dat aan de criteria van de NRC kan voldoen.

De kracht van de aërosol massaspectrometer is gebaseerd op de volgende drie onderdelen: deeltjes detectie, deeltjes selectie en de analyse van de deeltjes met MALDI massaspectrometrie. In het begin van dit onderzoek was de aërosol massaspectrometer nog niet geheel aangepast en geoptimaliseerd voor (on-line) analyse van bacteriologische deeltjes. Om het instrument geschikt te maken voor de detectie van bioaërosolen is de aërosol massaspectrometer is aangepast. Aangebrachte verbeteringen zijn de implementatie van een nieuw ontwerp ionenbron en de implementatie van vertraagde ion-extractie. Door de verbeteringen worden nu massaspectra verkregen van individuele aërosoldeeltjes met een massabereik tot 21 kDalton en met een resolutie van 2000 bij massa's van 6 kDalton. De gevoeligheid van het instrument is 1 zeptomol (1 zeptomol komt overeen met circa 600 moleculen) voor deeltjes die bestaan uit 1 soort eiwit. Deze gevoeligheid is voldoende voor de analyse van bacteriologische deeltjes. Naast deze instrumentele verbeteringen is de deeltjesproductie ook geoptimaliseerd om bioaërosolen van natuurlijke groottes te produceren op een controleerbare manier. De deeltjesproductie is alleen gebruikt om de principes van het instrument te onderzoeken; voor een 'echt' instrument is geen productie van deeltjes nodig.

In de lucht is de bacterieconcentratie laag ten opzichte van de totale deeltjesconcentratie. Daarom is een selectiestap ingebouwd in de aërosol massaspectrometer. De selectiestap is gebaseerd op fluorescentie. In een experiment waarin buitenlucht werd gemeten, werd 20% geïdentificeerd als potentieel biologisch. Dit percentage komt overeen met een concentratie van $1 \cdot 10^6$ bioaërosolen/ m^3 , hetgeen weer overeenkomt met de waarden voor de achtergrondconcentraties die in hoofdstuk 1 van dit proefschrift zijn gevonden. Roetdeeltjes kunnen mogelijk interfereren op de gebruikte selectiestap en daarom is het effect van roetdeeltjes op de gebruikte selectiestap onderzocht. Het resultaat was dat roetdeeltjes worden beschouwd als een mogelijke bron van interferentie, maar de verwachting is dat op basis van de massaspectra roet niet zal worden geïdentificeerd als biologisch

materiaal. Door de toegepaste selectiestap worden alleen massaspectra gegenereerd van potentiële bacteriebevattende deeltjes.

In de aërosol massaspectrometer wordt MALDI (matrix-assisted laser desorption/ionization) massaspectrometrie gebruikt voor de analyse van aërosoldeeltjes. MALDI is een algemeen toegepaste techniek voor de analyse van biologisch materiaal. In dit onderzoek is de aard van het monster anders dan in de standaardtechniek, namelijk individuele aërosoldeeltjes. Voor de analyse van dit soort monsters is dan ook een andere monstervoorbewerking nodig. De kwaliteit en de massaspectra ‘an sich’ worden bepaald door de gebruikte monstervoorbewerking en de samenstelling van het monster. Om de MALDI-techniek toe te passen voor online analyse is het nodig dat de monstervoorbewerking ook online plaatsvindt. Naast de ontwikkelde offline monstervoorbewerkingsmethoden (de crushed-crystal- en de premix-methode), is daarom de online-coating methode ontwikkeld en onderzocht. De toegepaste monstervoorbewerkingstechnieken resulteerden in verschillende massa spectra, maar de te analyseren moleculen werden, onafhankelijk van de gebruikte methode, gedetecteerd. Het effect van de samenstelling van de monsters op de massaspectra is onderzocht met vijftien combinaties van matrix materialen en oplosmiddelen. Het effect van de samenstelling van de monsters in aërosol-MALDI is minder uitgesproken dan gevonden in de literatuur voor standaard MALDI massaspectrometrie. In aërosol-MALDI heeft de keuze van de matrix meer effect op de vorming en detectie van insuline-ionen dan het gekozen oplosmiddel. De matrix PMC (een ‘proprietary made compound’ ter beschikking gesteld door TNO Defensie en Veiligheid, Rijswijk, Nederland) is het meest geschikt voor de analyse van biologische aërosolen. Deze matrix kan ook gebruikt worden voor online analyse.

Het laatste deel van dit onderzoek betreft de analyse van bacteriedeeltjes, om de geschiktheid van het apparaat voor de online analyse van deze deeltjes vast te stellen. De bacteriedeeltjes zijn met drie verschillende monstervoorbewerkingsmethoden geanalyseerd, namelijk de crushed-crystal-methode, de impaction and evaporation/condensation-methode en met de online-coatingmethode. Met de *offline* crushed-crystal-methode is de detecteerbaarheid van de biologische deeltjes aangetoond. De massaspectra omvatten een groot massabereik (tot 16 kDalton) en de resolutie van de pieken was 200-400 bij een massa van 12 kDalton.

In de massaspectra konden pieken met gelijkwaardige massa's als ribo-

Samenvatting

somale eiwitten worden aan getoond. Aërosol MALDI massaspectrometrie is ook toegepast op bacteriële sporen. In de massaspectra werden pieken met gelijkwaardige massa's als de SASP's worden gedetecteerd. SASP's zijn voorgedragen biomarker moleculen voor bacteriële sporen.

Tenslotte is *online* analyse uitgevoerd op bacteriedeeltjes middels de online-coatingmethode. Met de online-coatingmethode wordt getracht online extractie, menging en co-kristallisatie van matrix en de te analyseren moleculen te bewerkstelligen. De pieken in de online massaspectra hebben een lage resolutie maar waren wel reproduceerbaar. Het massabereik van de gedetecteerde pieken is tot 4 kDalton. Aan de hand van de verkregen resultaten werd vastgesteld dat de toegepaste methode van monstervoorbewerking nog niet optimaal is. Voor de online extractie, menging en co-kristallisatie is een oplosmiddel nodig waarin de matrix en de moleculen oplossen. In de uitgevoerde experimenten is water als oplosmiddel gebruikt. De gebruikte matrix bleek echter niet oplosbaar te zijn in dit oplosmiddel. Preliminair oplosbaarheidsexperimenten lieten zien dat isopropanol een mogelijk oplosmiddel is dat wel aan deze voorwaarden voldoet. Meer en uitgebreider onderzoek naar andere oplosmiddelen is nodig.

Uit het in dit proefschrift beschreven onderzoek kan geconcludeerd worden dat de ontwikkelde massaspectrometer potentieel een geschikt apparaat is om bacteriedeeltjes te meten en te analyseren. Deze geschiktheid is aangetoond met een offline monstervoorbewerkingsmethode. Echter, om dezelfde performance voor online analyse te verkrijgen is meer onderzoek nodig.

De gedane experimenten en verkregen resultaten hebben geleid tot meer inzicht in het mechanisme van en de processen in MALDI massaspectrometrie.

Ineke Kleefsman
Delft, September 2008

Acknowledgement

Aangezien een proefschrift zonder dankwoord niet compleet is en omdat ook dit proefschrift tot stand is gekomen met hulp en ondersteuning van veel mensen, is dit de aangewezen plek om die mensen met naam te noemen. Allereerst wil ik Professor Andreas Schmidt-Ott heel hartelijk bedanken voor het zijn van mijn promotor. De vrijheid die ik kreeg om mijn onderzoek uit te voeren, heb ik erg gewaardeerd.

Mijn grootste dank gaat uit naar Jan Marijnissen. Dank je wel dat ik mocht werken aan jouw ‘bacterie-snuffelaar’. Met jouw onuitputtelijke enthousiasme heb je me altijd weer te weten motiveren, ook wanneer ik dingen niet meer zag zitten. Ondanks je drukke programma’s had je altijd tijd voor me. Zelfs in de avonduren mocht ik langskomen in Breda, waar ik gastvrij werd ontvangen. Jetje, ook jij bedankt voor de gastvrijheid. Dank je wel voor het koken van de heerlijke ‘aërosol-diners’.

Peter Verheijen, ik wil jou bedanken voor je kritische opmerkingen, je hulp bij het schrijven van de MatLab routines, je geduld om mijn geschreven stukken te lezen en van goede commentaar te voorzien. Dank je wel ook voor de grappige aspecten die je altijd wist in te brengen in de gesprekken die we hadden.

Most results in this thesis I obtained together with Mike Stowers. I learned a lot from you, the details of the instrument, details about lasers and optics, new english words and grammar. It was a great pleasure to work with you, I enjoyed all the fruitful discussions we had. Thanks for your patience with me.

Een woord van dank naar TNO, de sponsor van dit onderzoeksproject, kan niet ontbreken. Arjan, heel erg bedankt voor je adviezen en hulp; voor je uitleg als ik het niet meer snapte. Ik waardeer je loyaliteit voor dit project. Jouw berekeningen voor de ionenbron zijn de basis voor enkele behaalde resultaten in dit proefschrift. Ingrid, we hebben elkaar vaak gezien op de vroege ochtend, wanneer ik bacteriekolonies bij je kwam

Acknowledgement

halen. Dank je wel dat je altijd klaar stond om weer een buis *E. coli* of een ander microorganisme voor mij te incuberen. Willem, we hebben samen wat uurtjes achter de microscoop doorgebracht. Je was altijd geduldig op zoek naar mijn beestjes die ik op een SEM-grid geïmpacteerd had. Dank je wel voor de mooie plaatjes die je van mijn monsters wist te maken. Ad, ik wil jou bedanken voor het uitvoeren van de standaard MALDI experimenten. Verder wil ik bij naam noemen: Charles, Olaf, Flip, Frank en Ruud en bedanken voor de samenwerking.

I would acknowledge the committee members. Thank you for reading my manuscript and the very useful comments. I want to name especially professor Piet Kistemaker.

Een goed werkend instrument is een voorwaarde voor het behalen van resultaten. Nico, Alex, Alex, Rien, Ruud, Cor, Carlo van de DCT-werkplaats en Henk van de glasblazerij, bedankt voor alle dingen die jullie voor mij hebben gemaakt en gerepareerd. Van de ICT-mensen wil ik Riccardo en Arno bedanken. In het bijzonder voor jullie hulp op afstand, zodat ik in het hoge noorden, herstellend van een gebroken been, toch mijn proefschrift kon afmaken.

Some of the results in this thesis have been generated by my students, intern shippers and post doc. I would like to thank Alyson Niewmeyer, Maria Svane, Patrick Sislian, Eliane Khoury and Sergei Ovsianko. It was a pleasure to work with you.

Heel belangrijk voor mij was de goede en gezellige werksfeer die er heerste bij de 'deeltjes'. Deze sfeer werd voornamelijk gecreëerd door de leden van de NPOB (NSM Party Organizing Board): Jan, Bas en Christian. Dank jullie wel voor jullie vriendschap, voor de gezellige en lekkere lunches die we hadden, voor de barbecues, voor de borrels, voor de koffiepauzes, de Mario-kart-sessies, de etentjes en nog veel meer. Jullie hebben ervoor gezorgd dat mijn TUDelft-carrière een hele waardevolle herinnering is geworden. Not only the NPOB members contributed to the nice working environment, I also have to thank the rest of the (former) particles: Henk, Sjaak, Vincent, Saul, Bart, Nooshin, Anna, Tomek, Yonshuang, Caner, George, Orion, Micha, Stefan, Antina, Raghu, Bas (aka Hein), Tobias, Simone, Ajay, Gabriele, Giacomo, Stephen, Andrezj, John, Valerie, Loes, Marcel, Corrado and Mario. Wil, Fieneke, Wil en Karin, bedankt voor de secretariële ondersteuning.

Dat het onderzoek een groot deel van je leven gaat bepalen dat weten

mijn vrienden. Lidwina, Annemarie, Miriam, Harolf, Sonja, Marco, Margreet, Catrina, Martine, Elly, Rene, de bijbelstudie. Bedankt voor jullie luisterende oren als ik weer eens veel te vertellen had over mijn onderzoek.

Dominee Wilschut, bedankt voor uw hulp bij het kiezen van de motto's bij de hoofdstukken in dit proefschrift.

Wim, jouw geduld, nuchterheid en liefde heb ik erg nodig gehad, dank je wel daarvoor.

Tenslotte wil ik mijn familie bedanken. Mijn ouders omdat ze mij en mijn zussen en broer altijd in de gelegenheid gesteld hebben om onderwijs te volgen en ons daarin ook met alles te steunen. Anja & Gerhard, Jos en Els dank jullie wel voor alles. Els bedankt voor het ontwerpen van de omslag van dit proefschrift. Ooms en tantes, ook jullie wil ik bedanken voor jullie interesse die jullie toonden in de voortgang van mijn onderzoek.

Tijdens mijn onderzoek heb ik een stukje van de grootsheid van de schepping mogen ervaren. Mijn allergrootste dank gaat dan ook uit naar God, Schepper van hemel en aarde.

Curriculum Vitae



Ineke Kleefsman was born on January 4th, 1979 in Groningen.

1991-1997	VWO Gomarus College Groningen
1997-2002	Pharmaceutical Engineering University of Groningen
1997-2003	Pharmacy University of Groningen
2003	Pharmacist Apotheek 't Hooge Zand Hoogezand
2003-2007	PhD research Particle Technology Group (Nanostructured Materials) Delft University of Technology
2007-current	Scientist Oral Dosage Forms N.V. Organon, Part of Schering-Plough Corporation